

Özlem Özcan

Ph.D. Thesis

AGU 2024

DEVELOPMENT OF HYBRID
MEMBRANE PROCESSES FOR
ENERGY AND WATER RECOVERY
FROM MUNICIPAL WASTEWATERS

Ph.D. THESIS

SUBMITTED TO THE DEPARTMENT OF MATERIAL SCIENCE
AND MECHANICAL ENGINEERING
AND THE GRADUATE SCHOOL OF ENGINEERING AND
SCIENCE OF ABDULLAH GUL UNIVERSITY
IN PARTIAL FULFILLMENT OF THE REQUIREMENTS
FOR THE DEGREE OF
DOCTOR OF PHILOSOPHY

By

Özlem ÖZCAN

June 2024

DEVELOPMENT OF HYBRID MEMBRANE
PROCESSES FOR ENERGY AND WATER
RECOVERY FROM MUNICIPAL
WASTEWATERS

A Ph.D. THESIS

SUBMITTED TO THE DEPARTMENT OF MATERIAL SCIENCE AND
MECHANICAL ENGINEERING
AND THE GRADUATE SCHOOL OF ENGINEERING AND SCIENCE OF
ABDULLAH GUL UNIVERSITY

IN PARTIAL FULFILLMENT OF THE REQUIREMENTS
FOR THE DEGREE OF
DOCTOR OF PHILOSOPHY

By

Özlem ÖZCAN

June 2024

SCIENTIFIC ETHICS COMPLIANCE

I hereby declare that all information in this document has been obtained in accordance with academic rules and ethical conduct. I also declare that, as required by these rules and conduct, I have fully cited and referenced all materials and results that are not original to this work.

Name-Surname: Özlem ÖZCAN

Signature :

REGULATORY COMPLIANCE

Ph.D. thesis titled “Development of Hybrid Membrane Processes for Energy and Water Recovery from Municipal Wastewaters” has been prepared in accordance with the Thesis Writing Guidelines of the Abdullah Gül University, Graduate School of Engineering & Science.

Prepared By	Advisor	Co Advisor
Özlem ÖZCAN	Prof. Dr. Niğmet UZAL	Prof. Dr. Erkan ŞAHİNKAYA

Head of the Material Science and Mechanical Engineering Program

Dr. Öğr. Üyesi Zeliha SORAN ERDEM

ACCEPTANCE AND APPROVAL

Ph.D. thesis titled “Development of Hybrid Membrane Processes for Energy and Water Recovery from Municipal Wastewaters” and prepared by Özlem Özcan has been accepted by the jury in the Material Science and Mechanical Engineering Graduate Program at Abdullah Gül University, Graduate School of Engineering & Science.

...../...../.....

JURY:

Advisor : Prof. Dr. Niğmet UZAL

Co-advisor : Prof. Dr. Erkan ŞAHİNKAYA

Member : Prof. Dr. Nadir DİZGE

Member : Doç. Dr. Kevser KAHRAMAN

Member : Prof. Dr. Nuray ATEŞ

Member : Doç. Dr. Adem YURTSEVER

APPROVAL:

The acceptance of this Ph.D. thesis has been approved by the decision of the Abdullah Gül University, Graduate School of Engineering & Science, Executive Board dated /..... / and numbered

...../...../.....

(Date)

Graduate School Dean
Prof. Dr. İrfan ALAN

ABSTRACT

DEVELOPMENT OF HYBRID MEMBRANE PROCESSES FOR ENERGY AND WATER RECOVERY FROM MUNICIPAL WASTEWATERS

Özlem ÖZCAN

Ph.D. in Material Science and Mechanical Engineering

Advisor: Prof. Dr. Niğmet UZAL

Co-advisor: Prof. Dr. Erkan ŞAHİNKAYA

June 2024

This thesis study aims to develop a hybrid innovative membrane-based process that maximizes circular benefit with the recovery of energy, nutrients, and water from municipal wastewater (MWW). This process was designed to be a sustainable alternative to the widely used advanced biological wastewater treatment plants (WWTP). For this purpose, the wastewater samples from the pre-sedimentation tank effluent of the Kayseri WWTP were used in laboratory-scale membrane-based process applications. In the first stage of the study, pre-concentration studies were performed to concentrate the organic matter and nutrients in the wastewater using the chemically enhanced primary sedimentation+direct ceramic microfiltration (CEPS+DCMF) process. Wastewater concentrated up to 8 times in the CEPS+DCMF process was fed to the anaerobic fluidized bed ceramic membrane bioreactor (AnFCMBR), which is the second stage of the study. The performance of the reverse osmosis (RO) process was evaluated for nutrient recovery performance in permeates of AnFCMBR and CEPS+DCMF processes. Chemical precipitation was performed on RO concentrate samples to recover struvite. With the innovative membrane-based hybrid wastewater treatment process, a net energy recovery potential of 0.126 kWh/m^3 was attained by operating the AnFCMBR process at 6 hours hydraulic retention time, while an energy requirement of 0.08 kWh/m^3 was attained and thus, an energy-positive process for treating MWW has been developed.

Keywords: Flocculation, direct ceramic microfiltration, anaerobic fluidized bed membrane bioreactor, ceramic membrane, energy-positive wastewater treatment

ÖZET

EVSEL ATIKSULARDAN ENERJİ VE SU GERİ KAZANIMINDA HİBRİT MEMBRAN PROSESLERİN GELİŞTİRİLMESİ

Özlem ÖZCAN

Malzeme Bilimi ve Makine Mühendisliği Anabilim Dalı Doktora

Tez Danışmanı: Prof. Dr. Niğmet UZAL

Eş-Danışman: Prof. Dr. Erkan ŞAHİNKAYA

Haziran-2024

Bu tez çalışması, evsel atıksudan enerji, nütrient ve su geri kazanımı ile döngüsel faydayı maksimize eden hibrit yenilikçi membran esaslı bir proses geliştirilmesi hedeflemiştir. Bu proses ile yaygın olarak kullanımda olan konvansiyonel ileri biyolojik atıksu arıtma tesislerine (AAT) sürdürülebilir bir alternatif olarak tasarlanmıştır. Bu amaçla, laboratuvar ölçekli membran esaslı proses uygulamalarında Kayseri İleri Biyolojik AAT ön çökeltim havuzu çıkışından alınan atıksu örnekleri kullanılmıştır. Çalışmanın ilk aşamasında organik madde ve nütrientin konsantre edilmesi için ileri kimyasal ön çöktürme+doğrudan seramik mikrofiltrasyon (CEPS+DSMF) prosesi uygulanmıştır. CEPS+DSMF çalışmalarında 8 kata kadar konsantre edilen atıksu, çalışmanın ikinci aşaması olan anaerobik akışkan yataklı seramik membran biyoreaktör (AnFSMBR)'e beslenmiştir. AnFSMBR ve yumaklaştırma+DSMF proseslerinin permeatlarında nütrient geri kazanım çalışmaları için ters osmoz (RO) uygulanarak, bu prosesin performansı değerlendirilmiştir. CEPS+DSMF prosesi ile evsel atıksuda organik madde konsantre hale getirilmiştir. RO konsantresinde strüvit geri kazanımı için kimyasal çöktürme uygulanmıştır. Yenilikçi membran esaslı hibrit atıksu arıtma prosesi ile 0,08 kWh/m³'lük enerji gereksinimine karşılık AnFSMBR prosesinin 6 saat hidrolik bekletme süresinde işletilmesi ile 0,126 kWh/m³'lük net enerji geri kazanımı potansiyeli sağlanmış ve dolayısıyla enerji pozitif bir evsel atıksu arıtma prosesinin geliştirilmiştir.

Anahtar kelimeler: Yumaklaştırma, doğrudan seramik mikrofiltrasyon, anaerobik akışkan yataklı membran biyoreaktör, seramik membran, enerji pozitif atıksu arıtımı

Acknowledgements

First and foremost, I would like to express my gratitude to my advisor Prof. Dr. Niğmet Uzal for her guidance, encouragement, and resources and for creating an incredible research and work culture. I would like to special thank my co-advisor Prof. Dr. Erkan Şahinkaya for giving me deep technical feedback when I needed it. I would also like to thank the research team members who helped me directly or indirectly during this long period of lab work.

I would like to thank my family, especially my father and my mother for being in favor of me in any case and believing in me. I am grateful to my husband, İskender Özcan, who supported and motivated me in every way. I would also like to thank my mother and father-in-law for supporting me through every success or failure.

This Ph.D. study was supported by the Scientific and Technological Research Council of Turkey (TUBITAK), 1001 program (Project No: 119Y134), YÖK 100/2000 Ph.D. program, and Abdullah Gül University Scientific Research Projects (Project No: FDK-2022-166T)

TABLE OF CONTENTS

1. TABLE OF CONTENTS	IV
2. LIST OF FIGURES	VI
3. LIST OF TABLES	IX
4. LIST OF ABBREVIATIONS	XI
5. CHAPTER 1	1
INTRODUCTION	1
6. CHAPTER 2	8
7. LITERATURE REVIEW	8
2.1 BIBLIOMETRIC ANALYSIS	8
2.2 CONVENTIONAL WASTEWATER TREATMENT TO RESOURCE RECOVERY	12
2.3 WATER, ENERGY, AND NUTRIENT RECOVERY FROM MUNICIPAL WASTEWATER.....	16
2.4 TECHNOLOGIES WATER, ENERGY, AND NUTRIENT RECOVERY FROM MUNICIPAL WASTEWATER	24
2.4.1 Membrane filtration applications.....	28
2.4.2.1 Membrane fouling	36
2.4.4 Anaerobic digestion.....	41
2.4.5 Anaerobic membrane bioreactors	44
2.4.6 AnMBR configurations.....	45
2.4.7 Integration of AnMBRs with different processes for resource recovery.....	55
2.4.8 Struvite Precipitation	59
2.4.8.1 Effect of pH	59
2.4.8.2 Effect of temperature	60
2.4.8.3 Effect of reaction time	60
2.4.8.4 Effect of Mg:P:N molar ratio.....	61
2.5 CONCLUSION AND FUTURE WORKS.....	61
8. CHAPTER 3	65
9. PRE-CONCENTRATION OF MUNICIPAL WASTEWATER USING FLOCCULATION ASSISTED DIRECT CERAMIC MICROFILTRATION PROCESS: OPTIMIZATION OF OPERATIONAL CONDITIONS	65
3.1 INTRODUCTION.....	65
3.2 MATERIALS AND METHODS	68
3.2.1 MEMBRANES AND CHEMICALS	68
3.2.2 WASTEWATER AND ANALYSIS	68
3.2.3 JAR TESTS.....	69
3.2.4 Experimental set-up and operational conditions.....	69
3.2.5 Membrane Cleaning.....	73
3.2.6 Specific fouling rate	73
3.3 RESULTS AND DISCUSSION.....	74
3.3.1 Flocculation performance at different PAM concentrations	74
3.3.2 Determination of optimum configuration.....	75
3.3.3 Optimization of operational conditions of the DCMF process.....	81
3.3.4 Optimization of pH.....	82
3.3.5 Optimization of flux and filtration/backwash time	84
3.3.6 Optimization of recovery rate.....	87
3.3.7 Long-term operation of CEPS+DCMF process and energy production potential.....	88
3.4 CONCLUSIONS	92
10. CHAPTER 4	94
11. LONG-TERM OPERATION OF FLOCCULATION ASSISTED DIRECT CERAMIC MICROFILTRATION FOR UP-CONCENTRATION OF MUNICIPAL WASTEWATER...	94
4.1 INTRODUCTION.....	94
4.2 MATERIALS AND METHODS	96
4.2.1 Materials and chemicals	96
4.2.2 Wastewater and Analysis	96
4.2.3 Experimental setup and operation	97
4.2.4 Membrane cleaning procedures.....	99

4.2.5	<i>Assessment of energy potential</i>	100
4.2.6	<i>Membrane characterization</i>	101
4.3	RESULTS AND DISCUSSION.....	101
4.3.1	<i>TMP behavior</i>	101
4.3.2	<i>Samples characteristics</i>	105
4.3.3	<i>Assessment of energy potential</i>	107
4.3.4	<i>Membrane characterization</i>	109
4.4	CONCLUSIONS.....	111
12.	CHAPTER 5	112
13.	PERFORMANCE EVALUATION OF AN ANAEROBIC FLUIDIZED BED CERAMIC MEMBRANE BIOREACTOR INTEGRATED WITH PRE-CONCENTRATION PROCESS FOR RESOURCE RECOVERY FROM MUNICIPAL WASTEWATER: STRATEGIES FOULING MANAGEMENT AND ENERGY GENERATION POTENTIAL	112
5.1	INTRODUCTION.....	112
5.2	MATERIALS AND METHODS.....	115
5.2.1	<i>Setup and operation of the AnFCMBR System</i>	115
5.2.2	<i>Wastewater</i>	119
5.2.3	<i>Energy balance</i>	121
5.2.4	<i>Membrane characterization</i>	121
5.3	RESULTS AND DISCUSSION.....	122
5.3.1	<i>AnFCMBR operation: optimization of filtration mode</i>	122
5.3.2	<i>Operation performance of AnFCMBR Systems</i>	123
5.3.3	<i>The evaluation of the operational performance of AnFCMBR configurations</i>	134
5.3.4	<i>Assessment of energy balance for the proposed process</i>	135
5.3.1	<i>Characterization of membranes</i>	138
5.4	CONCLUSION.....	140
14.	CHAPTER 6	141
15.	OPTIMIZATION OF REVERSE OSMOSIS AND STRUVITE PRECIPITATION TO MAXIMIZE NUTRIENT RECOVERY FROM THE COMBINED EFFLUENT OF ANAEROBIC FLUIDIZED CERAMIC MEMBRANE BIOREACTOR AND DIRECT CERAMIC MICROFILTRATION PROCESSES	141
6.1.	INTRODUCTION.....	141
6.2.	MATERIALS AND METHODS.....	144
6.2.1	<i>Wastewater and Analysis</i>	144
6.2.2	<i>Experimental set-up and operational conditions of RO system</i>	144
6.2.3	<i>Modelling of NH₄-N removal</i>	148
6.2.4	<i>Membrane Characterization</i>	148
6.2.5	<i>N and P recovery from RO concentrate by MAP crystallization</i>	149
6.2.6	<i>X-ray diffraction (XRD)</i>	149
6.3.	RESULTS.....	150
6.3.1	<i>RO tests with effluent of CEPS+DCMF</i>	150
6.3.1.1	<i>Operation of RO process in TRM using CEPS+DCMF process effluent</i>	150
8	152
6.3.1.2	<i>Operation of RO process in CM using CEPS+DCMF process effluent</i>	153
6.3.2	<i>RO tests with effluent of the CEPS+DCMF and AnFCMBR processes</i>	156
6.3.2.1	<i>Effect of TMP and CFV on RO performance</i>	156
6.3.2.2	<i>Effect of Recovery Rate on RO performance</i>	160
6.3.2.3	<i>Effect of pH on RO performance</i>	162
6.3.3	<i>Membrane Surface Characterization</i>	167
6.3.3.1	<i>ATR-FTIR</i>	167
6.3.3.2	<i>SEM-EDX</i>	168
6.3.4	<i>Struvite recovery from RO process concentrate</i>	169
6.4.	CONCLUSION.....	172
16.	CHAPTER 7	174
17.	CONCLUSIONS AND FUTURE PROSPECTS	174
7.1	CONCLUSIONS.....	174
7.2	SOCIETAL IMPACT AND CONTRIBUTION TO GLOBAL SUSTAINABILITY	176
7.3	FUTURE PROSPECTS.....	177
18.	BIBLIOGRAPHY	179

LIST OF FIGURES

Figure 1.1 Schematic representation of the research approach and thesis framework.....	7
Figure 2.1 The co-occurrence network visualization of “MWW treatment”	10
Figure 2.2 The co-occurrence network visualization of “sustainable MWW treatment”	11
Figure 2.3 The evaluation of resource composition and its associated economic value in the context of MWW [72].....	15
Figure 2.4 MWW production across regions in 2015 and predicted until 2050 [76].....	17
Figure 2.5 Concepts and illustrations for wastewater and reuse [79].....	18
Figure 2.5 Illustration of the nitrogen cycle, depicting both natural and anthropogenic transformations [100].....	21
Figure 2.6 Schematic representation of the phosphorus cycle [107].....	22
Figure 2.7 Different technologies are employed for reclaiming water from municipal WWTPs. [121].....	25
Figure 2.8 Methods that can be used to recover energy from municipal WWTPs [121]	26
Figure 2.9 Examples of technology for extracting nutrients from municipal WWTPs. The use of grey shading represents methods that have been implemented extensively in municipal WWTPs. Methods that do not have widespread application are indicated by not-shaded boxes. [121].....	28
Figure 2.10 Anaerobic treatment stages [226].....	44
Figure 2.11 Schematic diagram of novel AnMBR processes: (a) biogas-sparging AnMBR; (b) AnFMBR; (c) granular-sludge AnMBR; (d) AnDMBR and (e) AnFOMBR [231].....	46
Figure 2.12 Pre-concentration-based flow sheet for integrated resource recovery [283]	63
Figure 3.1 Optimization of DCMF filtration	70
Figure 3.2 Schematic diagram of the (a) PAM+DCMF and (b) CEPS+DCMF process	72
Figure 3.3 COD, TSS, and turbidity removals at varying PAM concentrations in jar tests	74
Figure 3.4 TMP profile as a function of time for (a) PAM+DCMF and (b) CEPS+DCMF	77
Figure 3.5 Comparison of specific fouling rate ($\text{g m}^{-2} \text{h}^{-1}$) for DCMF, PAM+DCMF, and CEPS+DCMF processes	78
Figure 3.6 TMP change in CEPS+DCMF process with different pH	83
Figure 3.7 Change in TMP in CEPS+DCMF process with filtration time with different filtration/backwash time	84
Figure 3.8 TMP change in CEPS+DCMF process with different fluxes.....	86
Figure 3.9 TMP change in CEPS+DCMF process with the different recovery rates.....	88
Figure 3.10 TMP profile as a function of time for continuous operation of CEPS+DCMF process	89
Figure 3.11 COD concentrations in the concentrate and permeate of continuously operated CEPS+DCMF process.....	90
Figure 3.12 Theoretical COD concentrations in different units of the proposed process used in mass balance and energy calculations	91
Figure 4.1 Schematic representation of the CEPS+DCMF process	97
Figure 4.2 The picture of the laboratory-scale DCMF system	98

Figure 4.3 The flow rates that will be achieved when operating the CEPS+DCMF process as a full-scale treatment plant.	100
Figure 4.4 TMP profile as a function of time during Phase I.....	102
Figure 4.5 TMP profile as a function of time during Phase II.....	103
Figure 4.6 TMP profile as a function of time during Phase III -Operating two membranes in parallel at a flux of 10 LMH (The red line indicates the time of chemical cleaning with NaOH solution).....	104
Figure 4.7 TMP profile as a function of time during Phase IV (The physical+chemical cleaning is applied are marked with blue arrows. At the time indicated by the red line, a new ceramic membrane was placed after the deformations in the ceramic membranes.).....	105
Figure 4.8 Theoretical potential energy generation that could be obtained from the operation of the CEPS+DCMF process.....	107
Figure 4.9 SEM images of the virgin (a), physically cleaned ceramic membrane (b), and physically+chemically cleaned ceramic membrane (c).....	110
Figure 5.1 Schematic diagram of AnFCMBR-SiS (a) and AnFCMBR-SiF (b).....	116
Figure 5.2 Images of AnFCMBR-SiS (a) and AnFCMBR-SiF (b).....	116
Figure 5.3 Experimental flow chart of AnFCMBRs operation.....	117
Figure 5.4 Schematic representation of strategy for generating the feed for the AnFCMBRs.....	120
Figure 5.5 TMP profile as a function of time for different filtration/relaxation times with an HRT of 24 hours for AnFCMBR-SiS.....	122
Figure 5.6 TMP profile as a function of time for different filtration/relaxation times with an HRT of 18 hours for AnFCMBR-SiS.....	123
Figure 5.7 TMP profile as a function of time at 24-hour HRT and 5/1 filtration/relaxation time for AnFCMBR-SiS.....	124
Figure 5.8 TMP profile as a function of time for operation at 18-hour HRT for AnFCMBR-SiS.....	126
Figure 5.9 TMP profile as a function of time at 12-hour HRT for AnFCMBR-SiS	128
Figure 5.10 TMP profile as a function of time at 6-hour HRT for AnFCMBR-SiS	129
Figure 5.11 TMP variations for the AnFCMBR at 3-hour HRT for AnFCMBR-SiS..	131
Figure 5.12 TMP variations for AnFCMBR-SiS (a) and AnFCMBR-SiF (b) at 12 hours of HRT.....	133
Figure 5.13 SEM images of the virgin (a), physically cleaned (b), and physically+chemically cleaned ceramic membrane (c) used in the AnFCMBR process at 3 hour HRT.....	139
Figure 6. 1 Schematic representation of RO system.....	145
Figure 6.2 Representation of the experimental flow chart of the RO process using the permeate of the AnFCMBR and CEPS+DCMF processes (CM: Concentrate mode, TRM: Total recycle mode, TMP: Transmembrane pressure, CFV: Cross-flow velocity).....	147
Figure 6.3 Permeability values and flux recovery rates obtained for TMP and CFV in RO tests.....	159
Figure 6.4 Permeability values and flux recovery rates obtained for different recovery rates in RO tests.....	162
Figure 6.5 Flux and flux recovery rates obtained for different pH in RO tests.....	165
Figure 6.6 A visual representation of the project generated to compare the NH ₄ -N recovery rate through the modeling designed in the Wave software.....	166
Figure 6.7 Comparison of the experimentally determined NH ₄ ⁺ removal efficiencies and the Wave software modeled NH ₄ -N recovery rate at different pH.....	167

Figure 6.8 ATR-FTIR spectra of the virgin, fouled during tests performed at a CFV of 0.8 and 1.0 m/s.....	168
Figure 6.9 SEM-EDX images of the BW30-XFR membrane before (a) and after (b) tests	169
Figure 6.10 XRD pattern of the precipitate obtained from MAP crystallization tests .	172



LIST OF TABLES

Table 2.1 Typical MWW composition [57].....	13
Table 2.2 Membrane processes for MWW reuse applications	30
Table 2.3 Overview of the impacts of various parameters on membrane fouling in different membrane processes	37
Table 2.4 A comparison of different AnMBR configurations [231]	47
Table 2.5 Scientific articles of relevance to the treatment of MWW using the AnMBR system.	49
Table 2.6 Overview of the main features of recent techniques used for recovering resources from MWW using AnMBR technology	57
Table 3.1 The characteristics of primary sedimentation tank effluent	69
Table 3.2 The procedure followed in the optimization of the CEPS+DCMF process ...	71
Table 3.3 The impacts of PAM concentration on pH, conductivity, and PO ₄ -P	75
Table 3.4 Characteristics of the concentrated wastewater after the DCMF process with different PAM concentrations and configurations.....	80
Table 3.5 The characteristics of raw wastewater and CEPS process effluent	82
Table 3.6 Effect of pH on COD removal performance of CEPS process conducted at 0.5 mg/L PAM.....	82
Table 3.7 Characteristics of the concentrated wastewater after DCMF at different pHs	83
Table 3.8 Characteristics of the concentrated wastewater after DCMF with different filtration/backwash time	85
Table 3.9 Characteristics of the concentrated wastewater after DCMF with different flux	86
Table 3.10 Characteristics of the concentrated wastewater with different recovery rates	88
Table 3.11 Energy balance for electrical energy requirements and potential production with CEPS+DCMF process	92
Table 4.1 Operating conditions for the CEPS+DCMF process	99
Table 4.2 Characterization of samples acquired by the CEPS+DCMF process.....	106
Table 4.3 Energy balance for electrical energy requirements and potential production with CEPS+DCMF process	108
Table 4.4 EDX data of the ceramic membrane used in the CEPS+DCMF process	110
Table 5.1 Operational conditions of AnFCMBR.....	119
Table 5.2 Feed characteristics of AnFCMBR systems.....	120
Table 5.3 Permeate and feed characteristics for operation at 24-hour HRT and 5/1 filtration/relaxation time for AnFCMBR-SiS	125
Table 5.4 Permeate and feed characteristics for operation at 18-hour HRT for AnFCMBR-SiS.....	127
Table 5.5 Permeate and feed characteristics for operation at 12-hour HRT for AnFCMBR-SiS.....	129
Table 5.6 Permeate and feed characteristics for operation at 6-hour HRT for AnFCMBR-SiS.....	130
Table 5.7 Permeate and feed characteristics for operation at 3-hour HRT for AnFCMBR-SiS.....	132
Table 5.8 Characteristics of feed and permeate in the AnFCMBR-SiS and AnFCMBR-SiF operation.....	133
Table 5.9 Performance results for 24, 18, 12, 6, and 3-hour HRT in AnFCMBR systems	135

Table 5.11 Energy requirement of processes.....	136
Table 5.11 Potential for methane-based electric generation for different HRT operations of the AnFCMBR process.....	138
Table 5.12 EDX data of the ceramic membrane used in the AnFCMBR-SiS process at 3-hour HRT.....	140
Table 6.1 Flux recovery rates obtained in TRM operation.....	150
Table 6.2 Characteristics of samples obtained by TRM operation of RO process.....	152
Table 6.3 Flux recovery rates obtained by operating the RO process in CM.....	153
Table 6.4 Characteristics of samples obtained by TRM operation of RO process.....	155
Table 6.5 Effect of CFV and TMP on the performance of RO	158
Table 6.6 Characteristics of samples obtained from tests on recovery rate optimization of RO.....	161
Table 6.7 Characteristics of samples on pH optimization of RO process at 60% recovery rate	163
Table 6.8 Inputs used in modeling created in Wave Software	165
Table 6.0.9 EDX data of BW30-XFR membrane.....	169
Table 6.10 PO ₄ -P and Mg ²⁺ concentrations of the samples obtained in MAP crystallization tests performed at different Mg/P molar ratios	170
Table 6.11 Characteristics of samples collected during MAP crystallization tests.....	171

LIST OF ABBREVIATIONS

AAS	Atomic absorption spectrometry
AC	Anion Chromatography
AnDMBR	Anaerobic Dynamic Membrane Bioreactor
AnFCMBR	Anaerobic Fluidized Bed Ceramic Membrane Bioreactor
AnFMBR	Anaerobic Fluidized Bed Membrane Bioreactor
AnFOMBR	Anaerobic Forward Osmosis Membrane Bioreactor
AnMBR	Anaerobic Membrane Bioreactors
AnOMBR	Anaerobic Osmotic Membrane Bioreactor
BOD	Biochemical Oxygen Demand
CAS	Conventional Activated Sludge
CEPS	Chemically Enhanced Primary Sedimentation
CEPT	Chemical Enhanced Primary Treatment
CFV	Cross Flow Velocity
CIP	Cleaning-In-Place
CM	Concentrate Mode
COD	Chemical Oxygen Demand
DCMF	Direct Ceramic Microfiltration
DMF	Direct Membrane Filtration
DOC	Dissolved Organic Carbon
DOM	Dissolved Organic Matter
EC	Electrical Conductivity
EDX	Energy-Dispersive X-Ray
GAC	Granular Activated Carbon
HRT	Hydraulic Retention Time
LCC	Life Cycle Cost
MAP	Magnesium Ammonium Phosphate
MBR	Membrane Bioreactors
MF	Microfiltration
MLSS	Mixed Liquor Suspended Solids
MWW	Municipal Wastewater
NF	Nanofiltration
OLR	Organic Loading Rate
OM	Organic Matter
ORP	Oxidation Reduction Potential
PAM	Polyacrylamide

PVDF	Polyvinylidene Fluoride
RO	Reverse Osmosis
sCOD	Soluble Chemical Oxygen Demand
SEM	Scanning Electron Microscopy
SRT	Sludge Retention Time
SS	Suspended Solids
TMP	Transmembrane Pressure
TN	Total Nitrogen
TP	Total Phosphorus
TRM	Total Recycle Mode
TDS	Total Dissolved Solid
TSS	Total Suspended Solids
TUIK	Turkish Statistical Institute
UF	Ultrafiltration
VFA	Volatile Fatty Acid
WWTP	Wastewater Treatment Plant



To my husband

Chapter 1

Introduction

The impact of demographic scaling up, urbanization, improved living standards, and technical progress has resulted in a remarkable increase in water demand. This demand is not limited to municipality usage but also includes agricultural and industrial sectors. It is also anticipated that about three-fourths of the world's population to live in urban regions by 2050. In addition to urban growth, water used for food production and irrigation imposes considerable tension on freshwater resources, in which the agricultural sector accounted for >70% of global freshwater withdrawals, and in some fast-growing economies, it increased up to 90% [1]. Currently, around two billion people globally lack access to potable water [2], while around half of the global population faces significant water scarcity at some periods of the year [3].

Considering that high water consumption increases the volume of wastewater generated, MWW is one of the main alternative sources for water reclamation and reuse. However, wastewater treatment and the use of effluents have two major advantages, including the reduction of environmental contamination and, hence, health risks, and conserving the limited freshwater reserves [4]. Consequently, it is essential to develop cutting-edge treatment techniques that are based on the concept of reusing wastewater to reduce the health and ecological risks of reclaimed water [5].

Beyond the environmental and health challenges, conventional methods of treating MWW involve significant energy input during the main stages of wastewater treatment plants. These stages include collecting and transferring wastewater to the plant, as well as physical and chemical treatment, biological treatment, treatment of sludge, and discharge [6]. In a conventional wastewater treatment plant, the

consumption of energy in the processes accounts for 25–40% of the operating costs [7], while the aeration process accounts for 75% of the total energy required. In addition, it has been stated that the nitrification process consumes approximately the same amount of oxygen and energy for the decomposition of organic substances [8].

In our country, approximately 71% of MWW treatment plants are categorized as advanced biological treatment plants that require a significant amount of energy. This emphasizes the necessity for further investigation into alternative approaches that place a higher emphasis on energy and water recovery during operations [9]. Essentially, recovering organic matter and nutrients in wastewater is crucial to minimize energy consumption and preserve resources. Ultimately, in the transition from linear to circular cycles through energy-saving and resource recovery systems wastewater treatment plants should be transformed into water and resource recovery facilities by recovering resources (water, energy, and nutrients) and, at the same time, reducing operating costs [10].

The use of membrane technologies to effectively and safely reuse MWW has gained widespread acceptance as an effective strategy [11, 12]. In membrane processes, the type of membrane plays a significant role, just as much as the type of process or the design of the membrane. The use of ceramic membranes in the treatment of MWW has received considerable attention in recent years. These materials provide exceptional qualities, like high fluxes, mechanical and chemical stability, as well as ease of cleaning, which make them very ideal for this specific function [12, 13]. Ceramic membrane-based wastewater treatment processes have demonstrated encouraging outcomes in laboratory-scale investigations and have been reported to go further than the performance of polymeric membranes [14-16].

Regarding the process type or configuration, MBRs are being recognized as a viable option for treating and reusing MWW, specifically targeting the effective removal of contaminants [17]. Therefore, reliance on aerobic biological treatment for wastewater reuse systems, which uses considerable energy, is currently shifting to anaerobic treatment, which instead produces bioenergy and high-quality effluent [18]. AnMBRs have received particular interest for wastewater reuse, in which an anaerobic bioprocess is combined with a membrane separation process. Research on both laboratory and pilot scales has revealed that AnMBRs offer potential as an alternative to

conventional processes for treating MWW [19]. Compared to aerobic MBRs, the AnMBRs have a smaller footprint and can be operated at a shorter HRT. Importantly, the AnMBRs can produce bioenergy in the form of methane that can be reused in the system operation or as other forms of alternative energy sources [20, 21].

Although AnMBRs offer numerous benefits, the anaerobic treatment of MWW faces a barrier because of its low organic content. This can limit the effectiveness of removing COD and producing biogas. Research has shown that MWW frequently includes a limited amount of organic carbon, which makes it less suitable for anaerobic treatment [22, 23]. Therefore, a different process integration is required to facilitate further development and optimization of AnMBR technology for MWW treatment. Recent studies have focused on pre-concentration or up-concentration of MWW to help solve the problem of low COD content in MWW for anaerobic treatment [24-28]. With the recent decrease in membrane pricing and improvement in membrane performance, there has been a lot of interest in the DMF of wastewater concerning various driving forces (e.g., pressure, osmosis, thermal, and electrical driving forces) [29]. A DMF system's high water recovery rate and excellent permeate quality result from membrane separation's function efficiently rejecting nutrients and organics from wastewater.

Despite continuous developments in the field of AnMBR technology, the state-of-the-art of this technology is not yet appropriate for MWW treatment to reach reuse quality effluents and lower COD content, due to investment costs and high shear stress on the biomass. Moreover, AnMBRs still face a significant challenge in controlling membrane fouling. Biogas sparging is the most commonly used strategy to manage membrane fouling. This process involves recirculating the produced biogas into the reactor to enable scouring effects. However, the energy demands associated with gas sparging, which range between 0.6 and 1.6 kWh/m³, reduce the attractiveness of AnMBRs [30]. Compared to AnMBRs, the AnFMBR has several benefits. The AnFMBR integrates the advantages of anaerobic fluidized bed reactors with membrane systems, resulting in enhanced efficacy in the treatment of wastewater. AnFMBRs have proven to be highly effective in reducing COD to levels below 20 mg/L and TSS to levels below 1 mg/L during the treatment of MWW [31]. Moreover, AnFMBRs have exceptional proficiency in managing low-concentration wastewater, proving them feasible for a diverse array of wastewater treatment purposes [32]. Incorporating GAC

AnFMBRs effectively manages membrane fouling while minimizing energy consumption, hence improving their overall operating efficiency [33]. Furthermore, nutrient-rich effluent of AnFMBRs effectively concentrates nutrients for subsequent recovery for fertilizer production [34]. However, it will be still necessary to implement additional advanced treatments to gather the nutrients that remain in treated MWW.

As an advanced treatment technology, the implementation of membrane processes, including RO and NF, which possess remarkable rejection capabilities, enable its potential reuse for irrigation and potable water [35, 36]. Moreover, RO membranes have shown high efficiency in treating MWW, resulting in improved rejection of ammonium which is essential for further nutrient recovery process [37]. Nevertheless, apart from the purified effluent stream, the RO process generates a membrane concentrate that is a highly concentrated wastewater stream with the potential to include abundant nutrients, salts, microorganisms, and organic compounds. Consequently, membrane concentrate treatment plays a crucial role in membrane-based wastewater purification, considering both its environmental impact and resource efficiency [38].

Various techniques for recovering nutrients from wastewater have been suggested and evaluated in the literature, including chemical precipitation [39], electrodialysis [40], enhanced biological phosphorus removal [41], adsorption processes [42], and gas permeable membranes [43]. Struvite precipitation, which is one of the most widely used processes for nutrient recovery, has the capability of simultaneously recovering ammonium and orthophosphate [44]. With the addition of a proper Mg source, NH_4^+ and PO_4^{3-} can be precipitated as struvite ($\text{MgNH}_4\text{PO}_4 \cdot 6\text{H}_2\text{O}$).

Based on the information that has been provided, it is evident that wastewater should be seen as a valuable resource rather than just waste. Consequently, it is imperative to develop alternative integrated methods to accomplish this goal. Therefore, this study aims to develop a novel membrane-based treatment process that generates its energy and maximizes its circular beneficial effects by recovering the organic matter, nitrogen, phosphorus, and water present in wastewater. This approach can be an alternative to the commonly used advanced biological treatment plants for MWW treatment.

There is an increasing perception of the environmental concerns associated with conventional methods of wastewater treatment technologies.

Conventional MWW treatment processes need to be renovated by adopting new process applications focusing on resource circularity and energy-self-sufficient processes. In this study, the development of a new integrated treatment process has been investigated (DCMF-AnFCMBR-RO) that facilitates water and nutrient recovery and is energy-self-sufficient, serving as an alternative to conventional MWW treatment methods. In accordance with this overarching purpose, a set of specific objectives were defined as follows:

- ✓ Achieving water quality that satisfies the criteria for discharge by implementing the DCMF, in addition to using it as a pre-concentration process to produce concentrated wastewater with the aim of enhancing the energy potential of AnFCMBR process. Enhancing the filtration and rejection efficiency of the DCMF process through the incorporation of polyelectrolytes.
- ✓ Reaching a state of energy self-sufficiency in the treatment process, owing to the methane generated by the organic matter removal in AnFCMBR.
- ✓ High water and nutrient recovery rates using the RO process.
- ✓ Enhancing nutrient recovery from RO concentrates through struvite precipitation.

The objectives mentioned above have been addressed in 7 chapters and the chapters are structured as follows (Figure 1.1):

The first chapter describes the topic, summarizes the goals and motivations that prompted this research, and provides an outline of the thesis structure. Chapter 2 provides a thorough analysis of the current body of literature and research, with particular attention paid to highlighting the gaps in the literature. Chapter 3 deals with evaluating the performance of PAM assisted direct ceramic membrane filtration process for municipal wastewater treatment and OM recovery in the concentrated stream. The

DCMF process was tested in two stages: (i) optimization of flocculant concentration and dosing point and (ii) optimization of operational conditions to control membrane fouling. Chapter 4 critically evaluates the long-term operating of the CEPS+DCMF process with the aim of developing a sustainable and effective up-concentration process for further energy recovery processes. To determine the optimum conditions, the effects of flux, membrane cleaning procedures, and the number of membranes used in the reactors were investigated. Chapter 5 presents the impact of different HRTs on the removal efficiency, membrane fouling, and energy potential during the operation of AnFCMBR system. Chapter 5 also provides a comparison of two different types of AnFCMBRs. These reactors' performances were compared at the HRT values that maximized the performance.

Chapter 6 discusses the effects of various operating conditions on the RO process to enhance the nutrient recovery rate and improve the quality of effluent, to underline the environmental benefits of optimizing resource use and minimizing waste. The performance of the RO system was evaluated using a mixture of effluents collected from the AnFCMBR and CEPS+DCMF processes, with a mixing ratio of 80% to 20%, respectively. Following the determination of optimal operating conditions in the RO process, further investigations were performed on RO concentrate samples to recover nutrients through struvite precipitation. Chapter 7 concludes the thesis with a general discussion and summarizes the conclusions, along with directions for future research.

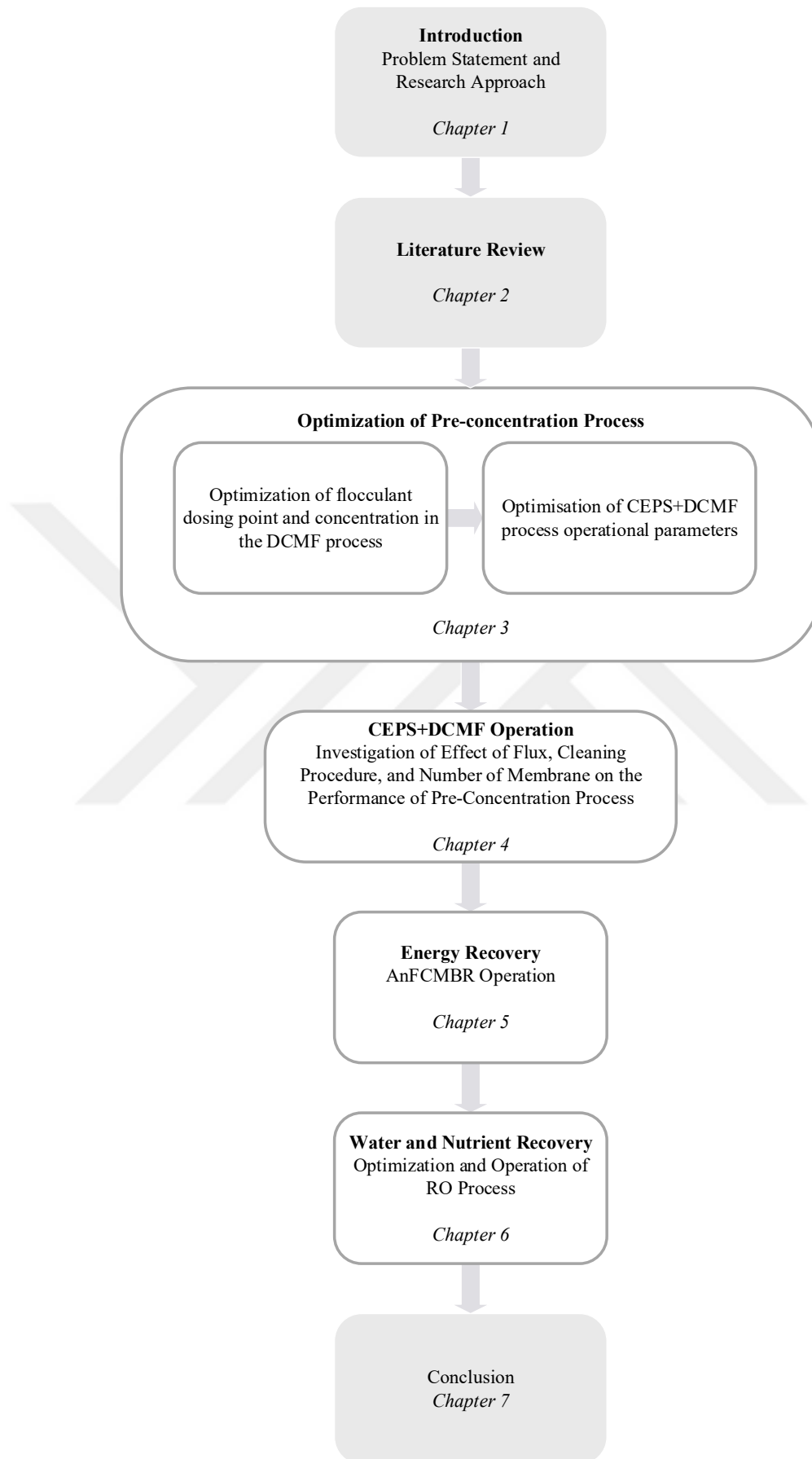


Figure 1.1 Schematic representation of the research approach and thesis framework

Chapter 2

Literature Review

2.1 Bibliometric analysis

Bibliometric analysis is a statistical method that could quantitatively analyze the research papers concerned with one special topic via mathematical ways. It could also assess the quality of the studies, analyze the key areas of research, and predict the direction of future studies [45]. Therefore, in order to review the research on sustainable MWW treatment from a bibliometric perspective, this study aims to identify the current advancements in this field and specifically analyze the trends and other significant indicators by surveying articles published on Scopus. The global literature about “MWW treatment” published between 2019 to 2024 was scanned in the Scopus collection database. The search terms applied to identify the closest matching publication included “MWW treatment” and “sustainable MWW treatment” which were used as the keywords in the titles, abstracts, and keywords of publications.

The information for the documents that meet the requirements contained year of publication, language, journal, title, author, affiliation, keywords, document type, abstract, and counts of citations which were exported into CSV format. The date of the retrieval was 23rd Feb 2024. VOSviewer (version 1.6.20, Leiden University) was used to analyze the co-occurrence. Two standard weight attributes are applied which are defined as “links attribute” and “total link strength attribute” [46].

The use of VOSviewer software provides a graphical analysis of bibliometric data and visualization of research results. All keywords that assisted with the full counting

method have been considered as an element of the analysis while conducting co-occurrence mapping. To obtain a more accurate result, the study set some constraints in the analysis. The number of keywords to be used can be adjusted by removing less relevant keywords. A minimum of five occurrences of a keyword was applied as a limiting factor. A VOSviewer thesaurus file can be used to indicate that different names refer to the same researcher, to merge terms, synonyms, and abbreviated terms with full terms, to correct spelling differences, and well ignore terms [47]. Thesaurus files have also been used to perform data cleaning in the study. A cluster of co-occurring keywords was generated by analyzing the Scopus data using VOSviewer. The final analysis incorporated keywords that were provided by the researchers in the Scopus database and were shown to be present in more than five occurrences within the same paper.

The Scopus database identified a total of 6,797 publications including 5,444 original research articles on the topic of “MWW treatment” which were identified in the Scopus database between 2019 and 2024. The shown Figure 2.1 illustrates the results of the analysis, whereby a minimum threshold of 683 keywords was adopted. Each term in the network is represented by a circle, with the scale of the circle directly proportional to the number of papers containing the term. Each color corresponds to a cluster of terms, with the length of curved lines indicating the frequency of term recurrence and the thickness representing the strength of connections between topic areas or keywords. The clusters demonstrate the correlation between different topics.

treatment”. Based on the information presented in Figure 2.2, we can draw the following conclusions: (i) Circular economy has received significant attention in research across different sustainability frameworks; (ii) Resource recovery is closely linked to sustainable wastewater treatment technologies; (iii) Special attention should be given to anaerobic digestion, life cycle assessment, and energy recovery.

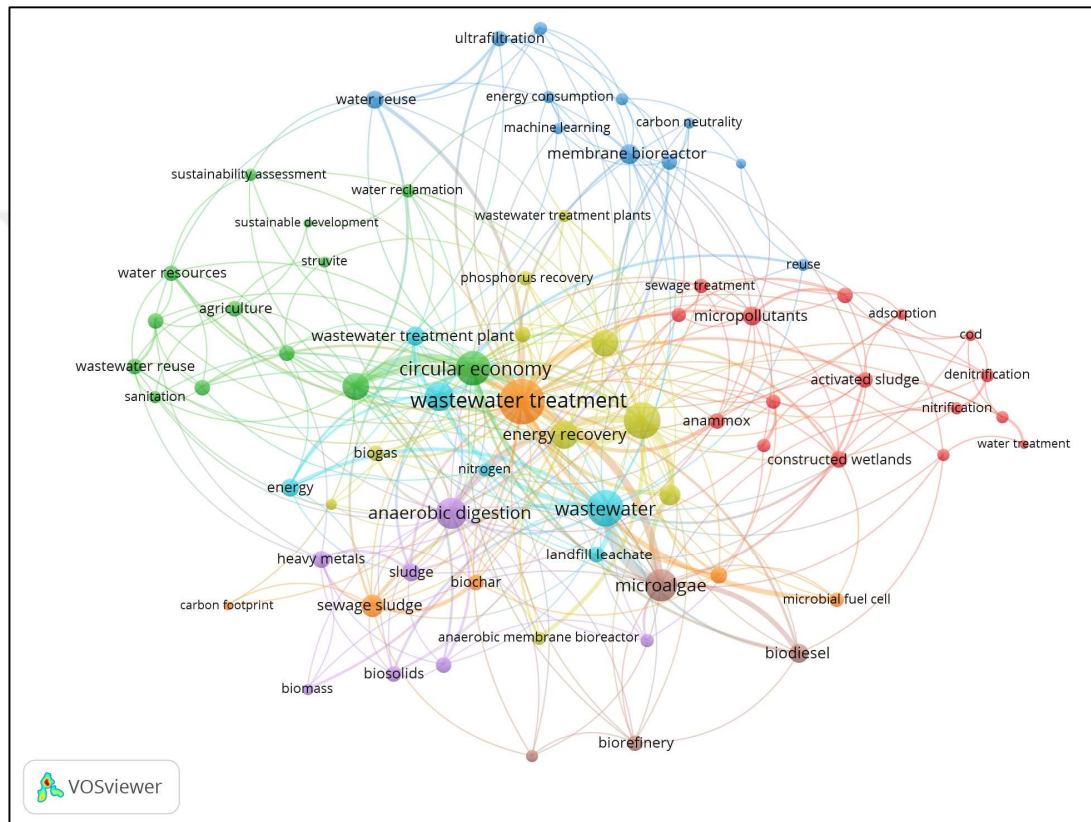


Figure 2.2 The co-occurrence network visualization of “sustainable MWW treatment”

Keywords that have occurrence scores above 10 are presented in Appendix, Table S1.2. Based on the results, it can be observed that the circular economy keyword shows the highest occurrence, with a score of 31 occurrences, following non-specific keywords that are similar to the search term "wastewater treatment, MWW, and wastewater". In recent years, there has been a growing acceptance of the concept that wastewater should be converted into several different types of valuable substances, consequently providing significant economic impact and value. Regardless, the main driver of this approach is the concept that recovering materials or reusing wastewater will effectively mitigate the pressure on natural resources [49].

The findings of the bibliometric analysis indicate that the approach used in this study aligns with the current global research trends and current research hotspots in the field of sustainable MWW treatment. Anaerobic digestion was found to be the fifth and ninth most significant keywords in both the general analysis of “MWW treatment” and the specific analysis of “sustainable MWW treatment”. Anaerobic wastewater treatment has been widely accepted as a reliable and advantageous approach in terms of both energy and environmental considerations [50].

2.2 Conventional wastewater treatment to resource recovery

Adequate water quality is crucial for the overall physical and mental wellness of beings. The quality of water is crucial not only for the survival of humans, animals, the ecosystem, and the agricultural sector but also for advancement in society and the economy. On a global scale, more than 80% of MWW is discharged into aquatic bodies without sufficient treatment [51].

MWW contains a great variety of pollutants, such as nutrients, oil and grease, detergents, biowastes, household chemicals, heavy metals, bathing and kitchen waste, salts, pathogens, medicinal constituents, and soluble and particulate organic matter [52]. The pollutants contribute to increasing levels of COD in water along with altering the pH, hardness, inorganic constituents, and pathogen load of the water. Untreated MWW is a threat to aquatic and marine animals, affects the yield of crops, and is the cause of several waterborne and water-related diseases. Such water-related diseases remain widespread across the country because almost less than 5% of wastewater emanating from urban settings and municipal use undergo pre-treatment before releasing to the environment [53]. When sources of water like rivers, lakes, ponds, and other sources become contaminated with oxygen-demanding wastes and pathogens, the water becomes unfit for human consumption unless disinfected. Safely managed wastewater is an affordable and sustainable source of water and energy.

The assessment of wastewater characteristics plays a crucial role in the design and operation of wastewater treatment facilities. This is because different types of

wastewaters require specific treatment methods to effectively eliminate or reduce their levels in the wastewater before its discharge or reuse. Table 2.1 presents an overview of the characteristic attributes commonly observed in MWW. The proper management of MWW is of crucial significance to mitigate potential health hazards and reduce environmental pollution [54]. Nutrients, specifically, present a substantial concern since they play a role in the main cause of eutrophication, a phenomenon that can have serious impacts on aquatic environments [55]. Therefore, it is crucial to remove them from MWW. According to the data presented in Table 2.1, the concentrations of phosphorus vary between 4 and 15 mg/L, whereas the concentrations of ammonia nitrogen range from 12 to 50 mg/L. The main determinant of the treatment process is the effluent quality criteria that are required by regulatory requirements. As an example, the European Water Framework Directive sets a maximum permissible concentration of nitrogen in effluent at 1 mg/L (for populations between 10,000 and 100,000) and phosphorus at 2 mg/L (for populations above 100,000) [56].

Table 2.1 Typical MWW composition [57]

Pollutant	Concentration (mg/L)		
	Low strength	Medium strength	High strength
Total solids	350	720	1200
TSS	100	220	350
TDS	250	500	850
Ammonia nitrogen	12	25	50
TN	20	40	85
Phosphorus	4	8	15
COD	250	500	1000
Sulphate	20	30	50
Chlorides	30	50	100

The conventional approach to treating MWW involves a first treatment phase, which is then followed by a secondary treatment phase. This secondary treatment phase often utilizes biological processes to remove organic contaminants and ensure compliance with discharge regulations. [58]. Presently, CAS stands as the prevailing wastewater treatment technology owing to its capacity to effectively manage significant and considerably fluctuating quantities of diluted wastewater while maintaining an acceptable HRT. CAS is widely regarded as a dissipative treatment method, as it involves the metabolism of organic chemicals by suspended bacteria or their conversion to CO₂ through aerobic processes, which need a significant amount of energy [59].

These conventional treatment processes generate significant amounts of sludge, which can be a challenge to manage [60]. Additionally, the removal of nutrients like nitrogen and phosphorus using conventional MWW treatment systems can be costly [61]. The use of potable water for waste conveyance and the incomplete removal of contaminants are recognized drawbacks of conventional MWW systems [62]. Municipal WWTPs are known sources of organic micropollutant discharges into the environment [63]. The effluent quality of these treatment plants plays a crucial role in selecting appropriate treatment technologies and influencing the ecology of receiving water bodies [64]. Furthermore, municipal sewage treatment plants primarily rely on biological processes designed to remove conventional contaminants like BOD and SS [65].

However, municipal WWTPs play a crucial role in transitioning towards a circular economy by focusing on resource recovery. The concept of circular economy emphasizes the creation of self-sustaining production systems where materials are reused continuously [66]. In the context of WWTPs, this involves shifting from a linear to a circular economy operation, facilitating resource recovery and more sustainable waste management [67]. WWTPs are increasingly being viewed as water resource recovery facilities, highlighting the shift towards considering wastewater as a source of resources rather than just contaminants [68].

The current treatment methods have limitations in effectively extracting the valuable materials included in wastewater. In recent literature, there has been a notable change in viewpoint, commonly referred to as 'zero-liquid discharge' [69] and 'integrated resource recovery' [70]. This transition represents a departure from the conventional removal of impurities towards the proactive recovery of valuable resources. A key benefit of this methodology is in its capacity for WWTPs to produce their sustainable energy, while also providing supplementary motivations for enhanced water treatment via more effective nutrient control. Although the existing technology facilitates the purification of wastewater to an acceptable level, so permitting its utilization as a viable water source for both potable and non-potable applications, the techniques for extracting energy and nutrients from wastewater are not as well developed.

The economic feasibility of energy and nutrient recovery practices continues to be the fundamental obstacle to their wide implementation. The data presented in Figure 2.3 illustrates that wastewater generally has solids with a concentration of less than 0.5%. These solids mostly consist of energy in the form of organic carbon, as well as ammonia and phosphorus. Considering the significantly small quantities, the economic feasibility of recovering these components in their diluted state is questionable. As a result, conventional methods of wastewater treatment have mostly concentrated on removing or reducing the amount of these constituents from wastewater to comply with effluent quality regulations or enable the reuse of water.

Furthermore, the studies on the economic value of wastewater resources have revealed that the non-water components (nutrients, energy, and metals) are anticipated to constitute 55% of the overall value, assuming full recovery [71]. Therefore, investors are confronted with acceptance, given that the precise capital and operational costs remain uncertain, and the economic advantages might not become clear for several years.

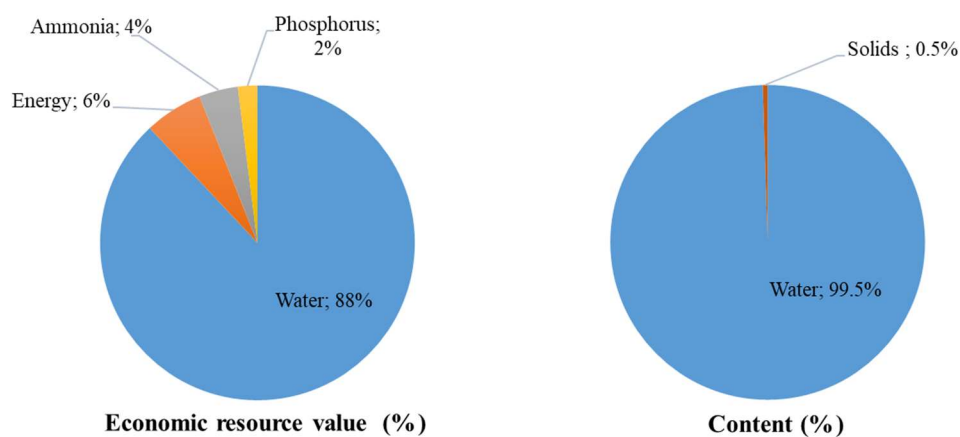


Figure 2.3 The evaluation of resource composition and its associated economic value in the context of MWW [72]

The direct benefits for both humans and the environment of conserving freshwater and decreasing the consumption of non-renewable resources are indisputable. Several factors can operate as accelerators for the transition toward resource recovery, exerting a substantial impact on decisions on the management of wastewater. Although water recovery from wastewater gets higher treatment costs in comparison to conventional water sources, the benefits of avoiding pollution far surpass the financial commitment.

As a result, the process of water recovery has become a crucial aspect of contemporary WWTPs. Furthermore, a similar situation can be expected in terms of the recovery of nutrients and energy. The reason for this forecast is the increased restrictions on effluent, which has led to a higher consumption of energy and an increased demand for renewable energy and alternating sources of phosphorus.

2.3 Water, energy, and nutrient recovery from municipal wastewater

In response to the growing water demands, suppliers are continuously exploring the most economically viable strategies to augment their water resources [73]. In earlier periods, the process of transporting surface water over longer distances or drilling deeper wells into freshwater aquifers was commonly employed [74]. However, the advent of climate change has introduced significant unpredictability to these evaluations of costs and benefits. Consequently, there has been a growing interest in alternate methods, particularly the reuse of MWW, due to their ability to withstand drought conditions [75].

Considering the projected growth in urban population in the foreseeable future, there is going to be a corresponding rise in the requirement for water resources in urban areas, primarily due to the leading quantities of wastewater. According to Qadir et al. [76], the global production of wastewater is projected to reach 470 billion m³ by 2030, representing a rise of 24% compared to the current amount. Furthermore, by 2050, it is likely to reach 574 billion m³, representing a 51% increase compared to the current level (Figure 2.4). These scenarios indicate that there will be an increasing amount of wastewater in the future, which presents a chance to deal with water scarcity in arid regions by collecting, treating, and utilizing wastewater for agricultural, aquacultural, agroforestry/landscaping, aquifer resupply, industrial, and direct or indirect drinking purposes.

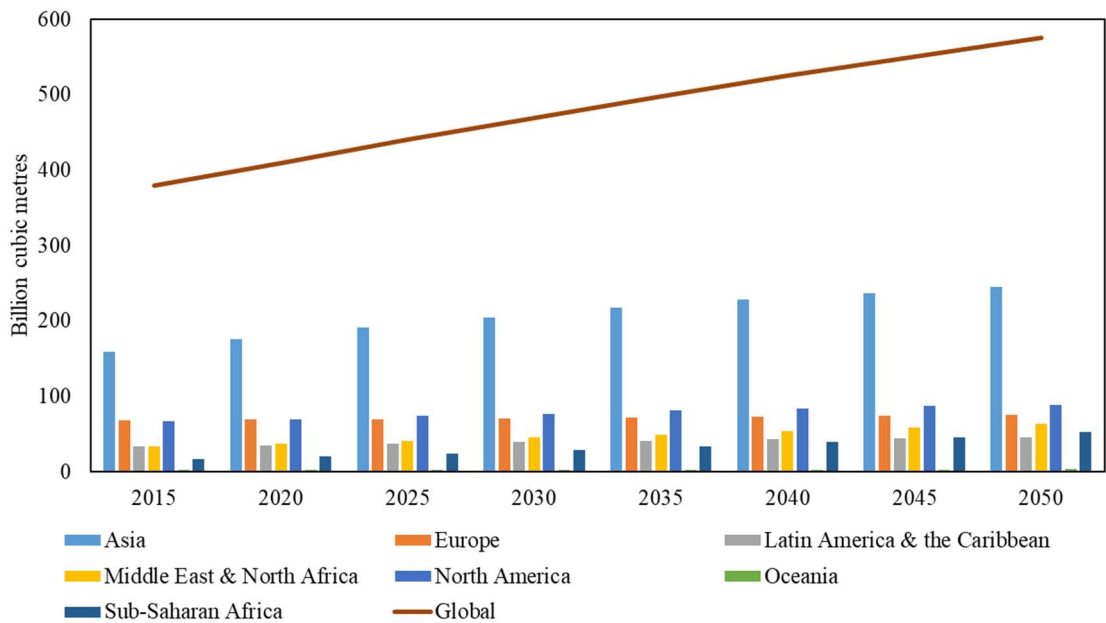


Figure 2.4 MWW production across regions in 2015 and predicted until 2050 [76]

With wastewater volumes increasing, there is huge potential for fit-for-purpose treatment and use as an unconventional water source for both potable and non-potable applications (Figure 2.5) [77, 78]. Depending on the treatment and quality standards required by regulation, wastewater can be recovered and safely used for drinking water, industrial applications, such as cooling power plants, manufacturing, such as textile production, irrigation of agriculture and/or municipal parks, recreational use, replenishing aquifers, returning in a good state to waterbodies to maintain environmental flows.

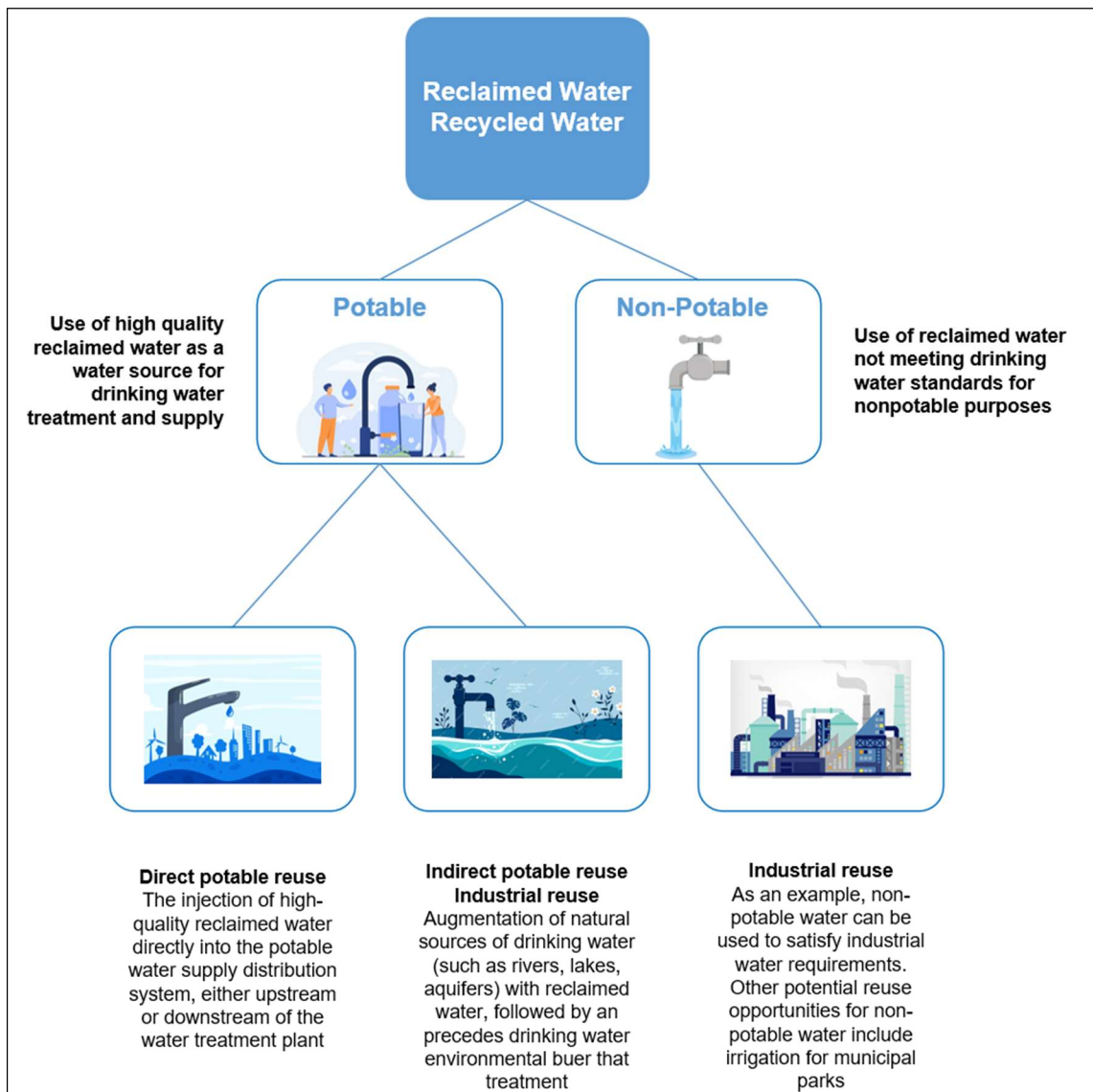


Figure 2.5 Concepts and illustrations for wastewater and reuse [79]

Furthermore, by 2030, the demand is anticipated to surpass the supply by 160 % [80]. Simultaneously, the amount of wastewater is rising. For context, the expected annual production of wastewater (more than 360 billion m³) is more than ten times greater than the world's desalination capacity (34.6 billion m³ in 2019), according to Jones et al. [81]. The potential of wastewater is not being fully utilized, even though there is a prediction that the intended reuse of treated municipal water will increase by 271% from about 7 billion m³.

Apart from the advantages associated with treated wastewater reuse, the process of distributing reusable water has impacts on the environment as it requires energy and infrastructure. [82]. However, urban regions typically meet their water requirements by

distributing water sourced from rural areas, which increases the environmental impact of water supply [83]. At this point, decision-makers should assess its distribution using region-specific criteria, considering its environmental impacts.

In conventional wastewater treatment, energy consumption is another essential issue. However, most WWTPs that are operational today are designed and built without considering energy demand, possibly because energy prices are not a major concern [84]. However, according to The International Energy Outlook 2016, the projected increase in global energy demand from 2012 to 2040 is estimated to be around 48%, with fossil fuels predicted to account for nearly 80% of this demand [85]. As a result, emissions related to fossil fuels are expected to rise by a comparable quantity. The need to significantly reduce the energy intensity of WWTPs is driven by these estimates. This can be achieved by developing treatment processes that prioritize energy efficiency and recovery.

CAS-based biological treatment systems have come under closer examination due to their comparatively high energy requirements, which typically range from 0.3 to 0.6 kWh/m³ [9]. These requirements are influenced by factors such as process setup, COD, and ammonium concentrations. Undoubtedly, energy consumption specifically associated with aeration might potentially make up to 50% of the overall energy needed in wastewater treatment plants [86]. As a result, a significant quantity of energy is used in order to promote the biological oxidation of organic and nitrogenous substances [87, 88]. Furthermore, it is crucial to recognize that the energy consumption for MWW treatment may increase even more if processes are enhanced to include advanced treatment methods in order to comply with strict effluent discharge criteria that are common in many nations [89, 90].

Wastewater treatment plants can produce the energy needed to treat wastewater and contribute to the energy needs of cities and municipalities that generate waste streams. As the volume of wastewater increases over time, the energy embedded in wastewater in 2030 would be enough to fulfil the energy needs of 196 million households, increasing to 239 million households by 2050. According to Verstraete et al. [91], utilizing the anaerobic conversion of organic carbon found in wastewater to produce methane, assuming that all the energy from the wastewater can be recovered, it is estimated that 380 billion m³ of wastewater can yield

53.2 billion m³ of methane, which has a caloric value of 1,908 billion MJ. There is enough energy in wastewater—1,908 billion MJ—to power 158 million homes, based on the average electricity use of 3,350 kWh per household [92]. These forecasts are derived from the highest achievable levels of energy recovery, without taking into account any technical or economic constraints in the energy recovery procedures from wastewater or current energy coverage networks. However, certainly, there is an urgent requirement for increased focus on the advancement of energy-efficient methods for the recovery of MWW.

The population growth will lead to a rise in water demand, wastewater production, and energy consumption for wastewater treatment, as well as an increase in the demand for agricultural production. The agricultural industries rely heavily on phosphorus and nitrogen. The current extraction of phosphorus, which is one of the most important resources in society, comes from non-renewable phosphate reserves and is therefore not sustainable [93-95]. If there is not a significant shift in the way that phosphorus is handled as a resource, it is possible that phosphate sources that can be obtained at reasonable prices will be depleted in the not-too-distant future [96, 97]. The increasing demand for sustainable nutrient management and pollution control has prompted the advancement of innovative technologies aimed at recovering nutrients from wastewater. However, a significant portion of the methods that are in use currently require a significant amount of chemical use in addition to an extensive use of energy in order to accomplish significant nutrient recovery [98]

Nitrogen is found in various forms in nature, including NH₄⁺, N₂, organic nitrogen molecules (such as amino acids and nucleic acids), and nitrogen oxides (NO₃⁻, NO₂⁻, NO, and N₂O). Despite the abundance of N₂ in the atmosphere, only a limited number of organisms in terrestrial and marine habitats have the ability to exploit this inert molecular nitrogen. Nitrogen-fixing prokaryotes, such as Azotobacter, Klebsiella, and Rhizobium, transform inert atmospheric N₂ into active ammonium molecules by the process of biological nitrogen fixation [99]. Figure 2.5 illustrates the primary chemical and biological processes that impact the global nitrogen cycle.

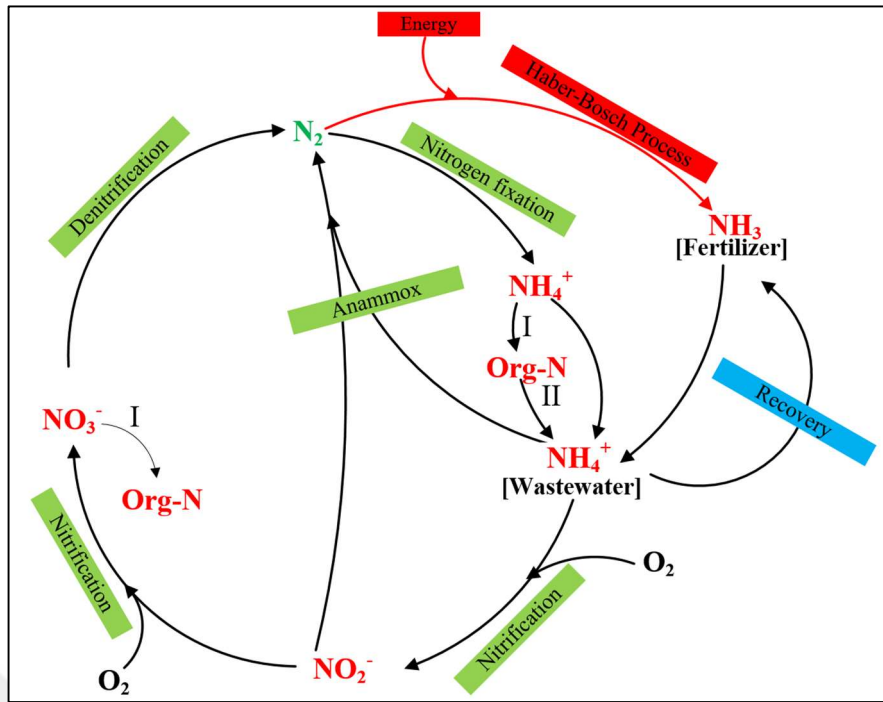


Figure 2.6 Illustration of the nitrogen cycle, depicting both natural and anthropogenic transformations [100]

The primary contributors to nitrogen pollution in aquatic ecosystems, from an environmental perspective, are the discharge of unutilized ammonium nitrogen due to the application of organic and inorganic nitrogen fertilizers in agricultural practices, as well as the release of nitrogen from domestic wastewater [101-103]. Furthermore, nitrogen-rich wastes include urea, leachate from landfills, and the liquid phase produced during the dewatering process of anaerobic digester sludge [104, 105]. WWTPs commonly employ nitrification and denitrification procedures to transform reactive ammonium nitrogen into inert nitrogen gas. Nevertheless, the process of nitrification necessitates aeration, while denitrification requires an electron donor. The process of nitrification-denitrification significantly amplifies the energy demand and treatment expenses, which is why nitrogen removal is affected [8]. Furthermore, the effectiveness of biological treatment techniques in removing nutrients relies on the careful tuning of various parameters, including SRT, HRT, pH, and alkalinity [106].

Phosphorus, similar to nitrogen, is a vital element for living creatures, but it also serves as a significant pollutant for aquatic habitats. The vital form of phosphorus for living organisms is phosphate. Phosphate is a constituent of nucleic acids, phospholipids, and ATP/ADP and is required for the proliferation of live cells. Figure

2.2 illustrates the movement of phosphorus from phosphate mines to water bodies in the global phosphorus cycle. Phosphorus can be removed from wastewater utilizing precipitation, adsorption, and/or biological processes. Cell creation requires minute quantities of phosphorus in biological processes. Hence, the effective removal of phosphorus from wastewater mostly necessitates enhancing biological treatment methods and implementing chemical treatment. Furthermore, the removal of phosphate through precipitation and adsorption necessitates adherence to specific operational conditions, including maintaining suitable pH levels and ensuring the presence of ions such as iron or calcium at the proper concentration within the surrounding environment [106].

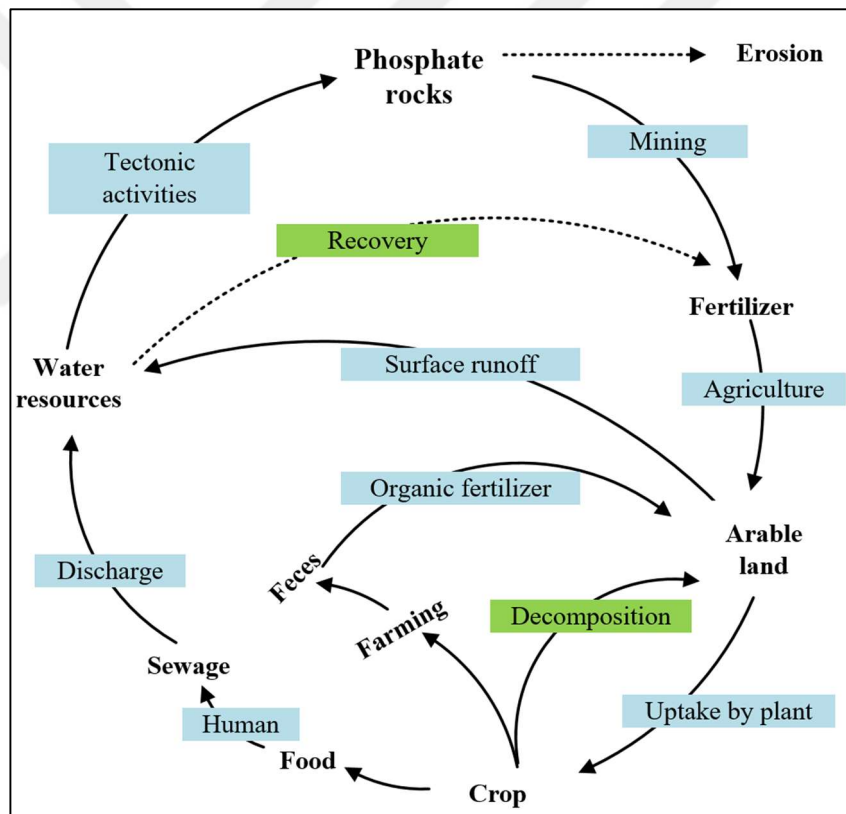


Figure 2.7 Schematic representation of the phosphorus cycle [107]

Nitrogen and phosphorus are predominantly utilized in fertilizers to enhance soil fertility and achieve greater yields from cultivable areas, which is progressively diminishing due to modern agricultural practices [108]. Due to the growing worldwide population, there is a rising demand for chemical fertilizers each year in order to

guarantee food security. Indeed, nitrogen is a renewable resource. Nevertheless, a select few organisms have the capability to directly utilize molecular nitrogen, which is abundant in the atmosphere. Consequently, fertilizer nitrogen is derived by transforming atmospheric nitrogen into ammonium nitrogen via the energy-intensive Haber-Bosch process. Phosphorus is scarce in nature, unlike nitrogen, and is mostly present in phosphate rocks as P_2O_5 . The global production of phosphorus for commercial purposes is projected to reach its maximum level by the year 2033. Furthermore, the reserves of phosphorus are expected to be completely exhausted within a timeframe of 50 to 100 years [109]. Hence, it is imperative to assess sustainable alternative nutrient sources.

According to the calculations made by Qadir et al. [76], 16.6 million tonnes of nitrogen, 3 million tonnes of phosphorus, and 6.3 million tonnes of potassium are present in the total volume of municipal wastewater that is generated each year. Depending on the level of treatment and the specific nutrient recovery procedure used, it is possible to extract anywhere from 10 to 80 percent of nitrogen and 33 to 96 percent of phosphorus from wastewater streams [110].

On a global scale, the substitution of industrial fertilizer with nutrients generated from wastewater is still occurring at a relatively low rate. Kok et al. [111] determined that, at its highest capacity, the recovery of phosphorus from urban wastewater alone could satisfy nearly 20% of the world's agricultural phosphorus requirement, which amounts to around 19.1 million tons per year. Despite recent improvements in nutrient recovery from wastewater streams, the existing nutrient recovery methods have not achieved complete efficiency levels of 100% [112, 113].

In our country, according to the data of the Ministry of Agriculture and Forestry, 1,241,209 tons of N-P-K equivalent fertilizer were produced in 2023, while 2,390,417 tons were consumed [114]. In 2023, 87,194 tons of P equivalent to the total P_2O_5 consumption is imported. Based on the 2022 wastewater data, approximately 4.6 billion m^3 out of the total 5.4 billion m^3 of wastewater released from the sewage network underwent treatment in wastewater treatment plants [115]. Assuming an average P content of 11 mg/L [116], there is a possibility of recovering 50,948 tons of P. The significance of recovering phosphorus from wastewater in reducing Turkey's dependency on imported phosphorus-based fertilizers is noticeable.

2.4 Technologies water, energy, and nutrient recovery from municipal wastewater

Approximately 99% by weight of the substances present in MWW is water [117]. Therefore, recycling and utilizing this water could be a more environmentally friendly choice compared to methods such as desalination or transferring freshwater across great distances [118]. Moreover, the primary motivation behind the recovery and reuse of residential wastewater is the scarcity of water resulting from the unequal distribution of fresh water worldwide and the water stress produced by climate change [119]. Secondary wastewater treatment processes incompletely remove BOD and only achieve a 95% reduction in TSS from discharges. These discharges still contain amounts of organic micropollutants, including pharmaceuticals, polychlorinated biphenyls, and pesticides. In order to comply with the stringent regulatory requirements regarding the levels of microorganisms and micropollutants in reclaimed water, it is necessary to commit the discharge from secondary wastewater treatment operations to additional processing on advanced treatment systems [120]. Figure 2.7 illustrates the categorization of treatment systems into filtration, disinfection, and advanced oxidation processes. The use of gray shading indicates the widespread implementation of techniques in municipal WWTPs, whilst the unshaded boxes represent technologies that are less frequently utilized.

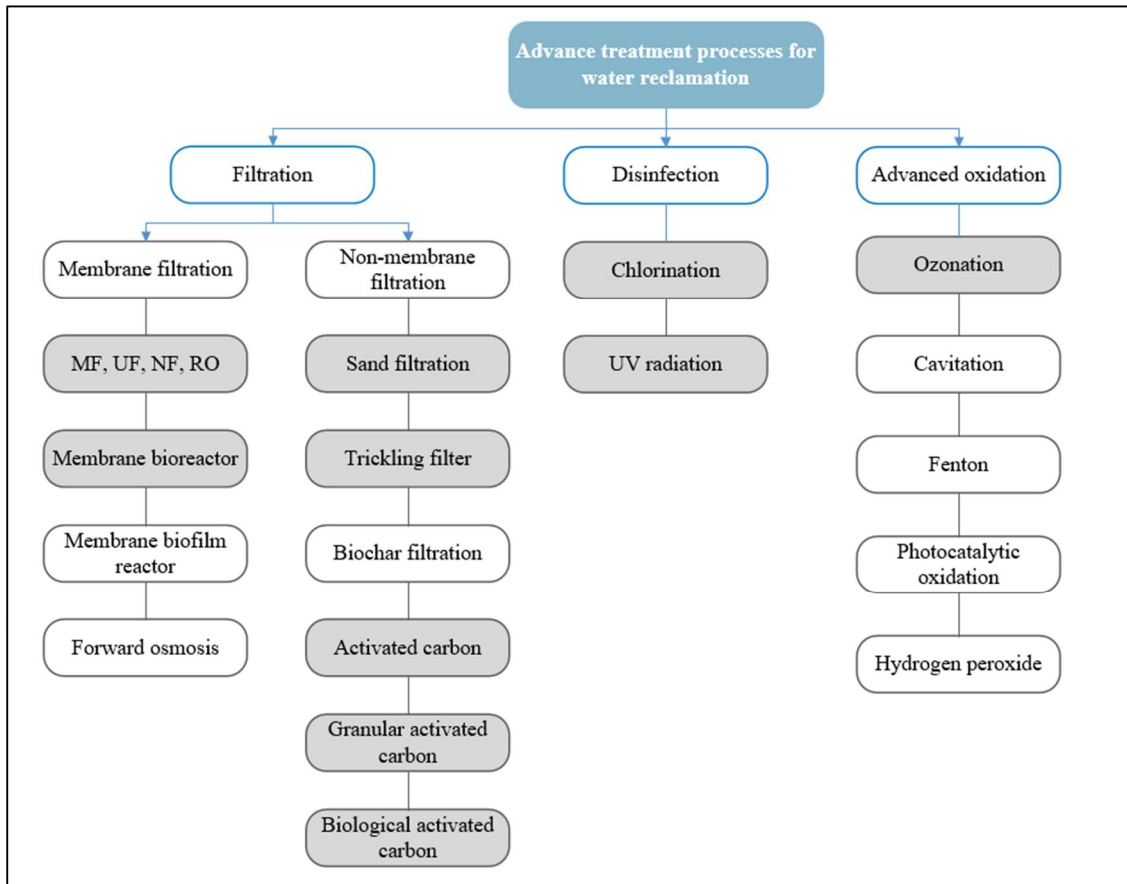


Figure 2.8 Different technologies are employed for reclaiming water from municipal WWTPs. [121]

The recovery of organic matter as a source of energy remains another significant concern, similar to the recovery of water from MWW. Although it may not be possible to fully recover all the energy from wastewater due to inherent losses in the conversion process, it is becoming more and more possible to create WWTPs that are energy-neutral or even produce more energy than they consume [122]. According to Shen et.al [123], a minimum of 12 plants in Europe and the USA have achieved energy self-sufficiency levels exceeding 90%. The Powerstep European research project is currently creating plans for WWTPs that are capable of producing as much energy as they consume, or even more, in six different real-life scenarios [124]. The process of capturing methane to generate electricity usually compensates for 25-50% of the energy needs of a wastewater treatment plant, assuming that traditional treatment methods are used [9]. In addition, combining the recovery of thermal energy from effluent with the recovery of chemical energy can result in achieving carbon neutrality or even better results [125]. Nevertheless, the water industry's significant focus on energy

sustainability has received criticism for potentially shifting attention away from optimizing the hydrological cycle in favor of energy and climate considerations [126].

As shown in Figure 2.8, it is feasible to extract fuels from wastewater using varying methods. The chemical energy content found in typical MWW is around 17.8 kJ per gram of COD [127]. This quantity surpasses the amount of electrical energy needed to operate the CAS process by approximately fivefold. However, in the CAS process, a significant amount of the energy stored in the COD is released as heat during microbial metabolism. As a result, the current configuration of the CAS process falls short of achieving energy self-sufficiency, generally ranging from 30% to 50%, depending on the country's issue at hand [128].

Anaerobic digestion plays a significant role in energy recovery from MWW, offering a sustainable and efficient method for treating organic matter while generating valuable biogas for energy production [129].

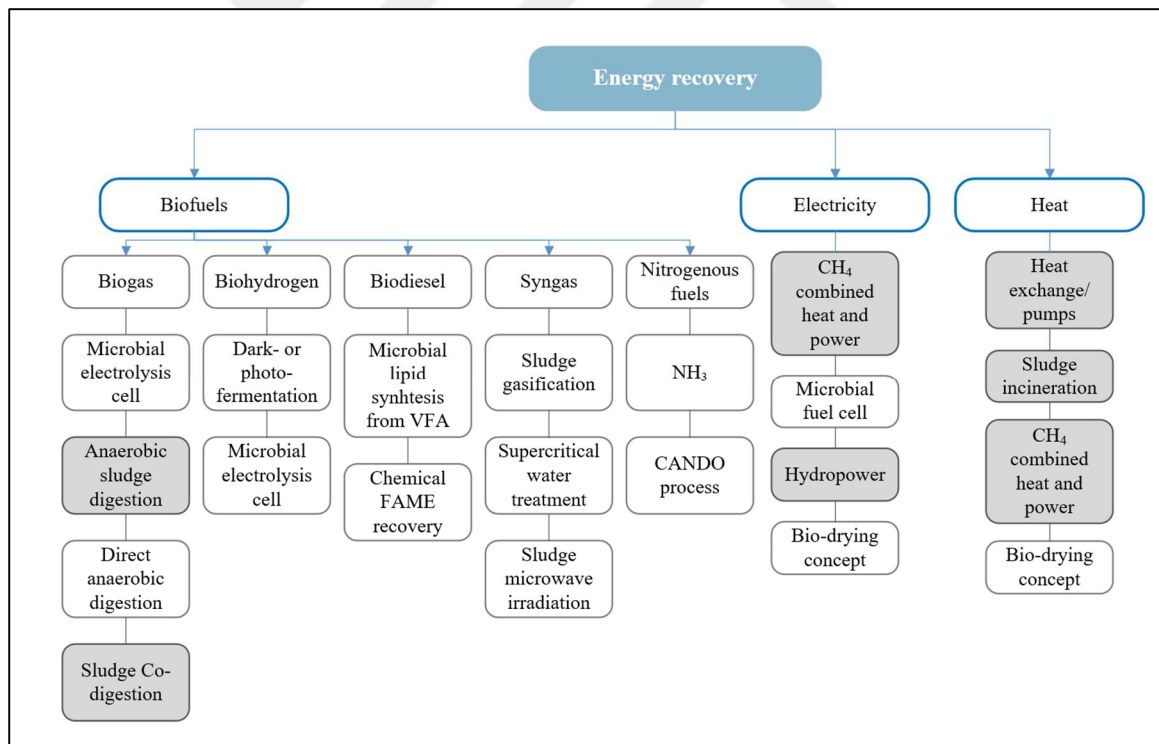


Figure 2.9 Methods that can be used to recover energy from municipal WWTPs [121]

The nutrient recovery approaches transform wastewater into a valuable resource, in addition to recovering energy and water, rather than treating it as just waste. The

primary objective of nutrient recovery from wastewater is to render the ammonium and phosphorus present in the wastewater suitable for agricultural purposes. Simultaneously, it permits the conservation of energy that is often consumed during the process of converting ammonium to molecular nitrogen by nitrogen recovery [130]. The recovery of ammonium nitrogen, typically present in wastewater, is achieved using methods such as adsorption, ammonium stripping, struvite precipitation, and membrane processes [131].

Extensive research has been conducted on nutrient-recovery methods, resulting in the development of several solutions (Figure 2.10). The effectiveness of recovering nutrients tends to decline as concentrations in the wastewater stream decline, consequently, a three-step sequential mechanism has been suggested:

- I. Accumulation of nutrients through biological, chemical, or physical processes.
- II. Nutrient extraction through biological, chemical, or thermal processes.
- III. Extraction and recovery of nutrients in the form of highly concentrated fertilizer, using chemical or physical processes.

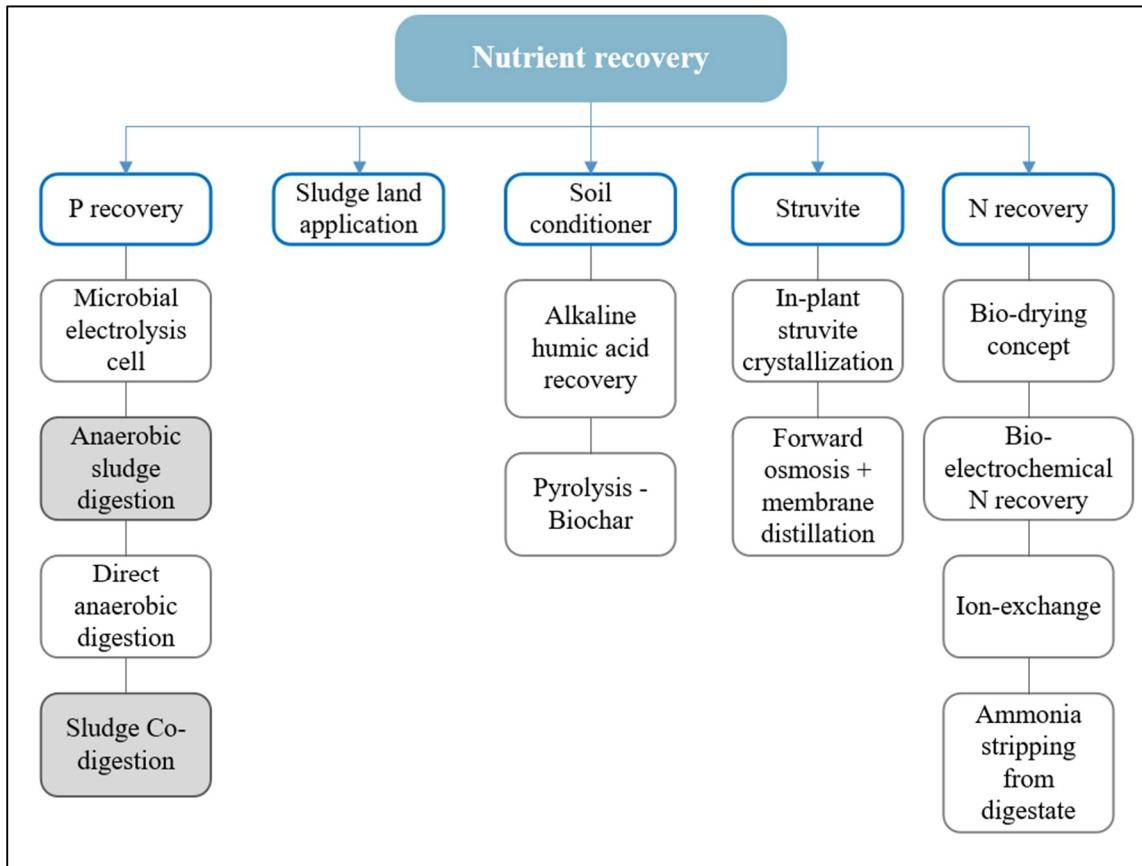


Figure 2.10 Examples of technology for extracting nutrients from municipal WWTPs. The use of grey shading represents methods that have been implemented extensively in municipal WWTPs. Methods that do not have widespread application are indicated by not-shaded boxes. [121]

The following Sections between 2.4.1 and 2.4.8 provide comprehensive knowledge on resource recovery processes, the challenges for these processes, and mitigation strategies for overcoming challenges.

2.4.1 Membrane filtration applications

Membrane processes are reliable and essential technologies for improved wastewater treatment and reuse methodologies. Their advantages involve reduced area requirements, acting as a physical barrier for particulate matter, and effectively preventing microorganisms without causing resistance or generating by-products. Membranes are integral components of various prominent large-scale advanced treatment systems employed globally for artificial groundwater recharging, indirect potable reuse, or industrial process-water supply.

Generally, three approaches are common in the reuse of domestic wastewater through membrane processes: (i) direct treatment of raw wastewater using integrated processes (ii) the integration of various processes with membrane processes following primary treatment, and (iii) the implementation of membrane processes as an advanced wastewater treatment process following secondary treatment. Table 2.2 provides a comprehensive overview of the research conducted on the utilization of various membrane processes for the purpose of generating reusable water from untreated, primarily treated, or secondarily treated wastewater.

UF membranes effectively remove colloids, organic matter, proteins, polysaccharides, most kinds of bacteria, and even certain viruses, resulting in the production of higher-quality treated effluents [132]. Membrane techniques such as NF and RO are effective in separating ions and dissolved particles from water due to their advantage of having smaller pore sizes [133].

MBRs are a combination of the activated sludge process with microporous membranes used for separating solids from liquids. They are commonly used on a pilot or real scale for treating MWW [134-137]. MBRs have several beneficial properties, including the ability to independently manage sludge and HRT, as well as the capability to maintain a higher level of mixed liquor-suspended solids. These advantages enable the use of smaller areas. However, MBRs also have some drawbacks when compared to the CAS treatment. These include increased process degree of complexity, sludge that is more difficult to remove water from, and a higher susceptibility to shock loading. Furthermore, MBRs are linked to increased expenses for equipment and operations, mostly due to the need for membrane cleaning and, in cases of high loading rates, greater aeration demands [138].

Table 2.2 Membrane processes for MWW reuse applications

Process (scale)	Feed Wastewater	Operating Conditions	Feed Characteristics	Permeate Quality/Removal Rate	Application for Reuse	References
UF (pilot scale)	Secondary effluent of WWTP	TMP: 0.1–0.7 bar UF: 0.03 µm	TSS: 96–165 mg/L COD: 167–307 mg/L PO ₄ -P: 1.0–3.9 mg/L NH ₄ -N: 3.0–33 mg/L	TSS: 3–9 mg/L COD: 42–103 mg/L PO ₄ -P: 0.8–3.4 mg/L NH ₄ -N: 4.0–33 mg/L	Crops irrigation	[139]
Prefilter +UF (pilot scale)	Secondary effluent of WWTP	UF: 0.01 µm Cross flow Inlet flow: 10 m ³ /h TMP: 0.3–1.2 bar	pH: 6.3–7.5 EC: 1584–1950 µS/cm TSS: 1–8 mg/L COD: 26–69 mg/L	Turbidity: < 0.2 NTU TSS: < 0.2 mg/L COD: 20–60 mg/L	Agricultural irrigation	[140]
Prefilters +UF (pilot scale)	Synthetic secondary sewage effluent	UF: 1 kDa (tubular); 25 kDa (spiral wound) UF modes: cross-flow TMP: 1.0–3.3 bar Flow velocity: 0.2 m/s	COD: 18.5–67 mg/L Turbidity: 9.43–46.4 NTU TSS: 13–30 mg/L Color: 41–81 EC: 320–366 µS/cm pH: 7.7–7.81	COD: 64.38–80.4% Turbidity: 96.75–99.61% Color: 0–53.49% Absorbance (254 nm): 76.6–91.94%	Non-potable reuse (not detailed)	[141]
GAC+MF (lab scale)	Secondary treated water of the sewage treatment plant	MF: 0.22 µm Flux: 98 LMH TMP: 0–0.4 bar	pH: 7.62–8.02 TSS: 4–20 mg/L COD: 10–30 mg/L TN: 30–50 mg/L TP: 15–30 mg/L	Turbidity: 0.1–0.4 NTU, 100% TSS: 100% COD: 8–25 mg/L, 53% TN: 20–40 mg/L 15% TP: 10–20 mg/L, 13%	Not mentioned	[142]

Process (scale)	Feed Wastewater	Operating Conditions	Feed Characteristics	Permeate Quality/Removal Rate	Application for Reuse	References
Coagulation +MF (lab scale)	Secondary effluent from WWTP	Coagulant: 10–50 mg/L alum MF: 0.1, 0.22 μm ; TMP: 0.34 bar	Turbidity: 19.7 \pm 87.9 NTU TOC: 7.2 \pm 6.5 mg/L pH: 7.0 \pm 0.2 TSS: 14.4 \pm 25.8 mg/L	Turbidity: 0.11–0.13 NTU, >93%; TOC: 1.30–1.56 mg/L, 23.5–35.5%	Not mentioned	[143]
Coagulation + PAC + UF (lab scale)	Secondary effluent from WWTP	UF: 50 kDa TMP: 1 bar Coagulant: FeCl ₃	pH: 7.4 Turbidity: 18 NTU TSS: 35 mg/L COD: 77 mg/L EC: 1350 $\mu\text{S/cm}$	COD: 13.33–21 mg/L Turbidity: 0.5–0.8 NTU	Not mentioned	[144]
CEPS+NF (pilot scale)	MWW	Coagulants: Alum and Ferric chloride Spiral-wound NF membrane: 0.002 μm ; TMP 8 bar; flow rate: 12.24 L/h	pH: 7.34 \pm 0.20 TSS: 358 \pm 22 mg/L COD: 358 \pm 29 mg/L PO ₄ ³⁻ : 25 \pm 1 mg/L	Turbidity: 0.92 NTU COD: 20.88 mg/L TDS: 100.84	Non-potable reuse	[145]
MF+UF (pilot scale)	Secondary effluent from urban WWTP	MF: 0.2 μm , hollow fiber, 0.2–0.8 bar (TMP) UF: 0.05 μm , flat sheet, 0.2–0.6 bar (TMP)	Turbidity: 4–20 NTU TSS: 11–87 mg/L	Turbidity: 0–0.9 NTU TSS: 1–7 mg/L	Not mentioned	[146]

Process (scale)	Feed Wastewater	Operating Conditions	Feed Characteristics	Permeate Quality/Removal Rate	Application for Reuse	References
MBR (pilot plant)	Mixed municipal and industrial wastewater	MF: 0.4 μm , flat sheet Flux: 83 LMH MLSS: 1600–2300 mg/L HRT: 8 h SRT: 25 days	pH: 7.3 \pm 0.62 SS: 223 \pm 32 mg/L COD: 250 \pm 64 mg/L	SS: <5 mg/L, >98% COD: 41–51 mg/L, >75%	Reused for process water in industries, cleaning, and recreational water supplies	[134]
MBR+ GAC (real scale)	Primary effluent of MWW plant	UF: 0.04 μm HRT: 3.2 h (MBR) + 0.58 h (GAC)	BOD5: 46.2–262.1 mg/L COD: 142–512 mg/L SS: 47.5–240 mg/L	BOD5: < 1.9 mg/L, >96% COD: < 48.3 mg/L, >65.9% SS: < 7.2 mg/L, >85%	Non-potable	[135]
MBR (pilot scale)	MWW	UF: 0.02 μm /300 kDa Flux: 75–150 LMH HRT: 5 d SRT: 5–30 days	COD: 200–800 mg/L SS: 100–600 mg/L NH ₃ -N: 10–30 mg/L Turbidity: 50–70 NTU pH: 7.5–8.5	COD: 9.4 mg/L, 97%; SS: nd, 100%; NH ₃ -N: 0.2–1.3 mg/L, 96.2%; Turbidity: < 2 NTU pH: 8.2	Use for municipal purposes or indirect use for industry with additional treatment	[136]
MBR (pilot scale)	MWW	UF: 0.45 μm Flux: 6.2 LMH HRT: 8 h SRT: 60 days	COD: 232 \pm 41 mg/L TSS: 220 \pm 52 mg/L TN: 42 \pm 5 mg/L TP: 3.2 \pm 0.4 mg/L pH: 7.3 \pm 0.1	COD: 9.0 \pm 3.6 mg/L, 96% TSS: 220 \pm 52 mg/L TN: 10.6 \pm 2.6 mg/L, 74% TP: 0.7 \pm 0.2 mg/L, 78% pH: 7.3	Urban or rural reuse	[147]

Process (scale)	Feed Wastewater	Operating Conditions	Feed Characteristics	Permeate Quality/Removal Rate	Application for Reuse	References
MBR+ NF (pilot scale)	MWW after primary treatment	UF: 200 kDa, hollow fiber NF: 150–300 Da, TMP: 0.1–0.5 bar (UF); 41 bar (NF)	EC: 1174±2 µS/cm pH: 7.2±0.1 TSS: 488±48 mg/L Turbidity: 248±11 NTU COD: 478±132 mg/L NO ₂ ⁻ : 64.35 mg/L PO ₄ ³⁻ : 9.631±1.428 mg/L	EC: 397 µS/cm pH: 8.06 TSS: 0 mg/L Turbidity: 0.23 NTU COD: < 5 mg/L NO ₂ ⁻ : 0.3728 mg/L PO ₄ ³⁻ : n.a. mg/L	Agricultural Irrigation (50% of MBR effluent and 50% of NF permeate)	[137]
UF+NF	Synthetic MWW after aerobic activated sludge process	UF: 30 kDa, PES NF: 270 Da, PA TMP: 1–6 bar	COD: 243.34 mg/L TP: 7.53 mg/L NH ₃ -N: 0.67 mg/L NH ₂ -N: 4.32 mg/L	COD: 3.68 mg/L TP: 0.19 mg/L NH ₃ -N: 0.14 mg/L NH ₂ -N: 0.14 mg/L	Inner industrial reuse, Garden irrigation	[148]
FO + NF (pilot plant)	Secondary effluent from WWTP	Flux: 2.4 LMH for FO Flux: 3.3 or 6.6 LMH for NF	<i>E. coli</i> : 0 CFU·100/mL TSS: < 1 mg/L Turbidity: 0.22 NTU EC: 5.33 dS/m	EC: 1 mS/cm SAR: 1.98 meq/L	Agricultural irrigation	[149]

Process (scale)	Feed Wastewater	Operating Conditions	Feed Characteristics	Permeate Quality/Removal Rate	Application for Reuse	References
RO	MBR effluent from domestic wastewater	TMP: 4–12 bars Initial Permeability: 3.6 LMH·bar	TOC: 6.0–8.0 mg/L COD: 12–13 mg/L TSS: < 2 mg/L EC: 631–894 $\mu\text{S}/\text{cm}$	TOC: 91–98% EC: 96–98%	Not mentioned	[150]
UF/NF/RO (pilot scale)	The secondary MBR effluent	UF: 25 and 30 LMH NF: 30 LMH RO: 30 LMH	EC: 56 mS/m pH: 6.5 TDS: 360 mg/L COD: <20 mg/L NH_4^+ : <0.4 mg/L PO_4^{3-} : 2.6 mg/L	EC: 37 $\mu\text{S}/\text{m}$ TDS: 19 mg/L COD: 2 mg/L PO_4^{3-} : 0.45 mg/L Turbidity 0.08 mg/L	Irrigation and industrial purposes	[151]
MF+RO (pilot scale)	Secondary treated effluent from sewage	MF: 26 m^3/d ; 0.4 μm RO: 19 m^3/d	TSS: 2 mg/L COD: 23 mg/L $\text{NH}_3\text{-N}$: 4.7 mg/L TDS: 364 mg/L pH: 7.2 Turbidity: 0.6 NTU	TSS: < 2 mg/L COD: < 2 mg/L $\text{NH}_3\text{-N}$: 0.71–1.43 mg/L TDS: 17–24 mg/L pH: 5.3–5.5 EC: 24–33 $\mu\text{S}/\text{cm}$	Both for potable and non-potable reuse	[152]
MBR+RO (pilot scale)	Primary treated MWW	UF: 0.04 μm , hollow fiber TMP: 0.42 bar (UF), 15.2 bar (RO)	TSS: 100–1930 mg/L Turbidity: 7–308 NTU COD: 122–2205 mg/L TN: 12.6–205 mg/L	TSS: <1 mg/L Turbidity: 0.01–0.13 NTU DOC: 1.04–4.1 mg/L TN: 17–21 mg/L	Not mentioned	[153]

Process (scale)	Feed Wastewater	Operating Conditions	Feed Characteristics	Permeate Quality/Removal Rate	Application for Reuse	References
AnMBR+RO (lab scale)	Synthetic MWW	Flux: 20 LMH	COD: 400 mg/L NH ₄ -N: 45 mg/L PO ₄ -P: 5 mg/L	Ammonium-N: 2.1 mg/L PO ₄ -P: 0.03 mg/L TOC: 0.13 mg/L EC: 47 µS/cm	Discharge to reservoirs for indirectly potable reuse	[154]
AnMBR + RO (lab scale)	Synthetic MWW	UF: 0.02 µm	Sucrose: 210 mg/L Meat extract: 41.7 mg/L Peptone: 60 mg/L NH ₄ Cl: 95.5 mg/L	TOC: 0.17±0.02 mg/L NH ₄ -N: 0.81±0.09 mg/L PO ₄ -P: < 0.01 mg/L EC: 24.19±1.21 µS/cm	NEWater product	[155]
NF-MBR+RO	MWW	NF: 200–300 Da Flux: 10 LMH MLSS: 513±96 mg/L	COD: 389±169 mg/L NH ₄ -N: 40.9±4.5 mg/L NH ₃ -N: nd PO ₄ ³⁻ : 23.6±3.2 mg/L EC: 859.5±18.9 mS/cm	NF permeate: COD: 99.6±0.8% DOC: 0.5–2.5 mg/L, 97.5%±1.8%	Not mentioned	[156]
RO (bench scale)	Primary treated effluent from sewage	AnMBR: 8 h HRT Hollow fiber UF membrane, 0.04 µm 10 LMH	pH: 7.9±0.5 TDS: 410.4±64.8 mg/L COD: 218±59 mg/L TN: 31.3±4.5 mg/L PO ₄ -P: 3.9±1.4 mg/L	pH: 6.0 ±1.9 TDS: 37.5 ±11.7 (93 %) COD: 1.9 ±2.5 (96 %) TN: 5.3 ±1.8 (86 %) PO ₄ -P: 0.3 ±0.3 (95 %)	Indirect potable water reuse	[157]

Despite the advantages of membrane processes in terms of water recovery, membrane fouling remains the main bottleneck of the process to be solved, which is discussed below in detail.

2.4.2.1 Membrane fouling

Membrane processes have the ability to produce very high-quality effluent that can be used for several types of wastewater reuse, but they can be quite cost-intensive to maintain. Membrane fouling is a major obstacle in wastewater applications, especially when flux rates are high. Choosing lower flux rates can reduce operational expenses, but it will require a higher initial investment due to the need for extra membrane units [158].

Membrane technology is characterized by complex interactions between the surfaces of the membrane, operating factors, and the chemical composition of the wastewater being treated [34, 145, 159, 160]. Membrane fouling, regardless of its characteristics, is a complex phenomenon that is influenced by multiple variables. Although it is difficult to create a clear rule for membrane fouling, several elements influence the rate at which fouling occurs. These factors include membrane properties, operational parameters, feed composition, as well as the properties of biomass for MBRs. Although it is difficult to establish a single rule for membrane fouling in MBRs, MF/UF, and NF/RO membranes, there are several groupings of elements that affect the rate at which fouling occurs [161, 162]. These factors include the constituents of the feed and biomass, the operating conditions, and the membranes themselves. Table 2.3 summarizes several factors that are outlined within these groups.

Table 2.3 Overview of the impacts of various parameters on membrane fouling in different membrane processes

Membrane Processes	Feed and Biomass Characteristics		Membrane properties		Operational conditions	
	Factors	Impact on fouling	Factors	Impact on fouling	Factors	Impact on fouling
MBRs	Fine particles and colloids	The accumulation of fine particles, organics, colloids, salts, and microorganisms [163].	Membrane material and composition	Order of antifouling resistance: ceramic membranes > composite membranes > polymeric membranes [164, 165]	Mode of Operation	When MBR is operated at constant permeate flux, fouling is noticed by TMP increase, while when operating MBR at constant TMP, fouling is noticed by flux decline [166, 167].
	Viscosity of Sludge	At high MLSS viscosities, the membrane fouling rate in MBRs will increase [168].	Water Affinity	MBR fouling is much more significant in hydrophobic membranes than in hydrophilic ones [169].	Rate of aeration or biogas sparging	Aeration and biogas sparging tend to reduce fouling in MBRs but will increase their operational cost [170, 171].
	Extracellular Polymeric Substances (EPS)	The existence of hydrophilic and hydrophobic species in EPS has an amphoteric influence on fouling [172].	Surface roughness and porosity	Homogenous MBR surfaces are less likely to foul as compared to irregular surfaces. MBRs with protruding projections have antifouling properties. MBRs with higher pore aspect ratios have a lower fouling tendency [169, 173].	SRT and HRT	Generally, increasing SRT will reduce fouling in MBRs because of MLSS accumulation and raising sludge viscosity [174]. Decreasing HRT will increase fouling in MBRs [175].
	Salinity of Wastewater	Higher salinity wastewater will increase the fouling tendency in MBRs [176].	Surface charge	Since the MBR's surface is negatively charged, positively charged ions in the influent result in inorganic fouling [177].	Food/Micro-organisms (F/M)	High F/M ratios can result in elevating EPS amounts because of high bacterial substrate utilization. High F/M will increase fouling in MBRs [178].
	Sludge floc size	Small flocs easily adhere to the membrane and increase hydraulic cake and osmotic pressure-induced resistance. [179]	Pore Size	Fouling can't be linked to pore size alone; influent composition and membrane material will influence the relation between MBR fouling and pore size [180].	OLR	Higher OLR will result in higher fouling in MBRs [181].

Membrane Processes	Feed and Biomass Characteristics		Membrane properties		Operational conditions	
	Factors	Impact on fouling	Factors	Impact on fouling	Factors	Impact on fouling
NF/RO	Presence of microorganisms	The adherence and multiplication of microorganisms on membrane surfaces can lead to the development of biofilm [182, 183].	Water Affinity	Membrane surface hydrophilicity has a negative impact on membrane fouling by natural organic matter [184].	Permeate flux	At higher water flux larger volume of water permeated through the membrane and thus greater amount of foulants brought towards the membrane surface due to the water convection [184].
	Humic substances, polysaccharides, proteins, lipids, nucleic acids and amino acids, organic acids	Significant flux decreases in RO membranes can be caused by organic fouling, which is composed of organic matter [185, 186].	Surface charge	When the surface and the foulant have similar charges, electrostatic repulsion forces between the foulants and the membrane prevent the foulant deposition on the membrane thereby reducing the fouling [187].	CFV	A higher cross-flow velocity permits a decrease of the concentration polarization by elevating the mass transfer rate and mitigating membrane fouling by enhancing the back transport of foulants, thus improving flux behavior [188, 189]
	Different minerals including calcium carbonate, calcium sulfate, and silica precipitate	Inorganics may exceed the equilibrium solubility and become supersaturated. This can lead to the deposition of these substances on the surface or within the pores of the membrane, leading to scaling [190].	Surface roughness	Membranes with rougher surfaces are observed to be more favorable for attachment of foulants resulting in faster fouling rates [191, 192].	Temperature	The effect of temperature on membrane fouling is virtually through the influence of hydrodynamic conditions (initial water flux level and mass transfer of foulant) and thermodynamic conditions (solution osmotic pressure, foulant solubility/stability, and foulant-foulant/foulant-membrane interactions) [193-195].
	Inorganic foulants and organic macromolecules	Colloidal fouling refers to the fouling of the membrane caused by the colloids or particles depositing on the host materials [196].			Feed spacer	The different geometry/configuration of the spacer influenced turbulence at the membrane surface and that, in turn, affected concentration polarization [197].

Membrane Processes	Feed and Biomass Characteristics		Membrane properties		Operational conditions	
	Factors	Impact on fouling	Factors	Impact on fouling	Factors	Impact on fouling
	DOM	Membrane fouling is mostly caused by low-molecular-weight DOM [198]			Pressure	Running the NF/RO below the critical pressure will reduce fouling [197].
					pH	Lowering the pH reduces the negative charge on particles, causing aggregate formation that deposits on the membrane surface [197].
MF/UF	Particle size	Depending on the particle size, the particles can cause fouling by blocking pores, narrowing pores, or forming cakes. Some other factors are also important, such as pH, ionic strength, and particle electric charges [199, 200].	Membrane pore size, pore size distribution, and pore geometry	The smaller the membrane pore size, the better pollutant removal rate can be achieved in conventional MF/UF, with alleviated membrane fouling [201].	Temperature	The permeate flux increased with a low degree of fouling at higher temperatures
	Dissolved inorganic and organic components, bacteria, colloids, and suspended solids	Concentration polarization occurs when dissolved and/or colloidal materials concentrate on or very near the membrane surface while fouling is the gradual build-up of contaminants on the membrane surface as gel layer formation [202].	Surface hydrophobicity	Hydrophilic membranes are thought to have a lower membrane fouling potential than hydrophobic membranes [203].	Cross-flow velocity	Higher cross-flow velocity leads to a decrease in the combination of feed solids in the gel layer mainly because these components become more widely diffused back towards a bulk, which leads to a reduction in the overall concentration polarization effect

Membrane Processes	Feed and Biomass Characteristics		Membrane properties		Operational conditions	
	Factors	Impact on fouling	Factors	Impact on fouling	Factors	Impact on fouling
	Biologically active organisms, mainly bacteria and (in some cases) fungi	The adherence and multiplication of microorganisms on membrane surfaces can lead to the development of biofilm [204].			Transmembrane pressure (TMP)	The force of the fluid flowing into the membrane increases as the TMP rises, resulting in a higher permeate flux
	pH and ionic strength of the feed	The charge on the membrane, the charge on the particles, conformation, and stability of, and thus adhesiveness of particles/molecules, as well as the size of the cake, are all influenced by the pH and ionic strength of the feed [205-207]				

Recent improvements in membrane studies have demonstrated potential in overcoming the issue of membrane fouling in several wastewater treatment processes. The significance of optimization of feed characteristics, operational parameters, and membrane properties for mitigation of membrane fouling that mentioned before in Table 2.3.

The primary strategy involves improving pre-treatment methods for wastewater before membrane filtration. To prevent fouling and improve treatment effectiveness, the lifespan of the membrane can be lengthened by modifying the composition of wastewater and conducting effective pre-treatment procedures [208]. Methods such as pre-coagulation, pre-adsorption, pre-filtration, pre-oxidation, and the use of novel membranes have been investigated in recent years in research publications [209-213]. However, it appears that pre-coagulation is predominantly mentioned in the literature. Another possible pre-treatment strategy to reduce fouling is the creation of membrane-based hybrid systems that integrate various membrane technologies. These integrated strategies not only enhance the effectiveness of treatment but also present opportunities for the recovery of resources and the implementation of circular economy approaches [214]. By combining the best functions of several membrane technologies, these integrated systems can overcome the challenges of fouling [215]. Lastly, using advanced materials and surface modifications to improve the resistance of membranes against fouling. Researchers make an effort to enhance membrane function by using nanomaterials or modifying the surface characteristics of membranes to minimize the adhesion of foulants. [216].

2.4.4 Anaerobic digestion

Currently, the most prevalent approach for energy recovery involves the generation of biogas through anaerobic sludge digestion, which is being applied globally on different scales [217]. Around 80% of the biodegradable COD fraction in the sludge can be transformed into usable biogas in fully mixed reactors [9]. Utilizing advanced reactor topologies can improve the efficiency of biodegradation and make it easier to collect dissolved methane from the broth [218]. However, if the methane that

has been recovered is not used in the same location, it requires the process of increasing its pressure and transporting it to customers. In areas where biogas is easily accessible and supplied over a widespread pipeline network, this method can be excessively costly [219]. Heating is a major expense when it comes to digesters, as much as 40% of the produced methane might be dissolved in the liquid mixture at moderate temperatures. The emission of this dissolved methane has the potential to contribute to climate change. Hence, it is crucial to exert meticulous management over anaerobic wastewater treatment and sludge digestion in order to mitigate the potential for methane emissions [59].

Anaerobic microorganisms aid in the degradation of organic compounds through a sequence of activities (Figure 2.6). An essential stage in this metabolic route is hydrolysis, when organic substances are decomposed into less complex molecules of reduced molecular weight, allowing them to be absorbed by microbial cells. Microorganisms accomplish this by excreting specialized proteins called enzymes (enzymatic hydrolysis) outside their cells. Enzymes facilitate hydrolysis reactions, in which complex organic polymers including lipids, proteins, and polysaccharides are enzymatically decomposed into more basic organic molecules. For example, lipids are broken down into fatty acids and glycerol, proteins into amino acids, and polysaccharides into monosaccharides like glucose, fructose, and galactose. Afterward, these organic chemicals are able to be absorbed into the cytoplasm of microorganisms, commencing the process of metabolism, which occurs in four distinct stages: (i) hydrolysis, (ii) acidogenesis, (iii) acetogenesis, and (iv) methanogenesis.

Hydrolysis is the primary stage in which intricate organic compounds are decomposed into less complicated ones. Subsequently, acidogenesis ensues, wherein the byproducts of hydrolysis undergo further transformation into volatile fatty acids, alcohols, and hydrogen. Acetogenesis is the process of converting these chemicals into acetate, hydrogen, and carbon dioxide. Methanogenesis is the final stage in which methane is generated by the decomposition of acetate and hydrogen [220].

The hydrolysis and acidification stages play a crucial role in the initial decomposition of organic material during the anaerobic digestion process, followed by acetogenesis and methanogenesis. Although hydrolysis is commonly regarded as the stage that determines the rate, acetogenesis or methanogenesis can also impose

limitations in the case of more complex substances [221]. However, anaerobic digestion procedures result in methane as a valuable end product; this process is dependent on the last stage, methanogenesis [222].

Research has indicated that the variety of methanogens and anaerobic methanotrophs has a substantial impact on the effectiveness of methanogenesis [223]. Acetogens play a crucial role in acetogenesis due to their unique capability to utilize various electron donors, separating them from other types of microorganisms [224]. Moreover, the suppression of acetogenesis can happen even without the presence of volatile fatty acids in some circumstances, emphasizing the intricate equilibrium necessary for effective acetogenesis [225]. The anaerobic treatment stages of hydrolysis, acidogenesis, acetogenesis, and methanogenesis are interrelated and necessary for the successful conversion of organic waste into biogas. Every stage has a distinct function in the decomposition and conversion of organic compounds, ultimately resulting in the generation of methane as a useful source of energy.

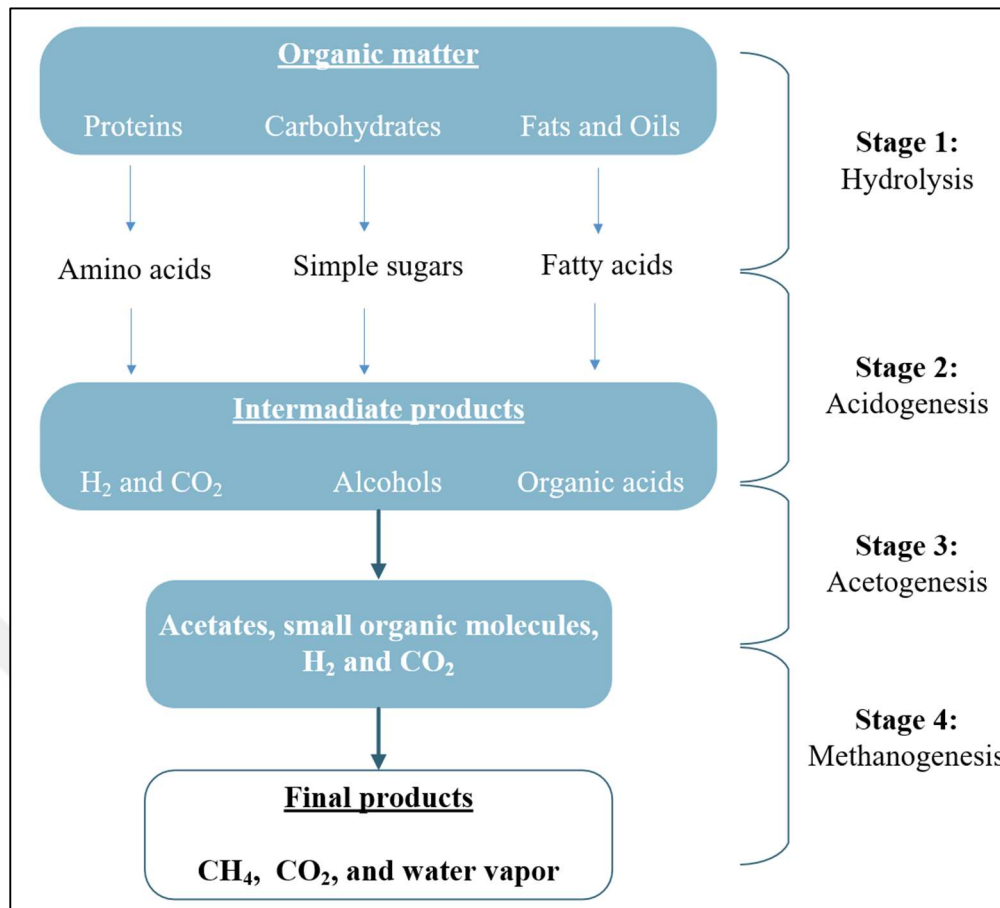


Figure 2.11 Anaerobic treatment stages [226]

2.4.5 Anaerobic membrane bioreactors

AnMBRs are a highly promising technology for treating urban wastewater. They offer several advantages over conventional anaerobic systems and aerobic MBRs. The advantages of this process encompass the production of bioenergy, the generation of high-quality effluent, the efficient disposal of sludge, the ability to tolerate substantial loads, the recovery of nutrients, the efficient use of space, reduced energy requirements, and the ability to operate in a decentralized manner [227].

AnMBR and aerobic MBR differ significantly in various parameters, such as fouling behavior, consumed energy, pollutant removal efficiency, and capacity throughput [228]. When it concerns energy consumption and the process's ability to operate sustainably, membrane fouling is the most crucial aspect. Wang, K. M., et. al. [229] analyzed to complement existing knowledge through the characterization of biomass properties within AnMBRs for MWW treatment, evaluating their impact on

membrane fouling and comparing them to those in aerobic MBR, to ascertain the main factors that determine differences in fouling behavior and characteristics between these two systems. They discovered that membrane fouling has a significant impact on energy consumption. To determine how the existing literature aligns intending to achieve 'energy-neutral' wastewater treatment, they analyzed published data on both energy production from AnMBR for MWW treatment and the specific energy usage of membranes. Analysis of literature data revealed that the level of extractable extracellular polymeric substrate is slightly higher in aerobic MBRs than in AnMBRs. However, AnMBR comprises considerably higher soluble microbial product concentrations, which have been widely reported to increase fouling propensity in aerobic systems. In addition, the study findings indicate that membrane fouling continues to be a significant obstacle. However, multiple research groups have previously shown the ability to create energy-sustaining scenarios at the pilot scale. Although aerobic MBR has reached a somewhat advanced stage of development, further investment is required in commercial module and aeration technologies to achieve significant reductions in specific energy demand on a full scale. Therefore, it is fundamentally feasible to accomplish energy-neutral wastewater treatment for AnMBR systems on a large-scale.

2.4.6 AnMBR configurations

Two primary configurations are widely used in AnMBRs: the submerged configuration and the external (side-stream) configuration. Lower energy consumption and gentler operating conditions, including permeate flux, are achieved in the submerged arrangement, which positions the membrane inside the reactor and results in lowered velocities. Conversely, the external configuration, which includes integrated membrane filtration in an external loop, provides higher flow rates and simplifies the process of replacing the membrane. Nevertheless, there is a tendency for increased energy consumption, and the elevated crossflow velocity may lead to a decrease in biomass activity. In traditional AnMBRs, the membrane modules are commonly combined with bioreactors such as a stirred tank reactor, an up-flow anaerobic sludge blanket reactor, an expanded granular sludge bed reactor, or an AnFMBR [230].

The recent novel AnMBR configurations, including AnFMBR, granular-sludge AnMBRs, AnDMBR, and AnFOMBR, have been developed through extensive research focused on improving fouling control, bioreactor integration, and membrane material or module design [231]. Figure 2.7 displays the schematic diagram of five representative AnMBR configurations, which have the ability to mitigate membrane fouling and reduce energy usage to varying degrees.

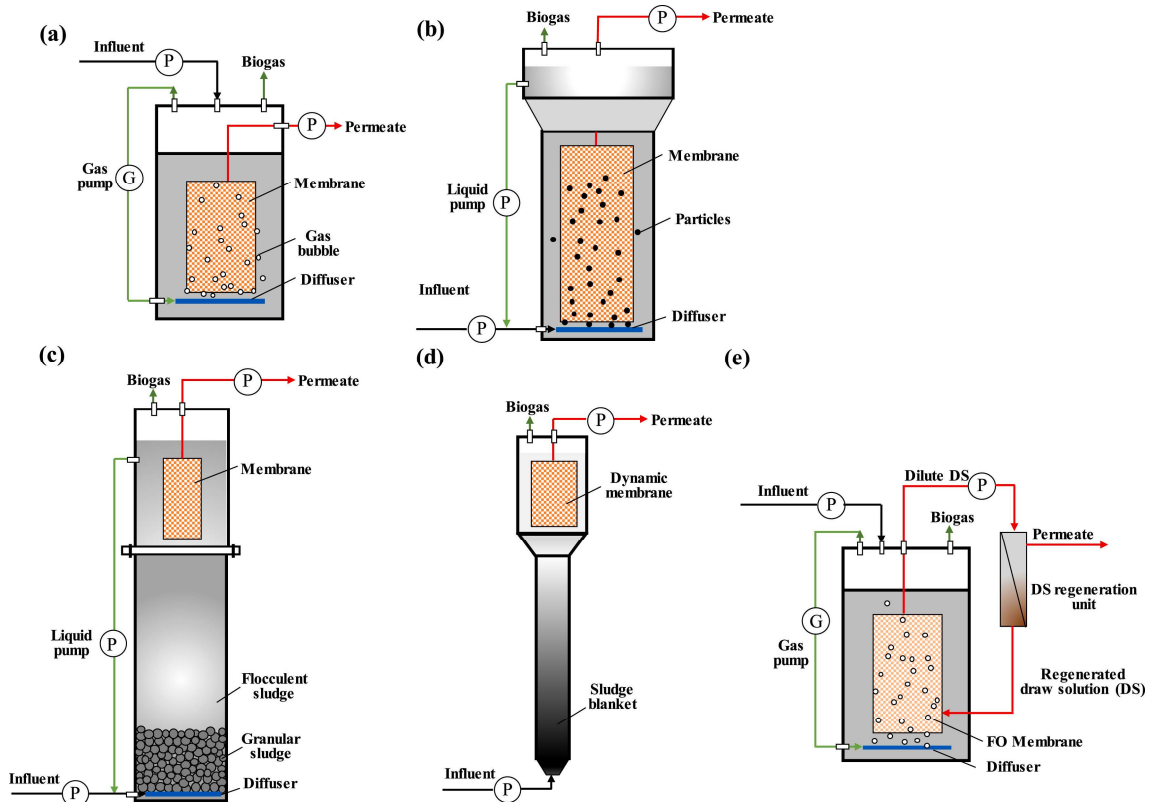


Figure 2.12 Schematic diagram of novel AnMBR processes: (a) biogas-sparging AnMBR; (b) AnFMBR; (c) granular-sludge AnMBR; (d) AnDMBR and (e) AnFOMBR [231].

In order to effectively evaluate the AnMBR system from a technical-economic point of view, other aspects are included in Table 2.4. Additional factors to consider are the specifications for the membrane and bioreactor configuration, the effectiveness of the treatment and filtration processes, the techniques used for membrane maintenance, and any other technical restrictions. Certain AnMBR systems demand specialized membrane modules, specifically flat-sheet ceramic membranes, which are beneficial for AnFMBR when used with not damaging carriers that have a certain density that is sufficient. This innovative integration enables the membrane surface to experience a

more effective flow of particles, while also preventing any significant harm to both the membrane and particles during extended periods of operation. The use of an inexpensive and rough mesh in the AnDMBR offers a cost-effective technical solution with minimal energy usage [20].

Table 2.4 A comparison of different AnMBR configurations [231]

Comparison factors	Biogas-sparing AnMBR	AnFMBR	Granular-sludge AnMBR	AnDMBR	AnFOMBR
Membrane material	N.N	Ceramic preferred	N.N	Coarse pore mesh	FO membrane
Membrane module	N.N	Flat sheet preferred	N.N	N.N	N.N
Pore size (µm)	0.01–0.5	0.01–0.5	0.01–0.5	10–200	None
Membrane cost	Moderate	Moderate	Moderate	Low	High
Reactor types	N.N	Upflow preferred	Upflow preferred	N.N	N.N
Retention capability	High	High	High	Moderate to high	Excellent
Driving force	Pressure driven	Pressure driven	Pressure driven	Pressure driven	Osmosis driven
Filtration performance	Moderate	Moderate to high	Moderate to high	High	Low
Fouling mitigation technique	PC and CC	PC and CC	PC and CC	PC	PC and CC
Technical restriction	High energy consumption, affecting floc properties	Requirements of particles and membrane	Risks of granular sludge breakup	Formation and maintaining stable DM layer	Salt accumulation, flux decline, and draw solution regeneration

Note: N.N., not necessary; PC, physical cleaning; CC, chemical cleaning.

Numerous scholarly articles have been published in international journals that examine the efficacy of AnMBR systems in the context of municipal managing MWW. Relevant investigations of the five years, specifically the period 2019–2024, are presented in Table 2.5.

Untreated or pretreated MWW, domestic wastewater, or synthetic wastewater that reflects MWW has been utilized as incoming loads for treatment. Regardless of the loading type, the focus is on treating wastewater with low levels of soluble organic matter. In the case of synthetic MWW, the rate at which COD is removed is typically over 95%, as all of the COD is in a soluble form [19]. The utilization of the up-flow anaerobic sludge blanket bioreactor is also widespread. Typically, researchers examine the performance and optimization of the AnMBR system using immersed membranes. Additionally, the AnFMBR is highly effective in treating low-strength dilute wastewater. Kim et al. [232] employed an AnFMBR using a tubular-shaped PVDF as a fluidizing agent to treat synthetic wastewater. The treatment was conducted at a temperature of 36.3 °C and a HRT ranging from 4 to 16 hours, over a total period of 240 days [107]. The fluidizing agent successfully reduced the fouling rate by creating a scouring effect, which in turn kept the transmembrane pressure below 0.1 bar and ensured a COD removal rate of over 90%. The energy consumption was 0.0109 kWh/m³, while the energy production from potential methane production was estimated at 0.246 kWh/m³, indicating that the AnFMBR is technically feasible.

Table 2.5 Scientific articles of relevance to the treatment of MWW using the AnMBR system

Reactor Type And Membrane Configuration	Type of Membrane	Flux (LMH)	Inlet COD (mg/L)	Operating Conditions	Outlet COD (mg/L)	COD Removal (%)	CH₄ Produced	Reference
AnOMBR	Forward osmosis Area: 70 cm ²	5.78	4000	35 °C pH = 7.48		93.4	0.21 m ³ CH ₄ /kgCOD	[233]
Granular activated carbon-synergized AnMBR	Hollow fiber PVDF Pore size: 0.1 μm Area: 20 m ²	16	277–348	5–35 °C HRT = 6–24 h pH = 6.8–7.3	<50	>86	0.24 m ³ CH ₄ /kgCOD	[234]
AnMBR submerged	Hollow fiber PVDF Pore size: 0.4 μm Area: 72 m ²	2.75– 17.83	362.2–481.9	25 °C HRT = 6–24 h OLR = 1.84 kgCOD/m ³ d	29.2–42.9	89.5–93.2	0.25–0.27 m ³ biogas/kgCOD CH ₄ content 75– 81%	[235]

AnMBR submerged	Hollow fiber PVDF Pore Size: 0.4 μm Area: (i–iii) 0.345 m^2 (iv) 0.146 m^2	(i) 14.16 (ii) 9.61 (iii) 7.23 (iv) 11.02	i. 350 ii–iv. 365	(i–iv) 25 °C (i) HRT = 4 h OLR = 2.05 kgCOD/ m^3d (ii) HRT = 6 h OLR = 1.52 kgCOD/ m^3d (iii) HRT = 8 h OLR = 1.18 kgCOD/ m^3d (iv) HRT = 12 h OLR = 0.72 kgCOD/ m^3d	89		(i) 0.16 $\text{m}^3\text{CH}_4/\text{kgCOD}$ (ii) 0.23 $\text{m}^3\text{CH}_4/\text{kgCOD}$ (iii) 0.24 $\text{m}^3\text{CH}_4/\text{kgCOD}$ (iv) 0.21 $\text{m}^3\text{CH}_4/\text{kgCOD}$	[236]
AnMBR external	Tubular ultrafiltration membrane Pore size: 0.045 μm and filtration area 0.93 m^2	10-14	892 \pm 271	HRT 7 h Temperature 18 \pm 2 °C VLR*: 2–2.5 kgCOD/($\text{m}^3\cdot\text{d}$)	111 \pm 16.6 - 160 \pm 22.3	87 \pm 1	0.18–0.23 $\text{Nm}^3\text{CH}_4/\text{kg}$ $\text{COD}_{\text{rem}}^{**}$	[237]
AnMBR submerged	Ultrafiltration membrane Pore size: 0.045 μm and filtration area 1.86 m^2	10-14	978 \pm 210	18 \pm 2 °C HRT 12.8–14.2	73.7 \pm 13.8 - 225.0 \pm 58.3	90	19.10 \pm 0.84 mg CH_4/L	[238]
AnMBR submerged	Hollow-fibre membrane module pore size 0.2 μm , total membrane area of 5.4 m^2	2.75– 17.83	not mention an average value	HRT 6 h Temperature 25 °C	50 \pm 22	>90	0.25–0.27 L biogas/g $\text{COD}_{\text{rem}}^{**}$; 75–81% methane in the biogas	[239]

AnMBR submerged	Hollow fiber PVDF Pore Size: 0.22 μm ; surface area: 0.06 m^2	6	320–360	OLR 3.0 kg COD/ $(\text{m}^3 \cdot \text{d})$ HRT 2.2 h Temperature 35 $^\circ\text{C}$	not mentioned	G- AnMBR: 91.9 \pm 1.5 EG- AnMBR: 91.3 \pm 2.1	0.12 L CH_4/g CODrem	[227]
AnMBR submerged	Hollow fiber PVDF Pore Size: 0.04 μm ; surface area: 0.146 m^2	i. 5.71 ii. 11.42 iii. 9.50 iv. 11.42	408	25.2 $^\circ\text{C}$ pH = 7.3 (i) HRT = 24 h (ii) HRT = 12 h (iii) HRT = 14.4 h (iv) HRT = 12 h	(i) 53.6 (ii) 42.1 (iii) 39.0 (iv) 44.0	(i) 88.9 (ii) 89.8 (iii) 89.0 (iv) 88.1	i. 0.15 $\text{m}^3\text{CH}_4/\text{kgCOD}$ ii. 0.15 $\text{m}^3\text{CH}_4/\text{kgCOD}$ iii. 0.18 $\text{m}^3\text{CH}_4/\text{kgCOD}$ iv. 0.19 $\text{m}^3\text{CH}_4/\text{kgCOD}$	[240]
AnMBR submerged	Hollow fiber PVDF Pore Size: 0.05 μm ; surface area: 0.270 m^2	i. 3.08 ii. 5.13 iii. 6.17	408	25.2 $^\circ\text{C}$ pH = 7.3 (i) HRT = 24 h (ii) HRT = 14.4 h (iii) HRT = 12 h (iv) HRT = 12 h	(i) 47.1 (ii) 42.8 (iii) 41.6	(i) 88.9 (ii) 88.9 (iii) 89.5	i. 0.16 $\text{m}^3\text{CH}_4/\text{kgCOD}$ ii. 0.2 $\text{m}^3\text{CH}_4/\text{kgCOD}$ iii. 0.18 $\text{m}^3\text{CH}_4/\text{kgCOD}$	[241]
AnFMBR submerged	Flat-tubular Ceramic (Al_2O_3) Pore size: 0.1 μm Area: 0.09 m^2	10.4	300.1	35 $^\circ\text{C}$ pH = 7.5 HRT = 8 h OLR = 0.9 $\text{kgCOD}/\text{m}^3\text{d}$	30.1	90.0	0.216 $\text{m}^3\text{CH}_4/\text{kgCOD}$	[232]

AnMBR submerged			269–712	32 °C HRT = 6–22 h OLR = 0.29–2.85 kgCOD/ m ³ d pH = 6.98–7.19		64.41–83.49		[242]
Sponge-based moving bed-AnOMBR/membrane distillation (AnOMBR/MD) system	Tubular forward osmosis membrane Area: 120 cm ² PVDF Pore Size: 0.45 μm Membrane distillation Pore Size: 0.45 μm Area: 200 cm ²	4.01	880–1120	45 °C HRT = 40–50 h pH = 7.3	<5	>99	0.11–0.18 m ³ CH ₄ /kgCOD	[243]
AnMBR external	UF membrane pore size: 0.03 μm area: 0.123 m ²	14-21	755±224-1403±532	27 °C (i) HRT = 41±1 h (ii) HRT = 25±1 h (iii) HRT = 26±2 h (iv) HRT = 26±2 h (v) HRT =41±13 h	79±18-121±15	95	(i) 5396±4435 L STP***/d (ii) 5558±3204 L STP/d (iii) 1901±597L STP/d (iv) 1359±999 L STP/d (v) 2241±924 L STP/d	[244]

AnMBR submerged	Hollow fiber PVDF Pore Size: 0.4 μm ; surface area: 72 m^2	10.8	364.4 \pm 94.8	(i) 15 $^\circ\text{C}$ (ii) 20 $^\circ\text{C}$ (iii) 25 $^\circ\text{C}$	< 50	84.5-90.7	0.205–0.244 NL/gCOD	[245]
AnMBR submerged	Hollow fiber PVDF Pore Size: 0.4 μm	(i) 9.39 (ii) 4.80 (iii) 3.61 (iv) 2.41	411.9 \pm 87.8	15 $^\circ\text{C}$ (i) HRT = 6 h (ii) HRT = 12 h (iii) HRT = 16 h (iv) HRT = 24 h OLR= 0.53-1.58 g-COD/L-reactor/d	30-100	77.4		[246]
AnMBR submerged	Flat sheet PVDF 0.5 m^2 pore size: <0.1 μm	13	439 \pm 34 - 453 \pm 26	18 $^\circ\text{C}\pm$ 3 T = 23 $^\circ\text{C}\pm$ 2 HRT= 6 h OLR=1.8 \pm 0.12 kg COD/ (m^3 .day)	147 \pm 8 - 177 \pm 21	73 \pm 4	0.24 0.29 L CH_4 /g COD	[247]
AnMBR external	Hollow fiber PVDF Pore Size: 0.4 μm area: 0.125 m^2	2.1	(i) 691 \pm 89 (ii) 709 \pm 110 (iii) 460 \pm 102 (iv) 489 \pm 78 (v) 594 \pm 63	34 $^\circ\text{C}$ HRT= 24 h	(i) 75 \pm 19 (ii) 79 \pm 29 (iii) 64 \pm 9 (iv) 71 \pm 22 (v) 69 \pm 7	(i) 89 \pm 4 (ii) 89 \pm 4 (iii) 85 \pm 3 (iv) 84 \pm 9 (v) 88 \pm 1	294.5 \pm 8.9 mL CH_4 /g VS	[248]

AnFMBR	Hollow fiber PVDF Pore Size: 0.04 μm area: 0.03 m^2	2-7	(i) 536.10 (ii) 602.20 (iii) 661.50 (iv) 706.00	pH: 6.5-7.8 (i) 25°C, HRT: 6.54 h (ii) 20°C, HRT: 2.68 h (iii) 15 °C, HRT: 5.22 h (iv) 10°C, HRT: 9.03 h	9.9 - 36.6	79-84		[249]
AnMBR external	Ceramic membrane Area 1.54 m^2		145.5 \pm 21.2- 169.9 \pm 45.9	HRT= 4 d and 3 d OLR=0.23-12.50 kg COD/ m^3day	114.04 \pm 36.1 0 - 67.85 \pm 11.10	87-93		[250]
AnMBR submerged	Hollow fiber PVDF Pore Size: 0.1 μm area: 0.1 m^2	3 \pm 0.1 5.7 \pm 0.5	454 \pm 79	36.5 °C 23.5 \pm 0.4 h 12.4 \pm 1.2 h	26 \pm 15 33 \pm 14	94.3 \pm 2.9 93 \pm 3	207 \pm 17.3 mL CH ₄ /gCOD _{rem} **	[251]

*VLR: Volumetric loading rate

**COD_{rem}: Removal amount of COD

***STP: Standard Temperature and Pressure

As revealed by most of the research under consideration, AnMBR technology is extremely efficient in removing organic load from the feed stream. The filtrate showed satisfactory COD removal, greater than 90% and in some cases 98–99%, indicating that AnMBR technology is an extremely competitive MWW treatment technique.

The operational parameters of the investigations show the number of scientific publications according to the different temperature conditions maintained within the bioreactor for the anaerobic treatment of MWW. In general, temperature affects the growth rate of the microbial population, the hydrolysis of organic components, and the solubility of components, such as CH₄ and CO₂. In addition to temperature, it was reported that a lower ORP can intensify methanogenesis [241]. It is possible that the biochar used by Chen et al. [241] provided optimal ORP conditions for microorganisms to convert propionic acid to methane. In another work, Chen et al. [234] investigated the effect of GAC on methane production. Specifically, Chen et al. found that *Methanosaeta*, which is responsible for methane generation, was more active in GAC-sludge samples even under low temperatures (15–5 °C).

The literature review of the present work has shown that AnMBR systems can effectively treat MWW and produce high-quality effluent. It is an environmentally friendly green technology with the possibility of utilizing the produced biogas for electricity and reusing treated water for irrigation.

The use of an external AnMBR may reduce the possibility of membrane fouling; however, it increases the overall cost of the AnMBR system. Therefore, AnMBRs with submerged membranes are prevalent. The efficiency of an AnMBR largely depends on process parameters, such as temperature, pH, HRT, and the concentration of pollutants.

2.4.7 Integration of AnMBRs with different processes for resource recovery

The integration of AnMBRs with other processes is an exciting new direction for wastewater treatment, energy generation, and resource recovery. It is clear that biological oxidation, an essential principle in the design and operation of present WWTPs, needs to be reconsidered in light of future MWW management strategies, particularly in light of the circular economy's development as a driving force in the effort to enhance energy and resource recovery. The generation of waste sludge is greatly decreased with the implementation of new A-B process designs, where the A-stage includes an anaerobic unit for the direct conversion of organic matter in MWW into biomethane. The B-stage, meanwhile, is mainly concerned with the chemical and physical recovery of nutrients [252]. AnMBRs have been extensively studied and shown to be the best option for the A-stage of the new A-B process. These bioreactors can directly capture COD from wastewater, which allows for energy recovery and minimizes sludge production [154, 253]. However, there are still several important barriers to AnMBR's continuing development. These difficulties stem from the fact that MWW is typically slightly dilute, the waste-to-resource approach requires pre-concentration of MWW before AnMBR [228]. It is possible to pre-concentrate wastewater using membrane filtration to obtain high-quality water while also enriching the non-water components for further recovery. Methods including MF, UF, and RO are currently employed in membrane processes. For instance, Dai et al. [254] demonstrated the efficient use of a UF-RO hybrid system in pre-concentrating MWW to achieve nitrogen and COD concentrations sufficient for the AnMBR process.

As mentioned previously, the development of advanced technologies to prevent membrane fouling will improve the effectiveness of AnMBR technology in recovering energy resources and decreasing the carbon footprint in MWW treatment. Table 2.6 provides a concise overview of the main features of recent techniques used for recovering resources from MWW using AnMBR technology.

Table 2.6 Overview of the main features of recent techniques used for recovering resources from MWW using AnMBR technology

Technology	Recovered resource	Main applications	Potentials	Limitations	Reference
Co-digestion	CH ₄	Renewable energy	Positive net energy balance when co-digestion >40% food waste	Severe fouling which leads to high operation and maintenance costs	[255]
Primary settling and CEPT	CH ₄	Renewable energy	Increase energy recovery through anaerobic digestion of primary settling Obtain a high-quality, methane-free effluent CEPT enhances the removal of pollutants Easy operation and low costs	The wastewater's physicochemical characteristics strongly affect the CEPT efficiency	[256]
Direct membrane filtration	Nutrient-rich water with negligible solids concentration	Agriculture Urban irrigation	Simultaneous energy, water, and nutrient recovery	Not full-scale applications evaluated yet Sensitive areas require nutrient removal	[257]
Forward osmosis	VFA and H ₂ CH ₄ Nutrient-rich water	Agriculture Urban irrigation Nutrient recovery	Low fouling propensity, easy cleaning, high rejection of contaminants, reduced volumetric flow rates, and dissolved methane losses	High energy requirements to operate the RO to produce regenerated water from diluted draw solutions	[258]
Microalgae	Microalgae-based bio-fertilizer after harvesting and composting or thermochemical processes (biochar)	Biofertilizer	Improves soil properties Reduce nutrient losses through a consistent release of nutrients Small carbon footprint. Up to 90% of nutrient content in wastewater	Further treatment is needed for biofertilizers. Low degradability of the cell wall Depends on solar radiation availability	[259]

				Extensive surfaces are required The harvesting phase is still challenging	
Photosynthetic Bacteria	Photosynthetic Bacteria-based biofertilizer after harvesting	Biofertilizer	High yield of hydrogen High tolerance over disturbances Assimilates C, N, and P in a single stage Content of many high-value substances Reduced sludge production	Further treatment is needed for biofertilizer Poor settling properties Depends on infrared light availability Still at the lab scale	[260]
Membrane contactors	Ammonium sulfate	Fertilizer	High N removal efficiencies (>99%) Reduce nitrogen load and aeration energy consumption	Membrane fouling needs further research before developing full-scale applications	
Electrodialysis	Solution with high N and/or P concentrations to produce ammonium sulfate and struvite	Fertilizer	Concentrates N and P from dilute streams such as wastewater MWW P recovery from sewage sludge ashes	Lab scale applications only	[257]
Bioelectrochemical systems	Free ammonia gas that can be absorbed in an acidic solution	Chemical industry Agriculture	High N removal efficiencies (70–90%) Suitable for nitrogen-rich streams: reject water, urine, landfill leachate	Not full-scale applications evaluated yet	
Ion exchange systems	Nutrient-rich water with negligible solids concentration	Fertilizer	Nutrient recovery from the effluent of an AnMBR AnMBR produces a solids-free high-quality permeate	Rarely applied in MWW due to media selectivity, bed clogging, and costly regenerations	[261]

2.4.8 Struvite Precipitation

The use of struvite precipitation as a method for recovering ammonia and phosphate has garnered considerable attention among researchers over the past few decades, and it is feasible on a full scale [262]. Chemical precipitation offers notable benefits in comparison to other technologies for the recovery of N and P and the formation of precipitates, such as $\text{MgNH}_4\text{PO}_4 \cdot 6\text{H}_2\text{O}$ (struvite) and $\text{Ca}_5(\text{PO}_4)_3(\text{OH})$. If the product of the ion concentrations of magnesium (Mg^{2+}), ammonium (NH_4^+), and phosphorus (PO_4^{3-}) exceeds the solubility product of the compounds, struvite crystallization will take place, as indicated in the following chemical equation.



Struvite, commonly known as magnesium ammonium phosphate (MAP), has the chemical formula MgNH_4PO_4 . In the industrial crystallization process, the formation of crystals normally follows three concepts: supersaturation, nucleation, and growth [263]. Supersaturation is often associated with solution pH and ion concentration, both of which are the driving forces behind determining nucleation. Secondly, the crystals that emerge from collisions between ions are nuclei, the process of nuclei formation is defined as the nucleation process. In addition, the process of nuclei growth to crystal is the growth process. Nucleation and growth processes are two essential factors in the study of crystallization kinetics, which are also important in controlling the size and morphological structure of crystals [264]. Nucleation and crystal growth are not independent of each other but often occur simultaneously.

The formation and growth of struvite crystals in WWTPs are affected by various parameters, such as pH, temperature, reaction time, molar ratio of Mg^{2+} , NH_4^+ , and PO_4^{3-} ions, Mg^{2+} source, and the presence of other ions like calcium or carbonates [265].

2.4.8.1 Effect of pH

The crystallization process generally occurs when the solution reaches a supersaturated state, and the supersaturation degree is the driving force for the crystallization process. The main approach to increase the supersaturation of struvite is

increasing the ions concentration or pH value. Compared with increasing the ions concentration, it is more convenient to increase the pH value of the solution [266].

Struvite crystallization is favored by alkaline pH levels, with optimal conditions typically falling within the range of 8.5-9 [267]. Studies have shown that increasing pH can lead to a decrease in the mean crystal size of struvite [268]. Additionally, within the pH range of 8.5-9, struvite solubility is lower, and crystallization rates are higher [269]. Higher pH levels have been found to promote struvite formation [270].

2.4.8.2 Effect of temperature

Research has shown that specific temperatures can impact struvite formation differently. For example, temperatures of 33 °C and 40 °C are not ideal for struvite precipitation as they can result in decreased purity and ammonia losses [271]. Conversely, studies have demonstrated that crystallization between 10 and 50 °C, under certain pH levels and stirring conditions, can lead to the retrieval of a high phosphorus percentage in the form of fine struvite crystals [267]. Furthermore, higher temperatures have been linked to increased crystal growth and size of struvite [272]. However, some studies suggest that temperature changes may have a mild effect on struvite reaction rates, with temperature increases causing almost negligible changes in crystal size in certain cases [273]. Moreover, temperature variations can influence the solubility of struvite, a critical aspect of its crystallization process. Investigations have revealed that temperature fluctuations can alter the solubility of struvite, making the crystals more soluble under specific temperature conditions [274].

2.4.8.3 Effect of reaction time

The kinetics of struvite crystallization are intricate, with fractional order reactions indicating multiple steps rather than a single step, impacting the overall process [267]. Moreover, the presence of nucleation sites such as brucite particles can decrease induction times and increase crystallization rates, thereby affecting the reaction kinetics [275]. Additionally, prolonged reaction times facilitate the formation of struvite crystals from intermediate phases, while variations in reaction time can affect crystal growth rates, crystal lattice defects, and overall process efficiency [276].

2.4.8.4 Effect of Mg:P:N molar ratio

The concentration of reacting ions is one critical factor for determining the supersaturation of the struvite crystallization process. It can be said that the molar ratio of reacting ions in solution makes a significant contribution to the struvite crystallization process. Chemical equation of the struvite precipitation reaction shows in wastewater solution by the Mg:P:N theoretical molar ratio of 1:1:1. However, to ensure that phosphorus is removed with high efficiency, an excessive amount of ammonium or magnesium or both elements is often added. In a study conducted by Gong, et al. [277], the molar ratio of Mg:P was increased from 0.8 to 1.2. Consequently, the rate of phosphorus removal increased from 80.8 to 95.5%. This is because other insoluble compounds of magnesium and phosphorus were formed along with struvite crystals [278].

2.5 Conclusion and Future works

Current studies are focusing on strategies to maximize the recovery of resources from MWW focus on avoiding or handling such a dilute and complex mixture [59, 69, 91]. Energy and nutrient recovery are simply not economically viable when using current technologies and practices. Intervention at both the household and WWTP levels may be required, with source separation, co-digestion, and pre-concentration representing three feasible strategies to facilitate maximum resource recovery.

Source separation is a notable strategy to maximize resource recovery as the problem of dilution is essentially avoided. Wastewater can be divided into concentrated black water and less concentrated grey water. The concentrated streams could effectively undergo direct anaerobic treatment for energy recovery, and dilute streams would present a more favorable approach to water recovery. Furthermore, urine can be source-separated from black water for nutrient recovery, as urine contains high concentrations of nitrogen and phosphorus. Separating wastewater at the source presents more tangible resource recovery opportunities, however, the considerable infrastructural

investment associated with upgrading collection systems has often limited its implementation [279].

An alternative strategy to address the diluted nature of MWW is to encourage the disposal of other organic wastes to maximize energy recovery through co-digestion at WWTPs. This can be achieved by encouraging households to add kitchen waste to wastewater using grinders [280]. Otherwise, on a community scale waste could be disposed of directly to digesters at WWTPs, including organics originating from municipal solids waste, industrial by-products, or agricultural crop residues [281]. The latter is more favorable, as an addition at households may not significantly increase wastewater concentrations and would still require separation processes at the WWTP before anaerobic digestion. At the same time, co-digestion at the WWTP does not directly resolve the issue of dilute wastewater and therefore pre-concentration techniques in combination with co-digestion would be desirable.

Pre-concentration strategy is the term that denotes an advanced concentration process to increase the amount of organic matter separated from wastewater so that energy and nutrient recovery becomes more feasible [282]. Unlike source separation or the addition of other organics, pre-concentration manages dilute wastewater at a centralized WWTP. Pre-concentration would be most effectively implemented if applied to raw wastewater, however, additional opportunities do exist. Since pre-concentration essentially describes a separation technique that results in clean water and a concentrated stream, this strategy could be implemented at many stages of WWTPs. Current WWTP processes essentially perform pre-concentration, however, an increased emphasis on maximizing recovery is required and a major limitation involves the need for further treatment to recover high-quality water. This results in the heightened need to reinvent and optimize wastewater treatment for integrated resource recovery. This idealistic objective personifies efforts to purify wastewater and with continued technological development, may be realized for new or re-developments in the near future.

Pre-concentration could be effectively applied at several stages during wastewater treatment, with Figure 2.11 presenting a possible scenario [283]. Firstly, primary treatment aims to remove suspended solids and can be achieved by gravity separation in clarifiers as well as fine screening. The pre-concentration process would then recover

high-quality water whilst simultaneously concentrating organic compounds. The resultant sludge from both primary treatment and pre-concentration would then undergo anaerobic digestion to produce biogas for energy production, utilizing a combined heat and power system. Solids and liquids from the digester are separated to produce biosolids and sludge centrate respectively. Biosolids are utilized for beneficial reuse, whilst centrate can undergo further processing to concentrate nutrients to enable phosphorus recovery. The composition of the remaining liquid is highly dependent on the rejection of each pre-concentration technique. Ideally, this stream would have a very low volume and the additional process that would be required for the concentration management may involve a low-energy nitrogen removal technique.

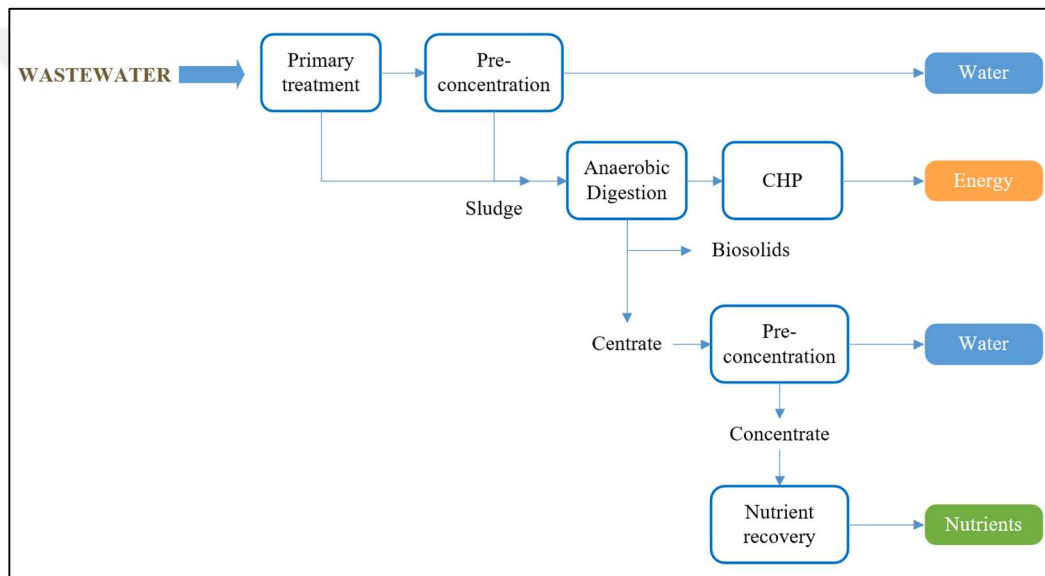


Figure 2.13 Pre-concentration-based flow sheet for integrated resource recovery [283]

Water, energy, and food security are intricately interconnected. Essential human entitlements and the factors that pave the way for economic and social progress encompass the availability of secure potable water and sanitation facilities, dependable and affordable energy necessities, and food that is both safe and nutritional. The establishment of a reliable water supply is influenced by the presence and accessibility of sufficient water resources. Water is crucial for maintaining energy security due to its significant usage in the extraction and processing of fossil fuels, the cultivation of biofuels, and the generation of electricity. Moreover, agriculture is the largest consumer of water worldwide, making water availability crucial for food production.

In the future, as the population continues to grow, there will be more competition and pressure to access limited natural resources on a worldwide basis. The projected limitations of natural resources highlight the necessity for a comprehensive strategy and improved alternatives to enhance their security currently. This approach takes into account the interdependence of each sector and aims to create solutions that are compatible with sustainable development. Various possibilities are available to enhance the security of water, energy, and food. An essential aspect of this thesis is the utilization of waste as a valuable resource in multi-purpose systems.

AnMBRs have the capability to transform existing WWTPs by enabling the simultaneous extraction of purified water, energy, and nutrients. Ongoing attempts to increase the concentration of MWW to a level that is sufficient for AnMBR treatment and following resource recovery may promote the process. Investigating innovative bioreactor designs, such as AnFMBR, has demonstrated significant potential for reducing energy consumption and improving performance. This advancement is likely to contribute to wastewater treatment plant operations becoming net energy positive.

The primary nutrients, phosphorus, and nitrogen, have the ability to form struvite crystals, which can be used as a fertilizer for various purposes in agriculture. Efficient struvite recovery from wastewater streams relies on optimizing the influencing conditions. Struvite recovery can enhance a sustainable MWW management strategy, thereby promoting a circular economy. In the context of the circular economy, it is possible to recycle nutrients that have been lost and reintroduce them into the soil.

Chapter 3

Pre-concentration of municipal wastewater using flocculation assisted direct ceramic microfiltration process: Optimization of operational conditions¹

3.1 Introduction

Due to the scarcity and depletion of natural resources, wastewater should be considered as a renewable resource, from which water, OM, and nutrients can be recovered [284]. In conventional wastewater treatment processes, large amounts of energy are consumed for aeration to promote biological oxidation for OM degradation and nutrient removal [7]. OM in MWW can be regarded as a resource for energy production via anaerobic digestion [285] to generate methane, hydrogen, or volatile fatty acids (VFAs) as the concentration of OM is generally in the range of 250–1000 mg

¹ This chapter was published as:

Ozcan, O., Sahinkaya, E., & Uzal, N. (2022). Pre-concentration of Municipal Wastewater Using Flocculation-Assisted Direct Ceramic Microfiltration Process: Optimization of Operational Conditions. *Water, Air, & Soil Pollution*, 233(10), 420.

COD/L [286, 287]. Theoretically, the energy content in 1 g COD is around 3.5 kWh, which means the average MWW may contain 1.66 kWh/m³ energy. Hence, the energy contained in MWW maybe around four times higher than the energy required for a conventional activated sludge treatment process [284]. Conversion of OM in wastewater to methane, hydrogen, and VFAs under anaerobic conditions are alternative process for energy recovery. However, it is well known that the hydrolysis of suspended solids in MWW is the rate-limiting step at low temperatures [288] and may require a mesophilic temperature range of 25-37°C. However, increasing the reactor temperature to the proper values may lead to the anaerobic process as energy-consuming rather than producing as around 1.2 kWh/m³ energy is needed to increase water temperature for 1°C [288]. Hence, OM in the wastewater should be pre-concentrated to make the anaerobic treatment a more efficient and energy-positive process. Transitioning from aerobic towards anaerobic-based treatment processes offers the potential to considerably minimize the energy consumption of wastewater treatment by avoiding aeration and achieving energy-neutral wastewater treatment through biogas production [9, 254, 285, 289]. For the pre-concentration of MWW, DMF, dynamic sand filtration, centrifugation, CEPS, dissolved air flotation, biological adsorption processes, and high-rate activated sludge processes are applied individually or in combination [128, 284, 290]. DMF of MWW has a significant potential owing to the simplicity of operation, low net energy requirement, high quality of treated water, high-water recovery ratio and generation of the concentrated stream to be further used for energy generation [291-296]. Ceramic membranes are more attractive than polymeric membranes due to their high filtration flux, low fouling behavior, and unique thermal, and mechanical resistance [297-300]. ceramic membranes have become more widely used in recent years for various water and wastewater treatments as a result of ongoing material development and lower prices [301]. Although using ceramic membranes within the DMF process has become more attractive [302], limited studies have been reported on the use of CMs for DMF of MWWs [303, 304].

The main problem in the application of the DMF process alone is fouling and the flux decreases like other pressure-driven processes [305, 306]. To overcome membrane fouling by removing or agglomerating the colloidal substances from wastewater, the CEPS process is an effective approach that applies chemical coagulants to greatly improve the removal of pollutants from wastewater by precipitation [307]. CEPS has

several advantages in wastewater treatment such as low investment cost [286], low energy requirement [308], ease of operation and maintenance [309], etc. For all these reasons, CEPS has been commonly utilized both in MWW treatment and also in industrial wastewater treatment for recent decades [310]. Moreover, CEPS has come into prominence in recent years, especially in OM/nutrient recovery from MWW, and is used as an alternative to conventional wastewater treatment processes [311-314]. Czerwionka et al. [311] reported that biogas production was increased by 65-80% in anaerobic digesters after the CEPS process with an increase in OM removal efficiency of primary settling tanks. Zhao et al. [303] also emphasized the advantages of the pre-coagulation process as a MWW pre-concentration method. They reported that the pre-coagulation process reduced the loading on membrane filtration and high amounts of OM and phosphorus were recovered from the sewage. However, the coagulation process, in which iron or aluminum salts are widely used [315-318] as a fouling reducer for membrane processes, may cause metal contamination in both supernatant and sludge [319]. In addition, because the concentration of chemicals used in coagulation is higher than flocculation, it increases the treatment process cost. Metal salts used in the coagulation process may also negatively affect the anaerobic treatment performance of the concentrated stream [320]. Hence, in recent years, much research has been conducted on the recovery of OM from MWW, and still, the development of novel process alternatives is needed to develop energy-neutral processes. The DMF system is commonly implemented in previous studies for the pre-concentration of MWW [321, 322]. However, as few studies have been conducted on DMF applications using ceramic membranes, more research is required to optimize process performance and membrane cleaning strategies [304]. Furthermore, to the best of our knowledge, there is a gap in the literature for evaluation of the dosing point in the flocculation process using PAM, which would serve to increase process effectiveness. Particularly, in order to achieve long-term, sustainable membrane filtration, it is quite essential to consider the effect of PAM dosing point and operating parameters on permeate quality and membrane filtration performance. Hence, this study aims at evaluating the performance of PAM assisted direct ceramic membrane filtration process for MWW treatment and OM recovery in the concentrated stream. The developed novel process was tested and optimized first in lab-scale before implementing it in pilot and then real-scale processes. In order to demonstrate the feasibility of the process on a real scale, the potential energy

production potential was calculated based on the flow data of current municipal WWTP in Kayseri, Turkey.

3.2 Materials and methods

3.2.1 Membranes and Chemicals

Cationic polyacrylamide (PAM, Hydrofloc, Italy) of high molecular weight, medium-high cationic load, and bulk density of 0.7-0.8 g/cm³ has been used as the flocculating agent. The stock solution of 0.1wt% PAM was used as polyelectrolyte in the flocculation experiments. Sodium Hydroxide (NaOH, Merck) and nitric acid (HNO₃, Merck) were used in cleaning the ceramic membrane [323, 324]. All solutions were prepared using deionized water in the experiments. The raw material of the operated ceramic membrane was silicon carbide. The pore size of the membrane was 0.1 μm. The length × width × thickness of the membrane plate was 230 mm × 150 mm × 6 mm. The effective membrane area was 0.069 m².

3.2.2 Wastewater and analysis

Raw MWW was collected from the primary settling tank effluent of the Kayseri municipal WWTP (Turkey). The characteristics of samples are given in 3.1. Collected samples were stored at 4 °C and samples were warmed up to room temperature (20 ± 5 °C) before use. The turbidity of wastewater samples was measured using a turbidimeter (TN100, Thermo Scientific, USA). EC and pH were measured using a 3620 IDS WTW multiparameter (WTW GMBH, Germany). Anion Chromatography (AC) was performed on a Metrohm equipped with a Metrosep A Supp 5 (150 mm) analytical column and Metrosep C4 (4 mm) guard column to measure chloride (Cl⁻), sulfate (SO₄²⁻), phosphate-phosphorus (PO₄-P), and nitrite-nitrogen (NO₂-N). COD, TSS, and ammonia-nitrogen (NH₄-N) analyses were carried out following the “Standard Methods for Water and Wastewater” of the American Public Health Association [325].

Table 3.1 The characteristics of primary sedimentation tank effluent

Parameters	Raw Wastewater
pH	7.3
Conductivity ($\mu\text{S}/\text{cm}$)	1476 - 1653
COD (mg/L)	324.4 - 468
NO ₂ -N (mg/L)	1.1 - 1.2
NH ₄ -N (mg/L)	41.9 - 41.7
PO ₄ -P (mg/L)	9.8 - 12.2

3.2.3 Jar Tests

The flocculation performance of the cationic flocculant (PAM) was tested using a jar test with a six-paddled Jar Tester (Velp JLT6, Italy) on a bench of equal size. The procedure applied in jar test experiments is; after the dosing of 0.5, 1, 1.5, and 2 mg/L PAM, 2 minutes of rapid mixing (120 rpm), 15 minutes of slow mixing (15 rpm), and 15 minutes of sedimentation were performed. The supernatant liquid was carefully withdrawn from each beaker using a pipette from the supernatant for COD, turbidity, TSS, and PO₄-P analysis. For the control sample, wastewater was settled for 15 minutes without dosing PAM. All tests were conducted at room temperature in the range of 20–25 °C. Before jar tests, the pH of the wastewater samples was adjusted to 7.0. The jar test was performed in duplicate, and the samples were characterized in each jar test. The average values are presented with standard deviations.

3.2.4 Experimental set-up and operational conditions

After examining the effect of flocculant concentration on the removal of COD, turbidity, TSS, and PO₄-P in jar test experiments, three-step optimization experiments were performed in DCMF tests: (i) optimization of flocculant dosing point and concentration, (ii) optimization of operational conditions, and (iii) long-term operation. The methodology of DCMF filtration tests is summarized in Figure 3.1.

In the first step of the DCMF experiments, the polyelectrolyte dosing point and polyelectrolyte concentration were optimized. DCMF experiments were carried out for two different flocculant dosing points, including one-time PAM dosing in the CEPS process before DCMF (CEPS+DCMF) and continuous dosing of PAM during the DCMF process (PAM+DCMF). For the optimization of flocculant concentration and

dosing point, the pH, flux, recovery ratio, and filtration/backwash duration were kept constant at pH 7.0, 20 LMH flux, 90% recovery rate, and 5/1 min filtration/backwash duration, respectively. The experiments were carried out by changing only the flocculant concentration and dosing point. NaOH and H₂SO₄ solutions were used to adjust the wastewater pH to 7.0. The filtration cycle included 5 minutes of filtration suction and 1 minute of backwash. The flux was 20 LMH during the backwash. 10% of the feed flow was removed from the system as a concentrate to keep the recovery rate constant at 90%. The HRT value was computed as 187 minutes based on the feed flow rate employed during the operation of the DCMF reactor, which is low enough to eliminate biological oxidation.

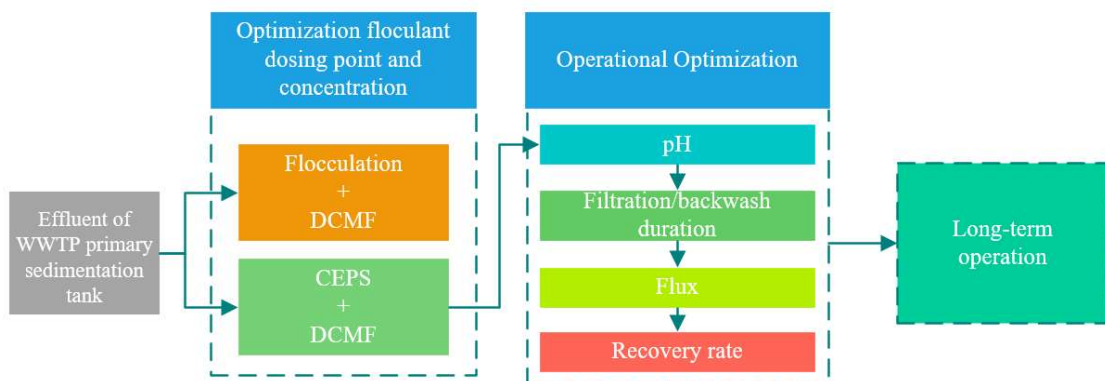


Figure 3.1 Optimization of DCMF filtration

In the second step of DCMF tests, the operating parameters of the DCMF process were optimized using the optimal flocculant dosing point and concentration determined in the first stage of DCMF tests (Figure 1.1). The operational parameters were optimized according to Table 3.2, by changing one parameter while keeping the others constant.

Table 3.2 The procedure followed in the optimization of the CEPS+DCMF process

Optimization Parameters	Operational conditions				
	pH	Flux (LMH)	Water recovery rate (%)	Poly concentration (mg/L)	Filtration/Backwash duration (min)
pH	6, 7, 8	20	90	0.5*	5/1
Filtration/backwash duration (min)	7	20	90	0.5*	5/1, 10/1, 10/2
Flux (LMH)	7	20, 30, 40	90	0.5*	10/2*
Recovery ratio (%)	7	20*	70, 80, 90	0.5*	10/2*

* These values were optimized in the dosing point optimization experiments.

Schematic diagrams of PAM+DCMF and CEPS+DCMF processes are given in Figure 3.2 a and b, respectively. The dimensions of the reactor used in the system are 40x20x8.5 cm giving the total and effective volumes of 5.2 L and about 3.2 L, respectively. A flat-sheet membrane module was vertically fixed in the tank and the filtrate was withdrawn through the membrane by a suction pump (Longer Pump, China). In addition, the formation of the cake layer was minimized by aeration of the membrane from the bottom of the reactor with a flow rate of 0.2 m³/(m²h). The concentrated and feed wastewater samples were characterized in each DCMF test, which was performed in duplicate. The average values are presented with standard deviations.

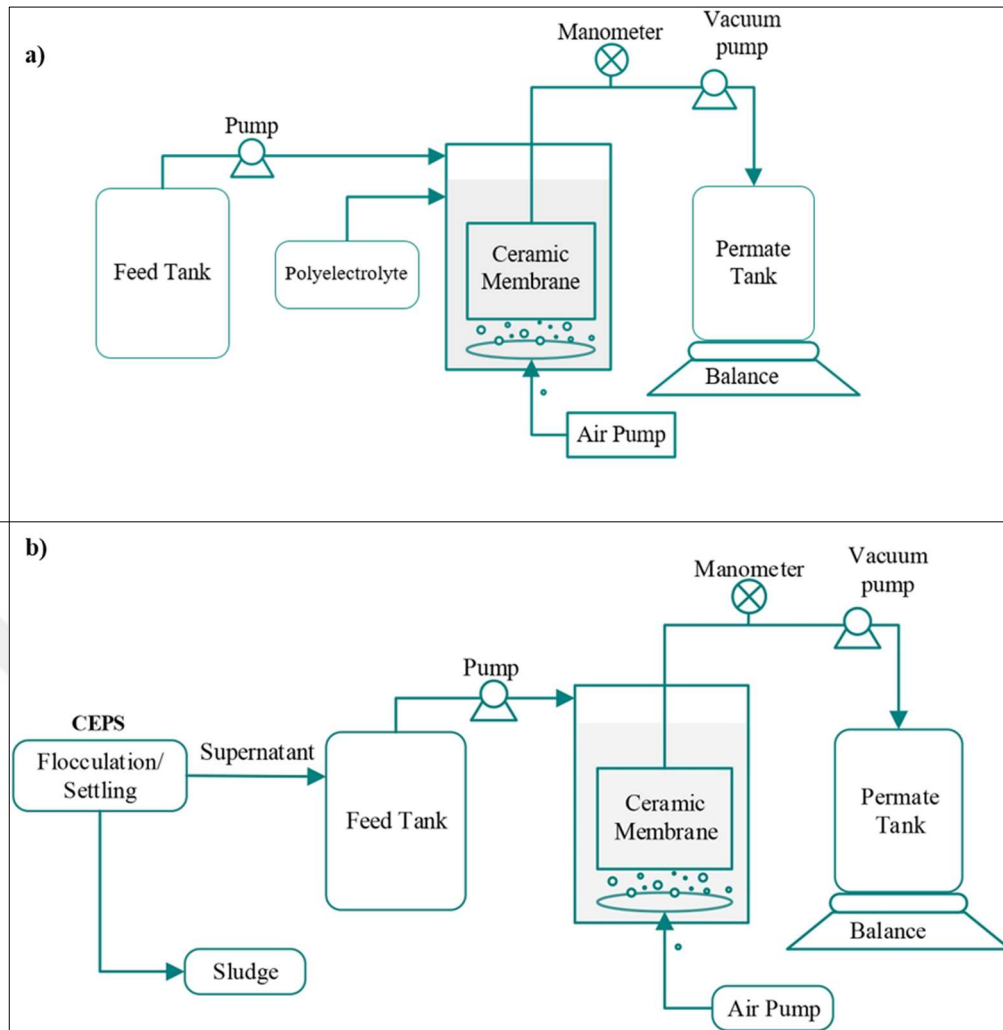


Figure 3.2 Schematic diagram of the (a) PAM+DCMF and (b) CEPS+DCMF process

In the third step, the long-term operation of the DCMF process was carried out after optimization of the dosing point and the operating conditions. CEPS+DCMF system was continuously operated for 20 days for treating primarily treated MWW. The system was operated for 6 hours for every run each day. During the long-term operation, 3 virgin membranes, the properties of which are given in Section 3.2.1, were used in a loop. The steps that take place in this loop are as follows; filtration was carried out in the DCMF reactor with one membrane, the second fouled membrane was physically cleaned after filtration, and the third membrane was chemically cleaned after physical cleaning. TMP behavior, as well as the characterization of concentrated wastewater and permeate, were investigated. During a typical operation, permeate was produced from 90% of the wastewater (23 mL/min) through the CM. Concentrated wastewater suspension was retained at a 10% rate. Once the TMP reached 700 mbar, the membrane

was cleaned by physical and chemical methods to recover its permeability. The membrane cleaning methods are given in detail in Section 3.2.5.

3.2.5 Membrane Cleaning

After each DCMF filtration experiment, the cake layer is physically cleaned with a sponge and backwashed with pure water. For the chemical cleaning of membranes, NaOH (0.5 M) and HNO₃ (0.5 M) solutions were used separately. According to the membrane cleaning procedure applied, the fouled membranes were taken out of the reactor and submerged in chemical solutions for offline cleaning. A three-stage cleaning procedure was applied to minimize flux loss in the ceramic membrane used in DCMF experiments. Details of the cleaning procedure are as follows:

- Physical cleaning: After each DCMF filtration, the cake layer was cleaned with a sponge, and soft brushing was applied to the membrane then 5 minutes backwash was applied with pure water to remove the remaining foulants from the membrane surface.
- Chemical cleaning with NaOH solution: Physically cleaned membrane was immersed in 0.5 M NaOH solution for 15 hours. After NaOH cleaning, backwashing was applied with pure water for 5 minutes to remove the remaining pore-blocking foulants.
- Chemical cleaning with NaOH (0.5 M) and HNO₃ (0.5 M) solutions: This procedure was applied after each parameter optimization during the DCMF tests. The membrane was first immersed in 0.5 M NaOH and then 0.5 M HNO₃ solution for 15 hours each. Following this chemical cleaning, the membrane was rinsed by backwashing with pure water for 5 minutes.

3.2.6 Specific fouling rate

The specific fouling rate (SFR, g m⁻² h⁻¹) is defined as the increase in the mass of foulants per square meter per hour and was calculated by using the Equation 3.1,

$$\text{SFR} = \frac{\Delta m}{(A \times \Delta t)} \quad (\text{Eq. 3.1})$$

where m is the foulant mass (g), A is the membrane area (m²), and t is the filtration duration (h).

3.3 Results and discussion

3.3.1 Flocculation performance at different PAM concentrations

Preliminary testing of polyelectrolytes with standard jar tests is essential for deciding the optimum polyelectrolyte dosage [326]. Therefore, COD, TSS, and turbidity removals at different PAM concentrations were determined by keeping pH at 7.0 in jar tests. Figure 3.3 shows the average COD, TSS, and turbidity removal rates and standard deviations for the duplicate jar test experiments. Even with the lowest concentration of 0.5 mg/L PAM, significant improvement in the sedimentation was observed, which in turn increased the removal efficiencies (Figure 3.3). The COD removals without and with 0.5 mg/L PAM were 22% and 26%, respectively. Increasing PAM dosage over 1 mg/L did not enhance COD removal efficiency, although 1, 1.5, and 2 mg/L PAM doses showed relatively similar values for COD removal efficiency (i.e., 31, 28, and 30%, respectively). Although the TSS removals were quite similar at 1 and 1.5 mg/L PAM dosages, the highest TSS removal (82%) was achieved at 2 mg/L PAM.

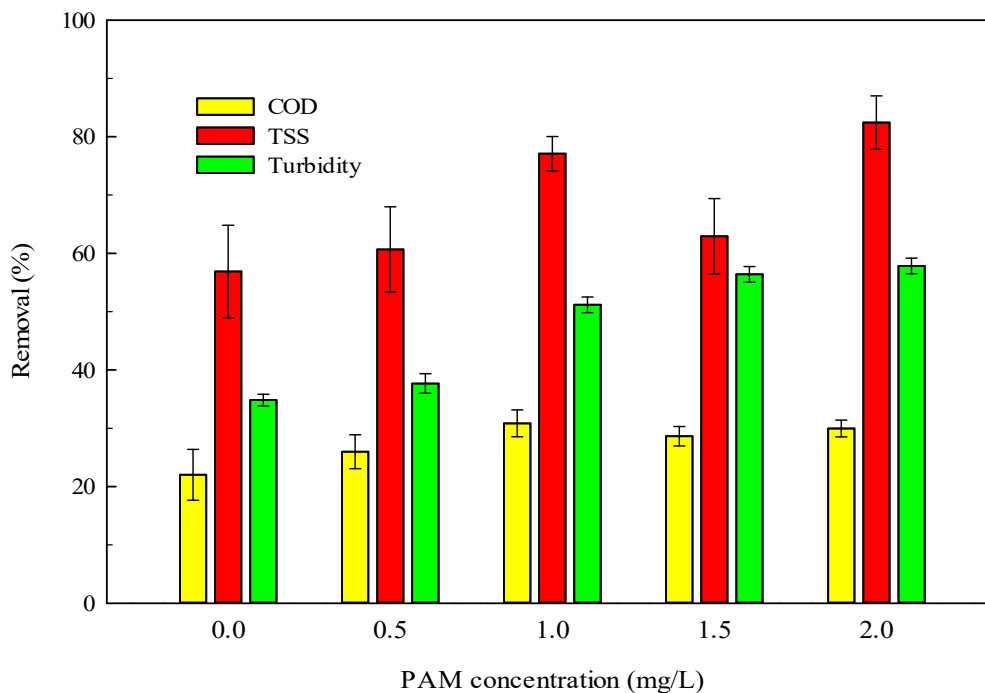


Figure 3.3 COD, TSS, and turbidity removals at varying PAM concentrations in jar tests

Besides COD, TSS, and turbidity measurements, the effluent of the jar test was also characterized in terms of pH, conductivity, and PO₄-P concentration (Table 3.3). After the PAM dosage, the pH was slightly changed ranging between 7.2 and 7.4. The performance of flocculants is inherently not pH-dependent and does not cause any significant changes in pH [327-329]. In addition, conductivity decreased to 1976±8 μS/cm in PAM-dosed samples. The highest PO₄-P removal (57%) was obtained at 2 mg/L PAM.

Table 3.3 The impacts of PAM concentration on pH, conductivity, and PO₄-P

Samples	pH	Conductivity (μS/cm)	PO₄-P (mg/L)
Raw wastewater	7.2±0.1	2010±25	5.6±0.4
Without PAM	7.3±0.2	2020±14	5.5±0.2
0.5 mg/L PAM	7.4±0.0	1976±8	5.6±0.1
1 mg/L PAM	7.4±0.1	1988±9	5.7±0.2
1.5 mg/L PAM	7.4±0.1	1982±9	5.0±0.6
2 mg/L PAM	7.4±0.0	1987±10	2.4± 0.7

3.3.2 Determination of optimum configuration

To determine the optimum PAM dosing point and its concentration, DCMF experiments were conducted for two different configurations: PAM+DCMF and CEPS+DCMF as detailed in Section 3.2.4.

The filtration performance of DCMF for two different configurations was determined in terms of the OM recovery and TMP elevation. The TMP changes for different configurations, i.e. PAM+DCMF and CEPS+DCMF, at varying PAM dosages were provided in Figure 3.4 a and b, respectively. To evaluate the impact of PAM on filtration performance, the DCMF experiment was also conducted in the absence of PAM dosing.

In the DCMF tests without PAM addition, TMP increased above 350 mbar after 240 minutes. For the PAM+DCMF tests, using 0.5, 1, 1.5, and 2 mg/L PAM concentrations, TMP increased above 350 mbar after 205, 187, 184, and 200 minutes, respectively. On the other hand, TMP increased above 350 mbar after 268, 269, and 266

minutes at 0.5, 1, and 1.5 mg/L PAM concentrations, respectively, in the CEPS+DCMF configuration. The positive effect of PAM dosing on TMP could not be obtained in PAM+DCMF experiments. Similarly, Malkoske et al. [330] evaluated the effect of coagulation and flocculation on low-pressure MF and UF processes and obtained the greatest reduction in membrane fouling in CEPS+DMF processes. Additionally, the high molecular weight polyelectrolytes may accumulate and form a gelatinous layer on the membrane surface, leading to a greater loss of flux and increasing the TMP [331]. As seen in Figure 3.4a, the PAM+DCMF cannot overcome the fouling problem due to this cake layer formation. Nevertheless, in the CEPS+DCMF process, gel layer formation on the membrane was prevented, which showed a positive effect in terms of TMP.



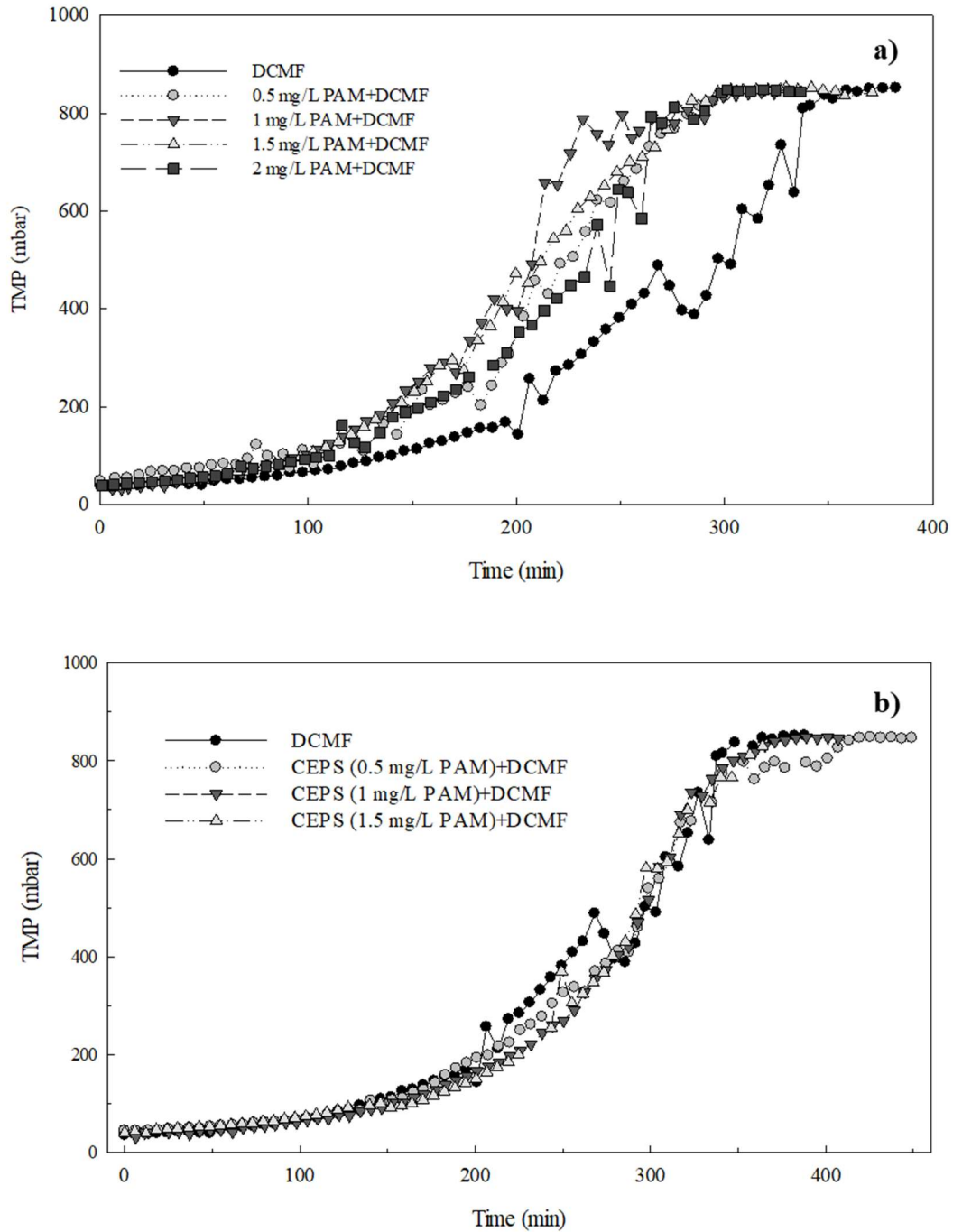


Figure 3.4 TMP profile as a function of time for (a) PAM+DCMF and (b) CEPS+DCMF

In order to investigate the effect of PAM dosing and the CEPS process on cake layer formation, the cake layer was collected with water and softly brushed after each filtration experiment, and the SFR was calculated. Firstly, the concentrations of TSS were converted to mass for comparison and the mass amounts of the cake layer were calculated. In the DCMF experiments without PAM, the mass of the cake layer was

270±88 mg. In the PAM+DCMF experiments, the mass of the cake layer was 10.3±1.3, 9.7±1.1, 12.9±1.4, and 13.3±0.9 g/m², respectively, at 0.5, 1, 1.5, and 2 mg/L PAM dosages. Nevertheless, for CEPS+DCMF experiments, the TSS of the cake layer was 3.3±0.6, 3.1±0.1, and 3.5±0.7 g/m², respectively, at 0.5, 1, and 1.5 mg/L PAM dosages. According to the mass of the cake layer, the average SFR values and standard deviations for the duplicate filtration experiments are presented in Figure 3.5. The increase in PAM dosage promoted the cake layer formation by supporting the adhesion of the solid matter on the membrane.

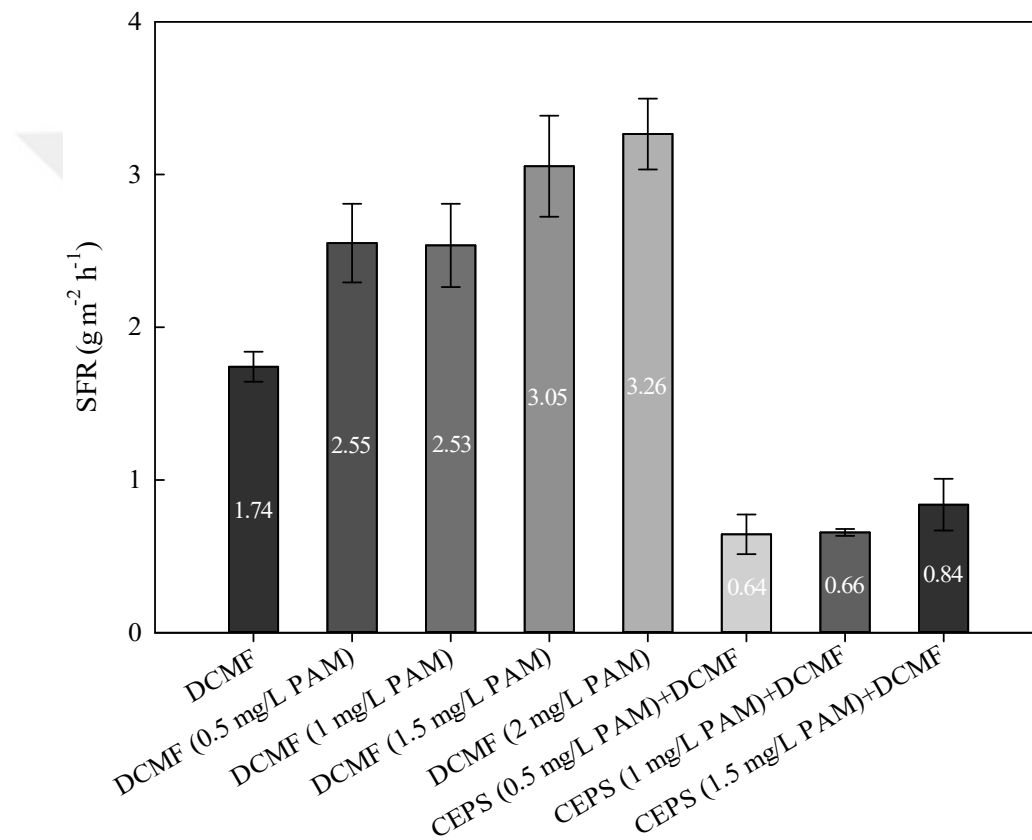


Figure 3.5 Comparison of specific fouling rate (g m⁻² h⁻¹) for DCMF, PAM+DCMF, and CEPS+DCMF processes

The characteristics of concentrated wastewater streams for two different DCMF configurations are given in Table 3.4. The PAM+DCMF experiments did not show better performance for the pre-concentration of the wastewater, like the performance of filtration performance based on TMP results. Since PAM+DCMF causes the polyelectrolyte to be attached to the reactor walls, membrane surface, and reactor equipment such as pipes and connections, COD content could not pass into the

concentrate stream with the sludge pump [332-334]. The highest COD concentration of the concentrate (520 ± 20 mg/L) was achieved for 0.5 mg/L PAM dosing in CEPS+DCMF (Table 3.4). The lowest concentration of $\text{NH}_4\text{-N}$ was obtained with 0.5 and 1.0 mg/L PAM CEPS+DCMF (37.9 and 35.7 mg $\text{NH}_4\text{-N/L}$) in concentrated wastewater samples. The low concentration of $\text{NH}_4\text{-N}$ is an advantage in further anaerobic energy recovery studies, as the high concentration of $\text{NH}_4\text{-N}$ will be toxic to methanogens [335]. Furthermore, $\text{PO}_4\text{-P}$ was recovered in the CEPS+DCMF process at higher performance. $\text{PO}_4\text{-P}$ concentration range in the concentrated streams of PAM+DCMF and CEPS+DCMF were between 8.0-9.9 mg $\text{PO}_4\text{-P /L}$ and 9.6-12.5 mg $\text{PO}_4\text{-P/L}$, respectively.



Table 3.4 Characteristics of the concentrated wastewater after the DCMF process with different PAM concentrations and configurations

Processes/Parameters		pH	Conductivity ($\mu\text{S}/\text{cm}$)	COD (mg/L)	$\text{NO}_2\text{-N}$ (mg/L)	$\text{NH}_4\text{-N}$ (mg/L)	$\text{PO}_4\text{-P}$ (mg/L)
DCMF		7.5 \pm 0.3	1667 \pm 105	495 \pm 4	1.3 \pm 1.0	47.8 \pm 0.9	8.1 \pm 0.6
DCMF+(0.5 mg/L PAM)		7.5 \pm 0.4	1642 \pm 47	340 \pm 42	1.5 \pm 0.1	44.3 \pm 2.2	8.1 \pm 0.6
DCMF+(1 mg/L PAM)		7.4 \pm 0.2	1380 \pm 404	352 \pm 4	1.4 \pm 0.2	44.1 \pm 8.4	9.9 \pm 3.2
DCMF+(1.5 mg/L PAM)		7.5 \pm 0.1	1628 \pm 66	325 \pm 18	1.2 \pm 0.1	38.2 \pm 1.1	8.0 \pm 0.8
DCMF+(2 mg/L PAM)		7.5 \pm 0.1	1782 \pm 19	331 \pm 41	1.1 \pm 0.1	49.4 \pm 0.1	9.7 \pm 2.7
CEPS+DCMF (0.5 mg/L PAM)	Feed*	7.4 \pm 0.1	1586 \pm 185	480 \pm 181	1.4 \pm 0.1	35.7 \pm 9.1	11.5 \pm 1.2
	Concentrate	7.5 \pm 0.1	1474 \pm 115	520 \pm 20	0.9 \pm 0.1	37.9 \pm 6.6	11.3 \pm 0.3
CEPS+DCMF (1.0 mg/L PAM)	Feed*	7.6 \pm 0.5	1599 \pm 62	352 \pm 90	0.9 \pm 0.1	36.8 \pm 13.3	10.8 \pm 2.2
	Concentrate	8.1 \pm 0.7	1599 \pm 75	341 \pm 98	1.0 \pm 0.1	35.7 \pm 11.8	9.6 \pm 2.3
CEPS+DCMF (1.5 mg/L PAM)	Feed*	7.5 \pm 0.2	1664 \pm 8	423 \pm 75	1.1 \pm 0.1	43.8 \pm 0.2	12.3 \pm 1.8
	Concentrate	7.8 \pm 0.5	1663 \pm 35	429 \pm 79	1.0 \pm 0.1	46.7 \pm 3.1	12.5 \pm 1.2

*Supernatant of CEPS process was used as feed.

PAM is known as a common polymer used for flocculation while it is non-toxic to humans, animals, and plants. However, residual monomers in PAM can cause some environmental problems [336]. Since the high concentration of the chemicals used will restrict the reuse of sludge in various applications with a circular economy approach, e.g. in agriculture, after appropriate treatment processes, small chemical dosages should be considered in the process [337, 338]. In addition to the OM recovery and fouling tendency, the chemical costs must be taken into account in deciding the optimum chemical dosage [339]. Therefore, the optimum flocculant concentration considering OM recovery, filtration performance, and the chemical cost was determined as 0.5 mg/L PAM.

3.3.3 Optimization of operational conditions of the DCMF process

The effective membrane fouling control approaches by determining optimum operational conditions may extend the lifespan of the membranes and reduce operational costs [340, 341]. The optimization of operational conditions is crucial to achieve sustainable long-term operations of DMF processes [321, 340]. After the determination of the optimum PAM concentration and process configuration, the operating conditions were optimized in terms of pH, flux, filtration/backwash duration, and water recovery ratio for the CEPS+DCMF mode of operation.

Influent and effluent wastewater characteristics in the CEPS process are presented in Table 3.5. There are no significant removals of $\text{NO}_2\text{-N}$, $\text{NH}_4\text{-N}$, and $\text{PO}_4\text{-P}$ at 2%, 4%, and no removal, respectively. However, the most significant removal was observed for TSS reduced from 184 ± 57 to 108 ± 55 after the CEPS process, which is crucial for controlling the cake layer developing on the membrane surface. Besides, COD was decreased from 496 ± 92 to 388 ± 86 mg/L in the CEPS process with 0.5 mg/L PAM dosing.

Table 3.5 The characteristics of raw wastewater and CEPS process effluent

Parameters	Raw WW	0.5 mg/L PAM dosing*
pH	7.4±0.2	7.5±0.2
Conductivity (µS/cm)	1624±199	1678±90
COD (mg/L)	496±92	388±86
TSS (mg/L)	184±57	108±55
NO ₂ -N (mg/L)	1.0±0.4	1.1±0.2
NH ₄ -N (mg/L)	47.0±1.3	46.0±2.2
PO ₄ -P (mg/L)	10.0±0.9	9.6±1.1

*The average values are presented here with ± indicating the standard deviations for 15 samples collected after every CEPS experiment.

3.3.4 Optimization of pH

After determining the optimum polyelectrolyte concentration, pH was optimized with jar tests at 0.5 mg/L PAM dosing. The pH of the raw wastewater was 7.3. In determining the optimum pH in jar tests, the pH of the samples was adjusted to 6, 7, and 8 using H₂SO₄ or NaOH solutions. Each jar test was performed in duplicate for different pH values and the conductivity and COD parameters were measured after each test and the results are presented in Table 3.6. COD removal efficiencies at pH 6, 7, and 8, were quite similar at 49.2, 46.1, and 49.2%, respectively. On the other hand, the lowest removal efficiency in terms of COD was obtained in the experiments conducted with the pH (7.3) of the raw wastewater. Filtration experiments were carried out at pH 7 and without pH adjustment due to the insignificant differences in COD removal obtained in the jar tests. It has also been stated that flocculation is not a process that requires pH adjustment, unlike the coagulation process [326, 342].

Table 3.6 Effect of pH on COD removal performance of CEPS process conducted at 0.5 mg/L PAM

pH	Conductivity (µS/cm)	COD (mg/L)	COD removal (%)
Raw wastewater	1639	305±5	-
7.3	1632±3	210±1	40.5±0.3
6	1762±8	180±7	49.2±2.0
7	1653±16	190±8	46.1±2.3
8	1794±7	180±9	49.2±2.5

The effect of pH on TMP is presented in Figure 3.6 for CEPS+DCMF experiments with 0.5 mg/L PAM. Although the pH had no noticeable impact on the TMP change, it was only revealed that the experiment that used the wastewater's natural pH performed better overall, particularly between the 280th and 380th minute of filtration.

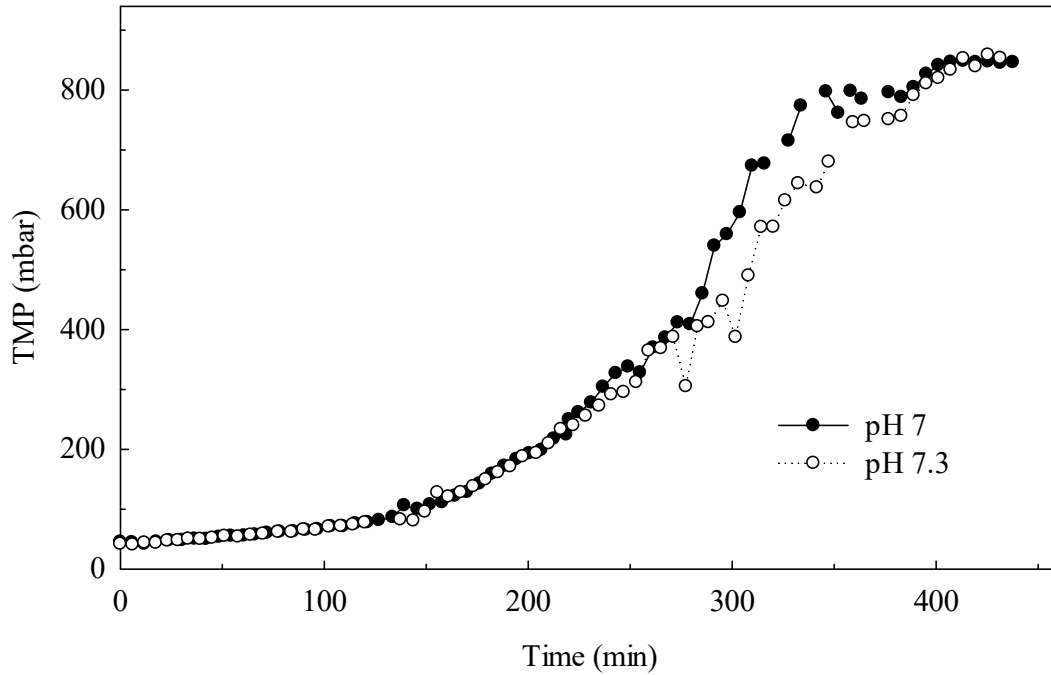


Figure 3.6 TMP change in CEPS+DCMF process with different pH

Concentrated wastewater characteristics at the optimum pH are given in Table 3.7. COD concentrations for pH 7 and 7.3 were 520 ± 20 and 510 ± 10 mg/L, respectively. The COD concentration in the CEPS+DCMF process concentrate was unaffected by the pH of the wastewater.

Table 3.7 Characteristics of the concentrated wastewater after DCMF at different pHs

Parameters	pH 7	pH 7.3
pH	7.5 ± 0.1	8.2 ± 0.1
Conductivity ($\mu\text{S}/\text{cm}$)	1474 ± 115	1600 ± 8
COD (mg/L)	520 ± 20	510 ± 10
$\text{NO}_2\text{-N}$ (mg/L)	0.9 ± 0.1	1.3 ± 0.0
$\text{NH}_4\text{-N}$ (mg/L)	37.9 ± 6.6	44.4 ± 11.1
$\text{PO}_4\text{-P}$ (mg/L)	11.3 ± 0.3	9.4 ± 0.5

At pH 7.0 and 7.3, there was no discernible difference in filtration performance. Therefore, the experiments were carried out at the wastewater's natural pH in the following optimization stages.

3.3.5 Optimization of flux and filtration/backwash time

Numerous studies have used intermittent filtration and/or backwash to mitigate membrane fouling [343-345]. In this study, the DCMF process was operated using aeration and frequent backwashing together to reduce membrane fouling. Thus, the formation of reversible fouling can be controlled with optimized backwash duration, resulting in less frequent chemical cleaning, and reduced operating costs [346]. In these DCMF experiments, net flux was kept at 20 LMH, and the TMP change against time at different filtration/backwash durations (5/1, 10/1, 10/2 minutes) are given in Figure 3.7. Major fouling of the membrane was detected when the system was operated with 10/1-minute filtration/backwash time. As can be seen in Figure 3.7, although the TMP increased in the system for 10/2 and 5/1 minutes of filtration/backwash times, the membrane operated with 10/2 filtration/backwash time had lower TMP after 250 minutes of filtration time.

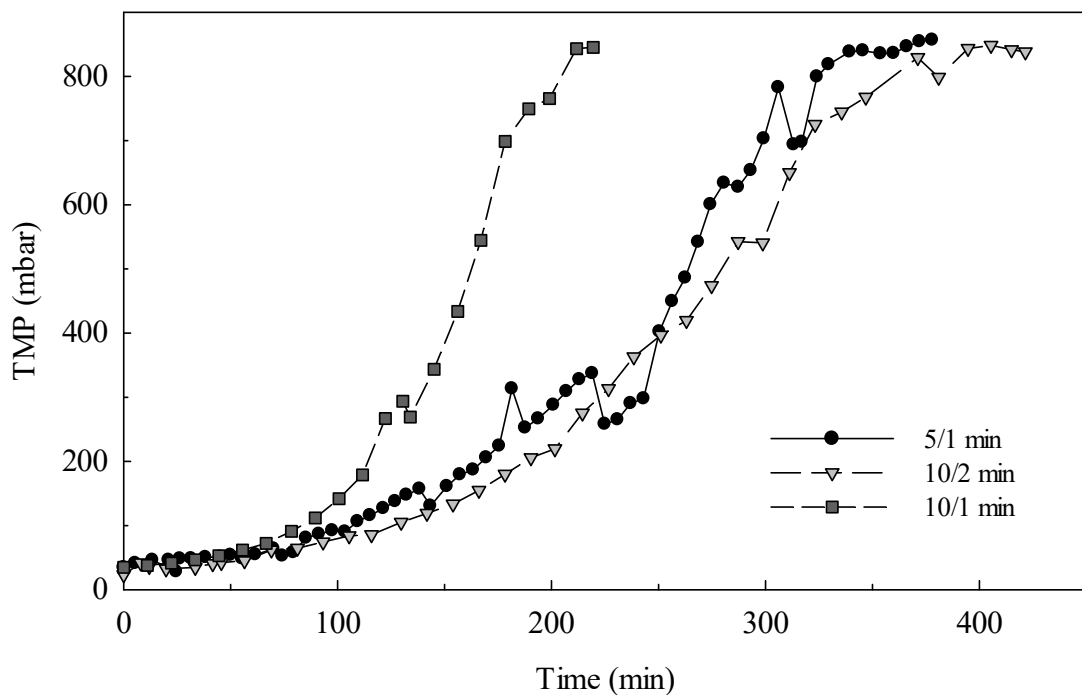


Figure 3.7 Change in TMP in CEPS+DCMF process with filtration time with different filtration/backwash time

The concentrated wastewater characterizations in the DCMF tests carried out for the optimization of filtration/backwash durations are given in Table 1.8. It was determined that the wastewater was not concentrated at the rate of 10/1 minute filtration/backwash, which ended after 220 minutes of filtration because of the fouling of the membrane. The COD in the concentrated streams were 480 ± 10 , 545 ± 34 , and 362 ± 39 mg/L at 5/1, 10/2, and 10/1 min filtration/backwash time, respectively.

Table 3.8 Characteristics of the concentrated wastewater after DCMF with different filtration/backwash time

Parameters	Filtration/backwash duration (min)		
	5/1	10/2	10/1
pH	8.2 ± 0.1	7.8 ± 0.0	7.9 ± 0.4
Conductivity ($\mu\text{S}/\text{cm}$)	1600 ± 8	1695 ± 52	1663 ± 108
COD (mg/L)	480 ± 10	545 ± 34	362 ± 39
NO ₃ -N (mg/L)	1.3 ± 0.0	1.0 ± 0.1	0.9 ± 0.4
NH ₄ -N (mg/L)	44.4 ± 11.1	49.4 ± 3.4	49.6 ± 0.8
PO ₄ -P (mg/L)	9.4 ± 0.5	9.0 ± 1.4	9.1 ± 0.1

The filtration/backwash duration of 10/2 minutes exhibited superior performance in terms of filtration performance. Then, filtration was carried out at 20, 30, and 40 LMH fluxes for the optimization of the process flux. The TMP behavior for the filtration is presented in Figure 3.8. For the DCMF operated at 30 and 40 LMH fluxes, the TMP increased above 350 mbar after 68 and 40 minutes, respectively, and these filtration experiments ended after 157 and 71 minutes, respectively. In the CEPS+DCMF experiment carried out at 20 LMH flux values, the TMP value increased over 350 mbar after the 220th minute and the experiment ended at the 424th minute. The higher fluxes required higher TMPs, often increasing the fouling rate and subsequently forcing more frequent cleaning, ultimately reducing productivity [347].

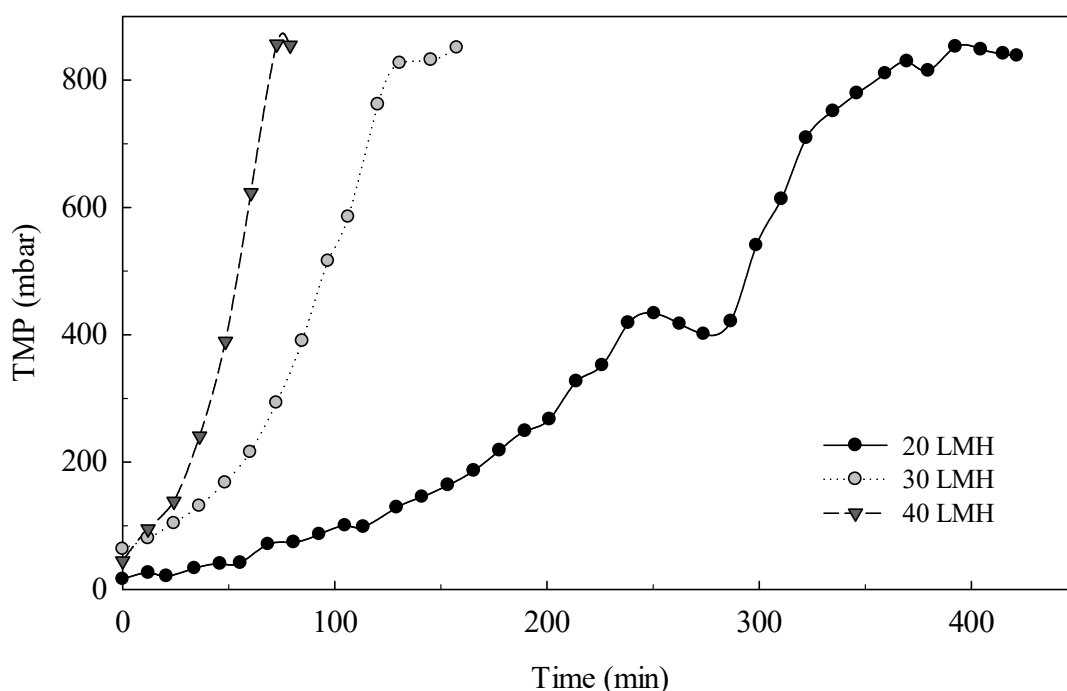


Figure 3.8 TMP change in CEPS+DCMF process with different fluxes

Characteristics of the concentrated wastewater after DCMF at 20, 30, and 40 LMH fluxes are given in Table 3.9. The highest COD concentration was reached at 20 LMH (545 ± 34 mg/L). These results were directly related to the duration of the experiment. Permeate production was approximately 7.8, 4.8, and 2.5 L for 20, 30, and 40 LMH fluxes, respectively. In the experiment conducted with a flux of 20 LMH, the duration of filtration extended up to 420 minutes (Figure 3.8).

Table 3.9 Characteristics of the concentrated wastewater after DCMF with different flux

Parameters	20 LMH	30 LMH	40 LMH
pH	7.8 ± 0.0	7.2 ± 0.1	7.4 ± 0.1
Conductivity ($\mu\text{S}/\text{cm}$)	1695 ± 52	1667 ± 30	1635 ± 7
COD (mg/L)	545 ± 34	420 ± 60	479 ± 27
$\text{NO}_3\text{-N}$ (mg/L)	1.0 ± 0.1	ND	1.0 ± 0.7
$\text{PO}_4\text{-P}$ (mg/L)	9.0 ± 1.4	9.2 ± 0.2	10.9 ± 0.4

In the CEPS+DCMF process, the optimum flux was determined as 20 LMH in terms of TMP and COD recovery. In DMF studies conducted in the literature with the polymeric membrane with a similar pore size (0.1μ), the flux values vary between 4.2 and 20.8 LMH [290, 292, 321]. However, ceramic membranes are usually operated at higher fluxes than the polymeric membranes, such as 20-40 LMH, but lower fluxes should be considered to reduce fouling, and associated energy demand for permeate withdrawing [345].

3.3.6 Optimization of recovery rate

The recovery rate of water in ceramic membrane filtration processes significantly impacts the overall effectiveness of wastewater treatment. Therefore, the effect of different water recovery rates of 70%, 80%, and 90% on DCMF system performance has been evaluated at 0.5 mg/L PAM, natural wastewater pH, the filtration/backwash time of 10/2 minutes, and at 20 LMH flux conditions. The TMP profile in the CEPS+DCMF experiments is given in Figure 3.9 for 70%, 80%, and 90% membrane recovery rates. In DCMF experiments conducted at different recovery rates, similar TMP changes were observed until the 200th minute, while TMP was lower at an 80% recovery rate in the rest of the filtration.

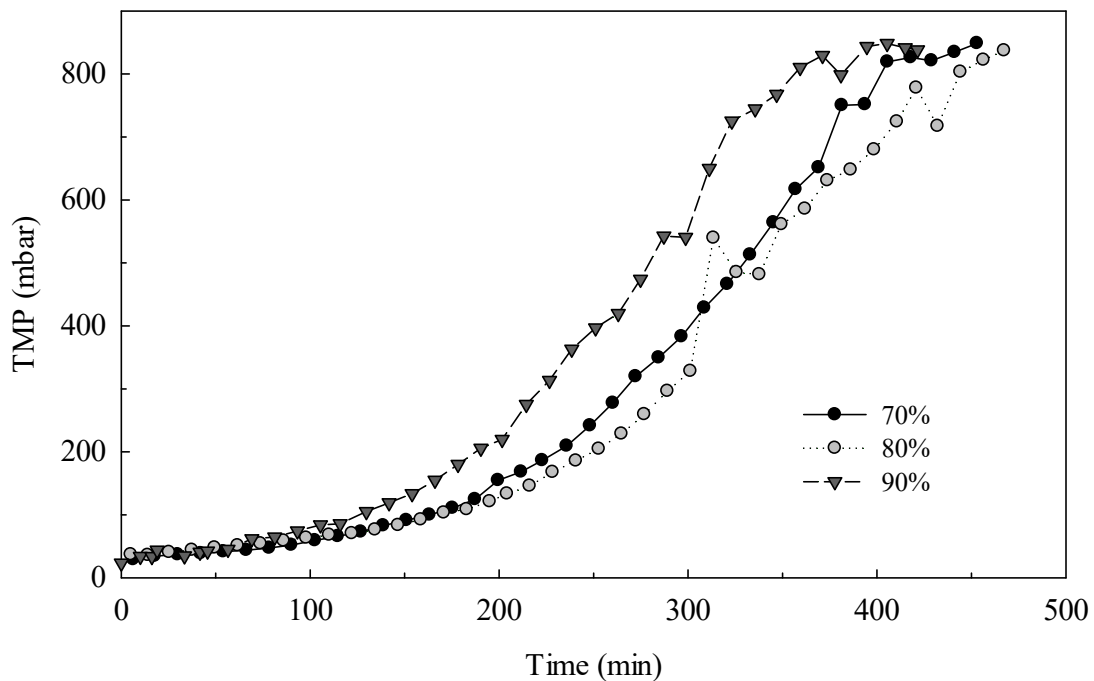


Figure 3.9 TMP change in CEPS+DCMF process with the different recovery rates

Characterization of concentrated wastewater obtained in CEPS+DCMF experiments conducted within the scope of optimization of the recovery rate is given in Table 3.10. Here, the best performance in terms of OM recovery was obtained for a 90% recovery rate and showed promising potential in energy recovery studies. In the literature, it is known that ceramic microfiltration membranes were used in recent years, and studies with high recovery rates were carried out in DCMF systems similar to the experimental setup used in this study [303, 304].

Table 3.10 Characteristics of the concentrated wastewater with different recovery rates

Parameters	70% Recovery	80% Recovery	90% Recovery
pH	8.0±0.1	7.7±0.2	7.8±0.0
Conductivity (µS/cm)	1689±76	1678±54	1695±52
COD (mg/L)	444±86	443±73	546±34
NO ₃ -N (mg/L)	1.1±0.2	1.4±0.2	1.0±0.1
PO ₄ -P (mg/L)	10.4±0.4	10.0±1.0	9.0±1.4

3.3.7 Long-term operation of CEPS+DCMF process and energy production potential

CEPS+DCMF system was operated for 20 days for long-term treatment of primarily treated MWW. Change in TMP with filtration time during the operation of the CEPS+DCMF process is presented in Figure 3.10. When the TMP reached the critical value of 700 mbar, the fouled membrane was subjected to off-line chemical cleaning. After each filtration, the membrane was physically cleaned with a sponge and chemically cleaned by immersing it in 0.5 M NaOH solution for 15 h. At the end of the 1st and 2nd cycles of operation, the membrane was cleaned by immersing it in 0.5 M HNO₃ solution in addition to physical and NaOH cleaning procedures, due to a decrease in time of the filtration duration. It can be noticed that the trend of TMP change with filtration time varied for three different filtration cycles. From the beginning of the filtration to around 16 h (1st cycle), the TMP showed a gentle increase to around 300 mbar in the first 10 h followed by a sharp increase to 700 mbar as the filtration time

went from 10 h to 16 h. Since the duration of the experiment gradually decreased in the first 6 filtrations, the HNO₃ cleaning procedure was also applied after the NaOH cleaning procedure.

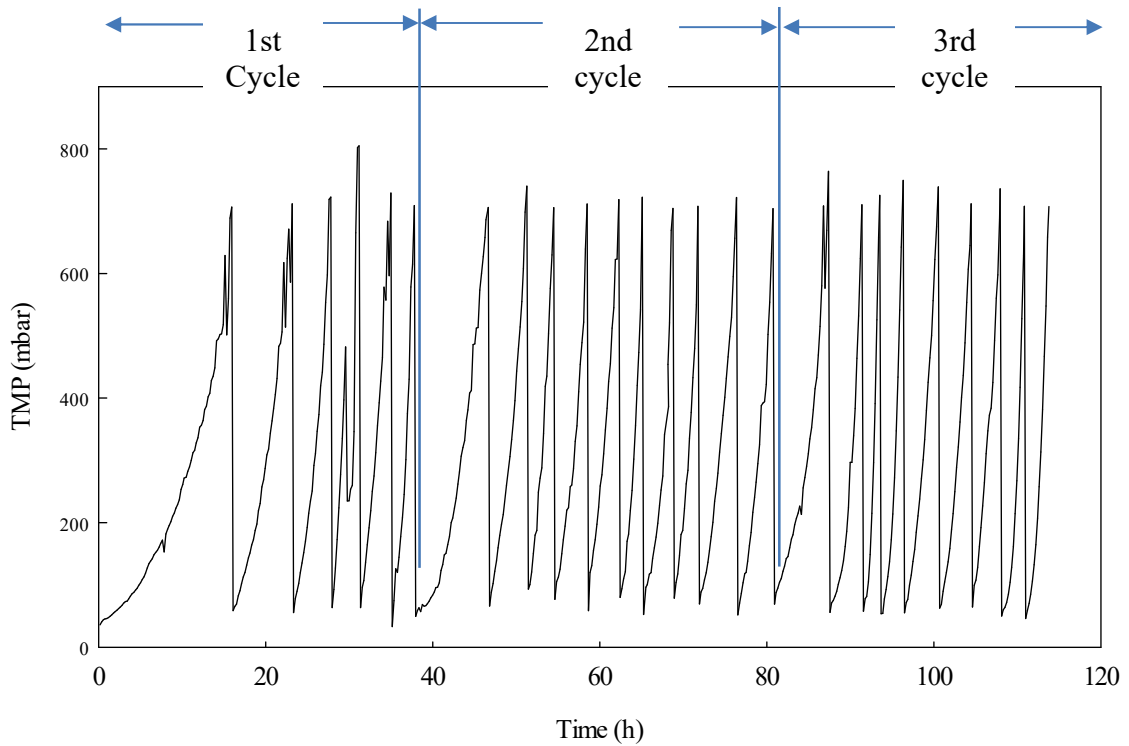


Figure 3.10 TMP profile as a function of time for continuous operation of CEPS+DCMF process

The CEPS+DCMF process was operated with a concentration factor of 10 and COD concentration increased during the operation (Figure 3.11). The COD concentration in the concentrate was 290 and 822 mg/L, initially and after 20 days of operation, respectively. Permeate COD concentration increased similarly to the concentrate concentration as it increased from 38 to 142 mg/L at initial and after 20 days of operation, respectively.

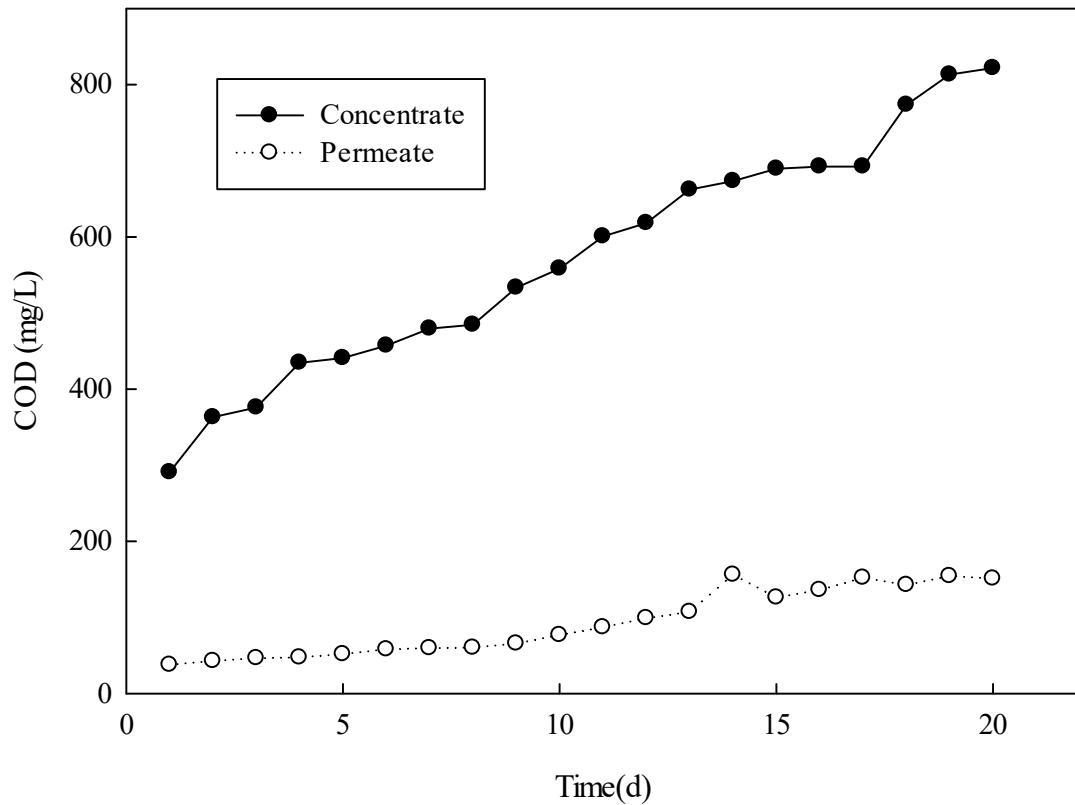


Figure 3.11 COD concentrations in the concentrate and permeate of continuously operated CEPS+DCMF process

COD concentration was used to quantify the amount of OM in concentrated wastewater and to predict the potential for energy production in further anaerobic processes. The process flow diagram and material balance obtained considering the experimental results are provided in Figure 3.12. The pre-settling tank flow rates were determined based on existing WWTP data. Approximately 1.25% of the wastewater is removed as sludge in the pre-settling tank. The pre-settling tank effluent is fed to the CEPS process and 10% sludge is removed. The COD concentration of the concentrated stream in this treatment process was calculated as 1432 mg/L. For each process, average COD concentrations were provided for mass balance calculations.

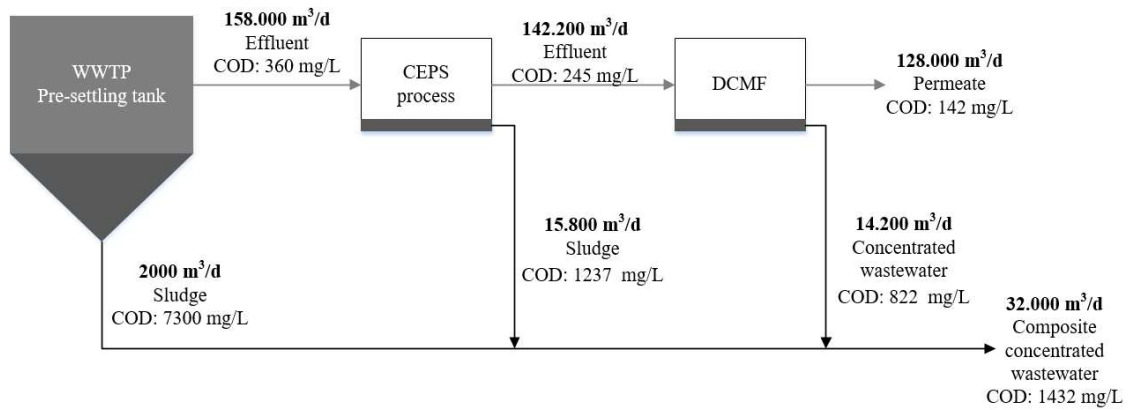


Figure 3.12 Theoretical COD concentrations in different units of the proposed process used in mass balance and energy calculations

For the real-scale WWTP from which wastewater is obtained, the influent flow rate of the pre-settling tank is 160,000 m³/d. According to mass-balance calculations provided in Table 3.11, 32,000 m³/d concentrate will be generated corresponding to 45,824 kg COD/d. The most frequently used basic technology to recover energy from sludge is anaerobic digestion to generate methane. Hence, methane generation is considered in the energy generation calculations. On the other hand, the energy requirement of the novel DCMF process was also included in the energy balance calculations. Thanks to the proposed OM recovery process 0.28 kWh/m³ of energy can be produced. However, the energy consumption of the existing conventional WWTP is 0.26 kWh/m³. In other words, the application of CEPS+DCMF has a high potential for the pre-concentration of OM from MWW for further energy recovery to achieve energy-positive wastewater treatment. The required energy and the potential energy generation for the suggested process are illustrated in Table 3.11. The detailed study in the table shows that the suggested process is an energy-positive process, which can be safely used for the treatment of MWW.

Table 3.11 Energy balance for electrical energy requirements and potential production with CEPS+DCMF process

Parameter	Value
Energy for permeate production	
Average TMP (m H ₂ O) ^a	4
Permeate flow rate (m ³ /s)	1.48
Power requirement for permeation (kW) ^b	58.07
Required pumping energy for permeation (kWh/m ³) ^c	0.011
Energy for feeding pumping	
Reactor head loss (m)	0.1
Feed flow (m ³ /s)	1.64
Power requirement for feeding (kW) ^b	1.61
Required pumping energy for feeding (kWh/m ³) ^c	0.0003
Energy for aeration	
Reactor head loss (m)	3
Air flow (m ³ /sn)	14.8
Power requirement for aeration (kW) ^b	435.6
Required energy for aeration (kWh/m ³)	0.082
Electrical energy production potential from methane	
Organic matter amount of concentrate (kg COD/d)	45,824
Methane production (m ³ CH ₄) ^d	16,038
Methane energy content (kWh/m ³) ^e	1.13
Electrical energy production from methane (kWh/m ³) ^f	0.37
Net energy production (kWh/m ³)	0.28
Electrical energy required for conventional treatment (kWh/m ³)	0.26

^a For the feeding pump head loss was assumed 0.1 m. Average TMP during long-term operation (0.23 bar), equivalent to a hydraulic head loss E of 2.3 m for permeation.

^b Energy requirement = $Q\gamma E/1000$, where Q (m³/s) is flow rate, $\gamma = 9800$ N/m³ and E (m) is head loss[348].

^c Assumed energy transfer efficiency of 65% in conversion of electrical energy to pump energy[348].

^d The CH₄ production potential of 1 g COD is around 0.35 L

^e The heating value of 1 m³ methane used in the calculation was 11.3 kWh[349].

^f The energy conversion efficiency is accepted as 33%.

3.4 Conclusions

In this study, a novel DCMF process configuration with PAM dosing was developed with the aim of concentrating OM from MWW for potential energy recovery. Different process configurations on the fouling behavior of DCMF were investigated

and the system operating conditions were optimized in terms of OM recovery and membrane fouling. Compared to the PAM+DCMF configuration, the CEPS+DCMF was a promising process, and dosing of 0.5 mg/L PAM was effective for the pre-concentration purpose. pH did not have a significant effect on filtration performance. pH had no noticeable impact on the effectiveness of the filtration process. In the DCMF operations, TMP increased above 350 mbar after 220, 68, and 40th minutes, respectively, at 20, 30, and 40 LMH fluxes. Membrane fouling was reduced at a filtration/backwash duration of 10/2 minutes. Thus, the formation of reversible fouling is controlled with the optimized backwash duration. COD concentration in concentrated wastewater was 444 ± 86 mg/L, 443 ± 73 mg/L, and 546 ± 34 mg/L, respectively, at recovery rates of 70, 80, and 90%. In the long-term operation of CEPS+DCMF for 20 days, COD reached 822 mg/L COD in concentrated wastewater. When evaluated with a holistic approach, according to the theoretical COD calculations 1432 mg/L COD can be obtained in the concentrated stream by using the CEPS+DCMF process. If the CEPS+DCMF process were utilized as a real-scale treatment, 0.28 kWh/m³ of energy could be generated. These results indicated that CEPS+DCMF has a high potential for the pre-concentration of OM from MWW for further energy recovery studies.

Chapter 4

Long-term operation of flocculation assisted direct ceramic microfiltration for up-concentration of municipal wastewater²

4.1 Introduction

Globally, in recent years studies on energy-self-sufficient and carbon-neutral wastewater treatment processes gathered more interest. There is wide acceptance that MWW may be repurposed as a valuable resource for energy, water, and nutrients [350]. MWW is generally described as having a moderate to low COD level, which makes it less suitable for direct anaerobic treatment. Advanced methods, such as dynamic sand filtration, dissolved air flotation, DMF, and biological adsorption, can be used to boost the content of COD in wastewater [91]. Recent investigations conducted at various

² This chapter was published as:

Ozcan, O., Sahinkaya, E., & Uzal, N. “Long-term operation of flocculation assisted direct ceramic microfiltration for up-concentration of municipal wastewater.”, 10th International Conference on Sustainable Solid Waste Management, Chania, Greece, 21 - 24 June 2023

scales, including short and long-term as well as lab and pilot-scale, have provided insights into the potential of DMF as a strategy for concentrating raw MWW [351]. However, the fundamental disadvantage still lies in the membrane fouling that is essential to the process. Regardless of whether they are in a submerged or side stream configuration, the membrane material is affected by accumulation caused by organic, inorganic, or biological fouling. This accumulation reduces the generation of permeates due to the development of gel, adsorption, deposition, pore blockage, or cake formation [352].

In light of the growing attention on resource recovery and environmental sustainability, the use of ceramic membranes for the up-concentration of MWW offers an environmentally friendly, energy-efficient, and more resistant to accumulation approach to MWW treatment [284]. The process of removing pollutants and potentially recovering resources from MWW through the use of DCMF is considered to be a straightforward and effective method [304]. However, for the DCMF process to be fully implemented, fouling and a decrease in flux must be overcome as they are the two major barriers [353]. The effective membrane fouling control approaches by determining optimum operational conditions may extend the lifespan of the membranes and reduce operational costs [340, 354].

In recent years, various experiments conducted at both lab and pilot scales, spanning short and long durations, have provided indications of the potential of DCMF as a means of up-concentrating raw MWW [24, 29]. However, the primary limitation continues to exist regarding the membrane fouling that is intrinsic to the process. In recent years, various non-traditional strategies such as photocatalysis, ultrasound, electro-filtration, membrane vibration, and rotating membranes have been studied as potential strategies for mitigating fouling on membrane surfaces during DMF processes [355-357]. Despite their prominence, such methods are still in their early stages and require further consideration of their economic and technical aspects to establish an affordable long-term operation. Additionally, the current literature primarily focuses on conventional methods to prevent fouling in membrane bioreactors, as this technology is well-established and widely used. However, further research is required to investigate the DMF process. In order to test the process's accurate performance, this research

should attempt to identify the optimum cleaning, fouling control, and operating strategy for long-term operations. [351, 354].

The conventional methods for mitigating fouling over low-pressure membranes are widely utilized and have demonstrated superior efficacy in wastewater treatment, while also being linked to comparatively economical operational expenses [358]. Chemically enhanced primary sedimentation (CEPS) is one of the most extensively used methods for reducing the fouling rate of membranes [29, 340, 359].

Nevertheless, there hasn't been any research on the efficiency of the cleaning strategy and the number of membranes in the DCMF of MWW integrated with the CEPS process during long-term operation. Therefore, this study was conducted to evaluate the long-term operation of the CEPS+DCMF process with the aim of developing a sustainable and effective up-concentration process for further energy recovery processes. To determine the optimum conditions the effect of flux, membrane cleaning procedure, and number of membranes used in the reactor were investigated.

4.2 Materials and methods

4.2.1 Materials and chemicals

The raw material of the operated flat sheet ceramic membrane was silicon carbide. The pore size of the membrane was 0.1 μm . The length \times width \times thickness of the membrane plate was 230 mm \times 150 mm \times 6 mm. The effective membrane area was 0.069 m².

Cationic polyacrylamide (PAM, Hydrofloc, Italy) was used as the flocculating agent in the CEPS process. The ceramic membrane's cleaning process involved the use of chemicals sourced from Merck, Germany, namely sodium hydroxide (NaOH), nitric acid (HNO₃), and hydrochloric acid (HCl). All solutions were prepared using deionized water in the experiments.

4.2.2 Wastewater and Analysis

In order to feed the CEPS+DCMF process, samples were acquired from the primary settling tank effluent of the municipal WWTP located in Kayseri, Turkey. In

Chapter 3, Table 3.1 presents the characteristics of the raw wastewater samples. The samples that were gathered were kept at a temperature of 4 °C. Prior to their use, the samples were allowed to reach room temperature, which was maintained at 20 ± 5 °C. The 3620 IDS WTW multiparameter (WTW GMBH, Germany) was used to measure EC and pH. The concentrations of chloride (Cl^-), sulfate (SO_4^{2-}), and phosphate-phosphorus ($\text{PO}_4\text{-P}$) were determined using anion chromatography (AC) on a Metrohm fitted with a Metrosep A Supp 5 (150 mm) analytical column and a Metrosep C4 (4 mm) guard column.

COD, TSS, and $\text{NH}_4\text{-N}$ analyses were carried out following the “Standard Methods for Water and Wastewater” of the American Public Health Association [360].

4.2.3 Experimental setup and operation

The schematic representation that summarizes the CEPS+DCMF process applied in this study is given in Figure 4.1. Specifically, the samples were placed into a jar test device and mixed with PAM for a duration of 2 minutes at a rapid speed of 120 rpm, followed by a slow mixing period of 15 minutes at 15 rpm. The mixture was then allowed to settle for 15 minutes, after which the supernatant was collected and used in the DCMF process. The total daily operating time of the system was 6 hours.

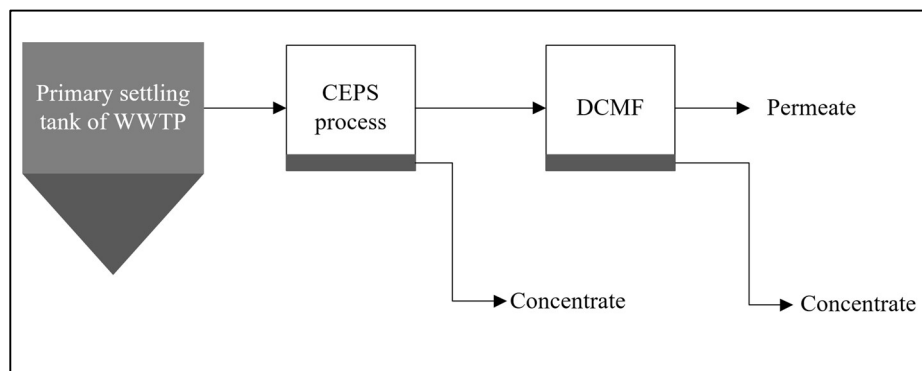


Figure 4.1 Schematic representation of the CEPS+DCMF process

Figure 4.2 represents a picture of the laboratory-scale setup utilized in DCMF investigations.

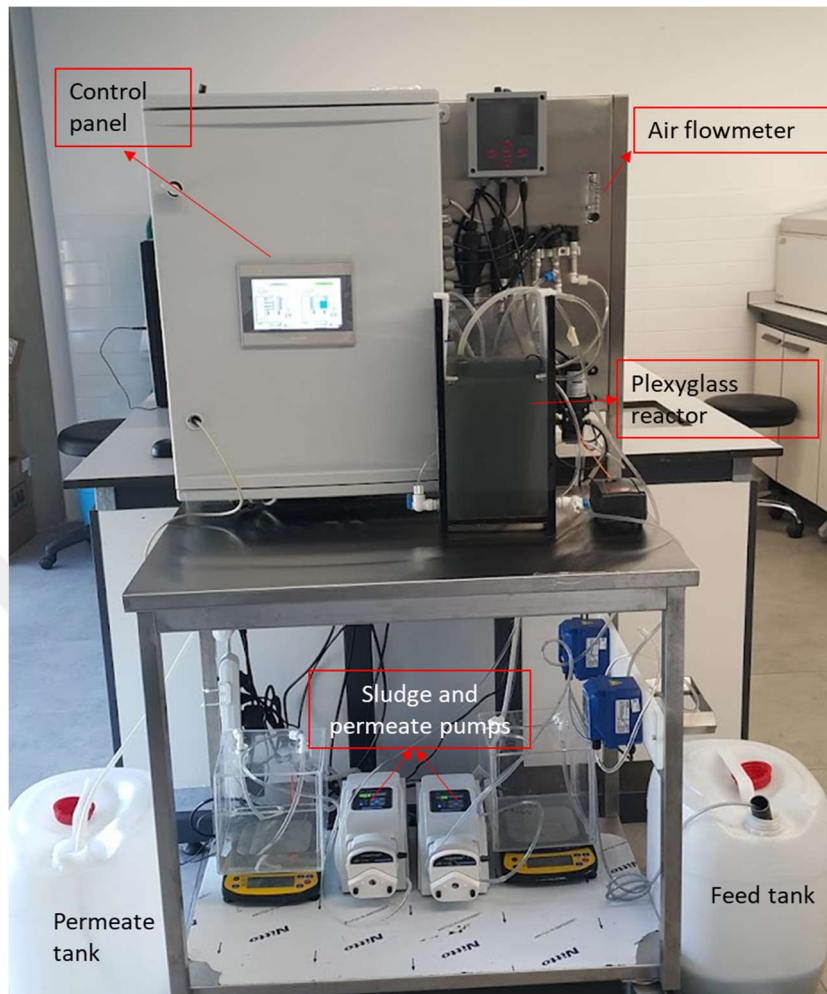


Figure 4.2 The picture of the laboratory-scale DCMF system

Experiments were performed at four different phases by changing the number of membranes in the reactor, flux values, and membrane cleaning procedure. The differences and operating times applied at each phase are given in Table 4.1.

Table 4.1 Operating conditions for the CEPS+DCMF process

Phases of Operation	Number of membranes	Flux (LMH)	Operating time (hour)	Membrane cleaning procedure
Phase I	1	20	30	Chemical cleaning (In-situ)
Phase II	1	20	110	Physical+chemical cleaning (Offline)
Phase III	2	10	190	Physical/Physical+chemical cleaning (Offline)*
Phase IV	2	20	580	Physical/Physical+chemical cleaning (Offline)*

**Chemical cleaning procedures were used when physical cleaning was no longer effective in preventing membrane fouling.*

4.2.4 Membrane cleaning procedures

The in-situ chemical backwashing (CIP, Cleaning-In-Place) procedure consisted of employing two solutions that were adjusted to pH 2 with HCl and contained 500 mg/L NaOH in order to use during backwashing. The flux of the backwash was set to 10 LMH and the duration of each backwash cycle was maintained at approximately 15 minutes for each solution.

The details of the ex-situ cleaning procedure are as follows.

- Physical cleaning: The cake layer is cleaned with a sponge and soft brush and backwash is applied with pure water for 5 minutes to the membrane.
- The membrane, which has been physically cleaned with water, is immersed in a 0.5 M NaOH solution for 15 hours. Following chemical immersing, 5 minutes of backwashing with pure water is performed. Lastly, the remaining chemicals are removed by soaking the membrane in pure water.
- When the membrane is not sufficiently cleaned using 0.5 M NaOH solution, further cleaning is performed using 0.5 M HNO₃ solution. The membrane is immersed in a 0.5 M HNO₃ solution for 15 hours. Lastly, the remaining chemicals are removed by soaking the membrane in pure water.

4.2.5 Assessment of energy potential

Assessing the energy production potential of the CEPS+DCMF process is crucial to showcasing its feasibility on a large-scale application. Within this context, the amounts of organic matter involved in the process of extracting energy from wastewater are directly correlated with the amount of energy that can be recovered. Therefore, the potential energy that can be derived from the CEPS + DCMF process was determined by calculating the amount of average COD present. Figure 4.3 provides the process flows that will be obtained if the CEPS+DCMF process is operated as a real-scale treatment plant. Additionally, it includes the flow rate data needed in energy calculations. The flow rates of the preliminary sedimentation tank are determined using data obtained from the current WWTP, where samples of raw wastewater were collected. In the current WWTP, about 1.25% of the influent wastewater is removed as sludge in the preliminary settling tank. In the proposed approach, the effluent of the primary settling tank will be transferred to the CEPS process, and the supernatant will be extracted at a rate equivalent to 90% of the influent flow rate. The DCMF process will be performed with a sludge stream concentration factor of 10.

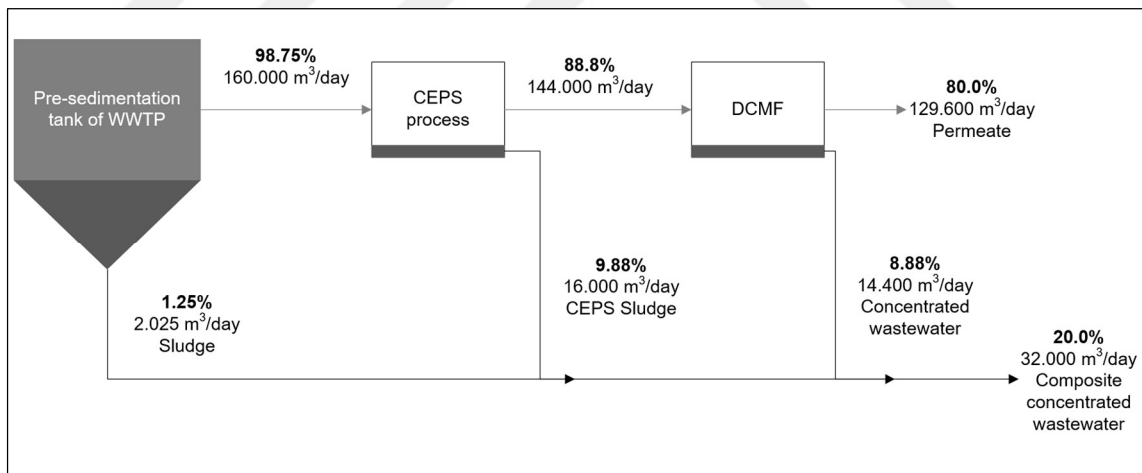


Figure 4.3 The flow rates that will be achieved when operating the CEPS+DCMF process as a full-scale treatment plant.

For energy potential calculations, the estimated production potential of CH₄ from 1 gram of COD is around 0.35 L [361]. Under standard conditions, it is generally accepted that each m³ of methane is equivalent to 10 kWh of energy, and the efficiency of converting this energy is accepted to be 33% [362]. Based on the total inflow of the

system, the energy that can be generated using this data is computed as kWh/m³ wastewater.

4.2.6 Membrane characterization

SEM-EDX analyses were performed to gather data on how fouling affects the morphology of the membrane surface and the efficacy of the cleaning methods used. SEM-EDX measurements were taken on the surfaces of the membranes using an analyzer manufactured by Zeiss, Leo 440, Randburg. The membranes were trimmed to an approximate dimension of 3×3 mm and subsequently subjected to a gold coating process prior to measurement. The analyses were conducted utilizing a voltage of 10 kV.

4.3 Results and discussion

4.3.1 TMP behavior

The time-course variation of TMP during the long-term operation of the CEPS+DCMF process for the first phase is given in Figure 4.4. The long-term operation experiments of the CEPS+DCMF process were started by applying in-situ chemical backwashing (CIP, Cleaning-In-Place) as the first step and the system was operated at 20 LMH flux for 30 hours (Figure 4.4). During the 5-day operation at 20 LMH flux, CIP was applied when the TMP value exceeded 700 mbar. An HCl-adjusted solution with a pH of 2 and a NaOH solution with a concentration of 0.5 M were used for backwashing processes, respectively. Attaining TMP values exceeding 700 mbar had been reached within 9 hours from the initial start of the long operational experiment. When the TMP value reached 700 mbar, the CIP procedure was performed, and the system was restarted. Nevertheless, the frequency of CIP application was reduced to 2 hours at the end of 27 hours of operation. It was shown that controlling fouling in DMF required more than a CIP cleaning approach.

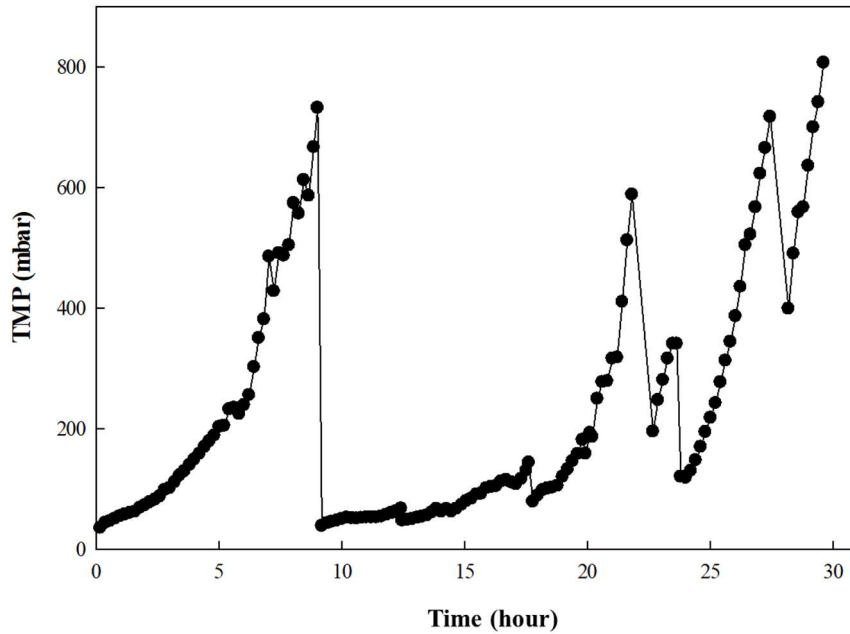


Figure 4.4 TMP profile as a function of time during Phase I

Since TMP rising could not be controlled during the first phase, physical and chemical cleaning procedures were applied in the period defined as the second phase (Figure 4.5). At this phase, physical and chemical cleaning was not effective due to the increasing concentration of wastewater during operation. External physical and chemical cleaning with 0.5 M NaOH solution was performed at this phase when the membrane became fouled with a TMP above 700 mbar during the process operational period. The increasing concentration of wastewater during the 20-day operation (at the end of 30 hours of operation) caused a change in the fouling tendency of the membrane. Based on the frequency of membrane cleaning, it concluded that using only NaOH for chemical cleaning was insufficient after 30 hours of operation. The time of the process involving both physical and chemical cleaning (using 0.5 M NaOH), as well as subsequent chemical cleaning using (0.5 M) HNO₃, is indicated by red lines in Figure 4.5.

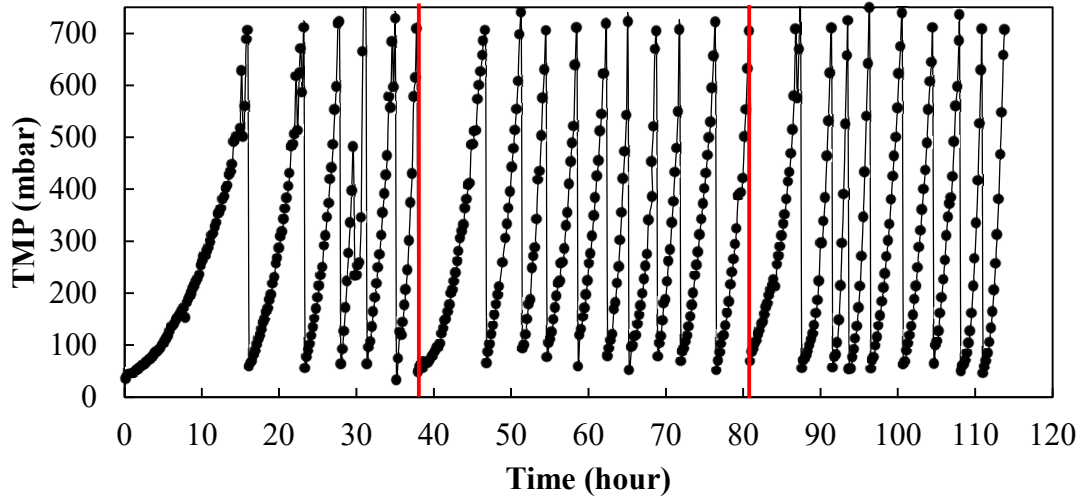


Figure 4.5 TMP profile as a function of time during Phase II

The higher fluxes required higher TMPs, often increasing the fouling rate and subsequently forcing more frequent cleaning, ultimately reducing productivity [363]. Literature reviews reveal a wide range of flux values (from 4.2 LMH to 20.8 LMH) in direct membrane filtration experiments using polymeric membranes that have a comparable pore size ($0.1 \mu\text{m}$) [290, 292, 321]. Lower fluxes should be evaluated to prevent fouling and manage TMP increasing, and the energy demand associated with permeate production, even though the ceramic membranes are typically operated at greater fluxes than polymeric membranes, such as 20-40 LMH [345]. In order to minimize this negative effect and mitigate the fouling, two membranes were integrated in parallel to the CEPS+DCMF system in the third operation phase, and the system was operated at 10 LMH flux with the same feed flow rate (Figure 4.6). Therefore, under the same flow rate operation, effective management of membrane fouling is achieved, allowing for a process duration of approximately 130 hours without the requirement of chemical cleaning. Chemical cleaning (using 0.5 M NaOH) was applied to the membrane after physical cleaning procedures were insufficient to control the rapid increase in TMP.

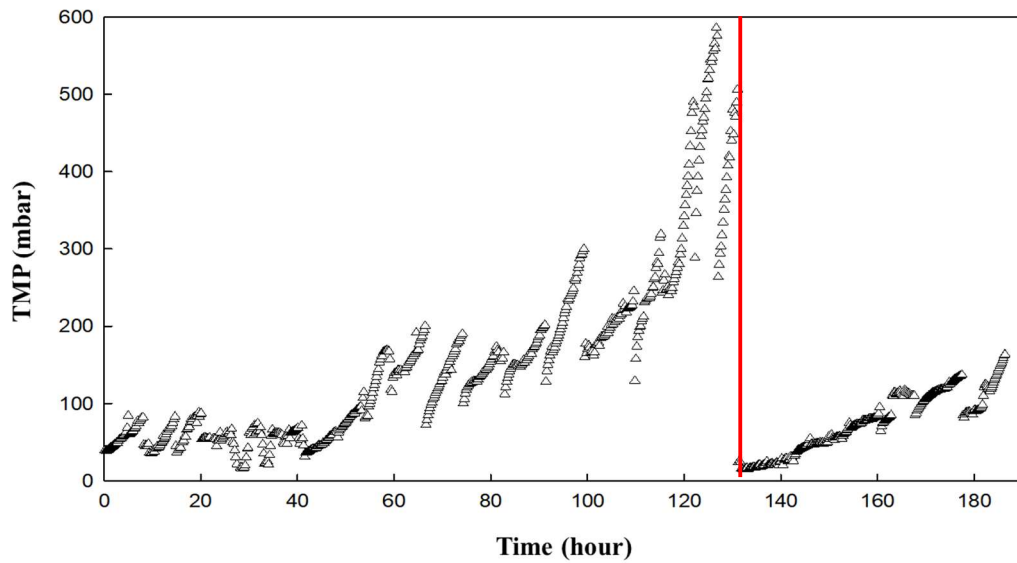


Figure 4.6 TMP profile as a function of time during Phase III -Operating two membranes in parallel at a flux of 10 LMH (The red line indicates the time of chemical cleaning with NaOH solution)

Finally, in the fourth operation phase, the CEPS+DCMF process was operated using two parallel membranes at 20 LMH flux (Figure 4.7). Blue arrows indicate the points in Figure 4.7 where physical and chemical cleaning (with 0.5 M NaOH solution) were performed. A pressure of 600 mbar was defined to provide efficient filtration and protect the membrane module from physical harm. Nevertheless, after the ceramic membranes were deformed a new ceramic membrane was installed at the 385th hour of operation (as indicated by the red line), and operation of the CEPS+DCMF process continued. After replacing the membrane modules, membranes become more resistance to fouling. This is indicated by the fact that the operation can be sustained only with physical cleaning until the 511th operating hour.

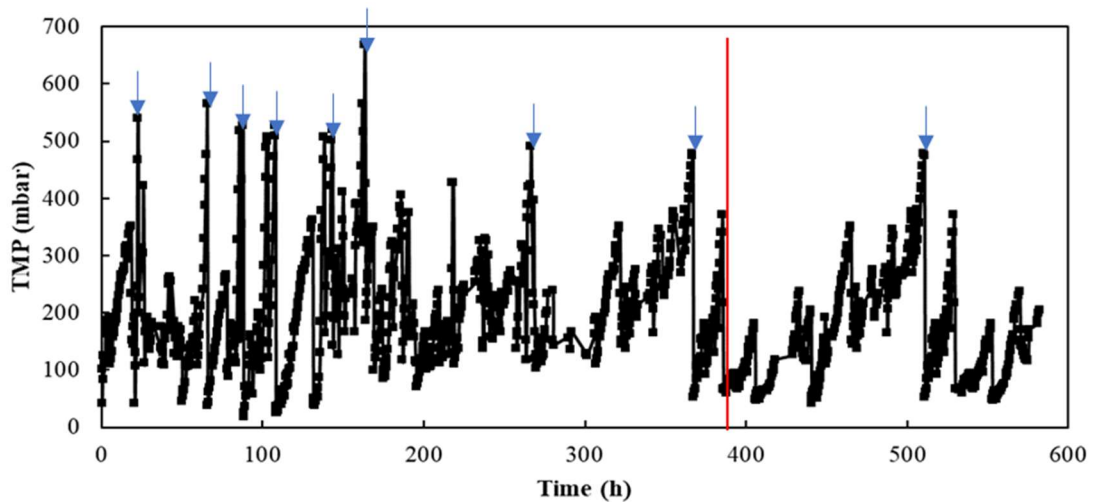


Figure 4.7 TMP profile as a function of time during Phase IV (The physical+chemical cleaning is applied are marked with blue arrows. At the time indicated by the red line, a new ceramic membrane was placed after the deformations in the ceramic membranes.)

4.3.2 Samples characteristics

Table 4.2 presents the findings of the characteristics of concentrate and permeate samples gathered from the DCMF process, which was fed the effluent of the CEPS process. During the first phase of the operation, the process terminated because the system was unable to effectively control the fouling of the membrane, resulting in insufficient up-concentration of the wastewater.

During the second phase of operation, it was found that the concentration of COD in the concentrate consistently increased over time throughout the operation of the CEPS+DCMF process.

During the third phase of operation, COD in the concentrate reached a maximum concentration of 1752 mg/L, and COD in the permeate ranged from 46 to 81 mg/L. The COD removal efficiency of CEPS+DCMF was ranged between 73% and 88%. Hence, CEPS+DCMF achieves its goal of efficiently removing and concentrating organic substances. By feeding the wastewater from the lower part of the membrane region, most of the particulate COD settled in the concentration zone and was collected from the system as a concentrated stream [364]. Therefore, compared to the raw wastewater, the COD in the supernatant was substantially reduced.

In the fourth phase of the CEPS+DCMF process, which was operated with two membranes in parallel at 20 LMH flux, the COD concentration in the concentrate increased to 2225 mg/L in the DCMF process, whereas the average COD value in the permeate was 61±14 mg/L. The CEPS process concentrated the wastewater approximately 8 times at this phase, resulting in an average COD removal of 70%. The influent samples of the CEPS+DCMF process were concentrated about 8 times in terms of COD in this phase of operation. On the other hand, it is not unexpected that the inorganic ions such as Cl⁻, SO₄²⁻, and PO₄-P were not removed highly in any operation phase because MF membranes have a higher pore size [365]. Although PO₄-P was not effectively removed, its concentration in the concentrate samples increased. The concentration of PO₄-P in the CEPS supernatant samples used in the DCMF process ranged from 8.1 to 9.3 mg/L. It reached a maximum concentration of 10.7±0.8 mg/L in permeate samples during the 4th phase of operation. Additionally, the DCMF concentrate samples had the highest concentration at 15.9±5.5 mg/L during the 2nd phase operation. According to research by Van Nieuwenhuijzen, A. F. et al. [366] on the characterization and fractionation of MWW based on particles, 11% of the phosphorus is bonded to settleable particles. Therefore, PO₄-P, which is considered to have become concentrated by adhering to particulate matter or the membrane in the reactor, also caused an increase in permeate samples.

Table 4.2 Characterization of samples acquired by the CEPS+DCMF process

Phases of Operation	Samples	pH	EC (µS/cm)	COD (mg/L)	Cl ⁻ (mg/L)	SO ₄ ²⁻ (mg/L)	PO ₄ -P (mg/L)
CEPS process	Feed	6.9-7.7*	1768-2080*	269-324*	197-352*	78-121*	7.9-10.1*
	Concentrate	7.2-7.7*	1817-2260*	1147-1239*	199-362*	54-120*	9.8-25.7*
	Supernatant	7.1-7.9*	1846-2070*	147-191*	197-358*	74-92*	8.1-9.3*
Phase I	Concentrate	7.9±0.2	2110±320	192±35	337±50	68±32	10.6±3.2
	Permeate	8.5±0.2	2000±320	74±20	326±55	81±22	8.0±1.8
Phase II	Concentrate	7.4±0.5	2046±83	290-822*	302±43	100±13	15.9±5.5
	Permeate	7.7±0.5	1940±71	38-151*	300±39	101±8	9.5±2.1
Phase III	Concentrate	8.0±0.9	1873-2360	194-1752*	196-405*	57-121*	9.9±5.4
	Permeate	8.5±0.5	1767-2280	46-81*	198-400*	76-111*	9.1±3.8
Phase IV	Concentrate	7.6±0.3	2270±65	792-2225*	346±19	78±23	15.7±2.3
	Permeate	7.9±0.2	1891±428	61±14	204±32	51±10	10.7±0.8

**These values are the lowest and highest values daily measured during operation of the CEPS+DCMF process.*

4.3.3 Assessment of energy potential

The potential energy generation obtained from the CEPS+DCMF process has been calculated based on the COD concentration received from long-term operating experiments. Figure 4.8 shows the process flow rates and average COD concentrations that will be reached if the CEPS+DCMF process is used in a real-scale treatment plant. The pre-sedimentation tank flow rates are acquired from Kayseri WWTP current data. The DCMF process will be implemented in the sludge flow at a concentration factor of 10. With a proportional calculation, we found that the COD content of the concentrated wastewater which might be obtained using this treatment process is 2055 mg/L.

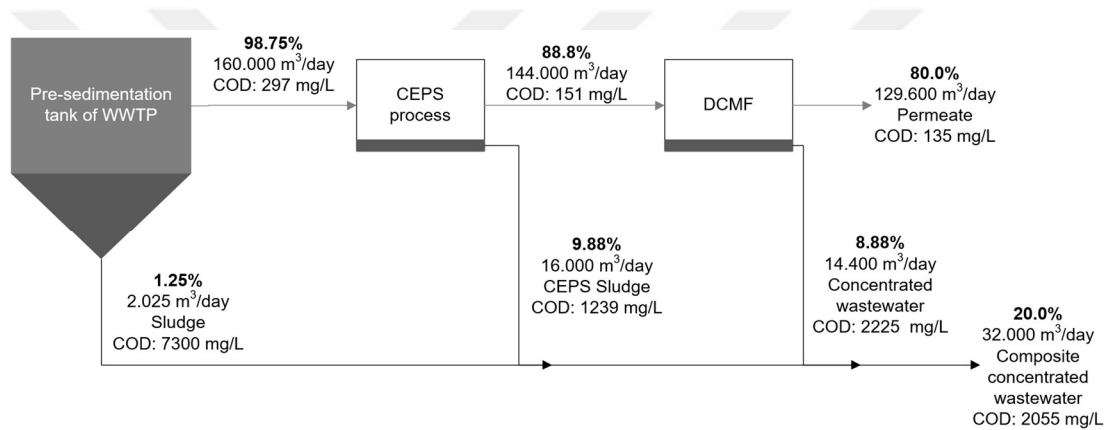


Figure 4.8 Theoretical potential energy generation that could be obtained from the operation of the CEPS+DCMF process

For the real-scale WWTP from which wastewater is gathered, the influent flow rate of the pre-settling tank is 160,000 m³/d. According to mass-balance calculations provided in Figure 4.8, 32,000 m³/d concentrate will be generated corresponding to 65,760 kg COD/d. The most frequently used basic technology to recover energy from sludge is anaerobic digestion to generate methane. Hence, methane generation is considered in energy generation calculations. On the other hand, the energy requirement of the novel DCMF process was also included in the energy balance calculations. Thanks to the proposed OM recovery process 0.45 kWh/m³ of energy can be produced. However, the energy consumption of the existing conventional wastewater treatment plant is 0.26 kWh/m³. In other words, the application of CEPS+DCMF has a high potential for the pre-concentration of OM from MWW for further energy recovery to achieve energy-positive wastewater treatment. The required energy and the potential

energy generation for the suggested process are illustrated in Table 4.3 The results of calculations in the table show that the suggested process is an energy-positive process, which can be safely used for the treatment of MWW.

Table 4.3 Energy balance for electrical energy requirements and potential production with CEPS+DCMF process

Parameter	Value
Energy for permeate production	
Average TMP (m H ₂ O) ^a	4
Permeate flow rate (m ³ /s)	1.48
Power requirement for permeation (kW) ^b	58.07
Required pumping energy for permeation (kWh/m ³) ^c	0.011
Energy for feed pump	
Reactor head loss (m)	0.1
Feed flow (m ³ /s)	1.64
Power requirement for feeding (kW) ^b	1.61
Required pumping energy for feeding (kWh/m ³) ^c	0.0003
Energy for aeration	
Reactor head loss (m)	3
Air flow (m ³ /sn)	14.8
Power requirement for aeration (kW) ^b	435.6
Required energy for aeration (kWh/m ³)	0.082
Electrical energy production potential from methane	
Organic matter amount of concentrate (kg COD/d)	65,760
Methane production (m ³ CH ₄) ^d	23,016
Methane energy content (kWh/m ³) ^e	1.63
Electrical energy production from methane (kWh/m ³) ^f	0.54
Net energy production (kWh/m ³)	0.45
Electrical energy required for conventional treatment (kWh/m ³)	0.26

^a For the feeding pump head loss was assumed 0.1 m. Average TMP during long-term operation (0.23 bar), equivalent to a hydraulic head loss E of 2.3 m for permeation.

^b Energy requirement = $Q\gamma E/1000$, where Q (m³/s) is flow rate, $\gamma = 9800 \text{ N/m}^3$ and E (m) is head loss[348].

^c Assumed energy transfer efficiency of 65% in conversion of electrical energy to pump energy[348].

^d The CH₄ production potential of 1 g COD is around 0.35 L

^e The heating value of 1 m³ methane used in the calculation was 11.3 kWh[349].

^f The energy conversion efficiency is accepted as 33%.

4.3.4 Membrane characterization

SEM and EDX analysis provides a better understanding of the characterization and development of fouling on the membrane surface after wastewater filtration. On virgin, physically, and physically+chemically cleaned ceramic membrane surfaces, SEM and EDX analyses were performed. Figure 4.9 presents images of the SEM analyses performed, and Table 4.4 provides the elemental composition obtained from the EDX results. In addition, the area where the EDX analysis was conducted is indicated in Figure 4.9 by a red box.

The pollutants that cannot be removed when the physical cleaning procedure is applied on the membrane surface after long-term operation studies and cause fouling in the membrane pores are seen in Figure 4.9b. According to the EDX analysis performed on the pollutant given in Figure 4.9b and Table 4.5, the fouling-causing pollutant consists primarily of the elements C, N, and P and originated from organic matter [367]. However, no pollutants were detected in the SEM images of the physically and chemically cleaned membrane surface (Figure 4.9c), and the elemental composition of the membrane is nearly similar to that of the virgin membrane (Table 4.4). The presence of Si, C, Al, and O in the EDX analysis of the virgin and physically+chemically cleaned membrane is attributable to the ceramic membrane's silicon carbide and aluminum oxide composition [368].

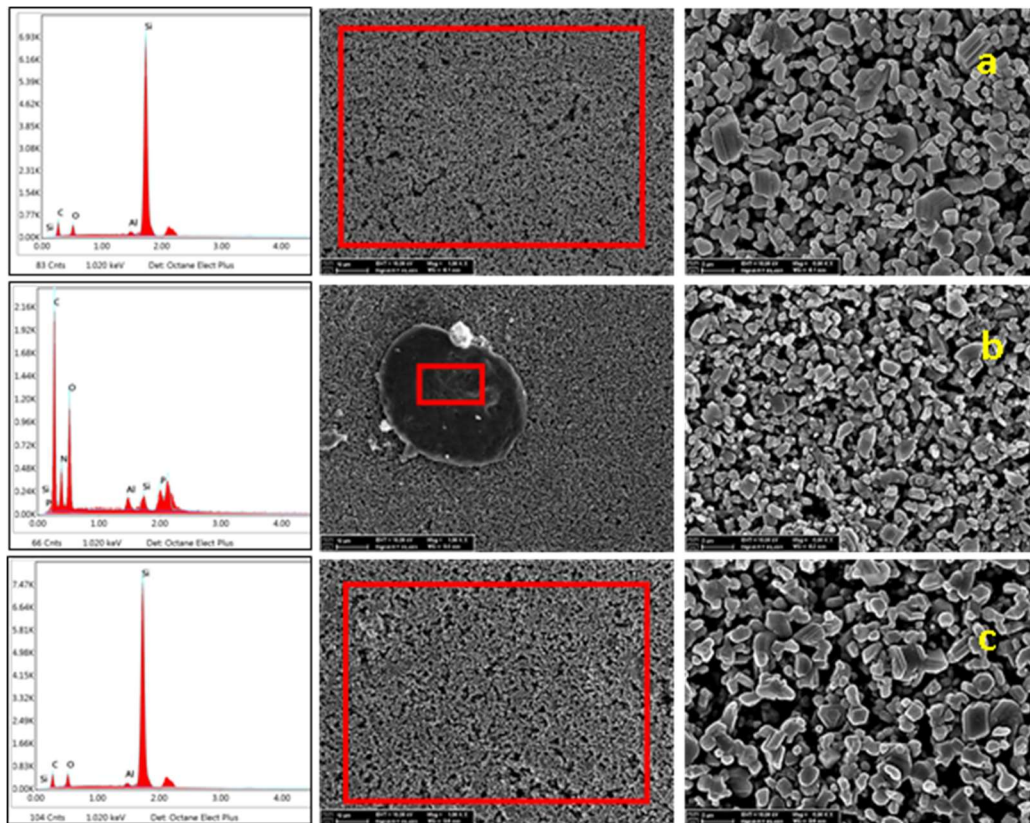


Figure 4.9 SEM images of the virgin (a), physically cleaned ceramic membrane (b), and physically+chemically cleaned ceramic membrane (c)

Table 4.4 EDX data of the ceramic membrane used in the CEPS+DCMF process

Element	Ratio (%)		
	a*	b**	c***
Si	51.91	1.39	51.94
C	37.03	42.97	35.86
Al	1.38	1.20	1.17
O	9.68	31.65	11.03
N	-	19.90	-
P	-	2.90	-

*Virgin ceramic membrane

** Physically cleaned ceramic membrane

*** Physically+chemically cleaned ceramic membrane

4.4 Conclusions

The CEPS+DCMF process was tested in long-term operational studies, which included performing experiments in four different phases. At each phase, evaluations were performed to assess the sustainable performance of the process in terms of TMP behavior, the capacity to concentrate organic matter, and the potential for energy production based on the organic matter content of the concentrate samples.

DCMF for up-concentration of MWW over the long term is possible through the use of straightforward and cost-effective procedures. The application of integrated CEPS and DCMF has a high potential for the up-concentration of organic matter in MWW for further energy recovery to achieve energy-positive wastewater treatment. The third and fourth operational phases demonstrated superior performance in both TMP and concentration capacity, as shown by the performed operating studies employing two parallel membranes and a flux of 10 and 20 LMH. The effective mitigation of membrane fouling is attained, enabling a process duration of roughly 130 hours without a requirement for chemical cleaning. The implementation of CEPS+DCMF on a full scale offers significant potential for concentrating organic matter from MWW, which can then be used to generate energy, resulting in a wastewater treatment process that produces more energy than it consumes. Therefore, the CEPS+DCMF technology can replace current MWW treatment technologies owing to its satisfactory organic matter removal and recovery performance, simple operation, and small footprint.

Chapter 5

Performance evaluation of an anaerobic fluidized bed ceramic membrane bioreactor integrated with pre-concentration process for resource recovery from municipal wastewater: Strategies fouling management and energy generation potential

5.1 Introduction

WWTPs are at the center of water-energy interactions as the plants consume energy to remove nutrients and thus reduce human footprint on the natural water environment [6]. With growing concerns over the scarcity of freshwater resources, the energy crisis, and climate change, MWW is receiving increased attention as a resource rather than a waste [9, 369, 370]. Organic substances in the content of wastewater are

defined as chemical energy potential and are found in chemical bonds of organic molecules [371]. Carbonaceous material originating from organics has the highest share in the total energy content of wastewater with 1.66 kWh/m^3 , and nitrogenous material offers an additional energy content of 0.30 kWh/m^3 [372].

Interest in anaerobic treatment as an alternative to conventional aerobic treatment for MWW is growing rapidly. Anaerobic treatment requires no aeration and produces both much less sludge and the generation of renewable energy in the form of methane [370, 373]. Although the anaerobic process has often been thought to be unsuitable for meeting stringent effluent quality regulations, integration of membranes into AnMBR can overcome this disadvantage [9, 374, 375]. Membranes not only retain the anaerobes in the reactor at a relatively short HRT but also maintain the long SRT that is required for effective treatment [376, 377]. However, membrane fouling caused by the deposition of foulants present in the wastewater on the membrane surface and/or with the pore matrix is the main challenge as it reduces membrane lifetime and increases capital/operational costs [378].

Biogas sparging along the membrane surface has been widely used to control membrane fouling within the AnMBR systems. However, the energy requirement for the biogas sparging often ranges from 0.7 to 3.4 kWh/m^3 , and this is even higher than the energy required to operate an aerobic MBR system ($0.5\text{--}1.0 \text{ kWh/m}^3$). Thus, biogas sparging may diminish the potential advantages of the AnMBRs over aerobic MBRs [379]. Recently, there has been an increased focus on AnFMBR processes due to fewer fouling issues and higher treatment performance, as the biomass remains in the bed, reducing membrane contact, while the upward movement of the bed effectively removes the cake layer [232, 362].

Moreover, recent literature uses GAC particles within the AnFMBR as the fluidized media, providing not only a high surface area for biofilm formation but also a mechanical scouring action on membrane surfaces to control membrane fouling. GAC fluidization occurs by fluid recirculation through a membrane reactor with relatively low energy consumption while providing excellent fouling control by mechanical scouring of membrane surfaces [380]. However, in long-term operations, exposure of polymeric membranes over time to particle sparging causes membrane damage [381]. There is growing attention to using ceramic membranes in AnFMBR systems are

garnering an increasing amount of attention and interest as a result of their superior chemical and thermal resistance, against polymeric membranes [382-384]. In addition, the excellent stability of ceramic membranes should prevent the damage of GAC fluidization and strong membrane-cleaning oxidants such as chlorine.

The chemical stability of ceramic membranes is expected to require only occasional maintenance cleaning and provide a higher flux than polymeric membranes. The high chemical resistance of the ceramic material enables the application of more aggressive cleaning methods compared to those used to clean polymeric membranes. Furthermore, silicon carbide ceramic membranes are considered a superior porous material compared to other ceramic membranes due to their possession of desirable characteristics such as high water permeability and a robust negative surface charge at neutral pH. These benefits can be beneficial in minimizing the fouling potential of membranes [385, 386]. Nevertheless, the utilization of ceramic membranes in full-scale implementations is still challenging due to their considerable investment costs [12]. However, the study investigated by Park, Sung Hyuk, et al. [387] compared the LCC of ceramic and polymeric membranes for a treatment plant. Despite the high initial investment cost, the LCCs of water from both types of membranes were found to be similar, with values of 0.28 USD and 0.274 USD for ceramic and polymeric membranes, respectively.

Although ceramic membranes offer several advantages, the use of the AnFMBR process for treating MWW is limited due to the medium-to-low organic matter level [21]. In this context, the pre-concentration of MWW by the use of various membrane technologies, such as direct membrane filtration, dynamic membrane filtration, and forward osmosis, has been proposed as a potential solution to overcome this limitation [24]. Nevertheless, no studies have yet been reported on the use of ceramic membranes in an AnFMBR system for the treatment of pre-concentrated MWW. Therefore, in this study, the pre-concentrated MWW was used for maximizing methane production in the up-flow AnFCMBR process. In addition to the composition of the wastewater, the operating parameters also play a significant impact on the performance of AnMBRs. HRT is an essential parameter that has a direct impact on the formation of membrane fouling [388]. Additionally, a higher OLR combined with a shorter HRT resulted in increased biomass growth and enhanced conversion of organic compounds into methane

[389]. Hence, it is necessary to identify the optimal HRT for ensuring a sustainable operation of the process.

In this section of the thesis study, the pre-concentrated MWW was used to maximize methane production and energy recovery in an up-flow AnFCMBR process. Specifically, the objectives of this study were: i) testing treatment of pre-concentrated MWW in a bench-scale AnFCMBR system equipped with flat-sheet ceramic membrane and GAC fluidization, ii) investigating the effect of different filtration/relaxation cycles on membrane fouling tendency, iii) showing the TMP behavior and COD the removal performance of AnFCMBR for different HRTs, (iv) investigating the effect of two different reactor types and the placement of membrane on membrane fouling tendency, and v) evaluating the energy requirements and production potential of the AnFCMBR system.

5.2 Materials and Methods

5.2.1 Setup and operation of the AnFCMBR System

The schematic diagram and images of the laboratory scale AnFCMBR systems used within the scope of biological treatment studies is given in Figure 5.1 and Figure 5.2, respectively. The up-flow AnFCMBR systems with two different reactor types were used: (i) AnFCMBR-membrane submerged into settling basin (Figure 5.1a) and (ii) AnFCMBR-membrane submerged into fluidized bed (Figure 5.1b). The main difference between these reactors was membrane placement location. In the following sections of this section, they will be referred to as AnFCMBR-submerged into settling basin (AnFCMBR-SiS) and AnFCMBR-submerged into fluidized bed (AnFCMBR-SiF), respectively.

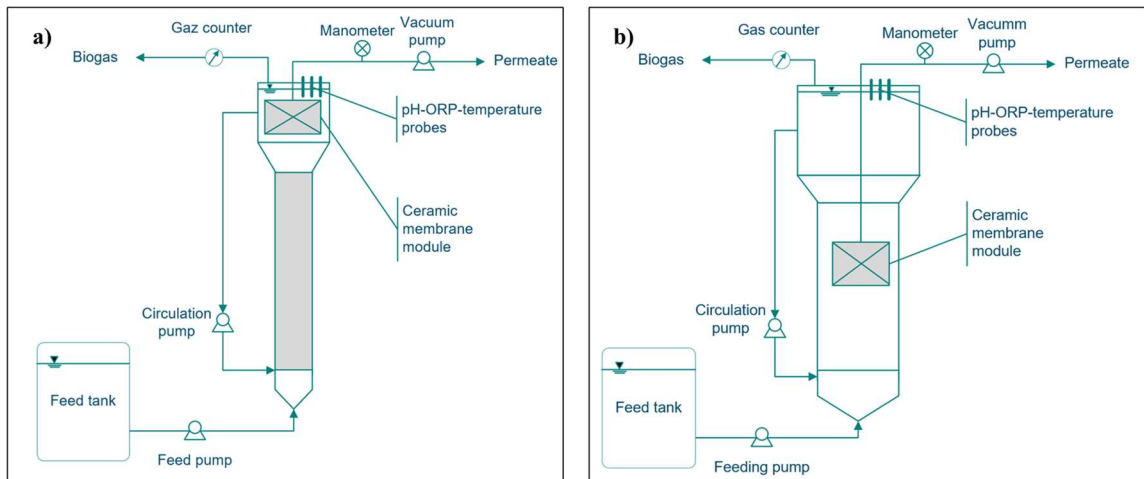


Figure 5.1 Schematic diagram of AnFCMBR-SiS (a) and AnFCMBR-SiF (b)



Figure 5.2 Images of AnFCMBR-SiS (a) and AnFCMBR-SiF (b)

In the first reactor (Figure 5.1a), the total volume of the system was approximately 8 L, the biomass fluidized media was in the lower part of the reactor (2 L), and the membrane was submerged into the settling basin of the reactor. In the second reactor (Figure 5.1b), the total volume of the system was approximately 6 L, the biomass fluidized media was in the lower part of the reactor (3 L), and the membrane was

submerged into the fluidized bed part of the reactor. Temperature, pH, and oxidation-reduction potential (ORP) were monitored for both reactors.

GAC with a diameter of between 0.85-0.60 mm was used as the fluidized media material in the systems. The circulation was used to obtain the fluidized bed in the system, and the bed fluidity rate was increased to at least 50%. Temperature, pH, and oxidation-reduction potential (ORP) were monitored in the reactors. The ceramic membrane was connected to a peristaltic pump (Longerpump, China) from the top open sections of the reactor to extract permeate at a desired constant membrane flux. A pressure transmitter was mounted before the suction pump to monitor TMP and the TMP was automatically recorded every 10 seconds.

A gas counter was used to measure the gas produced in the AnFCMBR system by volume. The methane concentration of the biogas collected in the gas sampling bag was quantified. In order to determine the methane content of the biogas, 20 mL of system gas was injected into a bottle half-filled with 10% potassium hydroxide solution and shaken. The total amount of gas in the bottle was measured by dipping the syringe into the bottle's septum thanks to the positive pressure.

Acclimation, optimization of filtration mode, and long-term operation studies were performed in the phases of AnFCMBR operation. Figure 5.3 represents a methodological approach to the sequential steps involved in the operation of AnFCMBR.

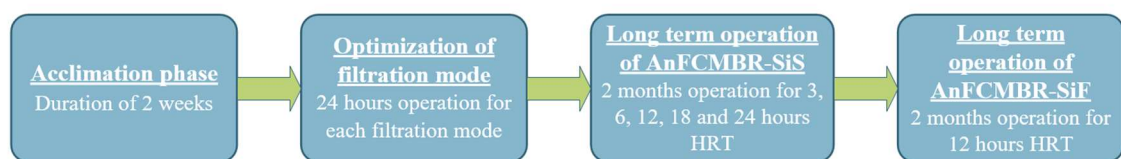


Figure 5.3 Experimental flow chart of AnFCMBRs operation

In the first phase of operation, the microbial culture inoculation in the reactor was performed by the use of anaerobic sludge gathered from the anaerobic digester of the Kayseri WWTP, which had an MLSS concentration of around 15 g/L. The continuous operation of AnFCMBR started with the start-up phase. During the start-up phase of the AnFCMBR, to adapt the microorganisms to the environment, continuous feeding

was started with an initial HRT of 2 days. The COD concentration and HRT were maintained constant throughout the start-up period. The feed was prepared using acetate (1000 mg/L) and carbonate (1000 mg/L). The acclimation of the sludge in the AnFCMBR system was carried out for 2 weeks. During acclimation, reactor pH, ORP, and temperature were measured as 9.5 ± 0.2 , -565.9 ± 44.6 mV, and $24.5\pm 0.1^\circ\text{C}$, respectively. In addition, MLSS and MLVSS were measured in the sludge samples taken from the reactor, and pH, EC, and COD were measured in the permeate and feed samples during the acclimation process. During the acclimation, the concentration of MLSS and MLVSS were 10.670 ± 3.2 and 5.650 ± 1.5 mg/L, respectively. COD was 828.3 ± 7.1 and 273.3 ± 3.5 in feed and permeate samples, respectively.

After the acclimation process was completed effectively, the AnFCMBR was operated with an HRT of 24 h to optimize the filtration mode. The optimization process involved running at various filtration/relaxation times (5/1, 10/1, and 10/2 min) to effectively manage membrane fouling. Each filtration/relaxation time was maintained for 24 hours. The AnFCMBR was operated in cycles including 5 or 10 minutes of filtration, followed by 1 or 2 minutes of relaxation. When TMP exceeds 500 mbar during the operation, the external membrane cleaning procedure, as described in Section 3.2.5, is applied. The internal membrane cleaning applied is performed for 10 minutes with 1 mg/L NaOCl as chemical backwashing.

HRT refers to the duration that wastewater remains in the bioreactor and determining the optimum HRT is crucial for COD removal and biogas production. Therefore, AnFCMBR was operated at 3, 6, 12, 18, and 24 h HRTs for 2 months for each HRT. In AnFCMBR, the flux has been increased from 1.6 LMH to 12.6 LMH as a result of changes in flow rate as the HRT decreased from 24 h to 3 h. The flux values, which were determined using the flow rate necessary to achieve the desired HRT and filtration mode for each phase operation phase are presented in Table 5.1.

Table 5.1 Operational conditions of AnFCMBR

AnFCMBR reactor type	HRT (h)	Feed flow (L/h)	Flux (LMH)	Filtration mode (min)*
AnFCMBR-SiS	24	0.083	1.6	5/1
	18	0.111	2.1	5/1/1
	12	0.167	3.1	5/1/1
	6	0.333	6.3	5/1/1
	3	0.667	12.6	5/1/2
AnFCMBR-SiF	12	0.167	2.1	5/1/1
<i>* Indicates filtration/relaxation or filtration/relaxation/backwash time.</i>				

5.2.2 Wastewater

The pre-sedimentation sludge of Kayseri WWTP was mixed with the concentrate stream from the pre-concentration process and then used as the feed for the AnFCMBR. The flow rate data gathered from the Kayseri WWTP was used to simulate a full-scale implementation of the process and ensure the results of these lab-scale studies can be performed on a pilot or full scale. The AnFCMBR was fed a mixture of 1.25:18.75 volume ratios of pre-sedimentation sludge and concentrate stream from the pre-concentration process. The description of the pre-concentration process is presented in Chapter 3 and our previous work [359]. Figure 5.4 is a flowchart representing the steps followed in preparing feed for the AnFCMBR process.

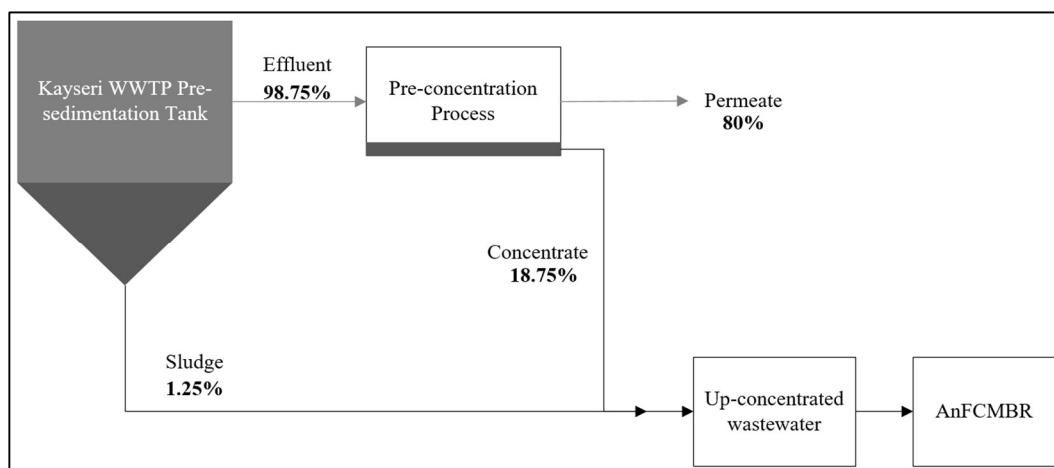


Figure 5.4 Schematic representation of strategy for generating the feed for the AnFCMBRs

Table 5.2 provides the characterization of the concentrated wastewater used in the AnFCMBR process, which was prepared following the flow chart presented in Figure 5.2, for each operational phase. pH, EC, COD, Cl⁻, SO₄²⁻, PO₄-P, and TSS were measured as described in Chapter 3. sCOD samples were filtered through 0.45 μm disposable filters before analysis and the concentration of COD was determined in the filtrate obtained.

Table 5.2 Feed characteristics of AnFCMBR systems

Reactor type	AnFCMBR-SiS					AnFCMBR-SiF
	24	18	12	6	3	
HRT (h)	24	18	12	6	3	12
pH	7.9±0.1	7.5±0.2	7.3±0.4	7.2±0.2	7.2±0.4	7.4±0.3
EC (μS/cm)	1913±18	1913±118	2011±410	2437±410	1876±87	1676±87
OLR (kg COD/m ³ /d)	1.3-3.9	1.8-4.9	1.7-5.1	4.2-7.7	7.7-22.6	1.6-5.1
COD (mg/L)	1313-3880	1213-3280	863-2544	1040-1930	963-2830	780-2563
Cl ⁻ (mg/L)	110-270	305-405	85-423	243-421	143-252	114-155
SO ₄ ²⁻ (mg/L)	57-125	33-80	32-88	55-84	64-83	28-40
PO ₄ -P (mg/L)	12.5-24.3	11.6-14.7	7.2-21.1	16.5-26.2	15.1-24.9	11.2-15.4
TSS (mg/L)	1210-2240	780-2680	640-1420	820-1510	930-1790	646-1930

5.2.3 Energy balance

The energy required for fluidizing the GAC (kWh/m³), the production of permeate (kWh/m³), and feeding were calculated.

The required energy can be found as follows;

$$E = N / Q$$

E is the energy requirement in kWh/m³, and Q is the wastewater flow fed to the reactor as m³/h.

$$N = Q \cdot \gamma \cdot H / \eta$$

N is the total pump power, Q is the sum of recirculation and inlet flow (m³/h), $\gamma = 9.81$ KN/m³, H is the total energy loss (m) and η is the efficiency of the pump (70%) [348, 362].

Total energy of methane produced (kWh/m³-wastewater):

- It is assumed that each m³ of methane is equivalent to 11.3 kWh of energy under standard conditions.
- The energy transfer efficiency is 45% when converting methane to electricity [45, 46].

The pre-concentration process was included in the calculation of the net energy balance. The total energy needed was determined based on the TMP value and the permeate flow.

5.2.4 Membrane characterization

The SEM-EDX investigations were performed to collect data regarding the impact of fouling on the membrane surface morphology and the effectiveness of the cleaning procedures applied. The membranes' surfaces were examined using a Zeiss, Leo 440, Randburg, analyzer for SEM-EDX measurements. The membranes were cut to a dimension of 3×3 mm and subsequently, membranes received a gold coating process before measuring them. The investigations were performed using a voltage of 10 kV.

5.3 Results and discussion

5.3.1 AnFCMBR operation: optimization of filtration mode

Effective methods for controlling membrane fouling by determining optimal operating conditions have the potential to increase membrane lifespan while decreasing operating costs [340, 341]. Consequently, following the acclimation phase, the duration of filtration/relaxation was optimized at 24 hours and 18 hours of HRT for AnFCMBR-SiS.

The effect of filtration/relaxation time on TMP for 24 h HRT operation for 24 h HRT is presented in Figure 5.5. The membrane suffered significant fouling when the system was run with a ratio of 10/1 min. The optimal TMP performance was achieved with 5/1 min filtration/relaxation time.

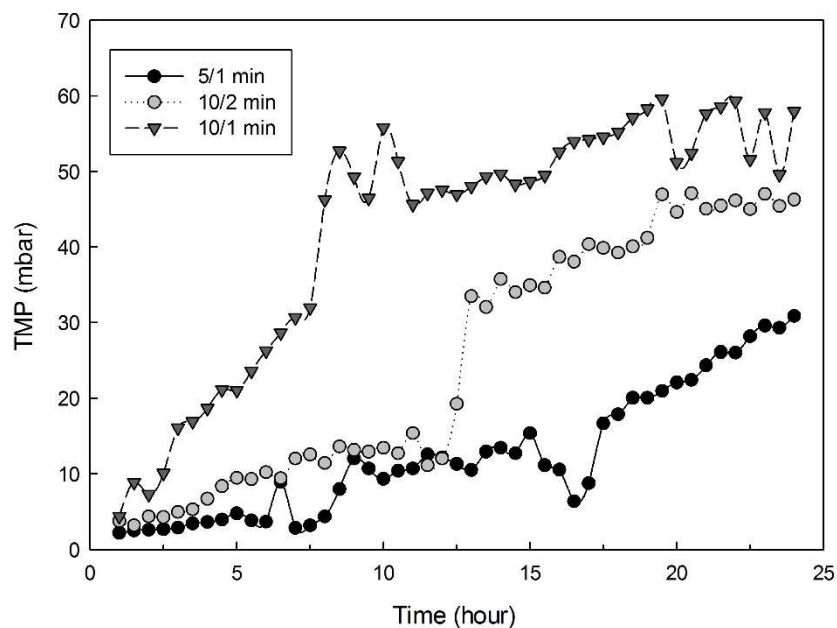


Figure 5.5 TMP profile as a function of time for different filtration/relaxation times with an HRT of 24 hours for AnFCMBR-SiS

HRT was reduced to 18 h to operate the AnFCMBR-SiS at different filtration/relaxation times (5/1, 10/1, and 10/2 min) to control membrane fouling and achieve an optimal AnFCMBR operation. The effect of filtration/relaxation time on TMP is presented in Figure 5.6. Similar TMP rising behavior was detected when the

system was operated with 5/1 and 10/1-min. The best performance in terms of TMP was obtained with 10/2 min filtration/relaxation time.

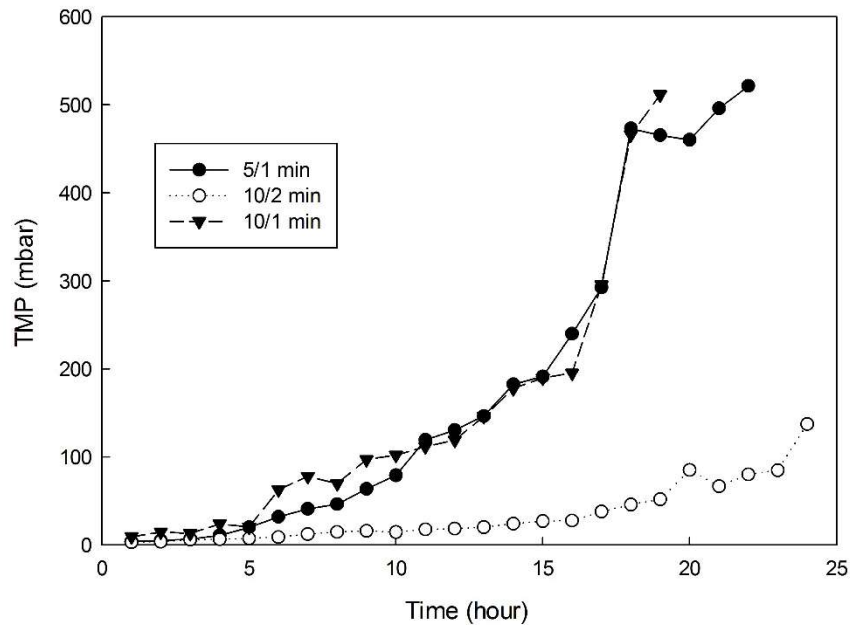


Figure 5.6 TMP profile as a function of time for different filtration/relaxation times with an HRT of 18 hours for AnFCMBR-SiS

5.3.2 Operation performance of AnFCMBR Systems

Following the optimization of the filtration/relaxation duration to 5/1 and 10/2 minutes for the AnFCMBR operation at HRTs of 24 and 18 hours, respectively, the HRT was adjusted to 24, 18, 12, 6, and 3 hours and the 1st reactor type of AnFCMBR was operated for 2 months at each HRT. Subsequently, the 2nd reactor type of AnFCMBR was operated for 2 months at 12 hours HRT.

The variation of TMP overtime during this operating period at 24 hours HRT and 5/1 filtration/relaxation time is given in Figure 5.7. A TMP value of 500 mbar serves as a significant indicator of increased fouling in the membrane [390]. Therefore, with the TMP value exceeding 500 mbar on the 20th and 45th day of operation, the membrane external cleaning procedure was applied. According to the research, AnFMBRs are capable of maintaining consistent TMP levels even when operated for extended HRTs such as 24 hours. The use of membrane relaxing techniques proves to be

beneficial in managing membrane fouling and ensuring the system operates at its optimal level of performance [391].

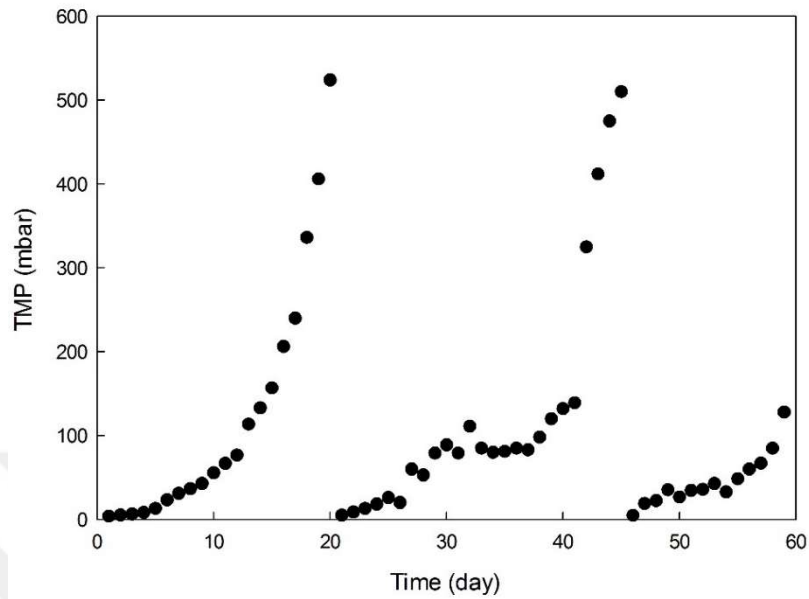


Figure 5.7 TMP profile as a function of time at 24-hour HRT and 5/1 filtration/relaxation time for AnFCMBR-SiS

Table 5.3 provides the characteristics of the feed and permeate samples collected over 2 months in the AnFCMBR process at 24 h HRT and 5/1 filtration/relaxation time. The characteristics of feed samples differed depending on the change in the characterization of the concentrated wastewater obtained from the pre-concentration process. Therefore, concentration ranges are given instead of mean values for COD, Cl^- , SO_4^{2-} and $\text{PO}_4\text{-P}$ parameters in Table 5.3. The COD concentration of feed samples ranges between 1313 and 3880 mg/L and the permeate concentration ranges from 33 to 139 mg/L. The AnFCMBR achieved an average COD removal of 89–96% and sCOD removal of 83-93%. SO_4^{2-} was found to be the highest 125 mg/L and 103 mg/L in feed and permeate, respectively. In a comparable manner, Li et al. [391] showed that AnFMBRs can successfully sustain high COD removal efficiency when operating at a 24-hour HRT, demonstrating the system's stable performance, with 93.6 % COD removal performance of AnFMBRs.

Table 5.3 Permeate and feed characteristics for operation at 24-hour HRT and 5/1 filtration/relaxation time for AnFCMBR-SiS

Parameters	Feed	Permeate
pH	7.9 ± 0.1	8.7 ± 0.1
EC (µS/cm)	1,913 ± 118	2,012 ± 158
COD (mg/L)	1,313 – 3,880	33 – 139
sCOD (mg/L)	854 - 2257	-
Cl ⁻ (mg/L)	110 – 270	106 – 216
SO ₄ ⁻² (mg/L)	57 – 125	58 – 103
PO ₄ -P (mg/L)	12.5 – 24.3	14.2 – 15.8
TSS (mg/L)	1,210 – 2,240	-

AnFCMBR-SiS operating period of 2 months at 18-hour HRT was started after 24 h HRT operation period. The variation of TMP over time during this operating period is given in Figure 5.8. The TMP reached 500 mbar on the 6th day of operation. After external chemical membrane cleaning, a 1-minute backwash was applied in addition to 10/2 min filtration/relaxation time. After the following rapid rise of TMP from the 6th day to the 20th day, the filtration and relaxation durations were reconsidered.

Studies have revealed that in cases of irreversible fouling, the relaxation frequency plays a crucial role as an important variable. It is widely accepted that depending only on the relaxation strategy is sufficient for sustaining permeability [392-394]. The efficiency of an AnMBR, as explored by Annop et al. [395], is influenced by the relaxation operation. In their research, four experiments were conducted to determine the most effective relaxation interval. Each experiment had a permeation duration of 4, 8, 12, and 16 minutes, with a constant relaxation period of 30 seconds. Among these experiments, the second one yielded the most favorable results, as fouling reached its peak. Interestingly, the longest permeation duration (16 minutes) led to rapid fouling, reaching its maximum within 30 minutes. It was observed that excessively frequent relaxation did not result in lower fouling development. Therefore, it is essential to establish an optimal relaxation period for sustainable operation [396]. Ugarte,

Patricia, et al. [394] measured the effect of different operating cycles in a laboratory scale MBR using flat sheet ceramic membrane to mitigate membrane fouling and preserve the continued operation along time considering two physical cleaning strategies: relaxation and backwashing. They found that the combination of relaxation and backwashing is more effective than relaxation in the reduction of fouling. In the 24-hour HRT operational period filtration/relaxation duration of 5/1 minutes produced more effective results in terms of TMP rising. Therefore, both in the light of literature data and results of the 24-hour HRT operational period, starting from day 20 of operation, the AnFCMBR was operated using a filtration/relaxation/backwash cycle of 5/1/1 minutes, with an extra 1 minute of backwash included in the 5/1 minute cycle, to ensure the long-term sustainability of the operation.

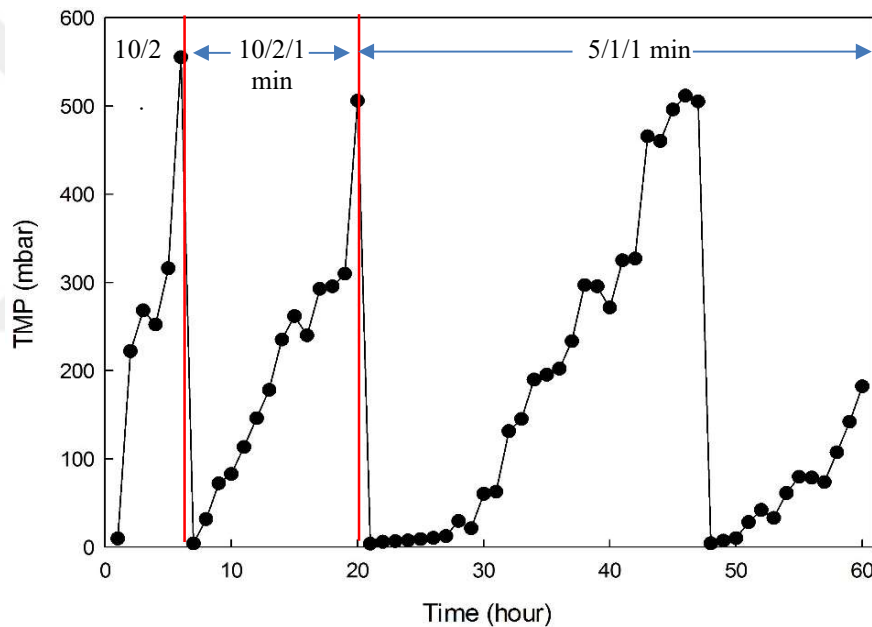


Figure 5.8 TMP profile as a function of time for operation at 18-hour HRT for AnFCMBR-SiS

The characterization of feed and permeate samples collected during 2 months of operation in the AnFCMBR process at 18 h of HRT is given in Table 5.4. The COD concentration of feed samples ranges from 1213 to 3280 mg/L and the permeate concentration ranges from 70 to 121 mg/L. The AnFCMBR achieved an average COD removal of 90–96% and sCOD removal of 84-95%. SO_4^{2-} was found to be the highest at 80 mg/L and 89 mg/L in feed and permeate, respectively. The amount of sulfur compounds in wastewater encourages the proliferation of sulfur-reducing bacteria while

inhibiting the growth of methanogens [397]. Therefore, that there is no significant removal of SO_4^{2-} can be assessed as evidence that sulfate-reducing bacteria do not inhibit the growth of methanogenic bacteria.

Table 5.4 Permeate and feed characteristics for operation at 18-hour HRT for AnFCMBR-SiS

Parameters	Feed	Permeate
pH	7,5 ± 0,2	8,1 ± 0,2
EC (µS/cm)	1913 ± 118	2012 ± 158
COD (mg/L)	1213 – 3280	70 – 121
sCOD (mg/L)	793 - 2564	-
Cl⁻ (mg/L)	305 – 405	342 – 384
SO₄²⁻ (mg/L)	33 – 80	54 – 89
PO₄-P (mg/L)	11,6 – 14,7	11,8 – 18,3
TSS (mg/L)	780- 2680	-

Following the operation period of 18 h HRT, the 2-month operating period at HRT of 12 h was performed, and the variation of TMP overtime during this operating period is given in Figure 5.9. AnFCMBR-SiS was operated on a 5/1/1 minute filtration/relaxation/backwash cycle because it offered a sustainable running period during the 18-hour HRT operation period. With the TMP value exceeding 500 mbar on the 22nd and 43rd day of operation, the membrane external cleaning procedure was applied.

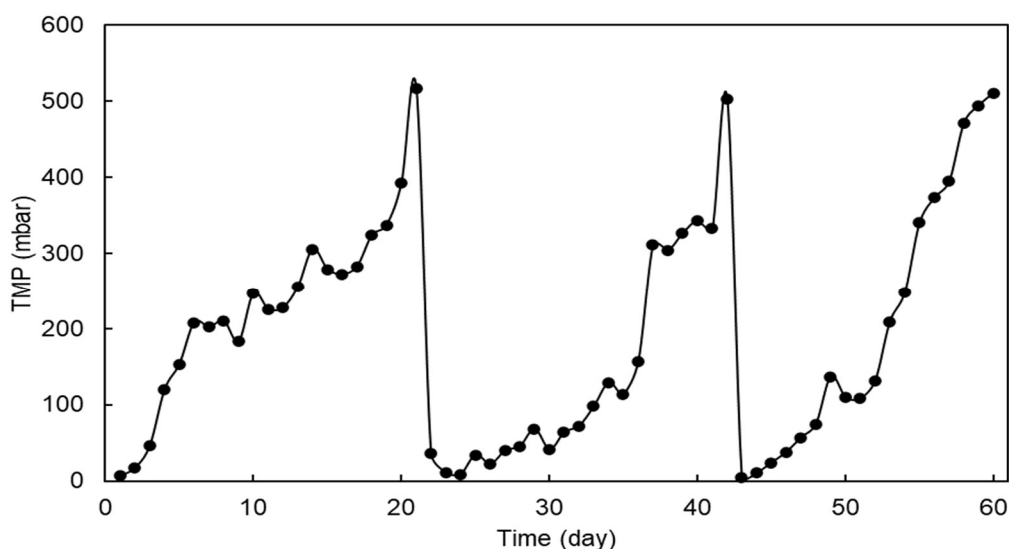


Figure 5.9 TMP profile as a function of time at 12-hour HRT for AnFCMBR-SiS

The characterization of feed and permeate samples collected during 2-months of operation in the AnFCMBR-SiS process is given in Table 5.5. The characterization of the feeding of the AnFCMBR-SiS process differed depending on the change in the characterization of the concentrated wastewater obtained from the CEPS+DCMF process. Therefore, concentration ranges are given instead of mean values for COD, Cl⁻, SO₄²⁻ and PO₄-P parameters. The COD concentration of feed samples ranges from 863 to 2544 mg/L and the permeate concentration ranges from 60 to 136 mg/L. The AnFCMBR-SiS achieved an average COD removal of 84–94%. Nevertheless, there was no accurate removal of Cl⁻, SO₄²⁻ and PO₄-P. In contrast, there was also found an increase in P concentration, reaching a maximum of 25.7 mg/L PO₄-P. Gouveia, J., et al. [237] found that there was no significant difference between the influent and effluent of the AnMBR and that there was an accumulation of PO₄-P concentration within the membrane module as well. On the other hand, they stated that the low level of phosphorus removal in the AnMBR effluent might be advantageous if the wastewater is used for agricultural or irrigation purposes. It offers an advantage in the subsequent step of nutrient recovery for our study.

Table 5.5 Permeate and feed characteristics for operation at 12-hour HRT for AnFCMBR-SiS

Parameters	Feed	Permeate
pH	7.3±0.4	7.7±0.3
EC (µS/cm)	2011±410	2043±310
COD (mg/L)	863-2544	60-136
Cl ⁻ (mg/L)	85-423	342-384
SO ₄ ⁻² (mg/L)	32-88	32-108
PO ₄ -P (mg/L)	7.2-21.1	11.1-25.7
TSS (mg/L)	640- 1420	-

After completing the 12-hour HRT was reduced to 6 hours to operate the AnFCMBR-SiS. With the TMP value exceeding 500 mbar during the operation, the membrane external cleaning procedure was applied eight times (Figure 5.10). Short filtration/relaxation/backwash time (5/1/1 minutes) intervals helped reduce fouling rates, but it was not very useful for avoiding TMP jumps [398]. The rapid increase in TMP is associated with the diffusion of organic compounds into membrane pores during the initial stages of membrane filtration, causing pore blockage which is not removed easily by applying relaxation and backwash [32]. The results suggest that combining periodic maintenance cleaning with membrane relaxation and backwash should be effective in reducing the fouling rate with the AnFCMBR-SiS system for the next operation period at 3-hour HRT.

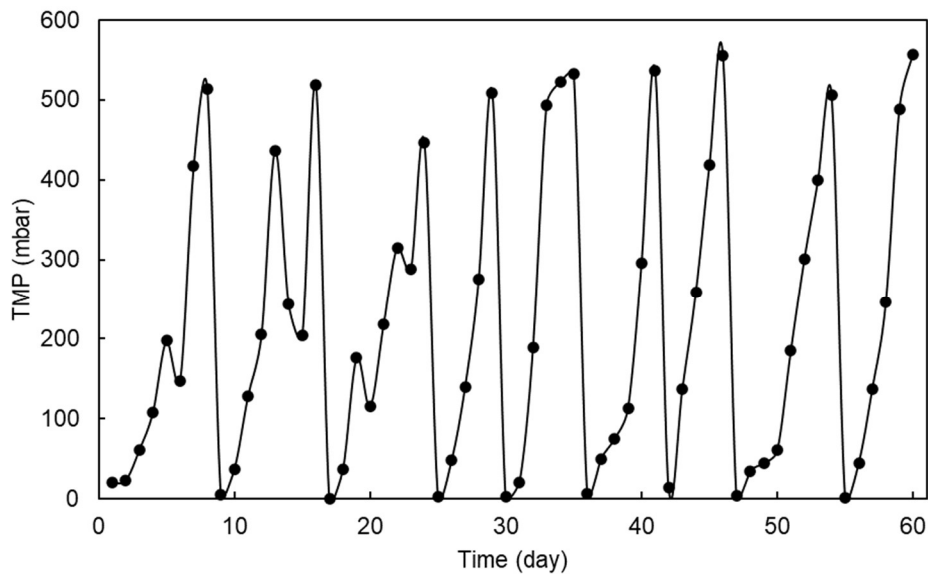


Figure 5.10 TMP profile as a function of time at 6-hour HRT for AnFCMBR-SiS

The characterization of feed and permeate samples collected during 2-months of operation in the AnFCMBR-SiS process is given in Table 5.6. The characterization of the feeding of the AnFCMBR-SiS process differed depending on the change in the characterization of the concentrated wastewater obtained from the CEPS+DCMF process. Therefore, concentration ranges are given instead of mean values for COD, Cl⁻, SO₄⁻², and PO₄-P parameters. SO₄⁻² was found to be the highest 84 mg/L and 82 mg/L in feed and permeate, respectively. The COD concentration of feed samples ranges from 1040 to 1930 mg/L and the permeate concentration ranges from 54 to 113 mg/L. The AnFCMBR-SiS achieved an average COD removal of 92–94%. A shorter HRT (6 hours) was predicted to lead to a reduction in COD removal, especially due to the developed microbial culture's biodegradation potential being limited. However, the AnFCMBR-SiS achieved significant COD removals at the shorter HRT, mainly because of the biofilm's accumulation during the operation at the previous HRT on the GAC particles, which enhances the removal efficiency [362].

Table 5.6 Permeate and feed characteristics for operation at 6-hour HRT for AnFCMBR-SiS

Parameters	Feed	Permeate
pH	7.2±0.2	7.6±0.4
EC (µS/cm)	2437±410	2084±310
COD (mg/L)	1040– 1930	54-113
Cl⁻ (mg/L)	243-421	225-415
SO₄⁻²(mg/L)	55-84	58-82
PO₄-P (mg/L)	16.5-26.2	19.7-32.3
TSS (mg/L)	820- 1510	-

Figure 5.11 represents TMP change during the 2-month operation of AnFCMBR-SiS duration at 3-hour HRT. By raising the flux to 12.6 LMH to provide the HRT value for three hours, the TMP value on the third day of operation reached above 500 mbar. Therefore, by installing two parallel membranes in AnFCMBR-SiS and increasing the backwashing time on the fourth day of operation, the HRT value of 3 h was sustained with a filtration/relaxation/backwash time of 5/1/2 minutes and flux of 6.3 LMH. The rapid increase in TMP value during the first stage of filtration with the cleaned membrane is caused by organic matter diffusion into the membrane pores [32]. Although the short relaxation and backwash durations used in MBR systems are effective at controlling fouling, researchers have shown that they are ineffective at

minimizing TMP jumps [398]. As a result, in addition to membrane relaxation and backwashing durations, periodic maintenance cleaning was used inside the reactor to control TMP during the 3-hour HRT operating period of AnFCMBR-SiS. When the TMP exceeded 500 mbar on the 19th day of operation, chemical backwashing was performed for 10 minutes with a 1 mg/L NaOCl solution. Since it was found that chemical backwashing was ineffective and TMP levels were rising rapidly, a physical+chemical cleaning method was performed on the membrane outside the reactor on day 28 and day 54 of the 2-month operation. The membrane permeability decreases dramatically during the relatively short HRT operation, resulting in a higher rate of membrane fouling and the need for more frequent membrane physical and chemical cleaning processes [390].

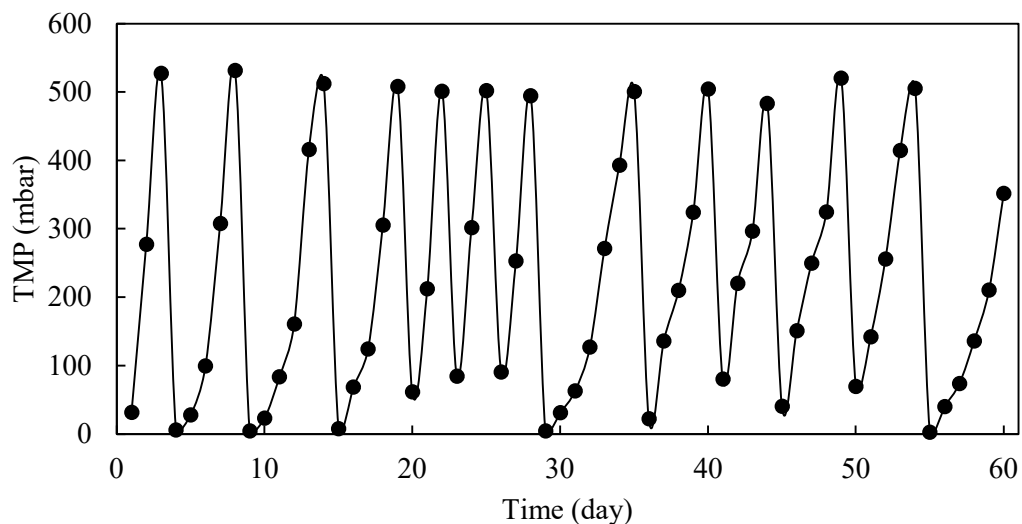


Figure 5.11 TMP variations for the AnFCMBR at 3-hour HRT for AnFCMBR-SiS

Table 5.7 shows the characteristics of feed and permeate samples collected during 3 hours of HRT operation in the AnFCMBR process. The feed COD concentration for the AnFCMBR process is between 963 and 2830 mg/L, whereas the permeate COD concentration is between 49 and 110 mg/L. Thus, COD removal was achieved between 88 to 94%. Similar high COD removal efficiencies (averaged 94% or higher) even at HRTs close to 2 h were reported by Bae et al. [399]. In another study, COD removal rates of 94.3–95.5% were found when AnMBR was operated at 8–48 hours of HRT and 1.08–6.46 LMH flux [400].

While the highest SO_4^{2-} concentration was obtained to be 83 mg/L in feed, it was 78 mg/L in permeate samples. When $\text{PO}_4\text{-P}$ concentrations in the feed are between 15.1-24.9 mg/L and 21.2-30.8 mg/L in permeate samples. The highest $\text{PO}_4\text{-P}$ concentration of 30.8 mg/L was found in the permeate samples during the operation of the AnFCMBR process. Chen, et al. [401] were reported that phosphorus removal in these bioreactors was limited. In addition, high concentrations of $\text{PO}_4\text{-P}$ have the potential for struvite recovery [402].

Table 5.7 Permeate and feed characteristics for operation at 3-hour HRT for AnFCMBR-SiS

Parameters	Feed	Permeate
pH	7.2±0.4	7.4±0.3
EC (µS/cm)	1876±87	1766±431
COD (mg/L)	963– 2830*	49-110*
Cl⁻ (mg/L)	143-252*	225-415*
SO_4^{2-}(mg/L)	64-83*	50-78*
$\text{PO}_4\text{-P}$ (mg/L)	15.1-24.9*	21.2-30.8*
TSS (mg/L)	930- 1790*	-

**These values are the lowest and highest concentrations measured during the operation of AnFCMBR.*

After completing 3-hour-HRT studies with the AnFCMBR-SiS configuration, the AnFCMBR-SiF was operated at 12 hours of HRT and 2.1 LMH of flux for 2 months. Figure 5.12 represents TMP change during the 2-month operation duration of AnFCMBR-SiS and AnFCMBR-SiF at 12 hours of HRT. When the TMP value exceeded 500 mbar during the operation, the membrane external physical+chemical cleaning procedure was applied eight times. After each cleaning application, the TMP remained less than 200 mbar without a significant membrane fouling until 4th day of operation. This is attributed to the scouring effect of the fluidized GAC particles on membrane fouling [380]. The TMP increased up to 250 mbar rapidly, then jumped above 300 mbar and exceeded 500 mbar in seven or eight days. However, in the AnFCMBR-SiS configuration, TMP exceeded 500 mbar in fifteen days at the same flow (0.167 L/h) and filtration/relaxation/backwash time (5/1/1 min).

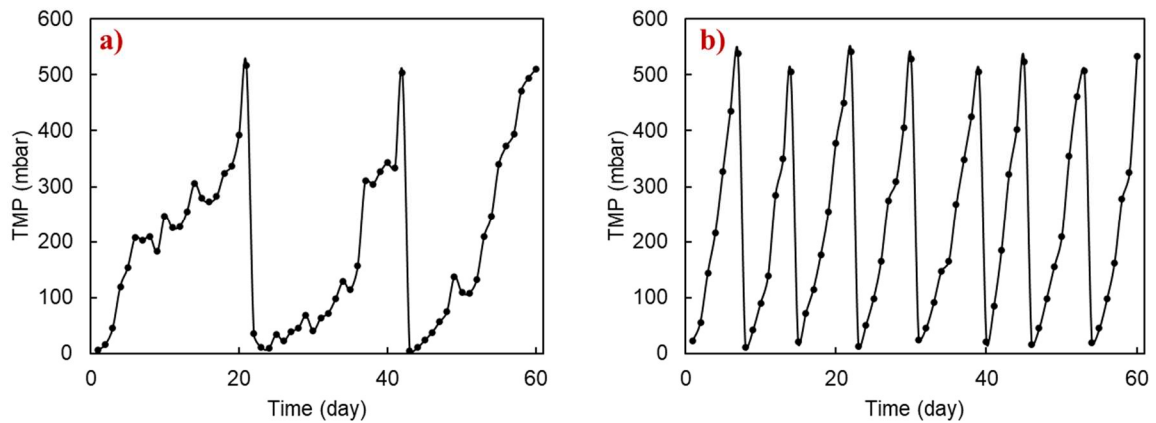


Figure 5.12 TMP variations for AnFCMBR-SiS (a) and AnFCMBR-SiF (b) at 12 hours of HRT

Table 5.8 shows a comparison for the characteristics of feed and permeate samples collected during the AnFCMBR-SiS AnFCMBR-SiF operation at 12 hour HRT. The feed COD concentration for the AnFCMBR-SiF process is between 780 and 2563 mg/L, whereas the permeate COD concentration is between 66 and 100 mg/L. Thus, COD removal was achieved between 87 to 97% which was similar to those observed in other AnMBRs [403]. AnFCMBR-SiS achieved an average COD removal of 84–94%. While the highest SO_4^{2-} concentration was obtained to be 49 mg/L in permeate, it was 40 mg/L in feed samples. These results reflect that sulfate-reducing bacteria were inactive to compete with the methanogens for COD utilization in the AnFCMBR-SiF [404]. When $\text{PO}_4\text{-P}$ concentrations in feed are between 11.2-15.4 mg/L and 19.5-23.9 mg/L in permeate samples. The highest $\text{PO}_4\text{-P}$ concentration of 23.9 mg/L was found in the permeate samples during the operation of the AnFCMBR-SiF process.

Table 5.8 Characteristics of feed and permeate in the AnFCMBR-SiS and AnFCMBR-SiF operation

Parameters	AnFCMBR-SiF		AnFCMBR-SiS	
	Feed	Permeate	Feed	Permeate
pH	7.4±0.3	7.7±0.4	7.3±0.4	7.7±0.3
EC ($\mu\text{S}/\text{cm}$)	1676±87	1792±100	2011±410	2043±310
COD (mg/L)	780– 2563*	66-100*	863-2544	60-136
Cl ⁻ (mg/L)	114-155*	131-302*	85-423	342-384
SO_4^{2-} (mg/L)	28-40*	26-49*	32-88	32-108
$\text{PO}_4\text{-P}$ (mg/L)	11.2-15.4*	19.5-23.9*	7.2-21.1	11.1-25.7
TSS (mg/L)	646- 1930*	-	640- 1420	-

*These are the lowest and highest concentrations measured during the operation of AnFCMBR.

5.3.3 The evaluation of the operational performance of AnFCMBR configurations

In AnFCMBR operation investigations, Table 5.9 compares the performance of AnFCMBR-SiS operated for 24, 18, 12, 6, and 3-hour HRT. It was found that decreasing HRT value enhanced flow values, however, there was no significant change in COD removal or methane content of produced biogas. Studies conducted at similar HRT values in the literature were reviewed and it was noted that comparable findings were obtained under similar operating conditions. Giménez et. al. [405] achieved 87% COD removal in AnMBR operated at 6-20 hours HRT, 4.2/0.8 minutes filtration/relaxation time and 2-6.67 LMH flux for the treatment of domestic wastewater and they were reported that the methane content of the produced biogas was 55%. In comparison, studies conducted using AnFCMBR showed that similar results were possible with shorter HRTs (1-3 hours) and higher flux levels (5-17 LMH) [362, 406].

In operating the AnFCMBRs, the methane content of the biogas and the amount of dissolved methane in the permeate stream were determined using the procedures described in Section 5.2.1. It is known that a decrease in the HRT value results in a reduction in the amount of methane that is available in the biogas [407]. While the methane content of the biogas was $45\pm 10\%$ at the 24-hour HRT, it was determined as $40\pm 11\%$ at the 3-hour HRT. Lim et al. [32] found a methane concentration of 46.0% while reaching an efficiency of 83.3% in removing COD during the operation of AnFMBR at 25°C it was operated with 1.2 LMH flux as in our study. Similarly, Jeong et al. [408] reported results for the evaluation of anaerobic ceramic MBR operated for treating domestic wastewater. They found that the average methane content was $41.4\pm 10.6\%$. Low permeate flows and operating below 30°C account for the relatively low methane content. Despite the reduction in the methane content of the biogas due to the decrease in the HRT, it was found that the amount of collected and dissolved biogas increased. If dissolved methane is recovered from the permeate stream, it has been found that 94 ± 11 L/m³ wastewater of biogas could be recovered at HRT in 3 hours.

When assessing the COD removal data, it is evident that the methane generation obtained was much below the expected theoretical methane yield. The theoretical methane production in lab-scale AnMBR processes faces challenges that hinder reaching its full potential. Despite efforts to maximize biogas production, certain

constraints impede the exploitation of the full potential of biogas production from AnMBRs, leading to low methane yield [407]. Additionally, achieving energy-neutral operation in AnMBRs, which involves maximizing gaseous and dissolved methane energy capture, can be more challenging in smaller-scale systems [409].

Table 5.9 Performance results for 24, 18, 12, 6, and 3-hour HRT in AnFCMBR systems

Parameters	AnFCMBR-SiS					AnFCMBR-SiF
	24	18	12	6	3	12
HRT(hour)	24	18	12	6	3	12
Flux (LMH)	1.6	2.1	3.1	6.3	6.3	2.1
Filtration mode (min)*	5/1	5/1/1	5/1/1	5/1/2	5/1/2	5/1/1
COD removal (%)	89-96	90-96	83-94	92-94	88-94	87-97
Amount of biogas (L/m ³ wastewater)	16.7	12.8	14.3	8.3	6.0	9.2
Dissolved biogas (L/m ³ wastewater)	15±2	28±5	62±3	88±7	94±11	59±5
Methane content of biogas (%)	45±10	43±5	42±6	42±9	40±11	43±7
Amount of total methane (L/m ³ wastewater)	14.3	17.5	32.0	40.4	40.0	29.3
Amount of theoretical methane (L/m ³ wastewater)**	105.7	136.5	136.4	236.0	610.3	200.5

* Indicates filtration/relaxation or filtration/relaxation/backwash time.

** It was calculated based on COD removal efficiency.

5.3.4 Assessment of energy balance for the proposed process

Energy balance calculations are essential for optimizing the performance of AnMBRs in MWW treatment in order to improve operational efficiency and sustainability. These calculations assess the overall energy demands on the system, covering energy consumption and recovery, in order to enhance performance and optimize the use of resources. Therefore, an overall assessment of the energy balance has been made for the membrane-based hybrid wastewater treatment process, demonstrating its feasibility for full-scale implementation.

The energy balance has been determined by calculating the amount of methane produced by AnFCMBR, the amount of energy that can be produced, and the amount of energy that is used by the system during the operation of both DCMF and AnFCMBR processes. The flow data used in energy calculations was received from the Kayseri WWTP and served as the basis for the energy balance. Figure 5.4 shows the process flow rates. In calculating the total energy requirements of the membrane-based hybrid wastewater treatment process, the energy required for permeate production, feeding, and aeration in the DCMF process and for circulation, permeate production, and feeding in the AnFCMBR process were considered (Table 5.10). The overall energy required for the operation of the processes was 0.08 kWh/m³. This value is significantly less than that reported in other studies with AnMBR using biogas sparging for domestic wastewater treatments [379].

Table 5.10 Energy requirement of processes

DCMF process		
Average TMP ^a	0.4	Bar
Influent flow rate of DCMF	1.66	m ³ /s
Permeate flow rate	1.49	m ³ /s
Aeration flow rate	7.5	m ³ /s
Water level	3	M
Reactor hydraulic head loss	3	m H ₂ O
Power requirement for aeration ^c	315.0	kW
Power requirement for permeation ^c	84.0	kW
Power requirement for feeding ^c	70.0	kW
AnFCMBR process		
Average TMP ^a	0.4	Bar
Permeate flow rate	0.38	m ³ /s
Feed flow rate	0.38	m ³ /s
Circulation flow rate	4.34	m ³ /s
Circulation E (Energy loss) ^b	0.5	m H ₂ O
Power requirement for circulation ^c	30.4	kW
Power requirement for permeation ^c	21.0	kW
Power requirement for feeding ^c	21.0	kW
Total power requirement	541	kW
Total energy requirement	0.08	kWh/m³

^a For the feeding pump head loss was assumed 0.1 m. Average TMP 0.4 bar is assumed to be equivalent to a hydraulic head loss E of 4 m for permeation

^b Local energy losses are considered.

^c Energy requirement = $Q\gamma E/\eta$; Flow rate, Q (m³/s), $\gamma = 9800$ N/m³, hydraulic head loss, E (m), and η efficiency of the pump (70%) [348, 362].

The potential energy amounts of the concentrated wastewater obtained from the pre-concentration process and the methane produced from the operation of the AnFCMBR process at different HRTs are given in Table 5.11. The volume of methane produced per m³ of treated wastewater increased from 14.3 L to 40.0 L when the HRT duration was reduced from 24 hours to 3 hours. Due to the different interactions, biogas production per unit volume of treated wastewater, gas composition, and dissolved methane concentration are dependent on operational parameters [412]. For AnMBRs, a large fraction of the produced methane will remain dissolved in the AnMBR effluent because of low influent COD and higher methane solubility at lower temperatures [412].

The energy potential per m³ of wastewater treated increased in proportion to the volume of methane produced, rising from 0.072 kWh/m³ to 0.203 kWh/m³ when the HRT duration was reduced from 24 hours to 3 hours. The innovative membrane-based hybrid wastewater treatment process requires only 0.08 kWh/m³ of energy. Similarly, Lee et al. [31] discussed the electrical energy required for operating an AnFMBR, emphasizing the low energy demand of 0.0087 kWh/m³ compared to other AnMBR systems.

Kong et. al [413] reported -0.014 kWh/m³ net energy potential for direct treatment of MWW using a submerged AnMBR for a range of HRTs from 24 h to 6 h at an ambient temperature of around 25 °C. In our work, a positive net energy potential was achieved using AnFCMBR-SiS at 18, 12, 6, and 3-hours HRT and using AnFCMBR-Si at 12-hours HRT. Thus, it has been revealed that energy-positive wastewater treatment is feasible with the implementation of the AnFCMBR process with integrated pre-concentration processes as opposed to the treatment of MWW by direct anaerobic processes. Therefore, MWW pre-concentration could improve the applicability and energy generation potential of AnMBR technology [48]. Nevertheless, the calculation of theoretical energy potential, based on the removal of COD, indicated that the AnFCMBR system has a wastewater theoretical energy potential ranging from 0.46 to 3.02 kWh/m³.

Table 5.11 Potential for methane-based electric generation for different HRT operations of the AnFCMBR process

Reactor	HRT (hour)	Biogas volume (L/m ³ wastewater)	Energy potential (kWh/m ³ wastewater)*	Net energy potential (kWh/m ³ wastewater)	Theoretical energy potential (kWh/m ³)**
1st	24	31.7	0.072	-0.008	0.46
	18	40.8	0.089	0.009	0.61
	12	76.3	0.163	0.083	0.61
	6	96.3	0.206	0.126	1.12
	3	100.0	0.203	0.123	3.02
2nd	12	68.2	0.149	0.069	0.94

* It is assumed that each m³ of methane is equivalent to 11.3 kWh of energy under standard conditions and the energy transfer efficiency is 45% when converting methane to electricity. [349, 414].

** It was calculated based on COD removal.

5.3.1 Characterization of membranes

On virgin, physically cleaned, and physically+chemically cleaned ceramic membrane surfaces, SEM and EDX analyses were performed. Figure 5.13 presents images of the SEM analyses performed, and Table 5.12 provides the elemental composition obtained from the EDX results. In addition, the area where the EDX analysis was conducted is indicated in Figure 5.13 by a red box. No pollutants were detected in the SEM images of the physically+chemically cleaned membrane surface (Figure 5.13c), and the elemental composition of the membrane is nearly similar to that of the virgin membrane (Figure 5.13a).

The presence of Si, C, Al, and O in the EDX analysis of the virgin and physically+chemically cleaned membrane is attributable to the ceramic membrane's silicon carbide and aluminum oxide composition [368]. It is known that frequent use of chemical cleaning procedures in long-term operations causes membrane surface deformations [410]. In the SEM images, it was determined that, compared to the virgin membrane, the surface of the used membrane had deformed during operation, increasing its porous structure (Figure 5.13b).

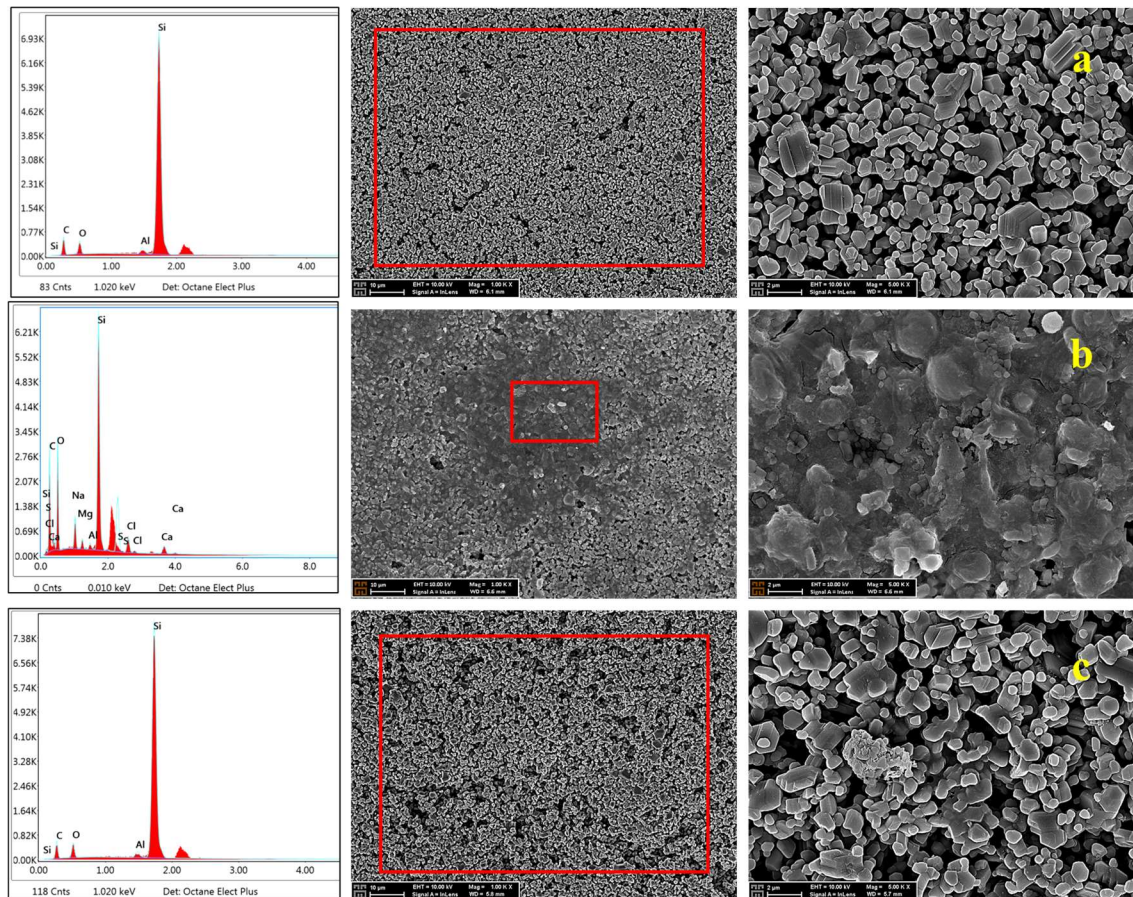


Figure 5.13 SEM images of the virgin (a), physically cleaned (b), and physically+chemically cleaned ceramic membrane (c) used in the AnFCMBR process at 3 hour HRT

The pollutants that cannot be removed when only the physical cleaning procedure is applied on the membrane surface after long-term operation studies and cause fouling in the membrane pores are seen in Figure 5.13b. According to the EDX analysis performed on the pollutant given in Figure 5.13b and Table 5.12, An increase in the content of O was seen, and elements such as S, Cl, Ca, and Na, which were not initially present in the virgin membrane, were identified in the EDX data. O and Ca elements may be speculated that Ca-P precipitates, e.g. hydroxyapatite ($\text{Ca}_5(\text{PO}_4)_3\text{OH}$), $\text{Ca}_3(\text{PO}_4)_2$, and CaHPO_4 . Meanwhile, there were other inorganic salt depositions including silicate, sodium chloride, and sulfate on the membrane surface. The inorganic component was easy to accumulate on the membrane surface by complexation or precipitation, and then more inorganic elements could be gathered in the cake layer [411].

Table 5.12 EDX data of the ceramic membrane used in the AnFCMBR-SiS process at 3-hour HRT

Element	Ratio (%)		
	a*	b**	c***
Si	51.91	26.2	52.99
C	37.03	34.15	35.42
Al	1.38	0.64	1.28
O	9.68	15.99	10.31
S	ND	10.62	ND
Cl	ND	3.74	ND
Ca	ND	4.30	ND
Na	ND	3.42	ND

*Virgin ceramic membrane

** Physically cleaned ceramic membrane

*** Physically+chemically cleaned ceramic membrane

ND: not detected

5.4 Conclusion

This chapter of the thesis focuses on an AnFCMBR treating pre-concentrated MWW using fluidized GAC particles to mitigate fouling. As a promising membrane thanks to its superior properties, the ceramic membrane was used in an AnFMBR for MWW treatment. Two different AnFCMBR configurations were tested for a total of 360 days at ambient temperature with a range of 3 to 24 hours of HRT using pre-concentrated MWW. The AnFCMBR process operating at varied HRT times showed sufficient COD removal efficiency ranging from 83 to 97%. Controlling TMP becomes more challenging in reactor configurations where the membrane is submerged in the fluidized media section.

The electrical energy that could be produced by using the methane was more than required for the operation of the system during the 3, 6, 12, 18-hour HRT operation phase. Operating the AnFCMBR process for 6 hours HRT yields 0.206 kWh/m³ energy, while the innovative membrane-based hybrid wastewater treatment process requires only 0.080 kWh/m³ of energy. AnFCMBR has a significant potential to perform the energy-self-sufficient treatment to achieve sustainable MWW treatment. For estimating the capital costs as well as the requirements for the operation and maintenance of full-scale systems, further work is required for different HRT values to predict and improve the lifespan and energy production potential of the ceramic membrane.

Chapter 6

Optimization of reverse osmosis and struvite precipitation to maximize nutrient recovery from the combined effluent of anaerobic fluidized ceramic membrane bioreactor and direct ceramic microfiltration processes

6.1. Introduction

As a result of climate change, economic growth, and rapid urbanization, 50% of the world's population is projected to face water stress in the not-too-distant future [415]. According to the data from the State Hydraulic Works in Turkey, the annual per capita available water quantity was around 1,322 m³ in 2022 [416]. However, according to the data from the TUIK, this quantity is projected to decrease to 1,120 m³ by the year 2030 [417]. In order to mitigate water scarcity, widespread implementation of effective water reuse strategies can provide substantial environmental, economic, and social advantages [418]. Furthermore, if these strategies incorporate the recycling of nutrients

found in the treated wastewater, particularly through composting, the benefits become much more significant.

Annually, as the global population grows, there is a corresponding increase in the demand for resources such as nitrogen, phosphorus, and potassium. Furthermore, the production of chemical fertilizers and water is essential to ensure food security and meet the needs of the growing population. Phosphorus, the primary constituent of a fertilizer, is scarce in nature and exists in phosphate rocks as P_2O_5 . It is projected that worldwide commercial phosphorus production will hit its highest point by 2033, and phosphorus deposits will be completely used up during the next 50 to 100 years [109]. Therefore, it is crucial to assess alternate and sustainable sources of nutrients. The presence of a significant amount of organic matter in MWW results in a high concentration of nitrogen, phosphorus, and potassium.

In the realm of nutrient recovery, numerous technologies are presently under investigation. These range from more conventional approaches like adsorption and chemical precipitation to more cutting-edge technologies like bioelectrochemical systems and osmotic MBRs [419]. Regarding water recovery, to comply with the restrictive legal requirements for reusable water, it is necessary to subject the effluent from secondary wastewater treatment processes to additional treatment on advanced treatment systems [120]. There are three main categories of advanced treatment systems: filtration, disinfection, and advanced oxidation. One of the most important technologies for advanced wastewater reclamation and reuse systems is the membrane process, which provides robust higher-quality treatment. RO process enables the production of highly purified water as a form of permeate from MWW and potentially even the recovery of nutrients [38]. This process effectively removes soluble ions, dissolved solids, organic materials, and even viruses from wastewater at high rates [420]. In municipal WWTPs, RO processes are used to provide advanced post-treatment to improve the quality of effluent water for subsequent use [421]. Currently, there is increasing interest in using a combination of biological processes and RO for the reuse of MWW due to high performance in removal [422-424]. Research demonstrates that these integrated biological treatment-RO procedures have the capability to consistently provide highly purified water that is better than the quality requirements set by the World Health Organization for drinking water [423]. In order to achieve these benefits,

operational conditions of RO process must be optimized to mitigate membrane fouling and to provide effective operation.

There is growing concern about the environmental sustainability of RO-based MWW reclamation procedures, as the concentrated stream is the unavoidable byproduct of RO units for wastewater reclamation. However, recovering nutrients from RO concentrate is crucial for sustainable water management because of the high nutrient concentrations in the concentrate [425]. Therefore, it is essential to investigate the impact of operational parameters on the ability to enhance concentrating nutrients, but so far, there is limited investigation documented in the existing literature regarding the recovery of nutrients from concentrates of MWW treatment without additional complex processes. Typically, the most straightforward method suggests returning the concentrate of membrane-based processes to the activated sludge process [426]. However, this is only feasible for a certain duration or, at the very least, the recycling process could provide difficulties in numerous facilities, particularly during extended periods of operation, because of the potentially elevated salt concentration in the membrane concentrates [38].

The literature suggests several potential approaches for recovering nutrients from RO concentrates in MWW treatment effluents. These include the utilization of electrochemical cells with cation exchange membranes [427], the crystallization of MAP [428], advanced oxidation [429], and the implementation of an integrated membrane system that incorporates polymeric ligand exchange resins [430]. However, a general assessment based on the literature suggests that advanced oxidation and additional membrane procedures would consume more than 2 kWh/m³ [431-435]. After all, MAP crystallization, being a commonly used cost-savings nutrient-recovery method, may effectively recover both NH₄⁺ and PO₄³⁻ simultaneously [44]. The process of MAP crystallization is regulated by a mixture of physio-chemical parameters that influence both the formation of nucleation and the growth of crystals. The factors that need to be considered include temperature, mixing energy, pH level, the concentration of Mg²⁺, NH₄⁺, and PO₄³⁻ ions, and the presence of competitive ions [436]. The most commonly used way to enhance the effectiveness of MAP crystallization is to optimize reaction parameters such as pH and the presence of struvite constituents [437].

The objective of this part of the thesis was to assess the efficiency of the system in the RO tests conducted to recover nutrients and water from the effluent of AnFCMBR and CEPS+DCMF. In order to achieve this goal, we examined the influence of different operational parameters, including TMP, CFV, recovery rate, and feed water pH value. Following the determination of optimal conditions in tests aimed at nutrient recovery in the RO process, studies were performed on concentrate samples to recover struvite via the MAP crystallization process. MAP crystallizations were performed with different Mg/P ratios and at different pH to determine optimum conditions.

6.2. Materials and Methods

6.2.1 Wastewater and Analysis

Wastewater samples were collected from the effluent of the AnFCMBR and pre-CEPS+DCMF processes. Collected samples were stored at 4 °C and samples were warmed up to room temperature (20 ± 5 °C) before use in the tests. The tests performed with the RO system involved the collection of samples at the end of each test.

The turbidity of wastewater samples was measured using a turbidimeter (TN100, Thermo Scientific, USA). EC and pH parameters were measured using a 3620 IDS WTW multiparameter (WTW GMBH, Germany). AC was performed on a Metrohm equipped with a Metrosep A Supp 5 (150 mm) analytical column and Metrosep C4 (4 mm) guard column to measure Cl^- , SO_4^{2-} , PO_4^{3-} , and NO_2^- . AAS (Perkin Elmer, 900T) device was used for the measurement of Ca^{2+} and Mg^{2+} ions in the samples. The measurements of the metals above the 1 mg/L concentration limit were measured by the flame method with the air-acetylene gas mixture, while the measurements of the lower concentration were measured by the graphite furnace method. COD and $\text{NH}_4\text{-N}$ analyses were carried out following the “Standard Methods for Water and Wastewater” of the American Public Health Association [360].

6.2.2 Experimental set-up and operational conditions of RO system

RO tests were performed using a laboratory-scale cross-flow RO unit (Sterlitech, USA) that can be operated at constant CFV and TMP (Figure 6.1). The temperature was maintained at a constant level of 25 ± 2 °C throughout the tests. Flux, temperature, and

EC were continuously monitored at regular intervals for each test period. The membranes used for the tests were immersed in distilled water for at least 24 hours before their use. To ensure the acquisition of consistent and reliable data, it was performed a one-hour operation with pure water at a TMP of 25 bar for compaction of virgin membrane. Prior to performing each test, the pure water flux was assessed under steady-state conditions for the compaction of the membrane. The decrease in the membrane's performance was assessed by monitoring the pure water flux following the wastewater tests.

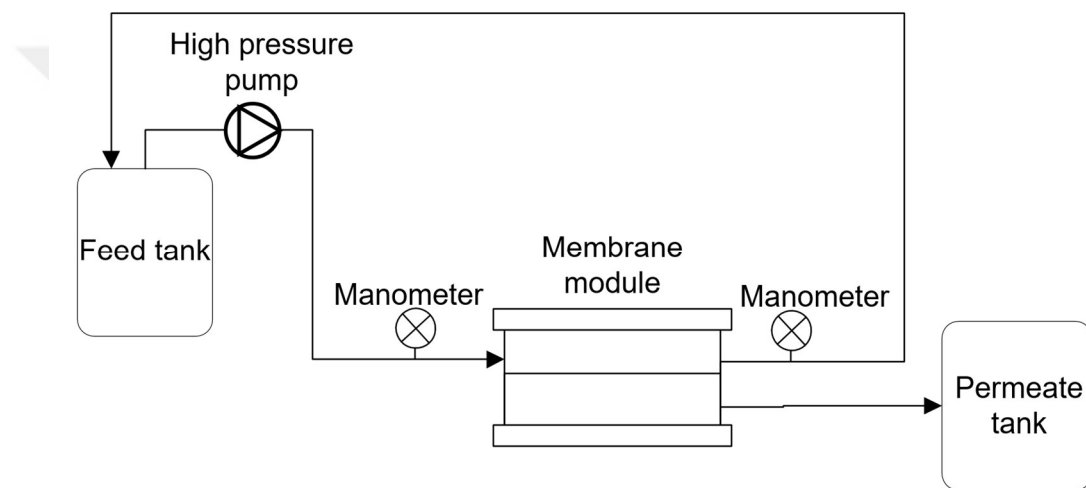


Figure 6. 1 Schematic representation of RO system

The permeate was collected from the system, whereas the concentrate was returned to the feed tank in CM. Thus, the residual water in the feed tank at the end of the test is concentrated. The operational capacity of the system was utilized to achieve a water recovery rate of up to 80%. Theoretical analysis suggests that the behavior of the membrane in this water recovery objective correlates to that of the final membrane element in a full-scale system. It is widely recognized that in a real-scale system, the concentration is most concentrated in the final element that has a membrane, as water permeates through all the other elements. Consequently, the net driving force within this element decreases due to the combined effects of flux drop and the elevation of osmotic pressure. Hence, at the end of the tests, the lab-scale RO system reflects the last operational element of a full-scale system. Therefore, at the initial phase of the tests, the conditions reflect the first element in the full-scale system.

The RO process, renowned for its high selectivity, has been employed to recover nutrients from the effluent of the AnFCMBR and CEPS+DCMF processes and to produce reusable water. Our objective was to evaluate the RO system's performance in nutrient and water recovery in terms of various operational parameters, namely feed compositions, membrane system operational modes (TRM and CM), TMP, CFV, system recovery rate, and pH. Figure 6.2 displays the experimental flow chart of the RO process, performed using the permeate samples gathered from the AnFCMBR and CEPS+DCMF processes. RO tests were performed using different samples in two phases: the first phase involved effluent from the CEPS+DCMF process, and the second phase combined effluent from both the CEPS+DCMF and AnFCMBR processes.

In the first phase, RO tests were performed in both TRM and CM to assess the system's performance with permeate samples from the CEPS+DCMF process. In TRM tests, the permeate was returned to the feed tank, and the RO system was operated until steady-state conditions were achieved. Steady-state conditions were determined by ensuring that the standard deviation calculated from the flux values obtained at regular intervals and continuous measurements during the RO tests were less than 5% of the average flux. In CM, tests maintained a recovery rate of 60%. The impact of varying CFV (0.8 m/s and 1.0 m/s) and TMP (8, 10, and 15 bar) was investigated. The evaluations were based on the flux recovery rates measured during the tests, as well as the characteristics of the permeate and concentrate samples.

In the second phase, after achieving steady-state operation of the AnFCMBR, a combined sample was used by mixing permeate samples from the CEPS+DCMF and AnFCMBR processes in a 20% to 80% ratio, respectively. These combined samples were then fed into the RO process, to optimize the effect of operating parameters including TMP, CFV, recovery rate, and pH levels to achieve maximum efficiency. Tests were maintained only in CM with a recovery rate of 60%. Following the optimization of the operational conditions of the RO system, the concentrated sample was produced under optimal conditions for subsequent MAP crystallization tests.

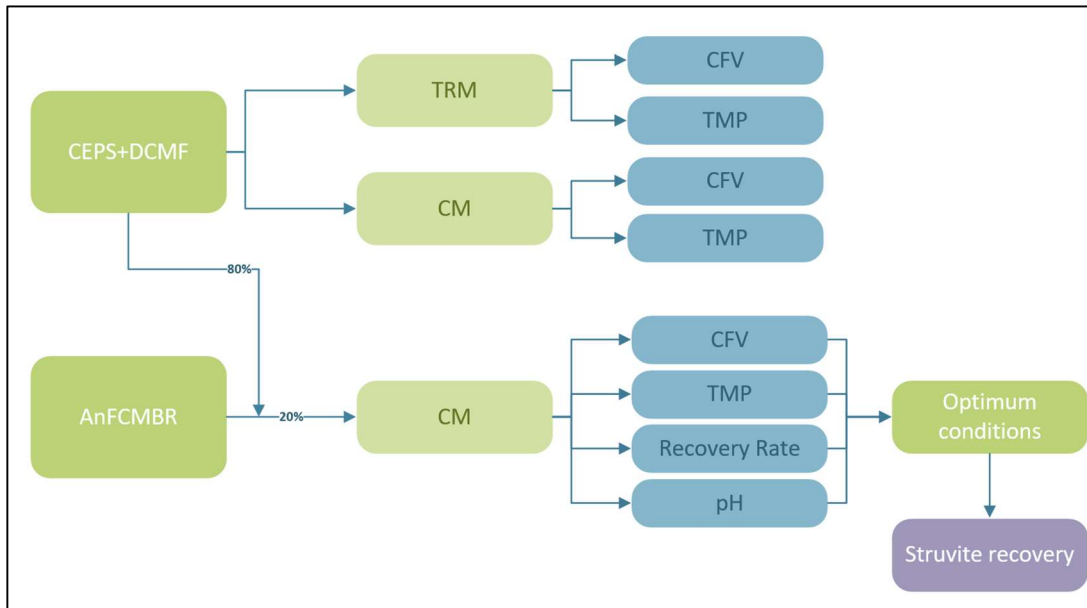


Figure 6.2 Representation of the experimental flow chart of the RO process using the permeate of the AnFCMBR and CEPS+DCMF processes (CM: Concentrate mode, TRM: Total recycle mode, TMP: Transmembrane pressure, CFV: Cross-flow velocity)

The investigation performed with the RO system involved the collection of samples at the end of each test. These samples were subsequently analyzed for parameters including COD, Cl⁻, PO₄-P, NO₂⁻, and SO₄²⁻.

The membrane flux value (L/m²h) represents the quantity of volume that passes through a given unit area of the membrane surface per unit time. This value can be calculated using Equation 6.1.

$$J_v = V/A.t \quad (\text{Eq. 6.1})$$

The symbol 'J_v' indicates the flux, while 'A' represents the effective surface area of the membrane in square meters. The volume of the water filtered across the membrane is indicated by 'V' in liters, and 't' in hours represents the time.

Equation 6.2 provided below was used to calculate the flux decline rate in RO tests for the purpose of making assessments regarding membrane fouling tendency.

$$\text{Flux recovery rate (\%)} = (J_{w2}/J_{w1}) \cdot 100 \quad (\text{Eq. 6.2})$$

In this context, the symbol J_{W2} represents the flux of pure water in units of L/m^2h , while J_{W1} represents the flux of pure water in units of L/m^2h that has been measured after the filtration of the wastewater.

Equation 6.3 was used to calculate the removal efficiency of each parameter, as obtained from the sample characteristics.

$$\text{Removal (\%)} = [(C_f - C_p) / C_f] \cdot 100 \quad (\text{Eq. 6.3})$$

Permeate concentration (C_p) is expressed in mg/L or $\mu S/cm$. Feed concentration (C_f) is expressed as mg/L or $\mu S/cm$.

6.2.3 Modelling of NH_4-N removal

The NH_4-N removal efficiency at pH 6, 7, and 8 was compared with the removal efficiency determined from modeling with the Wave software as part of the evaluation of the RO system performance at different pH values. The characteristics of the combination of 20% CEPS+DCMF and 80% AnFCMBR permeate samples were subsequently integrated into the program as feed characteristics. Subsequently, simulations were run at pH levels of 6, 7, and 8 using the software, and the results were compared with the data acquired from the lab-scale RO system.

6.2.4 Membrane Characterization

The surface of membranes was characterized after the RO test to evaluate the fouling phenomena. Before the characterization tests, the samples were dried at $50\text{ }^\circ C$ in a laboratory-scale oven.

The morphology of the virgin and fouled membrane surface was investigated by SEM on a Zeiss, Gemini-SEM 500 Field Emission microscope operated at 3 kV. Before the measurements, membranes were coated with gold.

ATR-FTIR was employed for the identification of functional groups of the virgin and fouled membranes of the deposited foulants using an FT-IR spectrometer (Thermo Nicolet Avatar 370). The analysis was conducted in the wavelength range of $4000-400\text{ cm}^{-1}$ [438].

6.2.5 N and P recovery from RO concentrate by MAP crystallization

The concentrate of the RO process was tested in nutrient recovery tests, which were gathered from the test performed under optimum operating conditions. The recovery of nutrients through the process of MAP crystallization was studied in batch reactors. In order to achieve the stated objective, the concentration levels of PO₄-P, NH₄-N and Mg²⁺ were quantified. The optimization of the conditions for the MAP crystallization was performed through a series of tests conducted in batch reactors, according to the following chemical equation.



As shown in the chemical equation the NH₄/PO₄/Mg requires a molar ratio of 1. However, the significance of the Mg/P ratio could be in the typically low concentration. PO₄³⁻ or Mg²⁺ was added to the wastewater to adjust Mg/P ratios of 0.67, 0.83, 1, and 1.1. The tests were conducted at a pH of 9 to determine the optimum Mg/P ratio. Subsequently, tests were performed at various pH levels (8, 8.5, 9, 9.5, and 10). During the optimization of the Mg/P ratio and pH, the batch reactors were stirred at 200 and 20 rpm for a duration of 20 and 60 minutes, respectively. Subsequently, the samples were filtrated through a 0.45 µm filter, resulting in the separation of the precipitate from the aqueous phase. The filtered precipitate samples were dried at a temperature of 40 °C for 24 hours [439].

6.2.6 X-ray diffraction (XRD)

The dried precipitate was then crushed to obtain smaller particles and made ready before analysis. XRD analysis was conducted using a Bruker/Siemens XRD analyzer equipped with Cu Kα = 1.54060 Å copper radiation to assess the quality of struvite in the precipitates formed during MAP crystallization. The analyses were performed at a scanning speed of 0.02° and a scanning range of 10-70° 2θ angles [277].

6.3. Results

6.3.1 RO tests with effluent of CEPS+DCMF

The first phase of the RO tests involved performance evaluation on CEPS+DCMF permeate samples with two different operational modes, focusing on nutrient recovery and the production of reusable water. The initial part of the RO tests with the effluent of the CEPS+DCMF process was conducted in TRM mode, while the subsequent tests were performed in CM. The following sections present the data and results obtained from these tests.

6.3.1.1 Operation of RO process in TRM using CEPS+DCMF process effluent

Initially, the tests were performed at TMP values of 8, 10, and 15 bar and CFV of 0.8 and 1 m/s in TRM operation. Table 6.1 displays the flux recovery rates received through the operation of the RO system in TRM operation. The average flux recovery rates observed were more than 94%. The experimental results indicate that the optimal conditions for achieving the highest flux recovery involve a TMP of 10 bar and a CFV of 1 m/s, resulting in a flux recovery of 97%. While the flux recovery rates did not show a significant variation, the highest level of membrane fouling was observed at a TMP of 10 bar and CFV of 0.8 m/s, resulting in a flux recovery rate of 94%. Basically, the flux decline is known to result from the increase in membrane resistance by cake formation and membrane pore blockage [440].

Table 6.1 Flux recovery rates obtained in TRM operation

CFV (m/s)	TMP (bar)	Flux recovery rate (%)
0.8	8	96
	10	95
	15	94
1	8	95
	10	97
	15	96

The tests performed using the RO system in TRM involved analyzing samples obtained from the permeate after reaching steady-state conditions. The findings of the sample characteristics are presented in Table 6.2. The EC values of RO feed water show a range of 1711 to 2125 $\mu\text{S}/\text{cm}$. Conversely, the obtained permeate samples have a range of 50-73 $\mu\text{S}/\text{cm}$. A study conducted using synthetic wastewater found that the BW30 membranes had an average EC rejection rate of 88% [441]. In our study, rejections of EC were higher with a range between 96 and 98%.

The feed samples of $\text{PO}_4\text{-P}$ concentration were approximately 8 mg/L and NO_2^- concentration ranging from 4-10 mg/L. However, the permeate samples indicated undetectable levels of both $\text{PO}_4\text{-P}^-$ and NO_2^- . In a similar way, it was observed that the feed COD concentration ranged between 16-45 mg/L, whereas the concentration in the permeate samples had COD concentrations below the detectable limit of 5 mg/L. Thus, it can be concluded that $\text{PO}_4\text{-P}$, NO_2^- and COD were completely rejected. Additionally, TMP, defined as the pressure variance across the membrane, impacts various aspects of the process. Studies have demonstrated that adjusting transmembrane pressure can result in modifications to membrane fouling characteristics [442] and the rejection mechanisms [443]. When the CFV was at 1 m/s, an increase in TMP from 8 bar to 15 bar resulted in a considerable decrease in the EC of the permeate from 73 ± 24 to 50 ± 3 $\mu\text{S}/\text{cm}$.

Table 6.2 Characteristics of samples obtained by TRM operation of RO process

TMP (bar)	CFV (m/s)	Sample	pH	EC ($\mu\text{S/cm}$)	COD (mg/L)	Cl⁻ (mg/L)	PO₄-P (mg/L)	NO₂⁻ (mg/L)	SO₄²⁻ (mg/L)
8	0.8	Feed	9	1996 \pm 360	26 \pm 4	388 \pm 12	8.0 \pm 1.6	6 \pm 4	110 \pm 3
		Permeate	9	73 \pm 24	<5	8 \pm 1	ND*	ND*	1 \pm 0
	1	Feed	8	2070 \pm 240	23 \pm 5	387 \pm 5	8.0 \pm 0.0	4 \pm 1	107 \pm 13
		Permeate	10	72 \pm 8	<5	6 \pm 0	ND*	ND*	1 \pm 0
10	0.8	Feed	8	2125 \pm 177	27 \pm 5	352 \pm 56	8.0 \pm 1.0	8 \pm 2	108 \pm 5
		Permeate	9	52 \pm 8	<5	5 \pm 2	ND*	ND*	1 \pm 0
	1	Feed	9	1711 \pm 240	16 \pm 3	386 \pm 5	8.0 \pm 0.1	6 \pm 5	104 \pm 8
		Permeate	9	72 \pm 8	<5	5 \pm 1	ND*	ND*	1 \pm 0
15	0.8	Feed	8	2037 \pm 75	45 \pm 5	358 \pm 61	8.0 \pm 1.3	10 \pm 4	110 \pm 6
		Permeate	10	61 \pm 2	<5	6 \pm 1	ND*	ND*	1 \pm 0
	1	Feed	9	1895 \pm 144	33 \pm 4	304 \pm 116	8.0 \pm 0	7 \pm 0	107 \pm 3
		Permeate	10	50 \pm 3	<5	3 \pm 1	ND*	ND*	1 \pm 0

ND*: Indicates concentrations below the detection threshold.

6.3.1.2 Operation of RO process in CM using CEPS+DCMF process effluent

Following the TRM operating mode, which constitutes the initial phase of optimization of CFV and TMP in RO tests, the subsequent phase involved conducting tests in the CM. Experimental investigations were performed using the RO system, with a 60% recovery rate, at the same CFV (0.8 and 1 m/s) and TMP (8, 10, and 15 bar) values in the CM. Table 6.3 presents the flux recovery rates acquired from the RO tests performed under the CM conditions. The tests indicated an average flux recovery rate of over 91%.

Experimental results also suggest that the most optimal conditions for achieving the highest rate of flux recovery refer to a TMP of 10 bar and a CFV of 1 m/s, resulting in a flux recovery rate of 98%. Research has shown that operational parameters like cross-flow velocity play a crucial role in mitigating fouling in RO systems, with higher velocities reducing the accumulation of foulants on the membrane surface [444].

Table 6.3 Flux recovery rates obtained by operating the RO process in CM

CFV (m/s)	TMP (bar)	Flux recovery rate (%)
0.8 m/s	8	96
	10	92
	15	97
1 m/s	8	94
	10	98
	15	91

During the operation of the RO system in CM, permeate was collected until the recovery rate reached 60%. Once the recovery rate reached 60%, samples of concentrate and permeate were sampled and analyzed. Their characteristics are presented in Table 6.4. The EC indicated a variation between 82 and 106 $\mu\text{S}/\text{cm}$ in the permeate samples. The permeate from the RO process is essential as it often meets stringent quality standards for reuse purposes. Studies reveal that the permeate produced by the RO process meets the requirements set by organizations including the Food and Agriculture Organization [36]. The feedwater samples indicated a COD concentration

within the range of 33-61 mg/L, whereas the permeate samples showed a concentration below the detectable limit of 5 mg/L. Thus, it was recognized that the COD had been completely removed. Based on the findings of the experiments performed under optimal conditions (i.e., 15 bar TMP and 0.8 m/s CFV) in terms of flux recovery, it was noticed that the maximum concentration of PO₄-P (16±2 mg/L) was achieved.



Table 6.4 Characteristics of samples obtained by TRM operation of RO process

TMP (bar)	CFV (m/s)	Sample	pH	EC ($\mu\text{S/cm}$)	COD (mg/L)	Cl ⁻ (mg/L)	PO ₄ -P (mg/L)	NO ₂ ⁻ (mg/L)	SO ₄ ²⁻ (mg/L)
8	0.8	Feed	9	1866±289	55±4	282±104	10±4	5±2	91±2
		Permeate	9	90±2	<5	10±1	ND*	ND*	2±0
		Concentrate	9	3320±339	153	573±133	8±1	22±8	205±25
	1	Feed	9	1467±66	61±8	299±139	8±1	13±3	101±12
		Permeate	10	103±15	<5	8±1	ND*	ND*	2±1
		Concentrate	9	3620±1428	211±157	661±378	5±5	24	219±0
10	0.8	Feed	9	1741±59	61±3	204±7	11±3	3±2	100±14
		Permeate	10	82±2	<5	7±2	ND*	ND*	2±0
		Concentrate	9	3175±7	135±7	434±36	11±5	7±6	214±29
	1	Feed	9	1780±11	33±6	280±115	8±2	10±7	99±3
		Permeate	10	86±9	<5	7±1	ND*	ND*	2±1
		Concentrate	9	3490±665	149±96	630±348	4±3	20±18	206±22
15	0.8	Feed	9	1757±43	48±10	205±10	9±4	2	103±15
		Permeate	9	82±4	<5	7±2	ND*	ND*	2±1
		Concentrate	9	3185±134	142±37	418±17	16±2	3	213±33
	1	Feed	9	1863±102	38±18	292±134	7±1	5±3	101±2
		Permeate	9	106±12	<5	11±0	ND*	ND*	2
		Concentrate	9	3410±509	125±64	608±302	5±0	9	209±2

ND*: Indicates concentrations below the detection threshold.

6.3.2 RO tests with effluent of the CEPS+DCMF and AnFCMBR processes

During the first phase of the tests performed to optimize the RO process, the parameters of CFV (0.8 and 1 m/s), and TMP (8, 10, and 15 bar) were tested under TRM and CM conditions using only effluent of CEPS+DCMF process. As the second phase of the RO tests, experiments were conducted under CM conditions to obtain nutrient-rich concentrate and reusable water by mixing the effluent samples of the CEPS+DCMF and AnFCMBR processes in a ratio of 80% to 20%, respectively. These rates have been determined based on daily average flow rates, assuming that the AnFCMBR system is operated at HRT for 3 hours.

Firstly, RO tests were performed at a 60% recovery rate, at different CFV (0.8 and 1 m/s) and TMP (8, 10, and 15 bar). Subsequently, tests were conducted at different recovery rates (60%, 70%, and 80%) at the optimized CFV and TMP values. Following the optimization of CFV, TMP, and the process recovery rate, the optimum pH value was determined. This step was the last phase of the process of identifying the most effective operating conditions. The last part of the RO test involved the implementation of the concentrate collection to determine optimum conditions in the subsequent nutrient (MAP) recovering investigations.

6.3.2.1 Effect of TMP and CFV on RO performance

The samples were tested for different CFV (0.8 and 1 m/s) and TMP (8, 10, and 15 bar), at a 60% recovery rate. Table 6.5 presents the characteristics of the feed sample used in the tests, as well as the concentrate and permeate samples obtained from the tests. The permeate samples showed a significantly lower EC range of 40-78 $\mu\text{S}/\text{cm}$, indicating a removal rate of over 95%. removal efficiency of Cl^- , $\text{PO}_4\text{-P}$, NO_2^- , and SO_4^{2-} . The results indicated that the removal efficiency of $\text{PO}_4\text{-P}$ and NO_2^- was 100%, while the average SO_4^{2-} and Cl^- removal efficiency was 99%. It is known that BW30 membranes have a negative surface charge within the pH range of 6 to 11 [445]. The wastewater samples used in this study have pH levels ranging from 8 to 10. Consequently, the membrane preserves a negative surface charge during the whole test.

Anions are repelled by the negatively charged surface of the membrane. Consequently, in addition to the mechanism of sieving, the repulsion of charges also played a significant part in the rejection of chloride and sulfate ions. The primary factors contributing to the high rejection of Cl^- and SO_4^{2-} were the membrane's sieving properties and charge repulsion [446]. Furthermore, the concentration of $\text{PO}_4\text{-P}$, a crucial factor in studies related to the recovery of nutrients such as struvite, exhibits a range of 17-23 mg/L in the samples of concentrate. The results of RO tests performed at a TMP of 15 bar and a CFV of 0.8 m/s indicated that the highest recovery of $\text{PO}_4\text{-P}$ was achieved at a concentration of 23 ± 5 mg/L. According to the characterization results, it was found that there was no significant difference in the removal efficiency, except for the COD removal efficiency. The test conducted at a CFV of 0.8 m/s and TMP of 15 bar provided the highest COD removal efficiency of 74%.

Table 6.5 Effect of CFV and TMP on the performance of RO

TMP (bar)	CFV (m/s)	Sample	pH	EC ($\mu\text{S/cm}$)	COD (mg/L)	Cl ⁻ (mg/L)	SO ₄ ²⁻ (mg/L)	NO ₂ ⁻ (mg/L)	PO ₄ -P (mg/L)
8	0.8	Feed	8.2±0.0	1635±22	49±18	181±3	52±10	29	15±3
		Concentrate	8.4±0.2	2940±14	175±62	365±2	125±65	42	18±8
		Permeate	8.8±0.4	73±1	22±18	1±0	1±0	ND*	ND*
	1	Feed	7.8±0.3	1656±11	35±12	178±1	58±0	1.9	13±3
		Concentrate	8.4±0.2	3160±354	102±27	363±12	108±1	2.2	17±5
		Permeate	8.5±0.7	78±4	14±4	1±0	1±0	ND*	ND*
10	0.8	Feed	8.2±0.1	1652±1	35±2	183±8	62±4	4	14±4
		Concentrate	8.5±0.2	3055±35	133±42	352±7	122±6	6	17±9
		Permeate	9.2±0.2	71±1	15±9	1±0.11	ND*	ND*	ND*
	1	Feed	7.9±0.1	1458±214	51±1	151±31	54±10	8±5	11±3
		Concentrate	8.3±0.0	2660±311	118±24	308±51	106±14	12±3	17±6
		Permeate	8.4±0.3	66±6	22±1	ND*	ND*	ND*	ND*
15	0.8	Feed	8.2±0.1	1658±10	29±7	178±1	60±0	4±2	14±3
		Concentrate	8.3±0.0	2980±71	107±30	349±12	116±1	5±2	23±5
		Permeate	8.7±0.0	72±16	8±2	ND*	1±0	ND*	ND*
	1	Feed	8.0±0.0	1486±232	41±6	154±31	59±3	10±1	11±0
		Concentrate	8.2±0.2	2695±460	106±29	301±57	113±7	17±1	19±2
		Permeate	8.4±0.3	68±20	18±12	ND*	ND*	ND*	ND*

ND*: Indicates concentrations below the detection threshold.

Figure 6.3 displays the results of tests conducted at varying CFV and TMP with a recovery rate of 60%, illustrating the pure water, wastewater, and pure water permeability (after wastewater tests) values as well as the flux recovery rates. The average flux recovery rates observed in all RO tests were greater than 93%. The tests performed at a TMP of 15 bar and a CFV of 0.8 m/s yielded the greatest flux recovery rate, reaching a value of 98%. The maximum wastewater permeability was attained during the RO tests conducted at a TMP of 8 bar, a CFV of 0.8 m/s, and a value of 3.6 LMH/bar. However, more severe biofouling can occur during operations at higher permeability. Rapid biofilm formation on the membrane is caused by the higher flux, which drives the convective transfer of nutrients, solutes, and bacteria to the membrane surface [447]. It has already been observed that a high permeability value has a negative effect on the flux recovery rate in the RO tests performed at a TMP of 8 bar, and a CFV of 0.8 m/s.

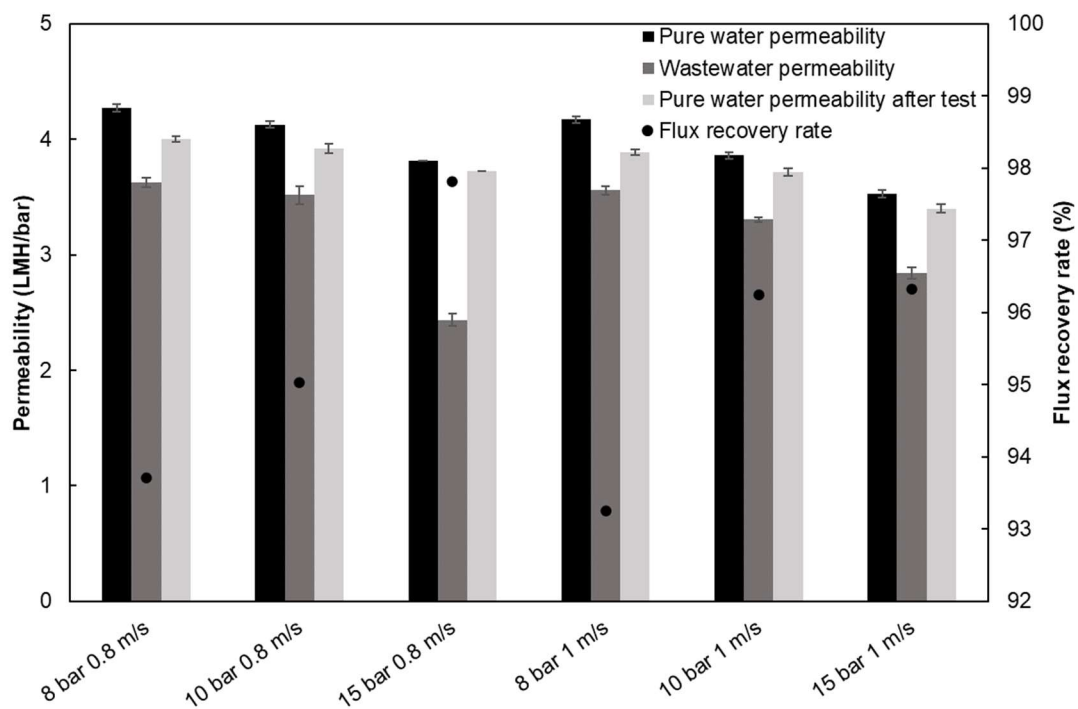


Figure 6.3 Permeability values and flux recovery rates obtained for TMP and CFV in RO tests

The experimental results indicate that the optimal conditions for achieving the highest recovery of $\text{PO}_4\text{-P}$ and flux recovery rate were achieved at a TMP of 15 bar and a CFV of 0.8 m/s. Hence, the recovery rate and pH level optimization studies the second

and third phases of the RO tests, respectively- were performed at a TMP of 15 bar and a CFV of 0.8 m/s.

6.3.2.2 Effect of Recovery Rate on RO performance

Following the TMP and CFV optimization, tests were performed at 60%, 70%, and 80% recovery rates, under optimal conditions of 0.8 m/s CFV and 15 bar TMP. Table 6.6 presents the characteristics of the feed, concentrate, and permeate samples. With regard to the tests performed at each recovery rate, the initial pH level in the feed samples ranged from 7.6 to 8.2, while the final pH level was between 8.3 and 8.5. As water is recovered, the concentration of ions and compounds in the remaining water increases, potentially affecting the pH of the solution. This concentration effect can result in pH level changes as the recovery rate increases [448].

When the rate of recovery increased from 60% to 80%, the content of $\text{PO}_4\text{-P}$ in the concentrate reduced from 23 ± 2 mg/L to 10 ± 1 mg/L. The findings of RO tests performed at a TMP of 15 bar and a CFV of 0.8 m/s indicated that the maximum recovery of $\text{PO}_4\text{-P}$ was achieved at a concentration of 23 ± 2 mg/L, with a corresponding recovery rate of 60%. The concentration of $\text{PO}_4\text{-P}$ is of major significance in studies regarding further MAP crystallization tests. The recovery rate in RO processes can have a significant impact on the recovery of phosphate. Higher recovery rates in RO systems can lead to challenges such as limitations in the system's maximum recovery ratio and increased fouling rates due to imbalances in driving force [449]. The presence of phosphate in the concentrate can affect the scaling behavior, with studies showing that calcium phosphate becomes increasingly insoluble at higher pH values [450]. In addition, as the recovery rate increases, so does the duration of the test. As a consequence, the chance of calcium phosphate crystallization may increase. It is essential to consider the overall recovery and concentration processes in water treatment systems. High recovery rates can lead to concentrate minimization challenges, especially when dealing with inorganic constituents like phosphate that can contribute to membrane scaling [451]. One key aspect to consider is the solubility of phosphate salts at different pH levels. Phosphate salts, such as calcium phosphate and magnesium phosphate, tend to have lower solubility at higher pH values [452]. A precipitate of calcium or magnesium phosphate, which forms at high pH values, can be avoided by

lowering the pH of the feed samples. However, high pH levels can lead to lower NH₄-N recovery [453].

Table 6.6 Characteristics of samples obtained from tests on recovery rate optimization of RO

Recovery rate (%)	Sample	pH	EC (μS/cm)	COD (mg/L)	Cl ⁻ (mg/L)	NO ₂ ⁻ (mg/L)	PO ₄ -P (mg/L)
60	Feed	8.2	1651	51±2	177±1	4±1	14±2
	Concentrate	8.3	2930	297±13	349±1	5±1	23±2
	Permeate	8.7	83	15±2	0,5±0	0,03±0	ND*
70	Feed	7.6	2415	30±1	440±1	0,6±0	15
	Concentrate	8.4	5230	223±11	1019±66	1,7±0	15±1
	Permeate	8.7	97	12±2	15±1	0,1±0	ND*
80	Feed	7.7	2500	30±1	440±1	0,6±0	16
	Concentrate	8.5	7220	302±16	1508±72	1,6±0	10±1
	Permeate	9.3	130	11±2	20±2	0,1±0	ND*

ND*: Indicates concentrations below the detection threshold.

Figure 6.4 presents the permeability values acquired from RO tests performed at various recovery rates while maintaining a TMP of 15 bar and a CFV of 0.8 m/s. The increase in the rate of test recovery resulted in a decline in the permeability and flux recovery rate. The noticed phenomenon is attributed to the extension of the testing duration, which is caused by the elevated recovery rate, leading to the membrane's fouling behavior. Upon reviewing the literature, it is obvious that the BW30-XFR membrane demonstrates a noteworthy level of efficacy, with a 60% recovery rate. [454]. When RO operates at higher concentrations and recovery rates, it faces challenges such as limitations in the system's maximum flux recovery ratio due to feed concentration and membrane constraints [455].

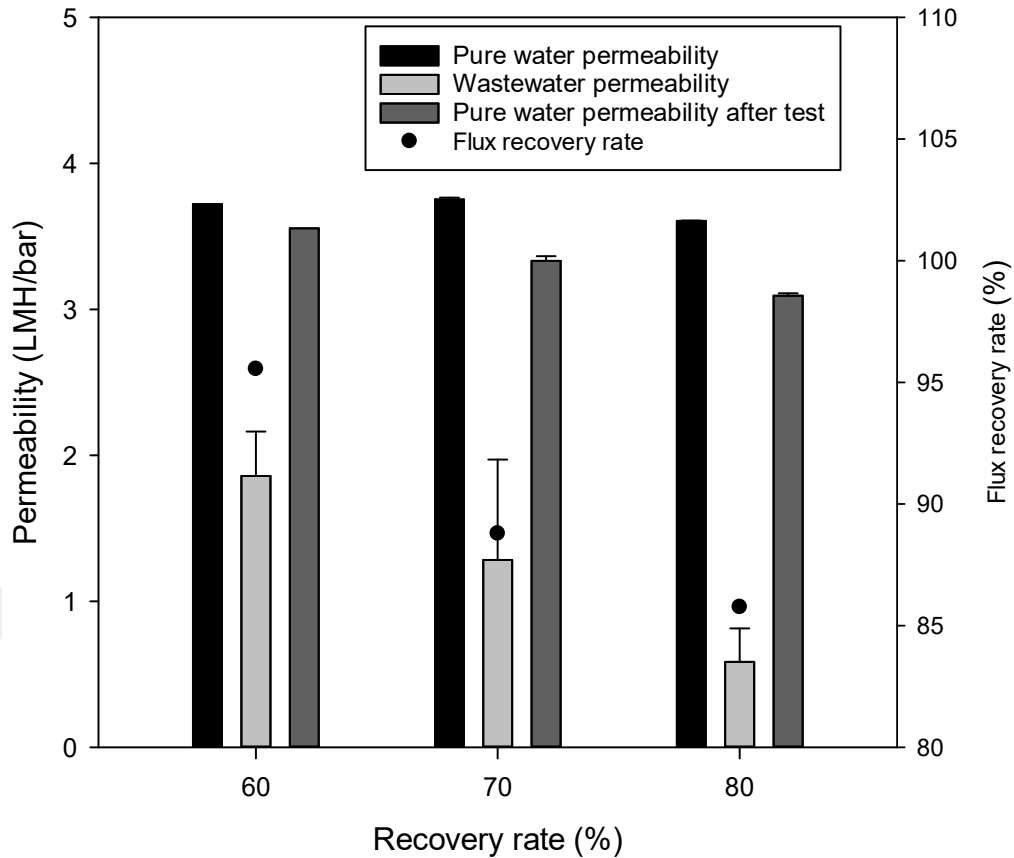


Figure 6.4 Permeability values and flux recovery rates obtained for different recovery rates in RO tests

6.3.2.3 Effect of pH on RO performance

As a last phase of optimization of RO, the performance of the RO process was investigated at pH values of 6, 7, and 8. Tests were performed using the optimized operating conditions of 15 bar TMP, 0.8 m/s CFV, and a 60% recovery rate. Table 6.7 presents the characteristics of the feed, concentrate, and permeate samples acquired from the tests. Studies have shown that the pH of the feed water significantly impacts ion rejection [456]. Specifically, at higher pH levels, the rejection of ammonium ions decreases due to the decrease in the hydration radius of uncharged ammonia [457]. This decrease in rejection at higher pH levels is attributed to the change in the speciation of ammonium compounds in solution, affecting their interaction with the membrane surface. Moreover, the effect of pH on membrane rejection mechanisms has been extensively studied in the context of various contaminants. For instance, feedwater pH has been found to impact membrane salt rejection through changes in salt partitioning caused by the electrostatic Donnan exclusion mechanism [458]. Additionally, the charge

density in the active layers of RO membranes plays a crucial role in the rejection of certain contaminants, where pH influences the membrane surface charge and, consequently, the rejection of ionic contaminants [449].

The concentration of PO₄-P, a crucial parameter for studies related to nutrient recovery, shows a variation between 14-34 mg/L in concentrate samples. The experimental studies performed at a pH of 6 provided a maximum concentration of PO₄-P at 34 mg/L in RO concentrate. The results represented in Table 6.9 indicate that higher PO₄-P recovery was achieved in the tests performed at pH 6 in contrast to those performed at pH 7 and 8. However, when a mass balance was established by using the system recovery rate and the feed PO₄-P concentration, it was revealed that 82.2% of PO₄-P was successfully recovered in the concentrate. Therefore, it can be assumed that 17.8% of PO₄-P was deposited on the surface of the membrane as it was not identified in the permeate. The concentrate has a pH of 7.2, and precipitation can be avoided by reducing the feed pH value to 6.5 or below. Similarly, with the increase in pH from 6 to 8, the NH₄-N concentration in the concentrate samples decreased from 124.6 mg/L to 95.6 mg/L. When considering the impact of pH increase on NH₄-N recovery in the concentrate of the RO process, it is crucial to understand that high pH levels can affect NH₄-N recovery adversely. Williams et al. [453] highlighted that high-pH concentrates can enhance desorption, which implies that an increase in pH may lead to reduced NH₄-N recovery efficiency.

Table 6.7 Characteristics of samples on pH optimization of RO process at 60% recovery rate

pH	Sample	pH	EC (μ S/cm)	COD (mg/L)	Cl ⁻ (mg/L)	PO ₄ -P (mg/L)	NH ₄ -N (mg/L)
6	Feed	6	2160	80±7	269±5	16.7±0.3	67.7
	Concentrate	7.2	4490	170±9	1110±4	34.3±0.3	124.6
	Permeate	6.7	85	11±5	14±0	ND*	4.8
7	Feed	7	1925	39±13	245±1	16.0±0.5	60.2
	Concentrate	7.8	3460	144±16	748±1	29.0±0.2	105.4
	Permeate	7.2	87	1±0	13±0	ND*	5.9
8	Feed	8	1750	75±10	268±4	16.4±0.3	66.1
	Concentrate	8.2	3360	158±9	551±10	14.7±0.4	95.6
	Permeate	7.8	82	8±3	8±0	ND*	9.5

ND*: Indicates concentrations below the detection threshold.

Figure 6.5 presents the permeability values acquired from RO tests performed at different pH levels. The study found that while the pure water permeability values were comparable. However, RO tests performed using wastewater samples showed a decline in wastewater permeability values. Specifically, by increasing the pH from 6 to 7 and 8, the permeability decreased from 2.7 LMH/bar to 2.4 LMH/bar and 1.9 LMH/bar. Regarding the flux recovery rates, it was noted that the RO test conducted at a pH of 7 resulted in the lowest flux recovery rate of 92%. It is important to consider the influence of pH on membrane fouling in RO systems, as membranes are susceptible to fouling, which can increase operational costs and reduce their efficiency [459]. Specifically, an increase in pH can lead to membrane fouling, which in turn can result in a decline in flux, an increase in operating pressure, more frequent membrane cleaning, and higher water production costs [460]. Research by Masse et al. [461] highlights that variations in pH levels can impact membrane fouling and cleaning, as well as permeate flux and quality during the processing of wastewater. When the pH of the feed solution in an RO process increases, it can have a negative impact on the permeability of the system. This is due to various factors such as electrostatic repulsion between carboxyl groups, which can lead to the prolongation of the chain and subsequently reduce the effective pore size of the membrane, resulting in a decrease in the stable permeation flux of the RO membrane [462]. Moreover, increasing the pH can lead to concentration polarization of solutes on the membrane surface or inside the membrane, limiting water flux in RO [463].

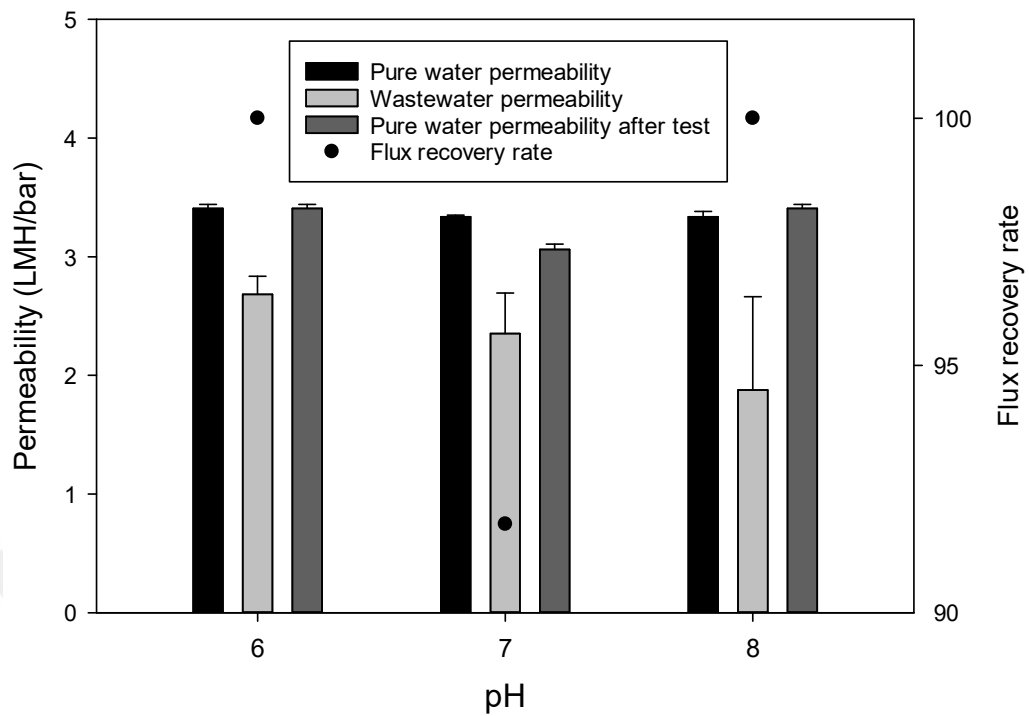


Figure 6.5 Flux and flux recovery rates obtained for different pH in RO tests

For assessing the performance of a RO system under different pH conditions, the removal efficiencies of $\text{NH}_4\text{-N}$ were evaluated at pH levels of 6, 7, and 8. These experimental results were then compared to the recovery of the $\text{NH}_4\text{-N}$ predicted by the Wave program. Figure 6.6 shows the project generated in the Wave software for modeling studies, while Table 6.8 presents the inputs utilized in indicated modeling studies.

Table 6.8 Inputs used in modeling created in Wave Software

Parameter	Inputs
Membrane	BW30-XFR
Design temperature ($^{\circ}\text{C}$)	25
Feed flow (m^3/h)	100
Permeate flow (m^3/h)	60
Recovery rate (%)	60
pH	6
pH adjustment chemical	HCl

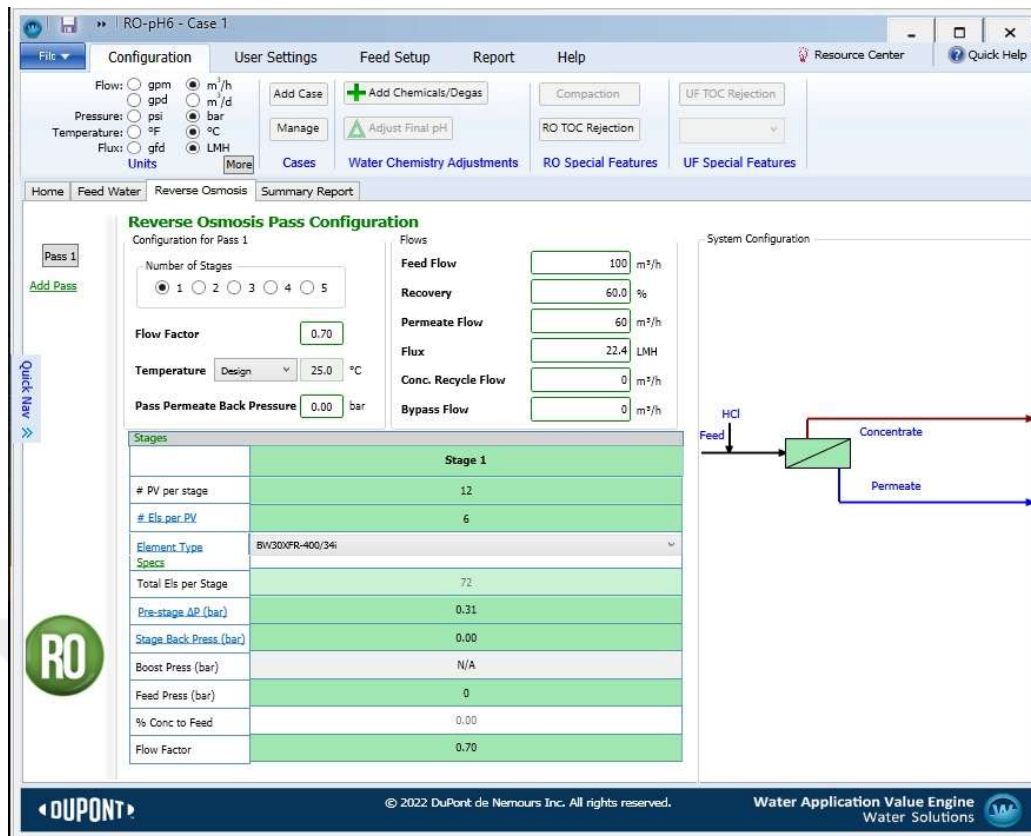


Figure 6.6 A visual representation of the project generated to compare the NH₄-N recovery rate through the modeling designed in the Wave software.

Figure 6.7 presents a comparison between the NH₄-N recovery rates obtained through modeling using the Wave software and achieved through RO tests at different pH levels (pH 6, 7, and 8). The RO modeling study found that the efficiencies assessed in the RO tests exhibited similar patterns to those indicated in the Wave software. Additionally, the NH₄-N recovery rate decreased as the pH value increased from 6 to 7 and 8. Furthermore, upon entering the feed characteristics and operating conditions gathered from the RO test performed at a pH of 6 and a TMP of 15 bar into the WAVE software, the energy demand of the RO process was estimated to be 0.62 kWh/m³.

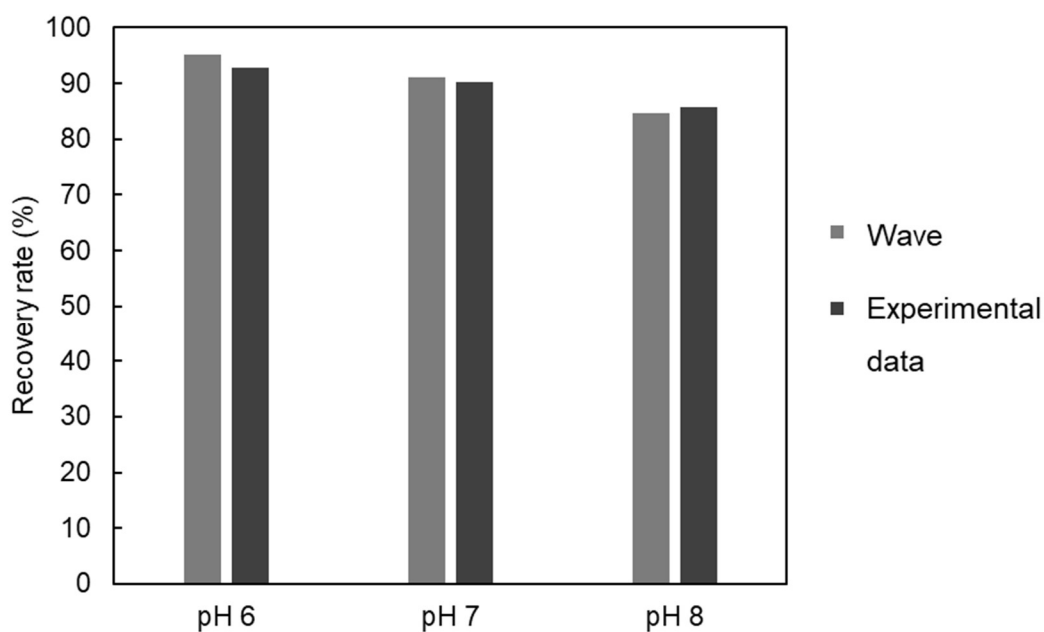


Figure 6.7 Comparison of the experimentally determined NH_4^+ removal efficiencies and the Wave software modeled $\text{NH}_4\text{-N}$ recovery rate at different pH

Finally, RO tests were performed to obtain concentrated wastewater for MAP crystallization studies at the optimized conditions: CFV of 0.8 m/s, TMP of 15 bar, recovery rate of 60%, and pH level of 6.

6.3.3 Membrane Surface Characterization

6.3.3.1 ATR-FTIR

Figure 6.8 presents the ATR-FTIR spectra of the BW30-XFR membrane used in the RO test, both pre- and post-experiment, within the $500\text{-}4,000\text{ cm}^{-1}$ range. The ATR-FTIR analysis was performed at a CFV of 0.8 and 1.0 m/s and a TMP of 15 bar. In the $500\text{-}4000\text{ cm}^{-1}$ region, peaks were associated with the PSF sublayer and the PA layer [464]. The strong peaks in the region between 1500 and 1800 cm^{-1} were associated with carbonyl groups and amide bands where the PA thin-film membranes presented their characteristic peaks [465]. The second specific peak with the presence of carbonyl groups and amide bands was indicated between 2700 and 3700 cm^{-1} [466]. In this region, a significant difference was determined for the membranes used in the tests performed with CFV of 0.8 and 1 m/s and virgin membranes in the range of $1640\text{-}1730\text{ cm}^{-1}$ [467]. Furthermore, noteworthy dissimilarities were noticed within the range of

2700 to 3700 cm^{-1} , which corresponds to the secondary peak region housing carbonyl groups and amide bands [468].

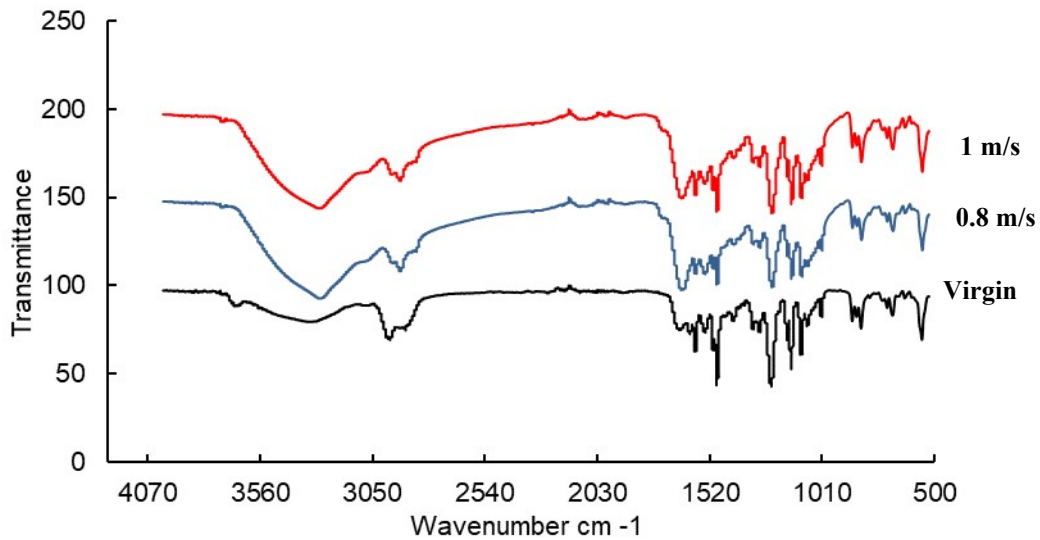


Figure 6.8 ATR-FTIR spectra of the virgin, fouled during tests performed at a CFV of 0.8 and 1.0 m/s

6.3.3.2 SEM-EDX

SEM and EDX analysis of the BW30-XFR membrane used in the RO tests, which was performed with a CFV of 0.8 m/s, 15 bar TMP, and 60% recovery rate, with the aim of revealing the change in membrane surface morphology before and after the test. The images of the SEM and EDX analyses performed on the surface of the BW30-XFR membranes, which were virgin membranes and were washed with distilled water after the tests, are presented in Figure 6.9 and the elemental composition obtained from the EDX results are presented in Table 6.9.

The pollutants that cause local fouling on the membrane surface after RO tests are clearly seen in Figure 6.9b. According to the results of the EDX analysis performed on the pollutant in Figure 6.9b, it was determined that the pollution that causes fouling mostly contains C and O elementally (Table 6.9) and is caused by organic matter [367]. The presence of C, N, O, and S elements obtained in the EDX analysis of the virgin

BW30-XFR membrane is due to the polyamide-based membrane of the BW30-XFR membrane. [469, 470].

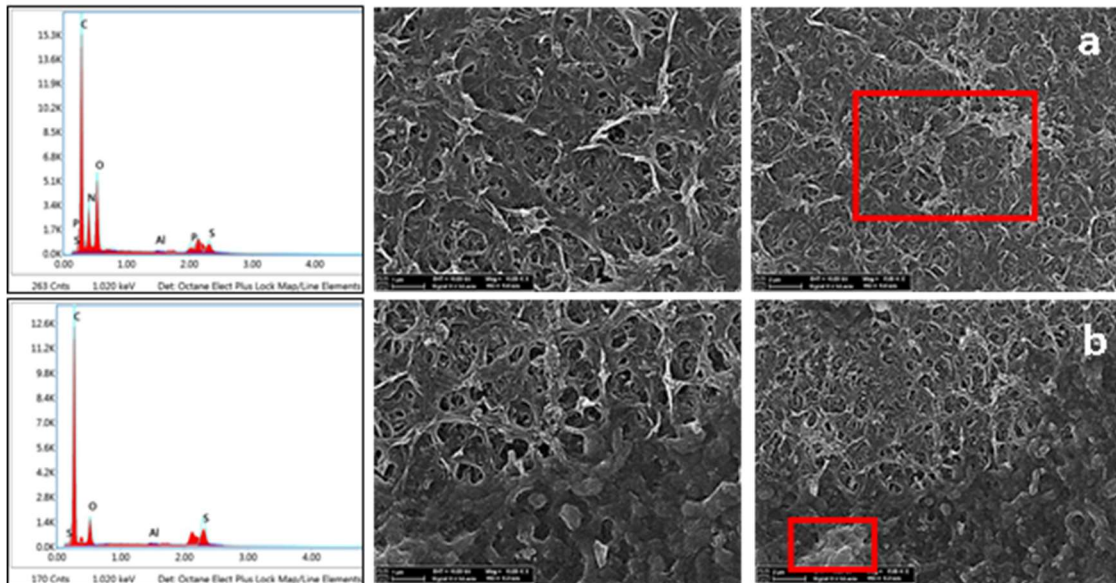


Figure 6.9 SEM-EDX images of the BW30-XFR membrane before (a) and after (b) tests

Table 6.9 EDX data of BW30-XFR membrane

Element	The weight ratio (%)	
	a*	b**
C	46.39	81.05
N	24.86	-
O	26.14	13.40
Al	0.13	0.25
P	1.04	-
S	1.44	5.29

*Virgin BW30-XFR membrane

** BW30-XFR membrane after RO test

6.3.4 Struvite recovery from RO process concentrate

Following the determination of optimal conditions for the RO process, the RO system was operated to gather a sufficient amount of concentrate sample to use in the optimization of the MAP crystallization process. MAP crystallization tests were performed at a pH of 9 and at Mg/P ratios of 0.67, 0.83, 1, and 1.1. The objective of the study was to investigate the impact of the Mg/P molar ratio on the crystallization

efficiency of MAP. The crystallization tests present the addition of PO₄-P in order to achieve the targeted Mg/P ratio. Table 6.10 presents the concentrations of PO₄-P and Mg²⁺ resulting from precipitation tests performed to recover struvite from the concentrate of the RO process. Tests performed at a molar ratio of 0.67 Mg/P showed the minimum concentration of PO₄-P (15.3±1 mg/L) in the supernatant samples. The experimental results showed that the supernatant samples presented the minimum concentration of Mg²⁺ (19.0±0.3 mg/L) at a molar ratio of 1.1 Mg/P. The experimental data indicates that the maximum PO₄-P removal rate of 82.6% was achieved at a molar ratio of 0.67 Mg/P. At the molar ratio of 1.10 Mg/P, the removal efficiency was 56.3%. According to Jaffer et al. and Matsumiya et al., a suitable Mg/P ratio for a MAP crystallization process is between 0.66–0.77, and usually, with an excessive amount of ammonia is available (ammonium to phosphorus ratio > 1) [265, 471]. Moreover, studies have demonstrated that at a Mg:P ratio of 1.4, MAP crystallization can lead to high removal percentages of nitrogen, phosphorus, and potassium [472]. Therefore, the results indicated in Table 6.10 and Figure 6.10 correlate with the current literature.

Table 6.10 PO₄-P and Mg²⁺ concentrations of the samples obtained in MAP crystallization tests performed at different Mg/P molar ratios

Molar ratio (P/Mg)	Sample	PO₄-P (mg/L)	Mg²⁺ (mg/L)
0.67	Feed	88.1	43.4±1.5
	Supernatant	15.3±1.0	21.4±0.4
0.83	Feed	96.7	43.4±1.5
	Supernatant	24±8.3	21.1±0.5
1	Feed	114	43.4±1.5
	Supernatant	58.7±1.6	19.7±0.3
1.1	Feed	140	43.4±1.5
	Supernatant	52.3±1.0	19.0±0.3

Following the determination of the optimum Mg/P molar ratio of 0.67, a series of tests were performed to investigate the effect of different pH levels of 8, 8.5, 9, 9.5, and 10 on the MAP crystallization process at 0.67 Mg/P ratio. Table 6.11 indicates the concentrations of PO₄-P, Mg²⁺, Ca²⁺, and NH₄-N in the samples obtained during the tests, along with the corresponding removal efficiencies for each of these ions. The increase in the pH level resulted in an associated increase in the removal of PO₄-P. The performed tests at a pH of 10 resulted in the 100% removal of PO₄-P, as it was not

detected in the supernatant. The pH range is a critical parameter affecting the crystallization rate, product quality, and the removal of PO₄-P [473]. Specifically, it has been observed that pH values above 9 can result in the deprotonation of NH₄-N, hindering the MAP crystallization process and increasing the recovery rate of NH₄-N and PO₄-P [277]. The characteristic results of MAP crystallization tests (Table 6.14) support this claim that the efficiency of NH₄-N and PO₄-P removal is enhanced as the pH level rises, and total removal of PO₄-P is achieved at a pH of 10.

The performed tests have shown that the removal efficiencies of NH₄-N and Mg²⁺ were very low, particularly at pH levels up to 9.5. The rapid decrease in PO₄-P has been suggested to be caused by the precipitation of Ca₃(PO₄)₂. Further research is required in this particular situation to promote the formation of MAP crystallization.

Table 6.11 Characteristics of samples collected during MAP crystallization tests

pH	Sample	PO ₄ -P (mg/L)	Mg ²⁺ (mg/L)	Ca ²⁺ (mg/L)	NH ₄ -N (mg/L)
7.3	Feed	100.6	43.4±1.5	82.3±0.1	71.8±2.1
8	Supernatant	65.4±4.6	34.8±1.9	46.4±1.5	69.7±1.2
8.5	Supernatant	30.1±4.2	33.8±0.6	43.1±1.9	69.1±2.1
9	Supernatant	10.7±0.9	32.6±0.6	29.3±7.5	70.3±0.1
9.5	Supernatant	3.1±0.5	25.4±0.7	33.9±1.2	65.9±0.3
10	Supernatant	ND*	22.1±0.7	33.5±0.8	63.7±0.9

ND: Indicates concentrations below the detection threshold.*

XRD analysis was performed on dried precipitate obtained in the tests carried out at pH 10, where the removal efficiencies are at the highest level with the aim of nutrient recovery from the RO process concentrate. The XRD pattern of the precipitate is presented in Figure 6.10. It was determined that the precipitate content was 24.9% crystalline and 75.1% amorphous structure. Due to the predominantly amorphous structure of the precipitate, it was not possible to identify characteristic peaks of MAP crystals.

In water reclamation plants, RO or nanofiltration is often used as the final membrane filtration step to produce purified high-quality water for reuse instead of discharge to the environment. In these reclamation plants, the concentrate corresponds to some extent to effluent coming from activated sludge treatment or the MBR

(membrane bioreactor) process (feed for the NF or RO process), but it typically has from two to four times higher concentrations of the various impurities [474, 475]. Upon reviewing relevant literature, it has been observed that impurities are present in the MAP sediment acquired during nutrient recovery from domestic wastewater. These impurities are attributed to components other than PO_4^{3-} , Mg^{2+} , and NH_4^+ found in the wastewater composition [476]

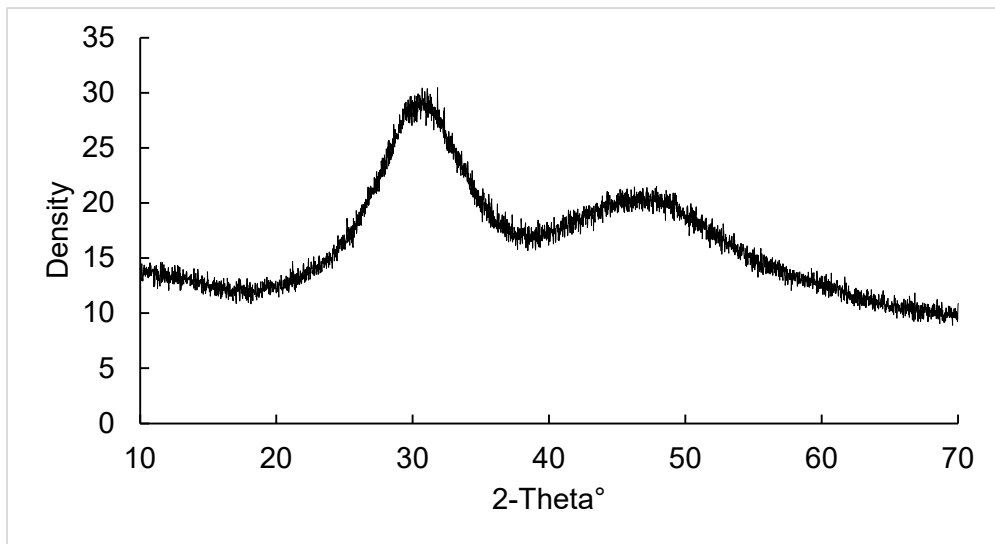


Figure 6.10 XRD pattern of the precipitate obtained from MAP crystallization tests

6.4. Conclusion

In this chapter of the thesis, it was aimed to evaluate and optimize the performance of the system in the RO tests performed to recover nutrients and water. The aim was achieved by investigating the effects of different operational parameters: feed composition, operational mode (TRM and CM), TMP, CFV, system recovery rate, and pH. In terms of nutrient and water recovery performance, 34.3 ± 0.3 mg/L $\text{PO}_4\text{-P}$ concentration, 92.8% NH_4^+ removal efficiency, and 100% flux recovery rate were obtained using RO process at 0.8 CFV, under 15 bar TMP, at 60% recovery rate and pH 6. In the struvite recovery studies in RO process concentrate, the highest L $\text{PO}_4\text{-P}$ removal efficiency was obtained at 100% at pH 10.

MAP crystallization tests were performed on the concentrate of the RO process in order to recover struvite. MAP crystallization process was performed at Mg/P ratios of 0.67, 0.83, 1, and 1.1. and pH of 8, 8.5, 9, 9.5, and 10 to investigate the impact of the Mg/P molar ratio and pH on the crystallization efficiency of MAP. The experimental data indicates that the 100% removal of PO₄-P was achieved at a molar ratio of 0.67 Mg/P and pH of 10.

This chapter focuses on an integrated approach that contributes to the sustainability of resources and ensures efficient treatment of MWW. In the not-too-distant future, it is anticipated that membrane concentrates will be regarded as invaluable raw materials for resource recovery, rather than as waste streams. Within the framework of this investigation, optimal resource recycling from effluent treated physically and biologically with membrane-based processes was attained. This integrated approach, which has considerable potential in terms of both economics and technology, is expected to be an additional investigation and to be implemented on a pilot or full scale.

Chapter 7

Conclusions and Future Prospects

7.1 Conclusions

The main aim of this PhD thesis was to investigate an integrated process (**DCMF-AnFCMBR-RO-MAP crystallization**) that is **self-sufficient** in terms of energy and provides water and nutrient recovery, as an alternative to conventional MWW treatment processes.

The novel DCMF process configurations were used to **maximize the energy potential** of wastewater by implementing pre-concentration with different PAM dosing points. The DCMF system was operated continuously in the optimized PAM dosing point as CEPS using 0.5 mg/L PAM and optimized operational parameters (natural pH of wastewater samples, 20 LMH, 10/2 min filtration/backwash time, and 90% recovery rate) to feed the AnFCMBR. Following the optimization, the long-term operation of the CEPS+DCMF process was performed at four different phases, and the theoretical energy potentials were calculated to be 0.33, 0.42, and 0.44 kWh/m³ based on the COD concentrations that could be achieved in the second, third, and fourth phases, respectively. These results indicated that the implementation of **CEPS+DCMF** on a full scale offers **significant potential** for concentrating organic matter from MWW. Therefore, the integrated CEPS+DCMF technology can replace current MWW treatment technologies thanks to its **remarkable efficiency** in organic matter removal and recovery performance, **straightforward operation**, and **small footprint**.

The operation of the **AnFCMBR** system to treat pre-concentrated MWW was investigated focusing on its ability to remove pollutants, **mitigate membrane fouling**, and **enhance the energy potential**. Two different types of AnFCMBR were operated, and the placement of the membrane was the main difference between the reactors. For the first AnFCMBR, the membrane module was submerged into the settling basin at the top of the reactor, and it was continuously operated for 300 days at five different HRT values (24, 18, 12, 6, and 3 hours). For the second AnFCMBR configuration, the membrane module was submerged into the fluidized bed section of the reactor, and it was continuously operated for two months at 12 hours of HRT. During the operation, with the TMP value exceeding 500 mbar the membrane external cleaning procedure was applied. **High COD removal efficiency** in the range of 83-97% was achieved in the AnFCMBR process operated at different HRTs. The volume of methane produced per m³ of treated wastewater increased from 14.3 L to 40.0 L when the HRT duration was reduced from 24 hours to 3 hours. AnFCMBR-SiS process operation at 6 hours HRT yields 0.126 kWh/m³ net energy production potential.

The performance of RO was evaluated for nutrient recovery studies using effluents obtained from AnFCMBR and CEPS+DCMF processes. An investigation was performed to evaluate the impact of different operational parameters, including feed compositions, operating mode (TRM and CM), TMP, CFV, system recovery rate, and pH. In terms of nutrient and water recovery performance, 34.3±0.3 mg/L PO₄-P concentration, **100% PO₄-P removal**, **92.8% NH₄⁺ removal efficiency**, and **100% flux recovery rate** were obtained using RO process at 0.8 CFV, under 15 bar TMP, at 60% recovery rate and pH 6.

Following the determination of optimal conditions in the RO process, MAP crystallization tests were performed to recover struvite from the concentrate of the RO process. MAP crystallization tests were performed to determine the optimum Mg/P ratio and pH. The tests were conducted using a molar ratio of 0.9 P/Mg, results revealed that the **removal efficiency of PO₄-P** was **100%** at a pH of 10.

Beyond the primary goal of meeting the discharge standard, an integrated DCMF-AnFCMBR-RO-MAP crystallization process was implemented to obtain sustainable process schemes for **the recovery of valuable resources** from MWW.

7.2 Societal Impact and Contribution to Global Sustainability

This thesis presents a novel hybrid MWW treatment process that was designed and optimized for operational conditions. It serves to provide guidance to institutions and organizations, such as treatment and design firms, municipalities, research institutions, and universities, as well as the public or private sector in this field. Furthermore, the data acquired from this thesis serves as a model of the strategies and procedures that should be used in wastewater treatment facilities, which suffer significant energy costs in our country.

The key aspect emphasized in this thesis is resource recovery. Sustainability and resource recovery from MWW are closely intertwined concepts that are gaining increasing attention in the field of environmental management. The treatment of wastewater is evolving from a mere disposal process to a resource recovery approach, where wastewater is seen as a valuable source of water, nutrients, and energy. This shift in perspective is essential for achieving Sustainable Development Goals (SDGs) related to SDG 6th clean water and sanitation, 7th affordable and clean energy, 11th Sustainable cities and communities, 13th Climate action, 14th Life below water, and 12th Sustainable consumption and production.

Various technologies and processes have been developed to enhance resource recovery from MWW. AnMBRs also applied in this thesis, have been identified as key components in sustainable wastewater treatment and resource recovery systems, as they can produce biomethane for renewable energy without the need for energy-intensive oxygen transfer. Nutrient recovery from MWW is highlighted as a crucial aspect of resource recovery, as it not only allows for the protection of phosphorus resources but also reduces eutrophication and enhances the sustainability of municipal sewage systems. Furthermore, the recovery of phosphate from wastewater can alleviate the burden of excessive fertilizer production and mitigate eutrophication issues caused by high phosphate concentrations in effluents. In the quest for sustainable wastewater management, the integration of resource recovery processes into wastewater treatment plants is essential. By adopting advanced technologies and retrofitting existing plants, it

is possible to transform wastewater treatment facilities into resource recovery factories that can produce freshwater, energy, and valuable materials from MWW streams.

7.3 Future Prospects

The combination of climate change and increasing demand for lifestyle products has led to a high value being placed on natural resources, as a result of ongoing pollution. The technology routes chosen were determined by the unrestricted access to natural resources. In the current situation, all natural resources have been polluted and have grown more expensive due to increased demand. The primary strategy is to adapt to the current conditions, which need the conservation of resources, efficient utilization, and economizing. Membrane separation techniques have become a better alternative to conventional separation techniques by offering higher recovery, ambient operating conditions, and lower energy requirements. Integration of more than one membrane process or hybridization offers the possibility to improve overall separation performance, overcome limitations, and result in higher value addition.

This thesis presents the development of an innovative membrane-based integrated treatment method that utilizes its own energy and serves the circular economy approach by recovering organic matter, nitrogen, phosphorus, and water from wastewater. The application of integrated CEPS and DCMF has a high potential for the up-concentration of organic matter in MWW for further energy recovery to achieve energy-positive wastewater treatment. An important issue with the utilization of treated MWW in agriculture is the elimination of toxicity and endocrine-disrupting substances. Industrial discharges into municipal sewage systems can lead to significant issues, including toxicity and the transfer of excessive organic matter into the wastewater treatment plants at the end of the pipe. Nevertheless, information is limited regarding their final fate and biodegradation in AnFCMBRs. Certainly, further investigation is necessary to determine the final fate of these crucial contaminants in AnFCMBR systems.

The controlled crystallization of compounds like struvite from wastewater using RO concentrate offers a means of recovering phosphorus, a critical nutrient, for reuse. This not only aids in nutrient recycling but also contributes to reducing the

environmental impact of RO concentrate discharges. In this study, struvite recovery tests in concentrate of RO process, 100% PO₄-P removal efficiency was obtained after optimization of the process. RO holds significant promise for enhancing nutrient recovery from the effluent of membrane-based MWW treatment processes, thereby promoting sustainable practices in water resource management. However, advancements in membrane technologies and process optimization may enhance the efficiency of ammonium recovery from MWW.

Additionally, there is a growing interest in recovering water, nutrients, and energy from wastewater streams due to increasing volumes of MWW and advancements in resource recovery technologies. In the future, a detailed techno-economic analysis of these hybrid membrane-based processes in nutrient recovery should be performed, such as process energy demand, CO₂ footprint, system robustness, operating costs, product quality, and market demands.

BIBLIOGRAPHY

- [1] U. Wwap, "World Water Assessment Programme: The United Nations World Water Development Report 4: Managing Water under Uncertainty and Risk," ed: Paris: UNESCO, 2012.
- [2] U. Nations, "Sustainable Development Goals Report," 2022. Accessed: 01.05.2024. [Online]. Available: https://unstats.un.org/sdgs/report/2022/Goal-06/?_gl=1*srgsyk*_ga*MTU5NTcyNTgyMS4xNjkwMTA2MjEy*_ga_TK9BQL5X7Z*MTcxNjA0ODU2MS44LjEuMTcxNjA1MDA2MC4wLjAuMA..
- [3] I. P. o. C. Change, "Fact sheet - Food and Water Climate Change Impacts and Risks," 01.10.2022 2022. [Online]. Available: https://www.ipcc.ch/report/ar6/wg2/downloads/outreach/IPCC_AR6_WGII_FactSheet_FoodAndWater.pdf
- [4] Y. A. Othman, A. Al-Assaf, M. J. Tadros, and A. Albalawneh, "Heavy metals and microbes accumulation in soil and food crops irrigated with wastewater and the potential human health risk: A metadata analysis," *Water-Sui*, vol. 13, no. 23, p. 3405, 2021
- [5] X. Lin *et al.*, "Occurrence and risk assessment of emerging contaminants in a water reclamation and ecological reuse project," *Sci Total Environ*, vol. 744, p. 140977, 2020
- [6] Y. Gu *et al.*, "Quantification of the water, energy and carbon footprints of wastewater treatment plants in China considering a water–energy nexus perspective," *Ecological indicators*, vol. 60, pp. 402-409, 2016
- [7] D. Panepinto, S. Fiore, M. Zappone, G. Genon, and L. Meucci, "Evaluation of the energy efficiency of a large wastewater treatment plant in Italy," *Applied Energy*, vol. 161, pp. 404-411, 2016
- [8] L. Luo, M. Dzakpasu, B. Yang, W. Zhang, Y. Yang, and X. C. Wang, "A novel index of total oxygen demand for the comprehensive evaluation of energy consumption for urban wastewater treatment," *Applied Energy*, vol. 236, pp. 253-261, 2019
- [9] P. L. McCarty, J. Bae, and J. Kim, "Domestic wastewater treatment as a net energy producer—can this be achieved?," *Environmental Science and Technology*, vol. 45, no. 17, pp. 7100-7106, 2011
- [10] M. Geissdoerfer, P. Savaget, N. M. Bocken, and E. J. Hultink, "The Circular Economy—A new sustainability paradigm?," *J Clean Prod*, vol. 143, pp. 757-768, 2017

- [11] J. Yang, M. Monnot, L. Ercolei, and P. Moulin, "Membrane-based processes used in municipal wastewater treatment for water reuse: state-of-the-art and performance analysis," *Membranes-Basel*, vol. 10, no. 6, p. 131, 2020
- [12] M. B. Asif and Z. Zhang, "Ceramic membrane technology for water and wastewater treatment: A critical review of performance, full-scale applications, membrane fouling and prospects," *Chem Eng J*, vol. 418, p. 129481, 2021
- [13] F. Kramer, R. Shang, L. Rietveld, and S. Heijman, "Fouling control in ceramic nanofiltration membranes during municipal sewage treatment," *Sep Purif Technol*, vol. 237, p. 116373, 2020
- [14] K. Guerra and J. Pellegrino, "Development of a techno-economic model to compare ceramic and polymeric membranes," *Separation Science and Technology*, vol. 48, no. 1, pp. 51-65, 2013
- [15] K. P. Goswami and G. Pugazhenthii, "Credibility of polymeric and ceramic membrane filtration in the removal of bacteria and virus from water: A review," *J Environ Manage*, vol. 268, p. 110583, 2020
- [16] M. T. Alresheedi, B. Barbeau, and O. D. Basu, "Comparisons of NOM fouling and cleaning of ceramic and polymeric membranes during water treatment," *Sep Purif Technol*, vol. 209, pp. 452-460, 2019
- [17] P. Krzeminski, L. Leverette, S. Malamis, and E. Katsou, "Membrane bioreactors – A review on recent developments in energy reduction , fouling control , novel configurations , LCA and market prospects," *J Membrane Sci*, vol. 527, no. December 2016, pp. 207-227, 2017
- [18] R. K. Dereli, F. P. van der Zee, I. Ozturk, and J. B. van Lier, "Treatment of cheese whey by a cross-flow anaerobic membrane bioreactor: Biological and filtration performance," *Environmental research*, vol. 168, pp. 109-117, 2019
- [19] Y. N. Kanafin *et al.*, "Anaerobic membrane bioreactors for municipal wastewater treatment: a literature review," *Membranes-Basel*, vol. 11, no. 12, p. 967, 2021
- [20] Y. Hu, X. C. Wang, H. H. Ngo, Q. Sun, and Y. Yang, "Anaerobic dynamic membrane bioreactor (AnDMBR) for wastewater treatment: A review," *Bioresource Technol*, vol. 247, no. June 2017, pp. 1107-1118, 2018
- [21] Z. Lei, S. Yang, Y.-y. Li, W. Wen, X. C. Wang, and R. Chen, "Bioresource Technology Application of anaerobic membrane bioreactors to municipal wastewater treatment at ambient temperature : A review of achievements , challenges , and perspectives," *Bioresource Technol*, vol. 267, no. July, pp. 756-768, 2018
- [22] P. L. McCarty, J. Bae, and J. Kim, "Domestic wastewater treatment as a net energy producer-can this be achieved?," *Environmental Science and Technology*, vol. 45, no. 17, pp. 7100-7106.2011/9// 2011

- [23] X. Song *et al.*, "Effects of sulphur on the performance of an anaerobic membrane bioreactor: Biological stability, trace organic contaminant removal, and membrane fouling," *Bioresource Technol*, vol. 250, no. November 2017, pp. 171-177, 2018
- [24] T. A. Nascimento and M. P. Miranda, "Continuous municipal wastewater up-concentration by direct membrane filtration, considering the effect of intermittent gas scouring and threshold flux determination," *J Water Process Eng*, vol. 39, 2021
- [25] T. A. Nascimento, F. Fdz-Polanco, and M. Peña, "Membrane-based technologies for the up-concentration of municipal wastewater: A review of pretreatment intensification," *Separation & Purification Reviews*, vol. 49, no. 1, pp. 1-19, 2020
- [26] O. Ozcan, E. Sahinkaya, and N. Uzal, "Long-term operation of flocculation assisted direct ceramic microfiltration for up-concentration of municipal wastewater,"
- [27] Y. Yang *et al.*, "Integrated electroflocculation-membrane process for pre-concentration of domestic wastewater: Filtration performance, organics recovery and membrane fouling characteristics," *Resources, Conservation and Recycling*, vol. 199, p. 107247, 2023
- [28] C. He, K. Wang, W. Wang, J. Luo, and K. Fang, "Chemically enhanced high-loaded membrane bioreactor (CE-HLMBR) for A-stage municipal wastewater treatment: Pilot-scale experiments and practical feasibility evaluation," *Sep Purif Technol*, vol. 307, p. 122853, 2023
- [29] S. Hube *et al.*, "Direct membrane filtration for wastewater treatment and resource recovery: A review," *Sci Total Environ*, vol. 710, pp. 136375-136375.2020/3// 2020
- [30] K. Manzoor, S. Shoukat, and S. J. Khan, "Treatment of Domestic Wastewater with Anaerobic Fluidized Membrane Bioreactor (An-FMBR) and Control of Membrane Fouling with Addition of Gac," presented at the 5th Conference on Sustainability in Civil Engineering, 2023.
- [31] R. Lee, P. L. McCarty, J. Bae, and J. Kim, "Anaerobic fluidized membrane bioreactor polishing of baffled reactor effluent during treatment of dilute wastewater," *Journal of Chemical Technology & Biotechnology*, vol. 90, no. 3, pp. 391-397, 2015
- [32] M. Lim, R. Ahmad, J. Guo, F. Tibi, M. Kim, and J. Kim, "Removals of micropollutants in staged anaerobic fluidized bed membrane bioreactor for low-strength wastewater treatment," *Process Saf Environ*, vol. 127, pp. 162-170.2019/07/01/ 2019
- [33] A. Szczuka, J. P. Berglund-Brown, J. A. MacDonald, and W. A. Mitch, "Control of sulfides and coliphage MS2 using hydrogen peroxide and UV disinfection for

- non-potable reuse of pilot-scale anaerobic membrane bioreactor effluent," *Water research X*, vol. 11, p. 100097, 2021
- [34] M. Zielińska and A. Ojo, "Anaerobic Membrane Bioreactors (AnMBRs) for Wastewater Treatment: Recovery of Nutrients and Energy, and Management of Fouling," *Energies*, vol. 16, no. 6, p. 2829, 2023
- [35] W. Suwaileh, D. Johnson, and N. Hilal, "Membrane desalination and water re-use for agriculture: State of the art and future outlook," *Desalination*, vol. 491, p. 114559, 2020
- [36] M. Hafiz, A. H. Hawari, R. Alfahel, M. K. Hassan, and A. Altaee, "Comparison of nanofiltration with reverse osmosis in reclaiming tertiary treated municipal wastewater for irrigation purposes," *Membranes-Basel*, vol. 11, no. 1, p. 32, 2021
- [37] C. Shin, A. Szczuka, R. Jiang, W. A. Mitch, and C. S. Criddle, "Optimization of reverse osmosis operational conditions to maximize ammonia removal from the effluent of an anaerobic membrane bioreactor," *Environmental Science: Water Research & Technology*, vol. 7, no. 4, pp. 739-747, 2021
- [38] K. Arola, B. Van der Bruggen, M. Mänttari, and M. Kallioinen, "Treatment options for nanofiltration and reverse osmosis concentrates from municipal wastewater treatment: A review," *Critical Reviews in Environmental Science and Technology*, vol. 49, no. 22, pp. 2049-2116, 2019
- [39] A. Siciliano, C. Limonti, G. M. Curcio, and R. Molinari, "Advances in struvite precipitation technologies for nutrients removal and recovery from aqueous waste and wastewater," *Sustainability-Basel*, vol. 12, no. 18, p. 7538, 2020
- [40] R. Mohammadi, W. Tang, and M. Sillanpää, "A systematic review and statistical analysis of nutrient recovery from municipal wastewater by electro dialysis," *Desalination*, vol. 498, p. 114626.2021/01/15/ 2021
- [41] C. Zhang, A. Guisasola, and J. A. Baeza, "A review on the integration of mainstream P-recovery strategies with enhanced biological phosphorus removal," *Water Res*, vol. 212, p. 118102, 2022
- [42] S. M. Muscarella, L. Badalucco, V. A. Laudicina, and G. Mannina, "Zeolites for the nutrient recovery from wastewater," in *Current Developments in Biotechnology and Bioengineering*: Elsevier, 2023, pp. 95-114.
- [43] S. Munasinghe-Arachchige, I. Abeysiriwardana-Arachchige, H. Delanka-Pedige, P. Cooke, and N. Nirmalakhandan, "Nitrogen-fertilizer recovery from urban sewage via gas permeable membrane: Process analysis, modeling, and intensification," *Chem Eng J*, vol. 411, p. 128443, 2021
- [44] H. Wu and C. Vaneeckhaute, "Nutrient recovery from wastewater: A review on the integrated Physicochemical technologies of ammonia stripping, adsorption and struvite precipitation," *Chem Eng J*, vol. 433, p. 133664, 2022

- [45] S. Haustein and V. Larivière, "The use of bibliometrics for assessing research: Possibilities, limitations and adverse effects," in *Incentives and performance: Governance of research organizations*: Springer, 2014, pp. 121-139.
- [46] P. Stephan, R. Veugelers, and J. Wang, "Reviewers are blinkered by bibliometrics," *Nature*, vol. 544, no. 7651, pp. 411-412, 2017
- [47] N. J. Van Eck and L. Waltman, "VOSviewer manual," *Leiden: Univeriteit Leiden*, vol. 1, no. 1, pp. 1-53, 2013
- [48] S. Vinardell *et al.*, "Advances in anaerobic membrane bioreactor technology for municipal wastewater treatment: A 2020 updated review," *Renewable and Sustainable Energy Reviews*, vol. 130, p. 109936.2020/09/01/ 2020
- [49] S. Guerra-Rodríguez, P. Oulego, E. Rodríguez, D. N. Singh, and J. Rodríguez-Chueca, "Towards the implementation of circular economy in the wastewater sector: Challenges and opportunities," *Water-Sui*, vol. 12, no. 5, p. 1431, 2020
- [50] U. Ghimire, G. Sarpong, and V. G. Gude, "Transitioning wastewater treatment plants toward circular economy and energy sustainability," *Acs Omega*, vol. 6, no. 18, pp. 11794-11803, 2021
- [51] U. WATER, "WATER QUALITY AND WASTEWATER," 2018. [Online]. Available: https://www.unwater.org/sites/default/files/app/uploads/2018/10/WaterFacts_water_and_wastewater_sep2018.pdf
- [52] L. Pelaz Pérez, "Nitrogen removal in domestic wastewater after anaerobic treatment," School of Industrial Engineering, University of Valladolid, 2016.
- [53] S. Agarwal, S. Darbar, and S. Saha, "Chapter 25 - Challenges in management of domestic wastewater for sustainable development," in *Current Directions in Water Scarcity Research*, vol. 6, A. L. Srivastav, S. Madhav, A. K. Bhardwaj, and E. Valsami-Jones Eds.: Elsevier, 2022, pp. 531-552.
- [54] R. Ordóñez, D. Hermosilla, N. Merayo, A. Gascó, C. Negro, and Á. Blanco, "Application of multi-barrier membrane filtration technologies to reclaim municipal wastewater for industrial use," *Separation & Purification Reviews*, vol. 43, no. 4, pp. 263-310, 2014
- [55] L. Zhu, C. Ding, T. Zhu, and Y. Wang, "A review on the forward osmosis applications and fouling control strategies for wastewater treatment," *Frontiers of Chemical Science and Engineering*, pp. 1-20, 2022
- [56] Y. Ye *et al.*, "Insight into chemical phosphate recovery from municipal wastewater," *Sci Total Environ*, vol. 576, pp. 159-171, 2017
- [57] Metcalf, amp, I. a. A. C. Eddy, T. Asano, F. Burton, and H. Leverenz, *Water Reuse: Issues, Technologies, and Applications*, 1st Edition ed. New York: McGraw-Hill Education (in en), 2007.

- [58] D. Crutchik and J. L. Campos, "Municipal wastewater reuse: is it a competitive alternative to seawater desalination?," *Sustainability-Basel*, vol. 13, no. 12, p. 6815, 2021
- [59] J. Frijns, J. Hofman, and M. Nederlof, "The potential of (waste) water as energy carrier," *Energ Convers Manage*, vol. 65, pp. 357-363, 2013
- [60] M. Stefanescu, G. Nechifor, C. Bumbac, I. Ionescu, and O. Tiron, "Improvement of active biological sludge quality for anaerobic digestion phase in the wastewater treatment plant by ultrasonic pretreatment," *REVISTA DE CHIMIE*, vol. 69, no. 1, pp. 31-33, 2018
- [61] C. Hu, D. Kendrick, T. C. Zhang, Y. H. Huang, M. F. Dahab, and R. Surampalli, "PERFORMANCE AND PHOSPHORUS REMOVAL IN MUSKEGON'S WASTEWATER LAND TREATMENT SYSTEM," in *WEFTEC 2005, 2005*: Water Environment Federation, pp. 6139-6151.
- [62] S. K. Ishii and T. H. Boyer, "Impact of urine source separation on wastewater treatment and sustainability initiatives at select US Universities: a triple bottom line evaluation," *Proc. Water Environ. Fed*, vol. 58, 2013
- [63] Y. Tong, B. K. Mayer, and P. J. McNamara, "Triclosan adsorption using wastewater biosolids-derived biochar," *Environmental science: water research & technology*, vol. 2, no. 4, pp. 761-768, 2016
- [64] K. Nebojša, P. Dušica, and M. Igor, "ANALYSIS OF TECHNICAL AND TECHNOLOGICAL PARAMETERS OF WASTE WATER TREATMENT PLANT FOR UP TO 15 000 EQUIVALENTS," *Arhiv za Tehnicke Nauke/Archives for Technical Sciences*, no. 19, 2018
- [65] H. Melcer, H. Monteith, and S. G. Nutt, "Variability of toxic trace contaminants in municipal sewage treatment plants," *Water Sci Technol*, vol. 20, no. 4-5, pp. 275-284, 1988
- [66] A. Genovese, A. A. Acquaye, A. Figueroa, and S. L. Koh, "Sustainable supply chain management and the transition towards a circular economy: Evidence and some applications," *Omega*, vol. 66, pp. 344-357, 2017
- [67] G. Mannina *et al.*, "Enhancing a transition to a circular economy in the water sector: The eu project wider uptake," *Water-Sui*, vol. 13, no. 7, p. 946, 2021
- [68] Á. Robles, J. Serralta, N. Martí, J. Ferrer, and A. Seco, "Anaerobic membrane bioreactors for resource recovery from municipal wastewater: a comprehensive review of recent advances," *Environmental Science: Water Research & Technology*, vol. 7, no. 11, pp. 1944-1965, 2021
- [69] W. Verstraete and S. E. Vlaeminck, "ZeroWasteWater: short-cycling of wastewater resources for sustainable cities of the future," *International Journal of Sustainable Development & World Ecology*, vol. 18, no. 3, pp. 253-264, 2011

- [70] W. Mo and Q. Zhang, "Energy–nutrients–water nexus: Integrated resource recovery in municipal wastewater treatment plants," *J Environ Manage*, vol. 127, pp. 255-267.2013/9// 2013
- [71] P. Christopher Stacklin, "The Value of Wastewater: An Econometric Evaluation of Recoverable Resources in Wastewater for Reuse," presented at the Water Environment Federation, New Orleans, 2012.
- [72] A. J. Ansari, F. I. Hai, W. E. Price, J. E. Drewes, and L. D. Nghiem, "Forward osmosis as a platform for resource recovery from municipal wastewater - A critical assessment of the literature," *J Membrane Sci*, vol. 529, pp. 195-206.2017/5// 2017
- [73] A. Danilenko, E. Dickson, and M. Jacobsen, "Climate change and urban water utilities: challenges and opportunities," 2010
- [74] L. Marston and X. Cai, "An overview of water reallocation and the barriers to its implementation," *Wiley Interdisciplinary Reviews: Water*, vol. 3, no. 5, pp. 658-677, 2016
- [75] C. T. Finnerty *et al.*, "The Future of Municipal Wastewater Reuse Concentrate Management: Drivers, Challenges, and Opportunities," *Environ Sci Technol*, vol. 58, no. 1, pp. 3-16, 2023
- [76] M. Qadir *et al.*, "Global and regional potential of wastewater as a water, nutrient and energy source," in *Natural resources forum*, 2020, vol. 44, no. 1: Wiley Online Library, pp. 40-51.
- [77] C. Tortajada, "Contributions of recycled wastewater to clean water and sanitation Sustainable Development Goals," *NPJ Clean Water*, vol. 3, no. 1, p. 22, 2020
- [78] U. N. E. Programme, "Wastewater – Turning Problem to Solution. A UNEP Rapid Response Assessment.," Nairobi, 2023.
- [79] Y. H. Wu *et al.*, "Effect of ultraviolet disinfection on the fouling of reverse osmosis membranes for municipal wastewater reclamation," *Water Res*, vol. 195, 2021
- [80] P. T. Vo *et al.*, "A mini-review on the impacts of climate change on wastewater reclamation and reuse," *Sci Total Environ*, vol. 494, pp. 9-17, 2014
- [81] E. R. Jones, M. T. Van Vliet, M. Qadir, and M. F. Bierkens, "Country-level and gridded estimates of wastewater production, collection, treatment and reuse," *Earth System Science Data*, vol. 13, no. 2, pp. 237-254, 2021
- [82] M. Mannan and S. G. Al-Ghamdi, "Environmental impact of water-use in buildings: Latest developments from a life-cycle assessment perspective," *J Environ Manage*, vol. 261, p. 110198.2020/05/01/ 2020

- [83] D. Lemos, A. C. Dias, X. Gabarrell, and L. Arroja, "Environmental assessment of an urban water system," *J Clean Prod*, vol. 54, pp. 157-165, 2013
- [84] S. Di Fraia, N. Massarotti, and L. Vanoli, "A novel energy assessment of urban wastewater treatment plants," *Energ Convers Manage*, vol. 163, pp. 304-313.2018/05/01/ 2018
- [85] J. Conti, P. Holtberg, J. Diefenderfer, A. LaRose, J. T. Turnure, and L. Westfall, "International energy outlook 2016 with projections to 2040," USDOE Energy Information Administration (EIA), Washington, DC (United States ..., 2016.
- [86] P. L. McCarty, "What is the best biological process for nitrogen removal: when and why?," ed: ACS Publications, 2018.
- [87] Y.-J. Liu, J. Gu, and Y. Liu, "Energy self-sufficient biological municipal wastewater reclamation: present status, challenges and solutions forward," *Bioresource Technol*, vol. 269, pp. 513-519, 2018
- [88] M. Zhang, J. Gu, and Y. Liu, "Engineering feasibility, economic viability and environmental sustainability of energy recovery from nitrous oxide in biological wastewater treatment plant," *Bioresource Technol*, vol. 282, pp. 514-519, 2019
- [89] A. Daverey *et al.*, "Recent advances in energy efficient biological treatment of municipal wastewater," *Bioresource Technology Reports*, vol. 7, p. 100252, 2019
- [90] L. Lu, J. S. Guest, C. A. Peters, X. Zhu, G. H. Rau, and Z. J. Ren, "Wastewater treatment for carbon capture and utilization," *Nature Sustainability*, vol. 1, no. 12, pp. 750-758, 2018
- [91] W. Verstraete, P. Van de Caveye, and V. Diamantis, "Maximum use of resources present in domestic "used water"," *Bioresource Technol*, vol. 100, no. 23, pp. 5537-5545, 2009
- [92] W. E. Council. *Energy efficiency indicators: Average electricity consumption per electrified household.* ,
- [93] P. Falkowski *et al.*, "The global carbon cycle: a test of our knowledge of earth as a system," *science*, vol. 290, no. 5490, pp. 291-296, 2000
- [94] D. Cordell, A. Rosemarin, J. J. Schröder, and A. Smit, "Towards global phosphorus security: A systems framework for phosphorus recovery and reuse options," *Chemosphere*, vol. 84, no. 6, pp. 747-758, 2011
- [95] Y. Zhang, E. Desmidt, A. Van Looveren, L. Pinoy, B. Meesschaert, and B. Van der Bruggen, "Phosphate separation and recovery from wastewater by novel electrodialysis," *Environ Sci Technol*, vol. 47, no. 11, pp. 5888-5895, 2013

- [96] S.-H. Lee, B.-H. Yoo, S.-K. Kim, S. J. Lim, J. Y. Kim, and T.-H. Kim, "Enhancement of struvite purity by re-dissolution of calcium ions in synthetic wastewaters," *J Hazard Mater*, vol. 261, pp. 29-37, 2013
- [97] J. Driver, D. Lijmbach, and I. Steen, "Why recover phosphorus for recycling, and how?," *Environmental technology*, vol. 20, no. 7, pp. 651-662, 1999
- [98] M. N. Hasan *et al.*, "Recent technologies for nutrient removal and recovery from wastewaters: A review," *Chemosphere*, vol. 277, p. 130328.2021/08/01/ 2021
- [99] N. Rascio and N. La Rocca, "Biological nitrogen fixation," 2013
- [100] D. Fowler *et al.*, "The global nitrogen cycle in the twenty-first century," *Philosophical Transactions of the Royal Society B: Biological Sciences*, vol. 368, no. 1621, p. 20130164, 2013
- [101] J. A. Camargo and A. Alonso, "Ecological and toxicological effects of inorganic nitrogen pollution in aquatic ecosystems: A global assessment," *Environ Int*, vol. 32, no. 6, pp. 831-49. Aug 2006
- [102] "<Carpenter et al. - 1998 - NONPOINT POLLUTION OF SURFACE WATERS WITH PHOSPHORUS AND NITROGEN.pdf>,"
- [103] G. D'Inverno, L. Carosi, G. Romano, and A. Guerrini, "Water pollution in wastewater treatment plants: An efficiency analysis with undesirable output," *European Journal of Operational Research*, vol. 269, no. 1, pp. 24-34.2018/8// 2018
- [104] B. P. Naveen, D. M. Mahapatra, T. G. Sitharam, P. V. Sivapullaiah, and T. V. Ramachandra, "Physico-chemical and biological characterization of urban municipal landfill leachate," *Environ Pollut*, vol. 220, no. Pt A, pp. 1-12. Jan 2017
- [105] G. Galvagno, C. Eskicioglu, and M. Abel-Denee, "Biodegradation and chemical precipitation of dissolved nutrients in anaerobically digested sludge dewatering centrate," *Water Res*, vol. 96, pp. 84-93. Jun 1 2016
- [106] M. F. Zuthi, W. S. Guo, H. H. Ngo, L. D. Nghiem, and F. I. Hai, "Enhanced biological phosphorus removal and its modeling for the activated sludge and membrane bioreactor processes," *Bioresour Technol*, vol. 139, pp. 363-74. Jul 2013
- [107] Z. Yuan *et al.*, "Human perturbation of the global phosphorus cycle: changes and consequences," *Environ Sci Technol*, vol. 52, no. 5, pp. 2438-2450, 2018
- [108] D. Cordell and S. White, "Peak Phosphorus: Clarifying the Key Issues of a Vigorous Debate about Long-Term Phosphorus Security," *Sustainability*, vol. 3, no. 10, pp. 2027-2049, 2011

- [109] Y. V. Nancharaiah, S. Venkata Mohan, and P. N. L. Lens, "Recent advances in nutrient removal and recovery in biological and bioelectrochemical systems," *Bioresour Technol*, vol. 215, pp. 173-185, Sep 2016
- [110] D. R. Kanter and W. J. Brownlie, "Joint nitrogen and phosphorus management for sustainable development and climate goals," *Environ Sci Policy*, vol. 92, pp. 1-8, 2019
- [111] D.-J. D. Kok, S. Pande, J. B. Van Lier, A. R. Ortigara, H. Savenije, and S. Uhlenbrook, "Global phosphorus recovery from wastewater for agricultural reuse," *Hydrol Earth Syst Sc*, vol. 22, no. 11, pp. 5781-5799, 2018
- [112] P. Drechsel, *Resource Recovery from Waste: Business Models for Energy, Nutrient and Water Reuse in Low-and Middle-income Countries*. Routledge, 2018.
- [113] T. Saliu and N. Oladoja, "Nutrient recovery from wastewater and reuse in agriculture: A review," *Environmental Chemistry Letters*, vol. 19, no. 3, pp. 2299-2316, 2021
- [114] T. C. T. v. O. Bakanlığı. "Gübre İstatistikleri-Yıllar Bazında Kimyevi Gübre Tüketim ve Üretim İstatistikleri." <https://www.tarimorman.gov.tr/Konular/Bitkisel-Uretim/Bitki-Besleme-ve-Tarimsal-Teknolojiler/Bitki-Besleme-Istatistikleri> (accessed.
- [115] TÜİK. "Su ve Atıksu İstatistikleri, 2022." <https://data.tuik.gov.tr/Bulten/Index?p=Su-ve-Atıksu-Istatistikleri-2022-49607> (accessed.
- [116] A. O. Erdoğan, G. E. Zengin, and D. Orhon, "Türkiye'de evsel atıksu oluşum miktarları ve karakterizasyonu," *İTÜDERGİSİ/e*, vol. 15, no. 1, 3, 2010
- [117] UNESCO, "The United Nations World Water Development Report-Wastewater: The untapped resource," 2017.
- [118] *Proposal for a Regulation of the European Parliament and of the Council on minimum requirements for water reuse*, 2018.
- [119] X. C. Wang, C. Zhang, X. Ma, and L. Luo, *Water cycle management: a new paradigm of wastewater reuse and safety control*. Springer, 2015.
- [120] S. Eslamian, *Urban Water Reuse*. Boca Raton London New York: Taylor & Francis Group, 2016.
- [121] P. Kehrein, M. Van Loosdrecht, P. Osseweijer, M. Garfi, J. Dewulf, and J. Posada, "A critical review of resource recovery from municipal wastewater treatment plants—market supply potentials, technologies and bottlenecks," *Environmental Science: Water Research & Technology*, vol. 6, no. 4, pp. 877-910, 2020

- [122] H. Gao, Y. D. Scherson, and G. F. Wells, "Towards energy neutral wastewater treatment: methodology and state of the art," *Environmental science: Processes & impacts*, vol. 16, no. 6, pp. 1223-1246, 2014
- [123] Y. Gu *et al.*, "Energy self-sufficient wastewater treatment plants: feasibilities and challenges," *Energy Procedia*, vol. 105, pp. 3741-3751, 2017
- [124] D. Ganora *et al.*, "Opportunities to improve energy use in urban wastewater treatment: a European-scale analysis," *Environmental Research Letters*, vol. 14, no. 4, p. 044028, 2019
- [125] X. Hao, R. Liu, and X. Huang, "Evaluation of the potential for operating carbon neutral WWTPs in China," *Water Res*, vol. 87, pp. 424-431, 2015
- [126] J. S. Guest *et al.*, "A new planning and design paradigm to achieve sustainable resource recovery from wastewater," ed: ACS Publications, 2009.
- [127] E. Heidrich, T. Curtis, and J. Dolfing, "Determination of the internal chemical energy of wastewater," *Environ Sci Technol*, vol. 45, no. 2, pp. 827-832, 2011
- [128] J. Wan, J. Gu, Q. Zhao, and Y. Liu, "COD capture: a feasible option towards energy self-sufficient domestic wastewater treatment," *Scientific reports*, vol. 6, no. 1, pp. 1-9, 2016
- [129] D. Wilkins, X.-Y. Lu, Z. Shen, J. Chen, and P. K. Lee, "Pyrosequencing of *mcrA* and archaeal 16S rRNA genes reveals diversity and substrate preferences of methanogen communities in anaerobic digesters," *Applied and environmental microbiology*, vol. 81, no. 2, pp. 604-613, 2015
- [130] M. K. Winkler and L. Straka, "New directions in biological nitrogen removal and recovery from wastewater," *Curr Opin Biotechnol*, vol. 57, pp. 50-55, Jan 29 2019
- [131] Y. Ye *et al.*, "A critical review on ammonium recovery from wastewater for sustainable wastewater management," *Bioresour Technol*, vol. 268, pp. 749-758, Nov 2018
- [132] D. G. Rao, R. Senthilkumar, J. A. Byrne, and S. Feroz, *Wastewater treatment: advanced processes and technologies*. CRC Press, 2012.
- [133] T. Wintgens *et al.*, "The role of membrane processes in municipal wastewater reclamation and reuse," *Desalination*, vol. 178, no. 1-3, pp. 1-11, 2005
- [134] M. Hosseinzadeh, G. Nabi Bidhendi, A. Torabian, and N. Mehrdadi, "A study on membrane bioreactor for water reuse from the effluent of industrial town wastewater treatment plant," *Iranian Journal of Toxicology*, vol. 8, no. 24, pp. 983-990, 2014

- [135] S. Purnell, J. Ebdon, A. Buck, M. Tupper, and H. Taylor, "Removal of phages and viral pathogens in a full-scale MBR: implications for wastewater reuse and potable water," *Water Res*, vol. 100, pp. 20-27, 2016
- [136] C.-H. Xing, E. Tardieu, Y. Qian, and X.-H. Wen, "Ultrafiltration membrane bioreactor for urban wastewater reclamation," *J Membrane Sci*, vol. 177, no. 1-2, pp. 73-82, 2000
- [137] D. Dolar, M. Racar, and K. Košutić, "Municipal wastewater reclamation and water reuse for irrigation by membrane processes," *Chemical and biochemical engineering quarterly*, vol. 33, no. 3, pp. 417-425, 2019
- [138] G.-H. Chen, M. C. van Loosdrecht, G. A. Ekama, and D. Brdjanovic, "Biological wastewater treatment: principles, modeling and design," IWA publishing, 2020, ch. Membrane Bio-reactors.
- [139] A. Pollice, A. Lopez, G. Laera, P. Rubino, and A. Lonigro, "Tertiary filtered municipal wastewater as alternative water source in agriculture: a field investigation in Southern Italy," *Sci Total Environ*, vol. 324, no. 1-3, pp. 201-210, 2004
- [140] D. Falsanisi, L. Liberti, and M. Notarnicola, "Ultrafiltration (UF) pilot plant for municipal wastewater reuse in agriculture: impact of the operation mode on process performance," *Water-Sui*, vol. 2, no. 4, pp. 872-885, 2010
- [141] S. Muthukumar, D. A. Nguyen, and K. Baskaran, "Performance evaluation of different ultrafiltration membranes for the reclamation and reuse of secondary effluent," *Desalination*, vol. 279, no. 1-3, pp. 383-389, 2011
- [142] K.-Y. Kim, H.-S. Kim, J. Kim, J.-W. Nam, J.-M. Kim, and S. Son, "A hybrid microfiltration–granular activated carbon system for water purification and wastewater reclamation/reuse," *Desalination*, vol. 243, no. 1-3, pp. 132-144, 2009
- [143] J.-D. Lee, S.-H. Lee, M.-H. Jo, P.-K. Park, C.-H. Lee, and J.-W. Kwak, "Effect of coagulation conditions on membrane filtration characteristics in coagulation–microfiltration process for water treatment," *Environ Sci Technol*, vol. 34, no. 17, pp. 3780-3788, 2000
- [144] D. Abdessemed, G. Nezzal, and R. B. Aim, "Coagulation—adsorption—ultrafiltration for wastewater treatment and reuse," *Desalination*, vol. 131, no. 1-3, pp. 307-314, 2000
- [145] S. Fida, S. Haydar, and M. Zeeshan, "Fouling reduction in nanofiltration membranes in the treatment of municipal sewage—effect of coagulant type used for prior chemically enhanced primary treatment," *Water Science & Technology*, vol. 86, no. 9, pp. 2375-2384, 2022
- [146] M. Gómez, F. Plaza, G. Garralón, J. Pérez, and M. A. Gómez, "A comparative study of tertiary wastewater treatment by physico-chemical-UV process and

- macrofiltration–ultrafiltration technologies," *Desalination*, vol. 202, no. 1-3, pp. 369-376, 2007
- [147] S. Chae *et al.*, "High reuse potential of effluent from an innovative vertical submerged membrane bioreactor treating municipal wastewater," *Desalination*, vol. 202, no. 1-3, pp. 83-89, 2007
- [148] L. Wang *et al.*, "Integrated aerobic granular sludge and membrane process for enabling municipal wastewater treatment and reuse water production," *Chem Eng J*, vol. 337, pp. 300-311, 2018
- [149] B. Corzo, T. de la Torre, C. Sans, R. Escorihuela, S. Navea, and J. J. Malfeito, "Long-term evaluation of a forward osmosis-nanofiltration demonstration plant for wastewater reuse in agriculture," *Chem Eng J*, vol. 338, pp. 383-391, 2018
- [150] M. Jacob, C. Guigui, C. Cabassud, H. Darras, G. Lavison, and L. Moulin, "Performances of RO and NF processes for wastewater reuse: Tertiary treatment after a conventional activated sludge or a membrane bioreactor," *Desalination*, vol. 250, no. 2, pp. 833-839, 2010
- [151] M. Aziz and G. Kasongo, "The removal of selected inorganics from municipal membrane bioreactor wastewater using UF/NF/RO membranes for water reuse application: A pilot-scale study," *Membranes-Basel*, vol. 11, no. 2, p. 117, 2021
- [152] L. Tam, T. Tang, G. N. Lau, K. Sharma, and G. Chen, "A pilot study for wastewater reclamation and reuse with MBR/RO and MF/RO systems," *Desalination*, vol. 202, no. 1-3, pp. 106-113, 2007
- [153] E. Dialynas and E. Diamadopoulos, "Integration of a membrane bioreactor coupled with reverse osmosis for advanced treatment of municipal wastewater," *Desalination*, vol. 238, no. 1-3, pp. 302-311, 2009
- [154] J. Gu, H. Liu, S. Wang, M. Zhang, and Y. Liu, "An innovative anaerobic MBR-reverse osmosis-ion exchange process for energy-efficient reclamation of municipal wastewater to NEWater-like product water," *J Clean Prod*, vol. 230, pp. 1287-1293.2019/09/01/ 2019
- [155] H. Liu, J. Gu, S. Wang, M. Zhang, and Y. Liu, "Performance, membrane fouling control and cost analysis of an integrated anaerobic fixed-film MBR and reverse osmosis process for municipal wastewater reclamation to NEWater-like product water," *J Membrane Sci*, vol. 593, p. 117442, 2020
- [156] M. F. Tay, C. Liu, E. R. Cornelissen, B. Wu, and T. H. Chong, "The feasibility of nanofiltration membrane bioreactor (NF-MBR)+ reverse osmosis (RO) process for water reclamation: Comparison with ultrafiltration membrane bioreactor (UF-MBR)+ RO process," *Water Res*, vol. 129, pp. 180-189, 2018
- [157] Y. Huang, P. Jeffrey, and M. Pidou, "A comparative evaluation of reverse osmosis membrane performance when combined with anaerobic or aerobic

- membrane bioreactors for indirect potable reuse applications," *J Water Process Eng*, vol. 50, p. 103295.2022/12/01/ 2022
- [158] G. K. Pearce, "UF/MF pre-treatment to RO in seawater and wastewater reuse applications: a comparison of energy costs," *Desalination*, vol. 222, no. 1-3, pp. 66-73, 2008
- [159] X. Du, Y. Shi, V. Jegatheesan, and I. U. Haq, "A review on the mechanism, impacts and control methods of membrane fouling in MBR system," *Membranes-Basel*, vol. 10, no. 2, p. 24, 2020
- [160] S. Min *et al.*, "Advanced strategies for mitigation of membrane fouling in anaerobic membrane bioreactors for sustainable wastewater treatment," *Chem Eng J*, vol. 485, p. 149996.2024/04/01/ 2024
- [161] S. Jiang, Y. Li, and B. P. Ladewig, "A review of reverse osmosis membrane fouling and control strategies," *Sci Total Environ*, vol. 595, pp. 567-583.2017/10/01/ 2017
- [162] L. Liu *et al.*, "Insight into key interactions between diverse factors and membrane fouling mitigation in anaerobic membrane bioreactor," *Environ Pollut*, vol. 347, p. 123750.2024/04/15/ 2024
- [163] R. Martínez, M. Ruiz, C. Ramos, J. Cámara, and V. Diez, "Fouling control of submerged and side-stream membrane bioreactors based on the statistical analysis of mid-term assays," *J Clean Prod*, vol. 326, p. 129336, 2021
- [164] Y. Jeong, Y. Kim, Y. Jin, S. Hong, and C. Park, "Comparison of filtration and treatment performance between polymeric and ceramic membranes in anaerobic membrane bioreactor treatment of domestic wastewater," *Sep Purif Technol*, vol. 199, pp. 182-188, 2018
- [165] C. Zhao, X. Xu, J. Chen, G. Wang, and F. Yang, "Highly effective antifouling performance of PVDF/graphene oxide composite membrane in membrane bioreactor (MBR) system," *Desalination*, vol. 340, pp. 59-66, 2014
- [166] P. van der Marel, A. Zwijnenburg, A. Kemperman, M. Wessling, H. Temmink, and W. van der Meer, "An improved flux-step method to determine the critical flux and the critical flux for irreversibility in a membrane bioreactor," *J Membrane Sci*, vol. 332, no. 1, pp. 24-29.2009/04/15/ 2009
- [167] V. Diez, D. Ezquerra, J. L. Cabezas, A. García, and C. Ramos, "A modified method for evaluation of critical flux, fouling rate and in situ determination of resistance and compressibility in MBR under different fouling conditions," *J Membrane Sci*, vol. 453, pp. 1-11.2014/03/01/ 2014
- [168] R. Lutze and M. Engelhart, "Effects of Sludge Characteristics on the Critical Flux of an AnMBR for Sludge Treatment," *Chemie Ingenieur Technik*, vol. 93, no. 9, pp. 1375-1382, 2021

- [169] H. Fan *et al.*, "Impact of membrane pore morphology on multi-cycle fouling and cleaning of hydrophobic and hydrophilic membranes during MBR operation," *J Membrane Sci*, vol. 556, pp. 312-320, 2018
- [170] B. Verrecht, S. Judd, G. Guglielmi, C. Brepols, and J. W. Mulder, "An aeration energy model for an immersed membrane bioreactor," *Water Res*, vol. 42, no. 19, pp. 4761-4770.2008/12/01/ 2008
- [171] S. Vinardell *et al.*, "Impact of permeate flux and gas sparging rate on membrane performance and process economics of granular anaerobic membrane bioreactors," *Sci Total Environ*, vol. 825, p. 153907.2022/06/15/ 2022
- [172] Y.-C. Juang, A. Su, L.-H. Fang, D.-J. Lee, and J.-Y. Lai, "Fouling with aerobic granule membrane bioreactor," *Water Sci Technol*, vol. 64, no. 9, pp. 1870-1875, 2011
- [173] S. Feng *et al.*, "Effects of fractal roughness of membrane surfaces on interfacial interactions associated with membrane fouling in a membrane bioreactor," *Bioresource Technol*, vol. 244, pp. 560-568, 2017
- [174] T. Jiang *et al.*, "Modelling the production and degradation of soluble microbial products (SMP) in membrane bioreactors (MBR)," *Water Res*, vol. 42, no. 20, pp. 4955-4964.2008/12/01/ 2008
- [175] N. Tran Thi Viet, D. C. Vu, and T. H. Duong, "Effect of Hydraulic retention time on performance of anaerobic membrane bioreactor treating slaughterhouse wastewater," *Environmental Research*, vol. 233, p. 116522.2023/09/15/ 2023
- [176] L. Wenhui Lee, X. Zhu, Z. Liu, Y. Gao, C. Chen, and X. Huang, "Probing the key foulants and membrane fouling under increasing salinity in anaerobic osmotic membrane bioreactors for low-strength wastewater treatment," *Chem Eng J*, vol. 413, p. 127450.2021/06/01/ 2021
- [177] H. Cai *et al.*, "Effects of surface charge on interfacial interactions related to membrane fouling in a submerged membrane bioreactor based on thermodynamic analysis," *Journal of colloid and interface science*, vol. 465, pp. 33-41, 2016
- [178] F. Meng and F. Yang, "Fouling mechanisms of deflocculated sludge, normal sludge, and bulking sludge in membrane bioreactor," *J Membrane Sci*, vol. 305, no. 1, pp. 48-56.2007/11/15/ 2007
- [179] T. Maliwan, W. Pungrasmi, and J. Lohwacharin, "Effects of microplastic accumulation on floc characteristics and fouling behavior in a membrane bioreactor," *J Hazard Mater*, vol. 411, p. 124991.2021/06/05/ 2021
- [180] S. Jeon *et al.*, "The effect of membrane material and surface pore size on the fouling properties of submerged membranes," *Water-Sui*, vol. 8, no. 12, p. 602, 2016

- [181] A. Al-Sayed, G. K. Hassan, M. T. Al-Shemy, and F. A. El-Gohary, "Effect of organic loading rates on the performance of membrane bioreactor for wastewater treatment behaviours, fouling, and economic cost," *Sci Rep-Uk*, vol. 13, no. 1, p. 15601, 2023
- [182] V. Nguyen, E. Karunakaran, G. Collins, and C. A. Biggs, "Physicochemical analysis of initial adhesion and biofilm formation of *Methanosarcina barkeri* on polymer support material," *Colloids and Surfaces B: Biointerfaces*, vol. 143, pp. 518-525, 2016
- [183] S. Creber, T. Pintelon, D. G. Von Der Schulenburg, J. Vrouwenvelder, M. Van Loosdrecht, and M. Johns, "Magnetic resonance imaging and 3D simulation studies of biofilm accumulation and cleaning on reverse osmosis membranes," *Food and Bioproducts Processing*, vol. 88, no. 4, pp. 401-408, 2010
- [184] M. Asadollahi, D. Bastani, and S. A. Musavi, "Enhancement of surface properties and performance of reverse osmosis membranes after surface modification: a review," *Desalination*, vol. 420, pp. 330-383, 2017
- [185] H. Lin *et al.*, "A critical review of extracellular polymeric substances (EPSs) in membrane bioreactors: Characteristics, roles in membrane fouling and control strategies," *J Membrane Sci*, vol. 460, pp. 110-125.2014/06/15/ 2014
- [186] Y. Chun *et al.*, "Organic matter removal from a membrane bioreactor effluent for reverse osmosis fouling mitigation by microgranular adsorptive filtration system," *Desalination*, vol. 506, p. 115016, 2021
- [187] W. Zhang, J. Luo, L. Ding, and M. Y. Jaffrin, "A review on flux decline control strategies in pressure-driven membrane processes," *Ind Eng Chem Res*, vol. 54, no. 11, pp. 2843-2861, 2015
- [188] R. Bian, K. Yamamoto, and Y. Watanabe, "The effect of shear rate on controlling the concentration polarization and membrane fouling," *Desalination*, vol. 131, no. 1-3, pp. 225-236, 2000
- [189] F. Zamani, J. W. Chew, E. Akhondi, W. B. Krantz, and A. G. Fane, "Unsteady-state shear strategies to enhance mass-transfer for the implementation of ultrapermeable membranes in reverse osmosis: a review," *Desalination*, vol. 356, pp. 328-348, 2015
- [190] A. Matin, F. Rahman, H. Z. Shafi, and S. M. Zubair, "Scaling of reverse osmosis membranes used in water desalination: Phenomena, impact, and control; future directions," *Desalination*, vol. 455, pp. 135-157.2019/04/01/ 2019
- [191] S. Al-Jeshi and A. Neville, "An investigation into the relationship between flux and roughness on RO membranes using scanning probe microscopy," *Desalination*, vol. 189, no. 1-3, pp. 221-228, 2006
- [192] M. Elimelech, X. Zhu, A. E. Childress, and S. Hong, "Role of membrane surface morphology in colloidal fouling of cellulose acetate and composite aromatic

- polyamide reverse osmosis membranes," *J Membrane Sci*, vol. 127, no. 1, pp. 101-109, 1997
- [193] B.-J. Wang, T.-C. Wei, and Z.-R. Yu, "Effect of operating temperature on component distribution of West Indian cherry juice in a microfiltration system," *LWT-Food Science and Technology*, vol. 38, no. 6, pp. 683-689, 2005
- [194] M. J. Campbell, R. P. Walter, R. McLoughlin, and C. J. Knowles, "Effect of temperature on protein conformation and activity during ultrafiltration," *J Membrane Sci*, vol. 78, no. 1-2, pp. 35-43, 1993
- [195] S.-J. You, X.-H. Wang, M. Zhong, Y.-J. Zhong, C. Yu, and N.-Q. Ren, "Temperature as a factor affecting transmembrane water flux in forward osmosis: Steady-state modeling and experimental validation," *Chem Eng J*, vol. 198, pp. 52-60, 2012
- [196] C. Y. Tang, T. Chong, and A. G. Fane, "Colloidal interactions and fouling of NF and RO membranes: a review," *Advances in colloid and interface science*, vol. 164, no. 1-2, pp. 126-143, 2011
- [197] M. Goosen, S. Sablani, H. Al-Hinai, S. Al-Obeidani, R. Al-Belushi, and a. Jackson, "Fouling of reverse osmosis and ultrafiltration membranes: a critical review," *Separation science and technology*, vol. 39, no. 10, pp. 2261-2297, 2005
- [198] Z. Du, M. Ji, and R. Li, "Enhancement of membrane fouling mitigation and trace organic compounds removal by electric field in a microfiltration reactor treating secondary effluent of a municipal wastewater treatment plant," *Sci Total Environ*, vol. 806, p. 151212, 2022
- [199] Y. Yu, Z. Yang, and Y. Duan, "Structure and flow calculation of cake layer on microfiltration membranes," *Journal of Environmental Sciences*, vol. 56, pp. 95-101, 2017
- [200] A. Gul, J. Hruza, and F. Yalcinkaya, "Fouling and chemical cleaning of microfiltration membranes: A mini-review," *Polymers*, vol. 13, no. 6, p. 846, 2021
- [201] F. Qu *et al.*, "Ultrafiltration membrane fouling caused by extracellular organic matter (EOM) from *Microcystis aeruginosa*: effects of membrane pore size and surface hydrophobicity," *J Membrane Sci*, vol. 449, pp. 58-66, 2014
- [202] M. W. Hakami, A. Alkudhiri, S. Al-Batty, M.-P. Zacharof, J. Maddy, and N. Hilal, "Ceramic microfiltration membranes in wastewater treatment: filtration behavior, fouling and prevention," *Membranes-Basel*, vol. 10, no. 9, p. 248, 2020
- [203] M. Zhang *et al.*, "Effects of hydrophilicity/hydrophobicity of membrane on membrane fouling in a submerged membrane bioreactor," *Bioresource Technol*, vol. 175, pp. 59-67, 2015

- [204] A. W. Mohammad, C. Y. Ng, Y. P. Lim, and G. H. Ng, "Ultrafiltration in food processing industry: review on application, membrane fouling, and fouling control," *Food and bioprocess technology*, vol. 5, pp. 1143-1156, 2012
- [205] Z. Lam, H. Anlauf, and H. Nirschl, "High-Pressure Jet Cleaning of Polymeric Microfiltration Membranes," *Chem Eng Technol*, vol. 43, no. 3, pp. 457-464, 2020
- [206] B. Zhang *et al.*, "Efficiencies and mechanisms of the chemical cleaning of fouled polytetrafluoroethylene (PTFE) membranes during the microfiltration of alkali/surfactant/polymer flooding oilfield wastewater," *Rsc Adv*, vol. 9, no. 63, pp. 36940-36950, 2019
- [207] H. Lee, J.-s. Kang, H. Kim, and S. Lee, "Salt cleaning of EfOM-fouled MF membrane for wastewater reclamation," *Desalination Water Treat*, vol. 180, pp. 55-66, 2020
- [208] F. Carstensen, A. Apel, and M. Wessling, "In situ product recovery: Submerged membranes vs. external loop membranes," *J Membrane Sci*, vol. 394-395, pp. 1-36.2012/03/15/ 2012
- [209] K. Li *et al.*, "Effect of pre-oxidation on low pressure membrane (LPM) for water and wastewater treatment: A review," *Chemosphere*, vol. 231, pp. 287-300.2019/09/01/ 2019
- [210] R. A. Ragio, L. F. Miyazaki, M. A. d. Oliveira, L. H. G. Coelho, R. d. F. Bueno, and E. L. Subtil, "Pre-coagulation assisted ultrafiltration membrane process for anaerobic effluent," *J Environ Chem Eng*, vol. 8, no. 5, p. 104066.2020/10/01/ 2020
- [211] B. Zhang *et al.*, "Pre-coagulation for membrane fouling mitigation in an aerobic granular sludge membrane bioreactor: A comparative study of modified microbial and organic flocculants," *J Membrane Sci*, vol. 644, p. 120129.2022/02/15/ 2022
- [212] S. S. Madaeni and E. Salehi, "Membrane-adsorption integrated systems/processes," *Integrated Membrane Systems and Processes*, pp. 343-373, 2016
- [213] D. Lu *et al.*, "Role of pre-coagulation in ultralow pressure membrane system for *Microcystis aeruginosa*-laden water treatment: Membrane fouling potential and mechanism," *Sci Total Environ*, vol. 710, p. 136340.2020/03/25/ 2020
- [214] Y. Zhao *et al.*, "Membrane bioreactors for hospital wastewater treatment: recent advancements in membranes and processes," *Frontiers of Chemical Science and Engineering*, pp. 1-27, 2022
- [215] H. Hamed, M. Ehteshami, S. A. Mirbagheri, S. A. Rasouli, and S. Zendehboudi, "Current status and future prospects of membrane bioreactors (MBRs) and

- fouling phenomena: a systematic review," *The Canadian Journal of Chemical Engineering*, vol. 97, no. 1, pp. 32-58, 2019
- [216] V. Kochkodan and N. Hilal, "A comprehensive review on surface modified polymer membranes for biofouling mitigation," *Desalination*, vol. 356, pp. 187-207.2015/01/15/ 2015
- [217] W. Rulkens, "Sewage sludge as a biomass resource for the production of energy: overview and assessment of the various options," *Energ Fuel*, vol. 22, no. 1, pp. 9-15, 2008
- [218] X. Ma, X. Xue, A. González-Mejía, J. Garland, and J. Cashdollar, "Sustainable water systems for the city of tomorrow—A conceptual framework," *Sustainability-Basel*, vol. 7, no. 9, pp. 12071-12105, 2015
- [219] K. Rabaey and R. A. Rozendal, "Microbial electrosynthesis—revisiting the electrical route for microbial production," *Nature reviews microbiology*, vol. 8, no. 10, pp. 706-716, 2010
- [220] A. Sikora, A. Detman, A. Chojnacka, and M. K. Błaszczuk, "Anaerobic digestion: I. A common process ensuring energy flow and the circulation of matter in ecosystems. II. A tool for the production of gaseous biofuels," *Fermentation processes*, vol. 14, p. 271, 2017
- [221] A. Hublin and B. Zelić, "Modelling of the whey and cow manure co-digestion process," *Waste management & research*, vol. 31, no. 4, pp. 353-360, 2013
- [222] T. Wang *et al.*, "Anaerobic digestion of sludge filtrate assisted by symbionts of short chain fatty acid-oxidation syntrophs and exoelectrogens: Process performance, methane yield and microbial community," *J Hazard Mater*, vol. 384, p. 121222, 2020
- [223] Y. Kong, H. Lei, W. Cheng, B. Wang, F. Pan, and F. Huang, "Shifting microbial communities perform anaerobic oxidation of methane and methanogenesis in sediments from the Shenhua area of northern south China sea during long-term incubations," *Front Earth Sc-Switz*, vol. 10, p. 1014976, 2022
- [224] M. Laskar, T. Kasai, T. Awata, and A. Katayama, "Humins assist reductive acetogenesis in absence of other external electron donor," *Int J Env Res Pub He*, vol. 17, no. 12, p. 4211, 2020
- [225] C. Huiliñir, E. Roa, D. Vargas, M. Roedel, and E. Aspé, "Kinetics of syntrophic acetogenesis in a saline medium," *Journal of Chemical Technology & Biotechnology: International Research in Process, Environmental & Clean Technology*, vol. 83, no. 10, pp. 1433-1440, 2008
- [226] T. Ngo, A. S. Ball, and E. Shahsavari, "The current status, potential benefits and future prospects of the Australian biogas sector," *Journal of Sustainable Bioenergy Systems*, vol. 11, no. 1, pp. 14-32, 2021

- [227] C. Chen *et al.*, "Impact of reactor configurations on the performance of a granular anaerobic membrane bioreactor for municipal wastewater treatment," *International Biodeterioration & Biodegradation*, vol. 121, pp. 131-138, 2017
- [228] X. Song *et al.*, "Resource recovery from wastewater by anaerobic membrane bioreactors: Opportunities and challenges," *Bioresource Technol*, vol. 270, pp. 669-677.2018/12// 2018
- [229] K. Wang, N. Martin Garcia, A. Soares, B. Jefferson, and E. McAdam, "Comparison of fouling between aerobic and anaerobic MBR treating municipal wastewater," 2018
- [230] H. Chen, S. Chang, Q. Guo, Y. Hong, and P. Wu, "Brewery wastewater treatment using an anaerobic membrane bioreactor," *Biochemical engineering journal*, vol. 105, pp. 321-331, 2016
- [231] Y. Hu *et al.*, "Recent developments of anaerobic membrane bioreactors for municipal wastewater treatment and bioenergy recovery: Focusing on novel configurations and energy balance analysis," *J Clean Prod*, vol. 356, p. 131856.2022/07/01/ 2022
- [232] M. Kim, T. Y. C. Lam, G. Y. A. Tan, P. H. Lee, and J. Kim, "Use of polymeric scouring agent as fluidized media in anaerobic fluidized bed membrane bioreactor for wastewater treatment: System performance and microbial community," *J Membrane Sci*, vol. 606, pp. 118121-118121.2020/7// 2020
- [233] T. Gao, H. Zhang, X. Xu, and J. Teng, "Integrating microbial electrolysis cell based on electrochemical carbon dioxide reduction into anaerobic osmosis membrane reactor for biogas upgrading," *Water Res*, vol. 190, p. 116679, 2021
- [234] C. Chen *et al.*, "Robustness of granular activated carbon-synergized anaerobic membrane bioreactor for pilot-scale application over a wide seasonal temperature change," *Water Res*, vol. 189, p. 116552, 2021
- [235] Z. Kong *et al.*, "Large pilot-scale submerged anaerobic membrane bioreactor for the treatment of municipal wastewater and biogas production at 25 °C," *Bioresource Technol*, vol. 319, p. 124123.2021/01/01/ 2021
- [236] J. Ji *et al.*, "One-year operation of a 20-L submerged anaerobic membrane bioreactor for real domestic wastewater treatment at room temperature: Pursuing the optimal HRT and sustainable flux," *Sci Total Environ*, vol. 775, p. 145799, 2021
- [237] J. Gouveia, F. Plaza, G. Garralon, F. Fdz-Polanco, and M. Peña, "Long-term operation of a pilot scale anaerobic membrane bioreactor (AnMBR) for the treatment of municipal wastewater under psychrophilic conditions," *Bioresource Technol*, vol. 185, pp. 225-233, 2015
- [238] J. Gouveia, F. Plaza, G. Garralon, F. Fdz-Polanco, and M. Peña, "A novel configuration for an anaerobic submerged membrane bioreactor (AnSMBR).

- Long-term treatment of municipal wastewater under psychrophilic conditions," *Bioresource Technol*, vol. 198, pp. 510-519, 2015
- [239] X. Mei, Z. Wang, Y. Miao, and Z. Wu, "A pilot-scale anaerobic membrane bioreactor under short hydraulic retention time for municipal wastewater treatment: performance and microbial community identification," *J Water Reuse Desal*, vol. 8, no. 1, pp. 58-67, 2018
- [240] J. Ji *et al.*, "Application of two anaerobic membrane bioreactors with different pore size membranes for municipal wastewater treatment," *Sci Total Environ*, vol. 745, p. 140903, 2020
- [241] L. Chen, P. Cheng, L. Ye, H. Chen, X. Xu, and L. Zhu, "Biological performance and fouling mitigation in the biochar-amended anaerobic membrane bioreactor (AnMBR) treating pharmaceutical wastewater," *Bioresource Technol*, vol. 302, p. 122805, 2020
- [242] J. Liu, X. Kang, X. Luan, L. Gao, H. Tian, and X. Liu, "Performance and membrane fouling behaviors analysis with SVR-LibSVM model in a submerged anaerobic membrane bioreactor treating low-strength domestic sewage," *Environmental Technology & Innovation*, vol. 19, p. 100844, 2020
- [243] N. C. Nguyen *et al.*, "Water and nutrient recovery by a novel moving sponge–Anaerobic osmotic membrane bioreactor–Membrane distillation (AnOMBR-MD) closed-loop system," *Bioresource Technol*, vol. 312, p. 123573, 2020
- [244] Á. Robles *et al.*, "A semi-industrial scale AnMBR for municipal wastewater treatment at ambient temperature: performance of the biological process," *Water Res*, vol. 215, p. 118249, 2022
- [245] C. Rong *et al.*, "Pilot plant demonstration of temperature impacts on the methanogenic performance and membrane fouling control of the anaerobic membrane bioreactor in treating real municipal wastewater," *Bioresource Technol*, vol. 354, p. 127167, 2022
- [246] J. Ji *et al.*, "Submerged anaerobic membrane bioreactor applied for mainstream municipal wastewater treatment at a low temperature: Sludge yield, energy balance and membrane filtration behaviors," *J Clean Prod*, vol. 355, p. 131831, 2022
- [247] A. Plevri, E. Barka, C. Noutsopoulos, and D. Mamais, "Enhancing the Performance of AnMBR Treating Municipal Wastewater at a High Organic Loading Rate with Iron Addition," *Energies*, vol. 16, no. 7, p. 3069, 2023
- [248] F. Yilmaz, E. Özbayram, N. Perendeci, E. Sahinkaya, and O. İnce, "Performance evaluation and microbial dynamics of submerged anaerobic membrane bioreactors for municipal wastewater treatment," *J Water Process Eng*, vol. 59, p. 104935, 2024

- [249] O. Casabella-Font, M. Ponzelli, M. Papapanou, J. L. Balcazar, M. Pijuan, and J. Radjenovic, "Impact of graphene oxide addition on pharmaceuticals removal in anaerobic membrane bioreactor," *Bioresource Technol*, vol. 383, p. 129252, 2023
- [250] S. Theuri, K. Gurung, V. Puhakka, D. Anjan, and M. Sillanpaa, "Effect of temperature variations in anaerobic fluidized membrane bioreactor: membrane fouling and microbial community dynamics assessment," *Int J Environ Sci Te*, vol. 20, no. 9, pp. 9451-9464, 2023
- [251] S. K. Tomar, S. K. Padhi, P. K. Dikshit, S. Yadav, and M. Balakrishnan, "Effect of hydraulic retention time on biological nutrients removal in an anaerobic membrane bioreactor treating low-strength drain wastewater," *Bioresource Technology Reports*, vol. 24, p. 101599, 2023
- [252] Y. Liu, J. Gu, and M. Zhang, *AB processes: Towards energy self-sufficient municipal wastewater treatment*. IWA publishing, 2019.
- [253] X. Zhang, J. Gu, and Y. Liu, "Necessity of direct energy and ammonium recovery for carbon neutral municipal wastewater reclamation in an innovative anaerobic MBR-biochar adsorption-reverse osmosis process," *Water Res*, vol. 211, p. 118058, 2022
- [254] W. Dai, X. Xu, B. Liu, and F. Yang, "Toward energy-neutral wastewater treatment: a membrane combined process of anaerobic digestion and nitrification–anammox for biogas recovery and nitrogen removal," *Chem Eng J*, vol. 279, pp. 725-734, 2015
- [255] R. Pretel, P. Moñino, A. Robles, M. Ruano, A. Seco, and J. Ferrer, "Economic and environmental sustainability of an AnMBR treating urban wastewater and organic fraction of municipal solid waste," *J Environ Manage*, vol. 179, pp. 83-92, 2016
- [256] R. Pretel *et al.*, "Designing an AnMBR-based WWTP for energy recovery from urban wastewater: The role of primary settling and anaerobic digestion," *Sep Purif Technol*, vol. 156, pp. 132-139, 2015
- [257] Á. Robles *et al.*, "New frontiers from removal to recycling of nitrogen and phosphorus from wastewater in the Circular Economy," *Bioresource Technol*, vol. 300, p. 122673, 2020
- [258] S. Vinardell, S. Astals, J. Mata-Alvarez, and J. Dosta, "Techno-economic analysis of combining forward osmosis-reverse osmosis and anaerobic membrane bioreactor technologies for municipal wastewater treatment and water production," *Bioresource Technol*, vol. 297, p. 122395, 2020
- [259] A. Guldhe *et al.*, "Prospects, recent advancements and challenges of different wastewater streams for microalgal cultivation," *J Environ Manage*, vol. 203, pp. 299-315, 2017

- [260] D. García, I. de Godos, C. Domínguez, S. Turiel, S. Bolado, and R. Muñoz, "A systematic comparison of the potential of microalgae-bacteria and purple phototrophic bacteria consortia for the treatment of piggery wastewater," *Bioresource Technol*, vol. 276, pp. 18-27, 2019
- [261] C. Liu, Q. Wang, F. Huang, and J. Zhang, "Removal of phosphorus from anaerobic membrane bioreactor effluent by ion exchange resin," *Separation Science and Technology*, vol. 51, no. 17, pp. 2833-2843, 2016
- [262] Q. Guan *et al.*, "A review of struvite crystallization for nutrient source recovery from wastewater," *J Environ Manage*, vol. 344, p. 118383.2023/10/15/ 2023
- [263] K. N. Ohlinger, PE, T. M. Young, and E. D. Schroeder, "Kinetics effects on preferential struvite accumulation in wastewater," *Journal of Environmental Engineering*, vol. 125, no. 8, pp. 730-737, 1999
- [264] E. Ariyanto, T. K. Sen, and H. M. Ang, "The influence of various physico-chemical process parameters on kinetics and growth mechanism of struvite crystallisation," *Advanced Powder Technology*, vol. 25, no. 2, pp. 682-694, 2014
- [265] Y. Jaffer, T. Clark, P. Pearce, and S. Parsons, "Potential phosphorus recovery by struvite formation," *Water Res*, vol. 36, no. 7, pp. 1834-1842, 2002
- [266] L. Song, Z. Li, G. Wang, Y. Tian, and C. Yang, "Supersaturation control of struvite growth by operating pH," *Journal of Molecular Liquids*, vol. 336, p. 116293, 2021
- [267] H. Sudibyo *et al.*, "Thermodynamics and kinetics of struvite crystallization from hydrothermal liquefaction aqueous-phase considering hydroxyapatite and organics coprecipitation," *Ind Eng Chem Res*, vol. 61, no. 20, pp. 6894-6908, 2022
- [268] H. Li, Q.-Z. Yao, Z.-M. Dong, T.-L. Zhao, G.-T. Zhou, and S.-Q. Fu, "Controlled synthesis of struvite nanowires in synthetic wastewater," *Acs Sustain Chem Eng*, vol. 7, no. 2, pp. 2035-2043, 2018
- [269] A. Korchef, S. Naffouti, and I. Souid, "Recovery of high concentrations of phosphorus and ammonium through struvite crystallization by CO₂ repelling," *Crystal Research and Technology*, vol. 57, no. 11, p. 2200123, 2022
- [270] G. Xu, J. Ren, K. Cui, and K. Guo, "Effect of operating conditions on phosphorus recovery from acidified plant oil wastewater by struvite crystallization," in *IOP Conference Series: Earth and Environmental Science*, 2023, vol. 1135, no. 1: IOP Publishing, p. 012014.
- [271] C. González-Morales, B. Fernández, F. J. Molina, D. Naranjo-Fernández, A. Matamoros-Veloz, and M. A. Camargo-Valero, "Influence of pH and temperature on struvite purity and recovery from anaerobic digestate," *Sustainability-Basel*, vol. 13, no. 19, p. 10730, 2021

- [272] S. Muryanto, "On precipitation of struvite ($\text{MgNH}_4\text{PO}_4 \cdot 6\text{H}_2\text{O}$)," *Journal of Science and Science Education*, vol. 1, no. 2, pp. 21-29, 2017
- [273] A. P. Bayuseno, D. S. Perwitasari, S. Muryanto, M. Tauviquirrahman, and J. Jamari, "Kinetics and morphological characteristics of struvite ($\text{MgNH}_4\text{PO}_4 \cdot 6\text{H}_2\text{O}$) under the influence of maleic acid," *Heliyon*, vol. 6, no. 3, 2020
- [274] L. Edahwati and S. Sutiyono, "Analysis of Air Flow Rate in Bulkhead Reactors on Struvite Mineral," *BIOMEJ*, vol. 2, no. 1, pp. 1-5, 2022
- [275] J. r. Hövelmann and C. V. Putnis, "In situ nanoscale imaging of struvite formation during the dissolution of natural brucite: implications for phosphorus recovery from wastewaters," *Environ Sci Technol*, vol. 50, no. 23, pp. 13032-13041, 2016
- [276] D. Kim, C. Olympiou, C. P. McCoy, N. J. Irwin, and J. D. Rimer, "Time-resolved dynamics of struvite crystallization: Insights from the macroscopic to molecular scale," *Chemistry—A European Journal*, vol. 26, no. 16, pp. 3555-3563, 2020
- [277] W. Gong, Y. Li, L. Luo, X. Luo, X. Cheng, and H. Liang, "Application of struvite-MAP crystallization reactor for treating cattle manure anaerobic digested slurry: Nitrogen and phosphorus recovery and crystal fertilizer efficiency in plant trials," *Int J Env Res Pub He*, vol. 15, no. 7, p. 1397, 2018
- [278] A. Siciliano, "Assessment of fertilizer potential of the struvite produced from the treatment of methanogenic landfill leachate using low-cost reagents," *Environ Sci Pollut R*, vol. 23, pp. 5949-5959, 2016
- [279] T. Tervahauta, T. Hoang, L. Hernández, G. Zeeman, and C. Buisman, "Prospects of source-separation-based sanitation concepts: a model-based study," *Water-Sui*, vol. 5, no. 3, pp. 1006-1035, 2013
- [280] K. Koch, B. Helmreich, and J. E. Drewes, "Co-digestion of food waste in municipal wastewater treatment plants: Effect of different mixtures on methane yield and hydrolysis rate constant," *Appl Energ*, vol. 137, pp. 250-255, 2015
- [281] V. K. Tyagi, L. Fdez-Güelfo, Y. Zhou, C. J. Álvarez-Gallego, L. R. Garcia, and W. J. Ng, "Anaerobic co-digestion of organic fraction of municipal solid waste (OFMSW): Progress and challenges," *Renewable and sustainable energy reviews*, vol. 93, pp. 380-399, 2018
- [282] C. He *et al.*, "Techno-economic feasibility of "membrane-based pre-concentration+ post-treatment" systems for municipal wastewater treatment and resource recovery," *J Clean Prod*, vol. 375, p. 134113, 2022
- [283] A. J. Ansari, "Resource recovery from wastewater using forward osmosis membranes," School of Civil, Mining and Environmental Engineering, University of Wollongong, 2017.

- [284] H. Guven, R. K. Dereli, H. Ozgun, M. E. Ersahin, and I. Ozturk, "Towards sustainable and energy efficient municipal wastewater treatment by up-concentration of organics," *Progress in Energy and Combustion Science*, vol. 70, pp. 145-168, 2019
- [285] D. L. Sills, V. L. Wade, and T. D. DiStefano, "Comparative life cycle and technoeconomic assessment for energy recovery from dilute wastewater," *Environmental Engineering Science*, vol. 33, no. 11, pp. 861-872, 2016
- [286] S. Aiyuk, J. Amoako, L. Raskin, A. Van Haandel, and W. Verstraete, "Removal of carbon and nutrients from domestic wastewater using a low investment, integrated treatment concept," *Water Res*, vol. 38, no. 13, pp. 3031-3042.2004/7// 2004
- [287] A. R. Bielefeldt, "Water Treatment, Industrial," in *Encyclopedia of Microbiology (Third Edition)*, M. Schaechter Ed. Oxford: Academic Press, 2009, pp. 569-586.
- [288] S. Xu, L. Zhang, S. Huang, G. Zeeman, H. Rijnaarts, and Y. Liu, "Improving the energy efficiency of a pilot-scale UASB-digester for low temperature domestic wastewater treatment," *Biochemical Engineering Journal*, vol. 135, pp. 71-78.2018/07/15/ 2018
- [289] M. Seib, K. Berg, and D. Zitomer, "Low energy anaerobic membrane bioreactor for municipal wastewater treatment," *Journal of Membrane Science*, vol. 514, pp. 450-457, 2016
- [290] Z. Jin *et al.*, "Efficient sewage pre-concentration with combined coagulation microfiltration for organic matter recovery," *Chem Eng J*, vol. 292, pp. 130-138.2016/5// 2016
- [291] B.-C. Huang, Y.-F. Guan, W. Chen, and H.-Q. Yu, "Membrane fouling characteristics and mitigation in a coagulation-assisted microfiltration process for municipal wastewater pretreatment," *Water research*, vol. 123, pp. 216-223, 2017
- [292] K. Kimura, D. Honoki, and T. Sato, "Effective physical cleaning and adequate membrane flux for direct membrane filtration (DMF) of municipal wastewater: Up-concentration of organic matter for efficient energy recovery," *Sep Purif Technol*, vol. 181, pp. 37-43.2017/6// 2017
- [293] K. Kimura, M. Yamakawa, and A. Hafuka, "Direct membrane filtration (DMF) for recovery of organic matter in municipal wastewater using small amounts of chemicals and energy," *Chemosphere*, p. 130244, 2021
- [294] T. A. Nascimento and M. P. Miranda, "Control strategies for the long-term operation of direct membrane filtration of municipal wastewater," *Journal of Environmental Chemical Engineering*, p. 105335, 2021

- [295] H. Gong, Z. Jin, X. Wang, and K. Wang, "Membrane fouling controlled by coagulation/adsorption during direct sewage membrane filtration (DSMF) for organic matter concentration," *Journal of Environmental Sciences*, vol. 32, pp. 1-7.2015/06/01/ 2015
- [296] T. A. Nascimento, F. R. Mejía, F. Fdz-Polanco, and M. Peña Miranda, "Improvement of municipal wastewater pretreatment by direct membrane filtration," *Environmental technology*, vol. 38, no. 20, pp. 2562-2572, 2017
- [297] H. Oh, S. Takizawa, S. Ohgaki, H. Katayama, K. Oguma, and M. Yu, "Removal of organics and viruses using hybrid ceramic MF system without draining PAC," *Desalination*, vol. 202, no. 1-3, pp. 191-198, 2007
- [298] F. Meng, S.-R. Chae, A. Drews, M. Kraume, H.-S. Shin, and F. Yang, "Recent advances in membrane bioreactors (MBRs): membrane fouling and membrane material," *Water research*, vol. 43, no. 6, pp. 1489-1512, 2009
- [299] Z. Liu, X. Zhu, P. Liang, X. Zhang, K. Kimura, and X. Huang, "Distinction between polymeric and ceramic membrane in AnMBR treating municipal wastewater: In terms of irremovable fouling," *Journal of Membrane Science*, vol. 588, p. 117229, 2019
- [300] M. Zielińska and M. Galik, "Use of ceramic membranes in a membrane filtration supported by coagulation for the treatment of dairy wastewater," *Water, Air, Soil Pollut.*, vol. 228, no. 5, pp. 1-12, 2017
- [301] C. Li, W. Sun, Z. Lu, X. Ao, and S. Li, "Ceramic nanocomposite membranes and membrane fouling: A review," *Water Research*, vol. 175, p. 115674.2020/05/15/ 2020
- [302] A. Hafuka, T. Takahashi, and K. Kimura, "Anaerobic digestibility of up-concentrated organic matter obtained from direct membrane filtration of municipal wastewater," *Biochemical Engineering Journal*, vol. 161, p. 107692.2020/09/15/ 2020
- [303] Y.-x. Zhao, P. Li, R.-h. Li, and X.-y. Li, "Direct filtration for the treatment of the coagulated domestic sewage using flat-sheet ceramic membranes," *Chemosphere*, vol. 223, pp. 383-390, 2019
- [304] Y.-x. Zhao, P. Li, R.-h. Li, and X.-y. Li, "Characterization and mitigation of the fouling of flat-sheet ceramic membranes for direct filtration of the coagulated domestic wastewater," *J Hazard Mater*, vol. 385, p. 121557.2020/03/05/ 2020
- [305] S. Hube *et al.*, "Direct membrane filtration for wastewater treatment and resource recovery: A review," *Science of The Total Environment*, p. 136375, 2019
- [306] S. G. Arhin *et al.*, "Membrane fouling control in low pressure membranes: A review on pretreatment techniques for fouling abatement," *Environmental Engineering Research*, vol. 21, no. 2, pp. 109-120, 2016

- [307] A. T. Nair and M. M. Ahammed, "The reuse of water treatment sludge as a coagulant for post-treatment of UASB reactor treating urban wastewater," *Journal of Cleaner Production*, vol. 96, pp. 272-281, 2015
- [308] G. De Feo, S. De Gisi, and M. Galasso, "Definition of a practical multi-criteria procedure for selecting the best coagulant in a chemically assisted primary sedimentation process for the treatment of urban wastewater," *Desalination*, vol. 230, no. 1, pp. 229-238.2008/09/30/ 2008
- [309] E. Jordao and I. Volschan, "Cost-effective solutions for sewage treatment in developing countries-the case of Brazil," *Water Science and Technology*, vol. 50, no. 7, pp. 237-242, 2004
- [310] W. A. Shewa and M. Dagnew, "Revisiting Chemically Enhanced Primary Treatment of Wastewater: A Review," *Sustainability*, vol. 12, no. 15, p. 5928, 2020
- [311] K. Czerwionka, A. Wilinska, and A. Tuszynska, "The use of organic coagulants in the primary precipitation process at wastewater treatment plants," *Water*, vol. 12, no. 6, p. 1650, 2020
- [312] A. Taboada-Santos, E. Rivadulla, L. Paredes, M. Carballa, J. Romalde, and J. M. Lema, "Comprehensive comparison of chemically enhanced primary treatment and high-rate activated sludge in novel wastewater treatment plant configurations," *Water Res*, vol. 169, p. 115258, 2020
- [313] J.-C. Huang and L. Li, "An innovative approach to maximize primary treatment performance," *Water science and technology*, vol. 42, no. 12, pp. 209-222, 2000
- [314] L. Lin, R.-h. Li, Y. Li, J. Xu, and X.-y. Li, "Recovery of organic carbon and phosphorus from wastewater by Fe-enhanced primary sedimentation and sludge fermentation," *Process Biochemistry*, vol. 54, pp. 135-139.2017/03/01/ 2017
- [315] A. Hög, J. Ludwig, and M. Beery, "The use of integrated flotation and ceramic membrane filtration for surface water treatment with high loads of suspended and dissolved organic matter," *J Water Process Eng*, vol. 6, pp. 129-135, 2015
- [316] A. Bezirgiannidis, A. Plesia-Efstathopoulou, S. Ntougias, and P. Melidis, "Combined chemically enhanced primary sedimentation and biofiltration process for low cost municipal wastewater treatment," *Journal of Environmental Science and Health, Part A*, vol. 54, no. 12, pp. 1227-1232, 2019
- [317] Y.-y. Li, L. Lin, and X.-y. Li, "Chemically enhanced primary sedimentation and acidogenesis of organics in sludge for enhanced nitrogen removal in wastewater treatment," *J Clean Prod*, vol. 244, p. 118705, 2020
- [318] A. Alengebawy, K. Jin, Y. Ran, J. Peng, X. Zhang, and P. Ai, "Advanced pre-treatment of stripped biogas slurry by polyaluminum chloride coagulation and biochar adsorption coupled with ceramic membrane filtration," *Chemosphere*, vol. 267, p. 129197, 2021

- [319] T. Chakraborty *et al.*, "Reusability of recovered iron coagulant from primary municipal sludge and its impact on chemically enhanced primary treatment," *Separation and Purification Technology*, vol. 231, p. 115894, 2020
- [320] A. Mudhoo and S. Kumar, "Effects of heavy metals as stress factors on anaerobic digestion processes and biogas production from biomass," *International Journal of Environmental Science and Technology*, vol. 10, no. 6, pp. 1383-1398, 2013
- [321] S. K. Lateef, B. Z. Soh, and K. Kimura, "Direct membrane filtration of municipal wastewater with chemically enhanced backwash for recovery of organic matter," *Bioresource technology*, vol. 150, pp. 149-155, 2013
- [322] K. Kimura, M. Yamakawa, and A. Hafuka, "Direct membrane filtration (DMF) for recovery of organic matter in municipal wastewater using small amounts of chemicals and energy," *Chemosphere*, vol. 277, p. 130244, 2021
- [323] K. Gruskevica and L. Mezule, "Cleaning Methods for Ceramic Ultrafiltration Membranes Affected by Organic Fouling," *Membranes*, vol. 11, no. 2, p. 131, 2021
- [324] X. Mei, P. J. Quek, Z. Wang, and H. Y. Ng, "Alkali-assisted membrane cleaning for fouling control of anaerobic ceramic membrane bioreactor," *Bioresource Technology*, vol. 240, pp. 25-32.2017/09/01/ 2017
- [325] APHA, "Standard methods for the examination of water and wastewater," *American Public Health Association (APHA): Washington, DC, USA*, vol. 21, 2005
- [326] M. F. Chong, "Direct flocculation process for wastewater treatment," in *Advances in water treatment and pollution prevention*: Springer, 2012, pp. 201-230.
- [327] A. Ahmad, S. Ismail, and S. Bhatia, "Optimization of coagulation– flocculation process for palm oil mill effluent using response surface methodology," *Environmental science & technology*, vol. 39, no. 8, pp. 2828-2834, 2005
- [328] A. Ahmad, S. Wong, T. Teng, and A. Zuhairi, "Improvement of alum and PACl coagulation by polyacrylamides (PAMs) for the treatment of pulp and paper mill wastewater," *Chemical Engineering Journal*, vol. 137, no. 3, pp. 510-517, 2008
- [329] O. Amuda and A. Alade, "Coagulation/flocculation process in the treatment of abattoir wastewater," *Desalination*, vol. 196, no. 1-3, pp. 22-31, 2006
- [330] T. A. Malkoske, P. R. Bérubé, and R. C. Andrews, "Coagulation/flocculation prior to low pressure membranes in drinking water treatment: a review," *Environmental Science: Water Research & Technology*, vol. 6, no. 11, pp. 2993-3023, 2020

- [331] T. T. H. Dang, C.-W. Li, and K.-H. Choo, "Comparison of low-pressure reverse osmosis filtration and polyelectrolyte-enhanced ultrafiltration for the removal of Co and Sr from nuclear plant wastewater," *Separation and Purification Technology*, vol. 157, pp. 209-214.2016/01/08/ 2016
- [332] Y. Du, W. H. Pennock, M. L. Weber-Shirk, and L. W. Lion, "Observations and a geometric explanation of effects of humic acid on flocculation," *Environmental Engineering Science*, vol. 36, no. 5, pp. 614-622, 2019
- [333] S. Wang, C. Liu, and Q. Li, "Fouling of microfiltration membranes by organic polymer coagulants and flocculants: Controlling factors and mechanisms," *Water research*, vol. 45, no. 1, pp. 357-365, 2011
- [334] T. Liu, Y. Lian, N. Graham, W. Yu, D. Rooney, and K. Sun, "Application of polyacrylamide flocculation with and without alum coagulation for mitigating ultrafiltration membrane fouling: Role of floc structure and bacterial activity," *Chemical Engineering Journal*, vol. 307, pp. 41-48, 2017
- [335] H. Wang, I. A. Fotidis, and I. Angelidaki, "Ammonia effect on hydrogenotrophic methanogens and syntrophic acetate-oxidizing bacteria," *FEMS microbiology ecology*, vol. 91, no. 11, 2015
- [336] D. Hennecke, A. Bauer, M. Herrchen, E. Wischerhoff, and F. Gores, "Cationic polyacrylamide copolymers (PAMs): environmental half life determination in sludge-treated soil," *Environmental Sciences Europe*, vol. 30, no. 1, pp. 1-13, 2018
- [337] M. I. Aguilar, J. Sáez, M. Lloréns, A. Soler, and J. F. Ortuño, "Nutrient removal and sludge production in the coagulation–flocculation process," *Water Research*, vol. 36, no. 11, pp. 2910-2919.2002/06/01/ 2002
- [338] M. Kacprzak *et al.*, "Sewage sludge disposal strategies for sustainable development," *Environmental Research*, vol. 156, pp. 39-46.2017/07/01/ 2017
- [339] I. M. Ismail, A. S. Fawzy, N. M. Abdel-Monem, M. H. Mahmoud, and M. A. El-Halwany, "Combined coagulation flocculation pre treatment unit for municipal wastewater," *Journal of Advanced Research*, vol. 3, no. 4, pp. 331-336, 2012
- [340] Z. Jin, F. Meng, H. Gong, C. Wang, and K. Wang, "Improved low-carbon-consuming fouling control in long-term membrane-based sewage pre-concentration: The role of enhanced coagulation process and air backflushing in sustainable sewage treatment," *J Membrane Sci*, vol. 529, pp. 252-262.2017/5// 2017
- [341] S. Hube *et al.*, "Direct membrane filtration for wastewater treatment and resource recovery: A review," *Sci Total Environ*, vol. 710, p. 136375.2020/03/25/ 2020

- [342] C. S. Lee, J. Robinson, and M. F. Chong, "A review on application of flocculants in wastewater treatment," *Process Safety and Environmental Protection*, vol. 92, no. 6, pp. 489-508.2014/11/01/ 2014
- [343] L. Jin, S. L. Ong, and H. Y. Ng, "Comparison of fouling characteristics in different pore-sized submerged ceramic membrane bioreactors," *Water research*, vol. 44, no. 20, pp. 5907-5918, 2010
- [344] J. Xue, Y. Zhang, Y. Liu, and M. G. El-Din, "Treatment of oil sands process-affected water (OSPW) using a membrane bioreactor with a submerged flat-sheet ceramic microfiltration membrane," *Water research*, vol. 88, pp. 1-11, 2016
- [345] B. Hofst, J. Ogier, D. Vries, E. F. Beerendonk, and E. R. Cornelissen, "Comparison of ceramic and polymeric membrane permeability and fouling using surface water," *Sep Purif Technol*, vol. 79, no. 3, pp. 365-374.2011/6// 2011
- [346] N. Kalboussi, J. Harmand, A. Rapaport, T. Bayen, F. Ellouze, and N. B. Amar, "Optimal control of physical backwash strategy-towards the enhancement of membrane filtration process performance," *Journal of Membrane Science*, vol. 545, pp. 38-48, 2018
- [347] M. Campinas, R. M. C. Viegas, C. Silva, H. Lucas, and M. J. Rosa, "Operational performance and cost analysis of PAC/ceramic MF for drinking water production: Exploring treatment capacity as a new indicator for performance assessment and optimization," *Separation and Purification Technology*, vol. 255, p. 117443.2021/01/15/ 2021
- [348] J. Kim *et al.*, "Anaerobic fluidized bed membrane bioreactor for wastewater treatment," *Environmental science & technology*, vol. 45, no. 2, pp. 576-581, 2011
- [349] S. Wang, U. Jena, and K. C. Das, "Biomethane production potential of slaughterhouse waste in the United States," *Energ Convers Manage*, vol. 173, pp. 143-157.2018/10// 2018
- [350] H. Gong *et al.*, "Organics and nitrogen recovery from sewage via membrane-based pre-concentration combined with ion exchange process," *Chem Eng J*, vol. 311, pp. 13-19, 2017
- [351] T. A. Nascimento and M. P. Miranda, "Control strategies for the long-term operation of direct membrane filtration of municipal wastewater," *J Environ Chem Eng*, vol. 9, no. 4, p. 105335.2021/08/01/ 2021
- [352] X. Shi, G. Tal, N. P. Hankins, and V. Gitis, "Fouling and cleaning of ultrafiltration membranes: A review," *J Water Process Eng*, vol. 1, pp. 121-138, 2014

- [353] Y. x. Zhao, P. Li, R. h. Li, and X. y. Li, "Direct filtration for the treatment of the coagulated domestic sewage using flat-sheet ceramic membranes," *Chemosphere*, vol. 223, 2019
- [354] S. Hube, J. Wang, L. N. Sim, T. H. Chong, and B. Wu, "Direct membrane filtration of municipal wastewater: Linking periodical physical cleaning with fouling mechanisms," *Sep Purif Technol*, vol. 259, 2021
- [355] M. Chai, Y. Ye, and V. Chen, "Separation and concentration of milk proteins with a submerged membrane vibrational system," *J Membrane Sci*, vol. 524, pp. 305-314, 2017
- [356] W. Xue, M. Jian, T. Lin, B. Ma, R. Wu, and X. Li, "A novel strategy to alleviate ultrafiltration membrane fouling by rotating membrane module," *Chemosphere*, vol. 260, p. 127535, 2020
- [357] S. A. Aktij, A. Taghipour, A. Rahimpour, A. Mollahosseini, and A. Tiraferri, "A critical review on ultrasonic-assisted fouling control and cleaning of fouled membranes," *Ultrasonics*, vol. 108, p. 106228, 2020
- [358] E. Obotey Ezugbe and S. Rathilal, "Membrane technologies in wastewater treatment: a review," *Membranes-Basel*, vol. 10, no. 5, p. 89, 2020
- [359] O. Ozcan, E. Sahinkaya, and N. Uzal, "Pre-concentration of Municipal Wastewater Using Flocculation-Assisted Direct Ceramic Microfiltration Process: Optimization of Operational Conditions," *Water, Air, & Soil Pollution*, vol. 233, no. 10, pp. 1-19, 2022
- [360] APHA, "Standard Methods for the Examination of Water and Wastewater. Federation. Water Environmental American Public Health Association, Washington, DC, USA," *Federation. Washington DC*, 2017
- [361] J. Tauber, V. Parravicini, K. Svardal, and J. Krampe, "Quantifying methane emissions from anaerobic digesters," *Water Science and Technology*, vol. 80, no. 9, pp. 1654-1661, 2019
- [362] M. Aslam, P. L. McCarty, C. Shin, J. Bae, and J. Kim, "Low energy single-staged anaerobic fluidized bed ceramic membrane bioreactor (AFCMBR) for wastewater treatment," *Bioresour technol*, vol. 240, pp. 33-41, 2017
- [363] M. Campinas, R. M. C. Viegas, C. Silva, H. Lucas, and M. J. Rosa, "Operational performance and cost analysis of PAC/ceramic MF for drinking water production: Exploring treatment capacity as a new indicator for performance assessment and optimization," *Sep Purif Technol*, vol. 255, pp. 117443-117443.2021/1// 2021
- [364] T. A. Nascimento and M. P. Miranda, "Continuous municipal wastewater up-concentration by direct membrane filtration, considering the effect of intermittent gas scouring and threshold flux determination," *J Water Process Eng*, vol. 39, p. 101733, 2021

- [365] R. Singh and N. Hankins, *Emerging membrane technology for sustainable water treatment*. Elsevier, 2016.
- [366] A. Van Nieuwenhuijzen, J. van der Graaf, M. Kampschreur, and A. Mels, "Particle related fractionation and characterisation of municipal wastewater," *Water Sci Technol*, vol. 50, no. 12, pp. 125-132, 2004
- [367] W. Li *et al.*, "Ceramic membrane fouling and cleaning during ultrafiltration of limed sugarcane juice," *Sep Purif Technol*, vol. 190, pp. 9-24.2018/01/08/ 2018
- [368] D. Hotza, M. Di Luccio, M. Wilhelm, Y. Iwamoto, S. Bernard, and J. C. Diniz da Costa, "Silicon carbide filters and porous membranes: A review of processing, properties, performance and application," *J Membrane Sci*, vol. 610, p. 118193.2020/09/01/ 2020
- [369] M. Valipour, "Variations of land use and irrigation for next decades under different scenarios," *Irriga*, vol. 1, no. 01, pp. 262-262, 2016
- [370] G. Zeeman *et al.*, "Anaerobic treatment as a core technology for energy, nutrients and water recovery from source-separated domestic waste (water)," *Water Science and Technology*, vol. 57, no. 8, pp. 1207-1212, 2008
- [371] J. Garrido, M. Fdz-Polanco, and F. Fdz-Polanco, "Working with energy and mass balances: a conceptual framework to understand the limits of municipal wastewater treatment," *Water science and technology*, vol. 67, no. 10, pp. 2294-2301, 2013
- [372] Y. D. Scherson and C. S. Criddle, "Recovery of freshwater from wastewater: upgrading process configurations to maximize energy recovery and minimize residuals," *Environmental science & technology*, vol. 48, no. 15, pp. 8420-8432, 2014
- [373] E. Foresti, M. Zaiat, and M. Vallero, "Anaerobic processes as the core technology for sustainable domestic wastewater treatment: Consolidated applications, new trends, perspectives, and challenges," *Reviews in Environmental Science and Bio/Technology*, vol. 5, no. 1, pp. 3-19, 2006
- [374] B.-Q. Liao, J. T. Kraemer, and D. M. Bagley, "Anaerobic membrane bioreactors: applications and research directions," *Critical Reviews in Environmental Science and Technology*, vol. 36, no. 6, pp. 489-530, 2006
- [375] D. C. Stuckey, "Recent developments in anaerobic membrane reactors," *Bioresource technology*, vol. 122, pp. 137-148, 2012
- [376] A. L. Smith, L. B. Stadler, N. G. Love, S. J. Skerlos, and L. Raskin, "Perspectives on anaerobic membrane bioreactor treatment of domestic wastewater: a critical review," *Bioresource Technol*, vol. 122, pp. 149-159, 2012

- [377] C. d. Chernicharo, "Post-treatment options for the anaerobic treatment of domestic wastewater," *Reviews in Environmental Science and Bio/Technology*, vol. 5, no. 1, pp. 73-92, 2006
- [378] P. Krzeminski, L. Leverette, S. Malamis, and E. Katsou, "Membrane bioreactors—a review on recent developments in energy reduction, fouling control, novel configurations, LCA and market prospects," *Journal of Membrane Science*, vol. 527, pp. 207-227, 2017
- [379] I. Martin, M. Pidou, A. Soares, S. Judd, and B. Jefferson, "Modelling the energy demands of aerobic and anaerobic membrane bioreactors for wastewater treatment," *Environmental technology*, vol. 32, no. 9, pp. 921-932, 2011
- [380] M. Aslam, P. L. McCarty, J. Bae, and J. Kim, "The effect of fluidized media characteristics on membrane fouling and energy consumption in anaerobic fluidized membrane bioreactors," *Sep Purif Technol*, vol. 132, pp. 10-15, 2014
- [381] C. Shin, K. Kim, P. L. McCarty, J. Kim, and J. Bae, "Integrity of hollow-fiber membranes in a pilot-scale anaerobic fluidized membrane bioreactor (AFMBR) after two-years of operation," *Separation and Purification Technology*, vol. 162, pp. 101-105, 2016
- [382] J. Heo, D. Kwon, E. Beirns, G.-Y. A. Tan, P.-H. Lee, and J. Kim, "Superior Methylparaben Removal by Anaerobic Fluidized Bed Ceramic Membrane Bioreactor with PVDF Tubular Fluidized Biocarrier: Reactor Performance and Microbial Community," *J Environ Chem Eng*, p. 109153, 2022
- [383] M. Aslam, P. Yang, P. H. Lee, and J. Kim, "Novel staged anaerobic fluidized bed ceramic membrane bioreactor: Energy reduction, fouling control and microbial characterization," (in English), *J Membrane Sci*, vol. 553, pp. 200-208. May 1 2018
- [384] V. Gitis and G. Rothenberg, "The basics," in *HANDBOOK OF POROUS MATERIALS: Synthesis, Properties, Modeling and Key Applications Volume 1- Introduction, Synthesis and Manufacturing of Porous Materials*: World Scientific, 2021, pp. 1-147.
- [385] K. Cho, K. W. Seo, S. G. Shin, S. Lee, and C. Park, "Process stability and comparative rDNA/rRNA community analyses in an anaerobic membrane bioreactor with silicon carbide ceramic membrane applications," *Sci Total Environ*, vol. 666, pp. 155-164, 2019
- [386] E. Eray, V. Boffa, M. K. Jørgensen, G. Magnacca, and V. M. Candelario, "Enhanced fabrication of silicon carbide membranes for wastewater treatment: From laboratory to industrial scale," *J Membrane Sci*, vol. 606, p. 118080, 2020
- [387] S. H. Park, Y. G. Park, J.-L. Lim, and S. Kim, "Evaluation of ceramic membrane applications for water treatment plants with a life cycle cost analysis," *Desalination Water Treat*, vol. 54, no. 4-5, pp. 973-979, 2015

- [388] J. Ni, J. Ji, Y.-Y. Li, and K. Kubota, "Microbial characteristics in anaerobic membrane bioreactor treating domestic sewage: Effects of HRT and process performance," *Journal of Environmental Sciences*, vol. 111, pp. 392-399, 2022
- [389] M. A. Musa, S. Idrus, H. Che Man, and N. N. Nik Daud, "Wastewater treatment and biogas recovery using anaerobic membrane bioreactors (AnMBRs): Strategies and achievements," *Energies*, vol. 11, no. 7, p. 1675, 2018
- [390] A. Foglia, Ç. Akyol, N. Frison, E. Katsou, A. L. Eusebi, and F. Fatone, "Long-term operation of a pilot-scale anaerobic membrane bioreactor (AnMBR) treating high salinity low loaded municipal wastewater in real environment," *Sep Purif Technol*, vol. 236, p. 116279.2020/04/01/ 2020
- [391] Y. Li, Q. Hu, and D.-W. Gao, "Dynamics of archaeal and bacterial communities in response to variations of hydraulic retention time in an integrated anaerobic fluidized-bed membrane bioreactor treating benzothiazole wastewater," *Archaea*, vol. 2018, 2018
- [392] T. Zsirai, P. Buzatu, P. Aerts, and S. Judd, "Efficacy of relaxation, backflushing, chemical cleaning and clogging removal for an immersed hollow fibre membrane bioreactor," *Water Res*, vol. 46, no. 14, pp. 4499-4507, 2012
- [393] Y. Rahimi, A. Torabian, N. Mehrdadi, M. Habibi-Rezaie, H. Pezeshk, and G.-R. Nabi-Bidhendi, "Optimizing aeration rates for minimizing membrane fouling and its effect on sludge characteristics in a moving bed membrane bioreactor," *J Hazard Mater*, vol. 186, no. 2-3, pp. 1097-1102, 2011
- [394] P. Ugarte *et al.*, "Low-cost ceramic membrane bioreactor: Effect of backwashing, relaxation and aeration on fouling. Protozoa and bacteria removal," *Chemosphere*, vol. 306, p. 135587.2022/11/01/ 2022
- [395] S. Annap, P. Sridang, U. Puetpaiboon, and A. Grasmick, "Influence of relaxation frequency on membrane fouling control in submerged anaerobic membrane bioreactor (SAnMBR)," *Desalin Water Treat*, vol. 52, no. 22-24, pp. 4102-4110, 2014
- [396] J. Wu, P. Le-Clech, R. M. Stuetz, A. G. Fane, and V. Chen, "Effects of relaxation and backwashing conditions on fouling in membrane bioreactor," *J Membrane Sci*, vol. 324, no. 1-2, pp. 26-32, 2008
- [397] A. Noyola, J. M. Morgan-Sagastume, and J. E. Lopez-Hernandez, "Treatment of biogas produced in anaerobic reactors for domestic wastewater: odor control and energy/resource recovery," *Reviews in environmental science and bio/technology*, vol. 5, pp. 93-114, 2006
- [398] Z. Wang, J. Ma, C. Y. Tang, K. Kimura, Q. Wang, and X. Han, "Membrane cleaning in membrane bioreactors: A review," *J Membrane Sci*, vol. 468, pp. 276-307.2014/10/15/ 2014

- [399] J. Bae, C. Shin, E. Lee, J. Kim, and P. L. McCarty, "Anaerobic treatment of low-strength wastewater: A comparison between single and staged anaerobic fluidized bed membrane bioreactors," *Bioresource Technol*, vol. 165, pp. 75-80.2014/08/01/ 2014
- [400] R. Chen, Y. Nie, N. Tanaka, Q. Niu, Q. Li, and Y.-Y. Li, "Enhanced methanogenic degradation of cellulose-containing sewage via fungi-methanogens syntrophic association in an anaerobic membrane bioreactor," *Bioresource technology*, vol. 245, pp. 810-818, 2017
- [401] W.-H. Chen, Y.-T. Wong, T.-H. Huang, W.-H. Chen, and J.-G. Lin, "Removals of pharmaceuticals in municipal wastewater using a staged anaerobic fluidized membrane bioreactor," *International Biodeterioration & Biodegradation*, vol. 140, pp. 29-36.2019/05/01/ 2019
- [402] T. Nur, P. Loganathan, M. B. Ahmed, M. Johir, J. Kandasamy, and S. Vigneswaran, "Struvite production using membrane-bioreactor wastewater effluent and seawater," *Desalination*, vol. 444, pp. 1-5.2018/10/15/ 2018
- [403] Y. Li, L. N. Sim, J. S. Ho, T. H. Chong, B. Wu, and Y. Liu, "Integration of an anaerobic fluidized-bed membrane bioreactor (MBR) with zeolite adsorption and reverse osmosis (RO) for municipal wastewater reclamation: Comparison with an anoxic-aerobic MBR coupled with RO," *Chemosphere*, vol. 245, p. 125569.2020/04/01/ 2020
- [404] W.-H. Chen, C.-Y. Tsai, S.-Y. Chen, S. Sung, and J.-G. Lin, "Treatment of campus domestic wastewater using ambient-temperature anaerobic fluidized membrane bioreactors with zeolites as carriers," *International Biodeterioration & Biodegradation*, vol. 136, pp. 49-54.2019/01/01/ 2019
- [405] J. Giménez *et al.*, "Experimental study of the anaerobic urban wastewater treatment in a submerged hollow-fibre membrane bioreactor at pilot scale," *Bioresource Technol*, vol. 102, no. 19, pp. 8799-8806, 2011
- [406] M. Aslam, P. Yang, P.-H. Lee, and J. Kim, "Novel staged anaerobic fluidized bed ceramic membrane bioreactor: Energy reduction, fouling control and microbial characterization," *Journal of Membrane Science*, vol. 553, pp. 200-208.2018/05/01/ 2018
- [407] C. Chen *et al.*, "Challenges in biogas production from anaerobic membrane bioreactors," *Renew Energ*, vol. 98, pp. 120-134, 2016
- [408] Y. Jeong, K. Cho, E. E. Kwon, Y. F. Tsang, J. Rinklebe, and C. Park, "Evaluating the feasibility of pyrophyllite-based ceramic membranes for treating domestic wastewater in anaerobic ceramic membrane bioreactors," *Chem Eng J*, vol. 328, pp. 567-573.2017/11/15/ 2017
- [409] P. Parameswaran, "Sustainable and Total Recovery of Resources from Wastewaters through the Anaerobic Membrane Bioreactor Platform," *Merrill Series on The Research Mission of Public Universities*, 2022

- [410] A. Ullah, H. J. Tanudjaja, M. Ouda, S. W. Hasan, and J. W. Chew, "Membrane fouling mitigation techniques for oily wastewater: A short review," *J Water Process Eng*, vol. 43, p. 102293.2021/10/01/ 2021
- [411] B. Hu, X. Zuo, J. Xiong, H. Yang, M. Cao, and S. Yu, "Identification of fouling mechanisms in MBRs at constant flowrate: model applications and SEM-EDX characterizations," *Water Sci Technol*, vol. 77, no. 1, pp. 229-238, 2018
- [412] C. Shin, P. L. McCarty, and J. Bae, "Importance of dissolved methane management when anaerobically treating low-strength wastewaters," *Current Organic Chemistry*, vol. 20, no. 26, pp. 2810-2816, 2016
- [413] Z. Kong *et al.*, "Evaluation of bio-energy recovery from the anaerobic treatment of municipal wastewater by a pilot-scale submerged anaerobic membrane bioreactor (AnMBR) at ambient temperature," *Bioresource Technol*, vol. 339, p. 125551.2021/11/01/ 2021
- [414] M. Tena *et al.*, "Techno-economic evaluation of bioenergy production from anaerobic digestion of by-products from ethanol flex plants," *Fuel*, vol. 309, p. 122171.2022/02/01/ 2022
- [415] WHO. "World Health Organization, Drinking Water." <https://www.who.int/en/news-room/fact-sheets/detail/drinking-water> (accessed 15.03.2019).
- [416] DSİ, "Su Kaynakları İstatistikleri, DSİ 2022 Yılı Verileri," 2022. [Online]. Available: <https://www.dsi.gov.tr/Sayfa/Detay/1848>
- [417] TÜİK, "Su ve Atıksu İstatistikleri, 2022," 2022. [Online]. Available: <https://data.tuik.gov.tr/Bulten/Index?p=Su-ve-Atıksu-Istatistikleri-2022-49607>
- [418] M. Sgroi, F. G. Vagliasindi, and P. Roccaro, "Feasibility, sustainability and circular economy concepts in water reuse," *Current opinion in environmental Science & Health*, vol. 2, pp. 20-25, 2018
- [419] Y. Ye *et al.*, "Nutrient recovery from wastewater: From technology to economy," *Bioresource Technology Reports*, vol. 11, p. 100425.2020/09/01/ 2020
- [420] M. Elimelech and M. R. Wiesner, "Membrane separations in aquatic systems," *Environmental Engineering Science*, vol. 19, no. 6, pp. 341-341, 2002
- [421] S. R. Pandey, V. Jegatheesan, K. Baskaran, and L. Shu, "Fouling in reverse osmosis (RO) membrane in water recovery from secondary effluent: a review," *Reviews in Environmental Science and Bio/Technology*, vol. 11, pp. 125-145, 2012
- [422] Y. Li, L. N. Sim, J. S. Ho, T. H. Chong, B. Wu, and Y. Liu, "Integration of an anaerobic fluidized-bed membrane bioreactor (MBR) with zeolite adsorption

and reverse osmosis (RO) for municipal wastewater reclamation: Comparison with an anoxic-aerobic MBR coupled with RO," *Chemosphere*, vol. 245, 2020

- [423] X. Zhang, M. Zhang, H. Liu, J. Gu, and Y. Liu, "Environmental sustainability: a pressing challenge to biological sewage treatment processes," *Current opinion in environmental science & health*, vol. 12, pp. 1-5, 2019
- [424] X. Zhang, M. Zhang, and Y. Liu, "One step further to closed water loop: Reclamation of municipal wastewater to high-grade product water," *Chin. Sci. Bull*, vol. 65, pp. 1358-1367, 2020
- [425] A. M. Mohseni, "Use of microalgae for treating municipal wastewater reverse osmosis concentrate and resource recovery," RMIT University, 2020.
- [426] C. Kappel, A. J. Kemperman, H. Temmink, A. Zwijnenburg, H. Rijnaarts, and K. Nijmeijer, "Impacts of NF concentrate recirculation on membrane performance in an integrated MBR and NF membrane process for wastewater treatment," *J Membrane Sci*, vol. 453, pp. 359-368, 2014
- [427] C. Kappel *et al.*, "Electrochemical phosphate recovery from nanofiltration concentrates," *Sep Purif Technol*, vol. 120, pp. 437-444, 2013
- [428] A. Bogdan, A. A. Robles Aguilar, E. Michels, and E. Meers, "Municipal wastewater as a source for phosphorus," *Biorefinery of Inorganics: Recovering Mineral Nutrients from Biomass and Organic Waste*, pp. 83-94, 2020
- [429] A. Kaplan, H. Mamane, Y. Lester, and D. Avisar, "Trace organic compound removal from wastewater reverse-osmosis concentrate by advanced oxidation processes with UV/O₃/H₂O₂," *Materials*, vol. 13, no. 12, p. 2785, 2020
- [430] M. Kumar, M. Badruzzaman, S. Adham, and J. Oppenheimer, "Beneficial phosphate recovery from reverse osmosis (RO) concentrate of an integrated membrane system using polymeric ligand exchanger (PLE)," *Water Res*, vol. 41, no. 10, 2007
- [431] A. Y. Bagastyo, J. Radjenovic, Y. Mu, R. A. Rozendal, D. J. Batstone, and K. Rabaey, "Electrochemical oxidation of reverse osmosis concentrate on mixed metal oxide (MMO) titanium coated electrodes," *Water Res*, vol. 45, no. 16, pp. 4951-4959, 2011
- [432] E. Dialynas, D. Mantzavinos, and E. Diamadopoulos, "Advanced treatment of the reverse osmosis concentrate produced during reclamation of municipal wastewater," *Water Res*, vol. 42, no. 18, pp. 4603-4608, 2008
- [433] M. Y. Jaffrin, "Dynamic shear-enhanced membrane filtration: a review of rotating disks, rotating membranes and vibrating systems," *J Membrane Sci*, vol. 324, no. 1-2, pp. 7-25, 2008

- [434] C. Kazner, "Advanced wastewater treatment by nanofiltration and activated carbon for high quality water reuse," Aachen, Techn. Hochsch., Diss., 2011, 2012.
- [435] M. Mehrjouei, S. Müller, and D. Möller, "Energy consumption of three different advanced oxidation methods for water treatment: a cost-effectiveness study," *J Clean Prod*, vol. 65, pp. 178-183, 2014
- [436] Y. Wang, J. Mou, X. Liu, and J. Chang, "Phosphorus recovery from wastewater by struvite in response to initial nutrients concentration and nitrogen/phosphorus molar ratio," *Sci Total Environ*, vol. 789, p. 147970.2021/10/01/ 2021
- [437] X. Liu, G. Wen, Z. Hu, and J. Wang, "Coupling effects of pH and Mg/P ratio on P recovery from anaerobic digester supernatant by struvite formation," *J Clean Prod*, vol. 198, pp. 633-641, 2018
- [438] S. Saki, D. Senol-Arslan, and N. Uzal, "Fabrication and characterization of silane-functionalized Na-bentonite polysulfone/polyethylenimine nanocomposite membranes for dye removal," *Journal of Applied Polymer Science*, vol. 137, no. 36, p. 49057, 2020
- [439] T. A. H. Nguyen, "Removal and recovery of phosphorus from municipal wastewater by adsorption coupled with crystallization," 2015.
- [440] B. M. Harouna, O. Benkortbi, S. Hanini, and A. Amrane, "Modeling of transitional pore blockage to cake filtration and modified fouling index–Dynamical surface phenomena in membrane filtration," *Chemical Engineering Science*, vol. 193, pp. 298-311, 2019
- [441] S. Lee and R. M. Lueptow, "Reverse osmosis filtration for space mission wastewater: membrane properties and operating conditions," *J Membrane Sci*, vol. 182, no. 1-2, pp. 77-90, 2001
- [442] M. Xie, J. Lee, L. D. Nghiem, and M. Elimelech, "Role of pressure in organic fouling in forward osmosis and reverse osmosis," *J Membrane Sci*, vol. 493, pp. 748-754, 2015
- [443] M. Shen, S. Keten, and R. M. Lueptow, "Rejection mechanisms for contaminants in polyamide reverse osmosis membranes," *J Membrane Sci*, vol. 509, pp. 36-47, 2016
- [444] C. H. Koo, A. W. Mohammad, and F. Suja', "Effect of cross-flow velocity on membrane filtration performance in relation to membrane properties," *Desalin Water Treat*, vol. 55, no. 3, pp. 678-692, 2015
- [445] K. L. Tu, L. D. Nghiem, and A. R. Chivas, "Coupling effects of feed solution pH and ionic strength on the rejection of boron by NF/RO membranes," *Chem Eng J*, vol. 168, no. 2, pp. 700-706, 2011

- [446] G. Sert *et al.*, "Investigation of mini pilot scale MBR-NF and MBR-RO integrated systems performance—Preliminary field tests," *J Water Process Eng*, vol. 12, pp. 72-77.2016/08/01/ 2016
- [447] S. Suwarno *et al.*, "Biofouling in reverse osmosis processes: The roles of flux, crossflow velocity and concentration polarization in biofilm development," *J Membrane Sci*, vol. 467, pp. 116-125, 2014
- [448] J. J. Lee, Y. C. Woo, and H.-S. Kim, "Effect of driving pressure and recovery rate on the performance of nanofiltration and reverse osmosis membranes for the treatment of the effluent from MBR," *Desalin Water Treat*, vol. 54, no. 13, pp. 3589-3595, 2015
- [449] O. Coronell, B. Mi, B. J. Mariñas, and D. G. Cahill, "Modeling the effect of charge density in the active layers of reverse osmosis and nanofiltration membranes on the rejection of arsenic (III) and potassium iodide," *Environ Sci Technol*, vol. 47, no. 1, pp. 420-428, 2013
- [450] H. Deng, M. Jacob, M. Montaner, J.-S. Pic, and C. Guigui, "Reverse Osmosis Performance in MBR-RO Process with Recirculation of RO Concentrate to MBR for Water Reclamation," 2020
- [451] K. Ikehata *et al.*, "Water recovery from advanced water purification facility reverse osmosis concentrate by photobiological treatment followed by secondary reverse osmosis," *Environ Sci Technol*, vol. 52, no. 15, pp. 8588-8595, 2018
- [452] S. Phuntsho, F. Lotfi, S. Hong, D. L. Shaffer, M. Elimelech, and H. K. Shon, "Membrane scaling and flux decline during fertiliser-drawn forward osmosis desalination of brackish groundwater," *Water Res*, vol. 57, pp. 172-182, 2014
- [453] A. Williams, D. Zitomer, and B. K. Mayer, "Ion exchange-precipitation for nutrient recovery from dilute wastewater," *Environmental Science: Water Research & Technology*, vol. 1, no. 6, pp. 832-838, 2015
- [454] L. L. S. Silva, J. C. S. Sales, J. C. Campos, D. M. Bila, and F. V. Fonseca, "Advanced oxidative processes and membrane separation for micropollutant removal from biotreated domestic wastewater," *Environ Sci Pollut R*, vol. 24, no. 7, pp. 6329-6338.2017/03/01 2017
- [455] A. T. Bouma, "Split-feed counterflow reverse osmosis for brine concentration," *Desalination*, vol. 445, pp. 280-291, 2018
- [456] K. P. Lee, T. C. Arnot, and D. Mattia, "A review of reverse osmosis membrane materials for desalination—Development to date and future potential," *J Membrane Sci*, vol. 370, no. 1-2, pp. 1-22, 2011
- [457] I. A. Tałałaj, "Performance of integrated sequencing batch reactor (SBR) and reverse osmosis (RO) process for leachate treatment: effect of pH," *J Environ Health Sci*, vol. 20, no. 1, pp. 419-429.2022/6// 2022

- [458] J. Wang, M. D. Armstrong, K. Grzebyk, R. Vickers, and O. Coronell, "Effect of feed water pH on the partitioning of alkali metal salts from aqueous phase into the polyamide active layers of reverse osmosis membranes," *Environ Sci Technol*, vol. 55, no. 5, pp. 3250-3259, 2021
- [459] A. C. Mecha, "Applications of Reverse and Forward Osmosis Processes in Wastewater Treatment: Evaluation of Membrane Fouling," *Osmotically Driven Membr. Process.-Approach, Dev. Curr. Status*, 2018
- [460] M. F. Tay, "A novel nanofiltration based membrane bioreactor (NF-MBR) and reverse osmosis (RO) for water reclamation," 2019
- [461] L. Masse, M. Mondor, and J. Dubreuil, "Effect of pH level and acid type on total ammoniacal nitrogen (TAN) retention and fouling of reverse osmosis membranes processing swine wastewater," *Water Quality Research Journal of Canada*, vol. 50, no. 4, pp. 297-304, 2015
- [462] J. Liu, L. Duan, Q. Gao, Y. Zhao, and F. Gao, "Removal of typical PPCPs by reverse osmosis membranes: optimization of treatment process by factorial design," *Membranes-Basel*, vol. 13, no. 3, p. 355, 2023
- [463] M. Son, T. Kim, W. Yang, C. A. Gorski, and B. E. Logan, "Electro-forward osmosis," *Environ Sci Technol*, vol. 53, no. 14, pp. 8352-8361, 2019
- [464] S. Saki and N. Uzal, "Surface coating of polyamide reverse osmosis membranes with zwitterionic 3-(3,4-dihydroxyphenyl)-l-alanine (l-DOPA) for forward osmosis," *Water Environ J*, vol. 34, no. 3, 2020
- [465] I. M. El-Azizi and R. G. Edyvean, "Performance evaluation and fouling characterisation of two commercial SWRO membranes," *Desalin Water Treat*, vol. 5, no. 1-3, pp. 34-41, 2009
- [466] O. Akin and F. Temelli, "Probing the hydrophobicity of commercial reverse osmosis membranes produced by interfacial polymerization using contact angle, XPS, FTIR, FE-SEM and AFM," *Desalination*, vol. 278, no. 1-3, 2011
- [467] S. Saki and N. Uzal, "Surface coating of polyamide reverse osmosis membranes with zwitterionic 3-(3, 4-dihydroxyphenyl)-l-alanine (l-DOPA) for forward osmosis," *Water and Environment Journal*, vol. 34, no. 3, pp. 400-412, 2020
- [468] O. Akin and F. Temelli, "Probing the hydrophobicity of commercial reverse osmosis membranes produced by interfacial polymerization using contact angle, XPS, FTIR, FE-SEM and AFM," *Desalination*, vol. 278, no. 1-3, pp. 387-396, 2011
- [469] Ö. Aktaş *et al.*, "Treatment of a chemical industry effluent by nanofiltration and reverse osmosis," *Desalin. Water Treat*, vol. 75, pp. 274-283, 2017
- [470] A. S. Al-Hobaib, K. M. Al-Sheetan, M. R. Shaik, N. M. Al-Andis, and M. S. Al-Suhybani, "Characterization and Evaluation of Reverse Osmosis Membranes

Modified with Ag₂O Nanoparticles to Improve Performance," *Nanoscale Research Letters*, vol. 10, no. 1, p. 379.2015/09/29 2015

- [471] Y. Matsumiya, T. Yamasita, and Y. Nawamura, "Phosphorus Removal from Sidestreams by Crystallisation of Magnesium-Ammonium-Phosphate Using Seawater," *Water Environ J*, vol. 14, no. 4, pp. 291-296, 2000
- [472] V. G. Le, D. V. N. Vo, C. T. Vu, X. T. Bui, Y. J. Shih, and Y. H. Huang, "Applying a novel sequential double-column fluidized bed crystallization process to the recovery of nitrogen, phosphorus, and potassium from swine wastewater," *ACS ES&T Water*, vol. 1, no. 3, pp. 707-718, 2020
- [473] K. Ge, Y. Ji, and S. Tang, "Crystallization kinetics and mechanism of magnesium ammonium phosphate hexahydrate: experimental investigation and chemical potential gradient model analysis and prediction," *Ind Eng Chem Res*, vol. 59, no. 30, pp. 13799-13809, 2020
- [474] M. Umar, F. Roddick, and L. Fan, "Effect of coagulation on treatment of municipal wastewater reverse osmosis concentrate by UVC/H₂O₂," *J Hazard Mater*, vol. 266, pp. 10-18, 2014
- [475] C. Zhao, P. Gu, H. Cui, and G. Zhang, "Reverse osmosis concentrate treatment via a PAC-MF accumulative countercurrent adsorption process," *Water Res*, vol. 46, no. 1, pp. 218-226, 2012
- [476] J. F. Hallas, C. L. Mackowiak, A. C. Wilkie, and W. G. Harris, "Struvite phosphorus recovery from aerobically digested municipal wastewater," *Sustainability-Basel*, vol. 11, no. 2, p. 376, 2019

APPENDIX

Table S1.1 The most frequent co-occurrences for the articles about “MWW treatment” based on the search held on February 29, 2024

Keyword	Occurrences	Total link strength
wastewater	491	1049
wastewater treatment	478	954
MWW	451	911
sewage sludge	169	336
anaerobic digestion	151	368
microbial community	143	279
activated sludge	137	266
wastewater treatment plant	127	243
anammox	111	264
microalgae	108	283
adsorption	104	219
membrane fouling	97	211
nitrogen removal	93	186
heavy metals	86	185
MWW treatment	81	127
resource recovery	76	179
nutrient removal	73	147
sludge	73	187
pharmaceuticals	70	175
membrane bioreactor	69	154
micropollutants	68	164
circular economy	66	140
denitrification	62	136
sars-cov-2	62	148
landfill leachate	61	147
microplastics	61	124
water quality	59	103
water reuse	59	123
biodegradation	58	116

Keyword	Occurrences	Total link strength
biogas	55	135
biochar	54	133
covid-19	54	130
nitrification	54	138
phosphorus	54	149
antibiotic resistance	53	114
life cycle assessment	52	121
constructed wetlands	51	91
disinfection	51	128
wastewater reuse	51	94

Table S1.2 The most frequent co-occurrences for the articles about “MWW treatment” based on the search held on February 29, 2024

Keyword	Occurrences	Total link strength
wastewater treatment	74	83
MWW	46	52
wastewater	39	52
circular economy	31	46
sustainability	31	32
microalgae	23	41
sewage sludge	22	20
resource recovery	21	29
anaerobic digestion	19	37
life cycle assessment	17	27
energy recovery	15	30
nutrient removal	12	18
membrane bioreactor	11	16
sludge	11	12
wastewater treatment plant	11	14
adsorption	10	5
constructed wetlands	10	11
wastewater reuse	10	13

CURRICULUM VITAE

2008 – 2012	B.Sc., Environmental Engineering, İstanbul University, İstanbul, TURKEY
2015 – 2018	M.Sc., Environmental Engineering, Erciyes University, Kayseri, TURKEY
2018 – 2024	Ph.D. Materials Science and Mechanical Engineering, Abdullah Gül University, Kayseri, TURKEY

SELECTED PUBLICATIONS AND PRESENTATIONS

J1) Ozcan, O., Sahinkaya, E., Uzal, N. (2022). Pre-concentration of Municipal Wastewater Using Flocculation-Assisted Direct Ceramic Microfiltration Process: Optimization of Operational Conditions. *Water, Air, & Soil Pollution*, 233(10), 1-19.

J2) Ozcan, O., Sahinkaya, E., & Uzal, N. (2023). "Integration of direct microfiltration and reverse osmosis process for resource recovery from municipal wastewater". *Desalination and Water Treatment*, 303, 1-11

C1) Ozcan O., Şahinkaya E., Uzal N. "Evaluation of up-concentration potential for direct membrane filtration of municipal wastewater, 14th Conference on Sustainable Development of Energy, Water, and Environment Systems" Dubrovnik, Croatia, 10 - 15 October 2021, ss.753

C2) O.Ozcan, S.Qadri, M.Ozdemir, R.Alabdullah, S.Gulcimen, E.Sahinkaya, N.Uzal, "Reclamation of municipal wastewater using direct ceramic membrane filtration for agricultural reuse" 9th International Conference on Sustainable Solid Waste Management, Corfu, Greece, 15-18 June 2022